A Study on the Water Retention and Contaminant Retention Behavior of Fly Ash, Bentonite and Its Mixes

Thesis

submitted in partial fulfillment of the requirements
of the degree of

DOCTOR OF PHILOSOPHY

by

ABHIJIT DEKA

Roll No. 10610413

Department of Civil Engineering
Indian Institute of Technology Guwahati
Guwahati - 781 039, India
August 2015

Dedicated to my beloved family

CERTIFICATE

This is to certify that the thesis entitled **"A Study on the water retention and contaminant retention behavior of fly ash, bentonite and its mixes"** submitted by Abhijit Deka to the Indian Institute of Technology Guwahati, for the award of the degree of Doctor of Philosophy (PhD) in Civil Engineering is a record of bonafide research work carried out by him under my supervision and guidance. The thesis work, in my opinion, has reached the requisite standard fulfilling the requirement for the degree of Doctor of Philosophy.

The results contained in this thesis have not been submitted in part or full to any other University or Institute for award of any degree or diploma.

IIT Guwahati
Date:

Dr. Sreedeep Sekharan
Associate Professor
Department of Civil Engineering
Indian Institute of Technology Guwahati
Guwahati- 781039
India

STATEMENT

I do hereby declare that the matter embodied in this thesis is the result of investigations carried out by me in the department of Civil Engineering, Indian Institute of Technology Guwahati, Guwahati, Assam, India.

In keeping with the general practice of reporting scientific observations, due acknowledgements have been made wherever the work described is based on the findings of other investigators.

IIT Guwahati
Date:

Abhijit Deka

ACKNOWLEDGEMENTS

The major work of completing this research work was made possible with continuous guidance and support of my supervisor Dr. Sreedeep Shekharan. His help, motivation and enthusiasm are gratefully acknowledged. Special thanks are given to my doctoral committee members Dr. Anil Kumar Mishra, Dr. Bulu Pradhan, and Dr. S. Kanagaraj for their valuable suggestions and guidance at every stage of this research work.

I am indebted to my family members: father Late Jatin Ch. Deka, mother Hemlata Deka, sister Arunima Deka and brother Arup Kr. Deka for their support and encouragement in carrying out my research work.

Special thanks to my research colleagues for their love, friendship and support throughout my stay at Indian Institute of Technology Guwahati. They are: Dr. Akash, Mr. Angshuman, Mr. Asish, Mr. Babloo, Mr. Chandrabhanu, Mr. Janarul, Mr. Jibeesh, Dr. Malaya, Mr. Ravi Patil, Mr. Srikanth, Mr. Sudheer, and Mr. Sunil. I am really thankful to Mr. Hariram Upadhay for his help in carrying out laboratory experiments.

I am also thankful to all the faculty members, staff members of Civil engineering department, IIT Guwahati and to all those who have been related to this study, either directly or indirectly, in smooth completion of the project work. I am thankful to Sophisticated Analytical Instrument Facility (SAIF) center, Gauhati University for conducting the XRF test of the materials used in this research work.

Abhijit Deka

Contents

ABSTRACT

A need to explore cost-effective and environmentally sustainable alternate materials that can be used in multi-layered hydraulic and contaminant barriers has motivated this research. Natural clays or expansive soils like bentonite mixed with cohesionless soil like sand is used for the construction of low permeable waste containment liners and covers. Sand is a costly construction material that would obviously need replacement in waste management projects such as liners and covers. Fly ash can be a viable alternative to sand in these projects.

Unsaturated characteristics and contaminant interaction are important for the behavioral modeling and performance assessment of geomaterials used in liners and covers. This research was planned to investigate the unsaturated behavior and contaminant interaction of fly ash-bentonite mix. The unsaturated behavior was established in terms of water retention characteristics curve (WRCC) for four Indian fly ashes, bentonites and fly ash-bentonite mix. The study brings out the measurable range of suction in fly ash, which is otherwise missing in the literature. The importance of volumetric shrinkage curve and mandatory approach for WRCC parameterization of bentonite has been demonstrated in this study. The influence of fly ash type and content on the WRCC of fly ash-bentonite mix was investigated. The sensitivity of variation in WRCC parameters on unsaturated seepage modeling was studied for specific cases of measured WRCC. The contaminant retention capacity of fly ash, bentonite and selected fly ash-bentonite mix was determined by considering lead as a model contaminant. The study highlights the usefulness of fly ash in combination with bentonite for waste containment liners and covers. This would help in the mass utility of waste fly ash for a meaningful environmental application such as waste containment and also relieve the burden of storage space.

Keywords: Waste containment, liners, covers, fly ash, bentonite, mix, water retention, contaminant retention, seepage modeling, sensitivity, fitting parameters.

List of Figures

List of Tables

Nomenclature

a_{vg}, a_f	Fitting parameters primarily dependent on the air entry value (AEV)
C_v	Coefficient of consolidation
C_e	Equilibrium concentration
e	Void ratio
G_s	Specific gravity of soil solids
H	Total head
h_r	Suction corresponding to residual state
k_{sat}	Saturated hydraulic conductivity
K_f	Constant representing the retention capacity (mg/g)
m_{vg}, m_f	Fitting parameter which depend on θ_r
n_{vg}, n_f	Fitting parameters that are dependent on the rate of extraction of water from the soil
n	Constant representing intensity of the adsorbent respectively
Pb	Lead
q_e	Amount of contaminant adsorbed at equilibrium time
q_m	Maximum sorption capacity
$\gamma_{d\ max}$	Maximum dry unit weight
Q	Quartz
S_r	Degree of saturation
t_{50}	Time required for saturating 50% of the column depth
w	Gravimetric water content
w_b	Bentonite water content
w_m	Water content of the mixture
ψ_m	Matric suction
ψ_o	Osmotic suction
ψ	Total suction
$\theta(\psi)$	Volumetric water content at any suction, ψ
θ_r	Residual volumetric water content
θ_s	Volumetric water content at saturation
θ_{ds}	Volumetric water content at desaturation
γ_d	Dry unit weight

γ_w	Unit weight of water
ε	Permittivity
β	Bentonite content in the mixture

Abbreviation

AAS	Atomic Absorption Spectrophotometer
AEV	Air entry value
B1	Bentonite 1
B2	Bentonite 2
B3	Bentonite 3
B4	Bentonite 4
BFA	Badarpur fly ash
EGME	Ethylene glycol monoethyl ether
EQT	Equitensiometer
FFA	Farakka fly ash
FX	Fredlund and Xing
FSI	Free swell index
kPa	Kilopascal
LL	Liquid limit
LOI	Loss on ignition
L/S	Liquid to solid ratio
MDD	Maximum dry density
MPS	Matric potential sensor
NTPC	National thermal power corporation
NFA	Neyvelli fly ash
OMC	Optimum moisture content
PA	Pond ash
ppm	Parts per million
PL	Plastic limit
PI	Plasticity index
R^2	Regression coefficient
RETC	Retention curve
RH	Relative humidity
FESEM	Scanning electron microscope
SL	Shrinkage limit
SSA	Specific surface area

SWCC	Soil-water characteristic curve
TM	Tensiometer
vG	van Genuchten
WP4	Dew point potentiameter
WRCC	Water retention characteristic curve

Chapter 1

Introduction

1.1 General

Natural clays, bentonite and its mixes with specific geomaterials are the most widely used materials for the construction of hydraulic barriers such as liners and covers due to its low hydraulic conductivity (< 10^{-9} m/s) (Chalermyanont and Arrykul 2005). High plastic clays like bentonite exhibit low strength and high volume change with changes in water content, which is not desirable for the stability of hydraulic barriers. Cohesionless materials like sand or natural soil are mixed with high plastic soils in appropriate proportions to improve strength and volume change characteristics without compromising the requirement of hydraulic conductivity. Compacted sand-bentonite mixture is one of the most commonly adopted hydraulic barrier investigated in the past for hazardous and nuclear waste containment (Heineck et al. 2010; Gleason et al. 1997; Ogata and Komine 1993; Cowland and Leung 1991; Abeele 1986). However, sand is a costly construction material and its availability is restricted by the environmental impact associated with its dredging. Construction of hydraulic barriers in waste containment demands huge quantity of sand, which may not be economically feasible and at the same time hampers the progress of the project due to non-availability. Researchers have investigated the use of natural soil in the vicinity of construction site if appropriate quality and quantity burrow sites are readily available. Natural soils would exhibit wide variability in its properties and hence a strict quality control may be deemed necessary. Further researches are still on to find effective alternative materials for the construction of hydraulic barriers.

The above objective has motivated to explore the utility of waste material like fly ash as an alternative to sand. Fly ash is generated by the burning of pulverized coal in the thermal power plants. The collection, reuse, disposal and storage of fly ash have always been a challenging geoenvironmental problem. Several researches in the past have facilitated the use of fly ash in several construction and geotechnical projects (Horiuchi et al. 2000; Parsa et al. 1996). Some researchers have also explored the utility of fly ash as hydraulic barrier (Yeheyis et al. 2010; Çokça and Yilmaz 2004; Prashanth et al. 2001; Nhan et al. 1996). Fly ash being a cohesionless fine material may not be a successful hydraulic barrier. But at the same time its utility can be ensured if it is mixed with bentonite in appropriate proportion (Younus and Sreedeep 2012). Fly ash can be a

suitable substitute for improving the strength and volume change characteristics of bentonite (Kumar and Sharma 2004). This would help in the mass utility of waste fly ash for a meaningful environmental application such as waste containment and also relieve the burden of storage space.

Hydraulic barriers are mostly unsaturated and hence its water retention characteristic becomes important for its performance evaluation. Therefore, it is mandatory to study the water retention characteristic curve (WRCC) of fly ashes, bentonite and their mixes to explore its utility as hydraulic barriers. Such studies are not reported in the literature. WRCC is the representation of suction as a function of water content (gravimetric or volumetric) or degree of saturation (Fredlund 2002) and is the basic measured input for modeling the behavior of unsaturated geomaterials (Thieu et al. 2001; Fredlund 1998; Lam et al. 1987). It is essential to measure suction and the corresponding state variable (water content or saturation) precisely for obtaining a reliable WRCC. Suction is mainly composed of matric suction (ψ_m) and osmotic suction (ψ_o), which together is known as total suction (ψ). Matric suction is due to adsorptive and/or capillary forces existing in the soil matrix whereas osmotic suction is due to the presence of salts or contaminants present in the pore water (Fredlund and Rahardjo 1993). Some of the frequently used methods for measuring suction are tensiometer, filter paper, chilled mirror dew point sensor, relative humidity technique, and axis translation technique (Nam et al. 2009; Sreedeep and Singh 2006; Thakur et al. 2006; Leong et al. 2003; Likos and Lu 2003; Ridley 2003). The measured data could be used for mathematical quantification using different empirical or semi-empirical WRCC equations (Leong and Rahardjo 1997; Fredlund and Xing 1994; van Genuchten 1980).

Another important aspect which is important in waste containment barriers is the soil-contaminant interaction. Retention is the most important soil-contaminant interaction parameter required for modeling the fate of contaminant in geo-environment (Poly and Sreedeep 2011; Khan et al. 2010; Viotti et al. 2005). These characteristics are not studied in detail for fly ash-bentonite mixes, especially for Indian fly ashes.

Therefore the main objective of this study was to establish water retention and contaminant retention characteristics of fly ashes, bentonite and their mixes. The influence of spatial variability and content of fly ash on the above said characteristics of fly ash-bentonite mixes need to be investigated. Such a study would help to understand the possibility of generalizing WRCC model parameters for the given variations in the physical characteristics of fly ashes collected from different sources. Effort was made to

identify the measurable range of suction for fly ashes, which is not reported in the literature. The usefulness of precise volumetric shrinkage characteristics for unambiguous WRCC parameterization of high volume change geomaterial like bentonite was demonstrated in this study. Further, the sensitivity of given variability in WRCC on unsaturated seepage modeling was studied for specific cases. The contaminant retention characteristics of different fly ashes and fly ash-bentonite mixes were studied with lead metal ion (Pb^{2+}) as the model contaminant. The study investigated the removal efficiency of different fly ashes and fly ash-bentonite mixes by conducting 24 hr batch equilibrium test.

1.2 Motivation for this study

A need for alternate material for constructing hydraulic barriers has motivated this research work. The usefulness of cohesionless materials like fly ash along with bentonite as hydraulic barrier is not well explored. Such an effort not only help to prevent the use of costly construction material like sand but also ensure the utility of waste fly ash. It is understood that water retention and contaminant retention characteristics of fly ash-bentonite mixes is mandatory for establishing its utility as hydraulic barriers in waste containment. There are limited studies on the water retention and contaminant retention characteristics of fly ash-bentonite mixes reported in the literature. There are no such studies available for Indian fly ashes. It is also important to know the influence of spatial variability of fly ashes and its quantity on the water retention and contaminant retention characteristics of fly ash-bentonite mixes. This would have an impact when fly ash from different sources will be used in the same project.

1.3 Organisation of the thesis

This thesis consists of nine chapters. Chapter 1 deals with the introduction of the problem and motivation behind this research work. Chapter 2 explains the available literature related to this research and the background information leading to the scope of the attempted research. In chapter 3, details of the materials fly ashes and bentonites with their different characteristics are presented. The details of different techniques used for suction measurement and volumetric water content measurement are discussed. The results and discussions are included in chapters 4 to 7. In chapter 4, the results of the WRCC of different fly ashes are presented. Chapter 5 includes the results of WRCC for bentonites and fly ash-bentonite mixes. The result of WRCC parameter from chapter 4

and 5 were used to study its sensitivity on unsaturated seepage modeling for specific cases as presented in chapter 6. The result of the lead retention characteristics of fly ashes, bentonite and selected fly ash-bentonite mixes is presented in chapter 7. Finally, the conclusion and major outcome from the present study is reported in chapter 8, limitation and future scope of research in chapter 9.

Chapter 2

Review of Literature and Scope of the Present Study

2.1 General

An understanding on the utility of fly ash and bentonite in geotechnical and geoenvironmental applications is essential for proposing it as alternate material for hydraulic barrier. Focus has been laid on studies related to the determination of hydraulic characteristics of fly ash, bentonite and their mixes. Further, contaminant retention characteristics of fly ash, bentonite and its various mixes were reviewed. A critical appraisal of literature review was presented, based on which the scope of the present research work has been formulated.

2.2 Utilization of fly ash and bentonite as hydraulic barriers

Fly ash has potential application in geotechnical and geoenvironmental projects such as construction of embankment, hydraulic barrier, compacted pavements/ roads and as fertilizer in agriculture. There are numerous studies carried out over the past few decades to determine different geotechnical properties of fly ashes. Bentonite which consist of the montmorillonite mineral have been widely used in landfill liner and cover construction due to its very low hydraulic conductivity. Few of these studies are discussed below.

Pal and Ghosh (2014) studied the volume change behavior of fly ash-montmorillonite mixes by conducting consolidation and free swell test on various proportions of fly ash-montmorillonite mixes. Nine type of fly ash collected from Eastern India were used in this study. It was found that the coefficient of consolidation values of the fly ash samples resemble that of non-plastic silty sand and non-plastic sandy silt. It was also found from the Free Swell Index (FSI) test that the fly ash samples are non-swelling in nature. Also, fly ash sample shows no significant change in vertical compression as found from the consolidation test.

Kalyanshetti and Thalange (2013) investigated the effect of addition of fly ash on the engineering properties of fly ash-expansive soil mixes. The study carried out various test like compaction properties, Atterberg limits, free swell index, swelling pressure, California bearing ratio (CBR) (Soaked and Unsoaked) test using different proportions of fly ash. It was found that there was an appreciable reduction in the swelling

characteristics of soils up to extent of 40% to 50%. The CBR value was improved by 70% to 75% with addition of fly ash. It was also observed that addition of fly ash beyond 20% is not significant on the above properties.

Younus and Sreedeep (2012) investigated the utility of fly ash-bentonite mixes for application in landfill liner. The objective of the study was to maximize the utility of fly ash in waste containment facility. Hydraulic conductivity and unconfined compressive strength test was determined for different percentage of fly ash-bentonite mixes. The study recommended that a maximum of 70% by weight of class F fly ash can be used with bentonite in compacted clay liners. The study also concluded that bentonite and fly ash could not be used alone in landfill liner construction.

Amadi (2011) studied the efficacy of fly ash stabilization in enhancing the compatibility between lateritic soil and Municipal Solid Waste (MSW) leachate. The study conducted hydraulic conductivity test using different proportions of fly ash and found that hydraulic conductivity was minimum at 10% fly ash content while it increases above 10%.

Amadi (2011) studied the hydraulic conductivity of lateritic soil and fly ash mix. Soil mix was prepared at 0, 5, 10, 15, 20% fly ash content compacted at 2% wet of optimum moisture content with modified Proctor method. Fly ash was a class C type collected from the thermal power plant in Nigeria. From the study, it was found that the hydraulic conductivity decreases with increase in fly ash content up to 10% due to increase in fines content in the mixture. Above 10%, the hydraulic conductivity was found to increase again.

Sivapullaiah and Baig (2011) studied the gypsum treated fly ash for using as liner for waste containment facility. Lime content up to 10% was studied and permeability was determined by the falling head method. It was found that hydraulic conductivity of lime treated fly ash decreases significantly while its unconfined compressive strength increases.

Ahmaruzzaman (2010) gave an extensive review on the stabilization of fly ash and its utilization. The adsorption capacity of fly ash for various heavy metals was extensively discussed here.

Heineck et al. (2010) studied the effect of bentonite proportions on the hydraulic conductivity of bottom ash, fly ash and compacted sand by using flexible wall permeameter. The particle morphology was studied based on thin section micrographs. The proportions of bentonite used in the study were 0, 3, 6, 9 and 18%. The study

indicated that there was only a marginal reduction of hydraulic conductivity ($1.78x10^{-6}$ m/s to $1.39x10^{-7}$ m/s for bottom ash and from $5.67x10^{-7}$ m/s to $1.12x10^{-7}$ m/s for fly ash) of bottom ash and fly ash on addition of bentonite. Hydraulic conductivity reduction was achieved only when bentonite was added to sand (from $3.17x10^{-5}$ m/s to $5.15x10^{-10}$ m/s). Due to the solid particles of sand and longitudinal contact between them, the hydraulic conductivity of sand bentonite mixture was less whereas ash had angular and porous particles. The elevated cation concentration in pore water is an important aspect for high hydraulic conductivity of ash-bentonite mixtures. The cation exchanges decreased the swelling capacity of bentonite and thus increased the hydraulic conductivity of the mixtures. The microscopic analysis of bottom ash and fly ash indicated porous particles resulting in high hydraulic conductivity.

Shafique et al. (2010) studied the long term performance of two fine grained soils stabilized by class C fly ash at different proportion. Various test like plasticity index test, UCS test, vertical swell test were conducted. It was found that addition of fly ash content increases the strength while decreases the plasticity and swelling characteristics of fine grained soils.

Yeheyis et al. (2010) studied the feasibility of coal fly ash and fly ash-bentonite mixes to be used as a barrier material for mine waste containment. Hydraulic conductivity test were conducted on raw fly ash and fly ash-bentonite mixes. It was found that fly ash-bentonite mixes gave a low hydraulic conductivity suitable for landfill liner application. It also exhibited good metal retention characteristics due to high alkalinity of fly ash.

Prakash and Sridharan (2009) determined the permeability of different coal ashes and found to be in the range of silts. The permeability of class C fly ashes was found to be less than class F fly ashes, and its permeability was found to decrease with time.

Shantakumar et al. (2008) investigated fly ash collected from various location of electrostatic precipitator (ESP). It was found that fly ash properties changes from one location to another location of ESP unit.

Zha et al. (2008) studied the stabilization of expansive soils by fly ash and fly ash treated lime. They also found a significant change in the swell potential and plasticity property of expansive soil. It was also reported that fly ash treated expansive soil increases its unconfined compressive strength with curing period.

Das and Yudhbir (2006) compared the geotechnical properties of low calcium and high calcium fly ash. They found a distinct difference in morphology between fly ashes. The optimum moisture content (OMC) was directly proportional and maximum dry

density (MDD) was inversely proportional to the loss on ignition content of fly ashes. The strength of high calcium C class fly ash was 230 times higher than low calcium F class fly ash. They termed high calcium fly ash as cementious and pozzolanic and low calcium fly ash pozzolanic.

Edil et al. (2006) studied the effectiveness of self-cementing fly ash in the stabilization of soft fine grained soil. Six soft soil with different ranges of plasticity and four fly ashes with two high quality C class fly ash were used. CBR and resilient modulus (M_r) test were conducted to study the behavior. It was found that addition of fly ash increases the CBR and M_r of inorganic soils while there was no appreciable effect on organic soils

Mishra and Karanam (2006) investigated the use of class F fly ash for backfilling mine voids. They prepared a fly ash composite by mixing with lime and gypsum in suitable proportions. The study found that class F fly ash had greater potential to be developed into a strong engineering material with the addition of lime and gypsum. The fly ash composite exhibited favorable characteristics to substitute sand as backfilling material.

Shang et al. (2006) studied the stabilization of acid mine tailing with the help of coal fly ash. It was noted that the hydraulic conductivity of coal fly ash decreases from 10^{-6} cm/s to 10^{-9} cm/s due to chemical reactions between ash solids and acid mine drainage.

Chalermyanont and Arrykul (2005) studied the application of sand-bentonite mixtures in hydraulic containment liners. The dry percentage weight of bentonite was varied from 0 to 9%. At about 5% bentonite content, the hydraulic conductivity decreased approximately four orders of magnitude. Further addition of bentonite produced insignificant decrease of hydraulic conductivity, rather it decreased the shear strength of the mixture and increased swelling. At 3% bentonite content compacted at about 2% wet of optimum water content, the hydraulic conductivity of the mixture decreased to the required value for hydraulic containment application with friction angle greater than 38 degrees.

Das and Yudhbir (2005) developed a simplified model for predicting the pozzolana reactivity of fly ash in terms of compressive strength of fly ash. The study proposed a relationship in terms of chemical composition of fly ashes.

Yeo et al. (2005) studied the consolidation and hydraulic conductivity of various backfill mixtures used in soil-bentonite vertical cut off wall. Different percentage of sand

and bentonite were used for preparing the mixtures. The coefficient of consolidation, C_v was found to decrease with increase in backfill-fine content or backfill-bentonite content. It was found that more than 40% of fine was required in the backfill to achieve the hydraulic conductivity of $\leq 10^{-9}$ m/s when the backfill contained only low-plasticity clay. Again, when the backfill consists of clean, coarse-grained materials, a significant amount of dry bentonite (5% in this study) might be required to achieve a hydraulic conductivity $\leq 10^{-9}$ m/s.

Çokça and Yilmaz (2004) investigated the fly ash mixed with bentonite as a liner material. Type C fly ash was collected from the Soma thermal power plant in Turkey. Falling head permeability test was performed using oedometer. The hydraulic conductivity of fly ash mixed with 10% bentonite was found to be within the acceptable limit for liner design (10^{-9} m/s).

John et al. (2004) investigated the effects of soil-bentonite mixture for hydraulic conductivity and retention of lead from the solution. The study indicated that the hydraulic conductivity of the soil-bentonite mixture was found to be 10^{-10} m/s. Acid extraction and SEM/EDX analysis were carried out to study the sorption of lead by soil-bentonite mixture.

Kaniraj and Gayathri (2004) studied the permeability and consolidation characteristics of compacted fly ashes. It was reported that the consolidation and permeability characteristics of compacted fly ashes were comparable to that of non-plastic soil.

Kumar and Sharma (2004) studied the effect of fly ash on different engineering properties of expansive soil by conducting laboratory experiments. The hydraulic conductivity of expansive soil-fly ash mix decreased with an increase in expansive soil content. The study indicated that the plasticity characteristics of expansive soil were reduced by the addition of fly ash. Again, increase in fly ash content decreased the liquid limit and increased the plastic limit of the expansive soil. It was found that the free swell index of expansive soils could be effectively reduced up to 50% by addition of 20% fly ash.

Pandian (2004) determined the geotechnical characteristics of different Indian fly ashes for their effective utilization in many geotechnical applications. It had a low specific gravity, free draining nature, ease of compaction, good frictional properties which makes it suitable for construction of embankment, roads and reclamation of low lying areas.

Kaniraj and Gayathri (2003) studied the geotechnical characteristics of raw and fibre reinforced fly ash with 1% fibre content by dry weight. They found that inclusion of fibre into fly ashes increases the strength of the raw fly ash specimen and change their behavior from brittle to ductile nature.

Iyer and Scott (2001) presented an extensive review of the utilization of fly ash in various fields other than the construction industry. The application include production of zeolite and mullite, glass like materials, making of composite materials, adsorbent for waste containment, waste stabilization, recovery of different materials from fly ash, application in agricultural field.

Horiuchi et al. (2000) investigated the utilization of slurry fly ash as a fill material in different civil engineering projects. The study appraised the potential of fly ash for 1) Underwater fills, 2) Light weight backfills, 3) Light weight structural fills through both laboratory test and construction works. They found that coal fly ash reclaimed by slurry placement shows lower compressibility, higher ground density and higher strength than other methods. The higher strength increased the stability against liquefaction during earthquake.

Prashanth et al. (2001) studied the use of pozzolanic fly ash as a hydraulic barrier in landfill. The behavior of three different fly ashes collected from different sources and having different physico-chemical properties were investigated in this study. Various geotechnical properties like shrinkage, compaction, permeability, consolidation and strength was determined. From the study, it was clear that fly ash had a very low shrinkage and compacted fly ash undergoes a little volume change. The pozzolanic fly ash was found to develop good strength with time even without the addition of lime. As the fly ash consists of silt size particles, it exhibited low hydraulic conductivity. However, pozzolanic fly ashes with lime exhibited low permeability on curing because of the formation of gel compounds which blocked the pores.

Lin and Benson (2000) studied the effect of wet-dry cycles on plasticity and swelling characteristics of bentonite by conducting various tests. Three different types of liquids were used in the tests. The hydraulic conductivity of geosynthetic clay liner (GCL) was also studied for these liquid for various wetting cycles. The study indicated that the plasticity of the bentonite decreased for increasing wet-dry cycles when tap water and $CaCl_2$ was used as wetting liquid. On the other hand, the plasticity characteristic of the bentonite increased when wetted with deionized water. The swelling of bentonite increased when deionized and tap water was used for wetting and decreased when $CaCl_2$

was used. The hydraulic conductivity was found to be less for initial few cycles of wetting, but gradually increased as the cycle was increased.

Palmer et al. (2000) conducted laboratory and field hydraulic conductivity test on class F fly ash and other materials like class C fly ash, sand and bottom ash for its use in waste containment liners. The study revealed that mixture of class F and C fly ashes combined with a coarse aggregate (e.g. bottom ash) could be compacted to achieve hydraulic conductivity near or below 10^{-7} cm/s at compaction water content above optimum moisture content.

Ghosh and Subbarao (1998) studied the effect of fly ash stabilized with lime and gypsum on the hydraulic conductivity, and on the leaching of metals out of the stabilized fly ash. The effect of moulding water content, lime content, gypsum content, curing period and flow period on the hydraulic conductivity was investigated in detail. From the study, it was found that the addition of lime to fly ash reduced hydraulic conductivity. Again, gypsum in the presence of lime helped to decrease hydraulic conductivity even further. It made the matrix more stable and enhanced the pozzolanic reaction. Hydraulic conductivity of the stabilized material reduced with an increase in molding water content, and the reduction in hydraulic conductivity was less on the wet side of optimum. For all the mixes of fly ash and lime or fly ash, lime and gypsum there was a reduction in hydraulic conductivity with an increase in the curing period. The concentrations of As, Cd, Cr, Cu, Fe, Hg, Mg, Ni, Pb, and Zn in the effluent emanating from the hydraulic conductivity specimens of mixes with higher proportions of lime or lime and gypsum were below threshold limits acceptable for ground water.

Gleason et al. (1997) studied the performance of calcium and sodium bentonite for application in soil-bentonite mixtures for landfill liner and cover, Geosynthetic Clay Liners (GCLs) and cement-bentonite mixture for vertical cut-off wall. In case of hydraulic conductivity, three times more calcium bentonite was required for reducing the hydraulic conductivity to about 10^{-7} m/s than the sodium bentonite. Again, the hydraulic conductivity of the sand-bentonite mixtures increased when permeated with $CaCl_2$ solution. All the thin bentonite layers (simulating the use of GCL) has given hydraulic conductivity less than 10^{-7} m/s. Sodium bentonite was found to be approximately 10 times less permeable with tap water than the calcium bentonite.

Nhan et al. (1996) investigated coal fly ash for using as landfill liner material by conducting hydraulic conductivity test and contaminant retention study on coal fly ash,

lime and calcium bentonite ratio 7:2:1. Tests were conducted for both pure water and synthetic MSW leachate.

Parsa et al. (1996) studied the utilization of fly ash in stabilization/solidification of hazardous wastes. The process involved mixing the waste with fly ash and compacting the mix to form a solid which is easier to handle. This process produced a solid which was structurally sound and relatively impermeable.

Cowland and Leung (1991) carried out both field and laboratory testing to study the performance of bentonite amended weathered granite landfill liner. The field investigations were carried out on both flat and sloping ground. The study indicated that bentonite content of around 5-7% was adequate in reducing the hydraulic conductivity of the completely weathered granite (CWG) to 10^{-9} cm/s. Here, both water and leachate was used as the permeant in the field permeability test. The permeability was found to lie between 10^{-9} cm/s and 10^{-10} cm/s. Laboratory permeability test on the CWG gave decreasing value of the coefficient of permeability with increase in bentonite content.

Abeele (1986) studied the permeability of bentonite-silt ratio for its effective utilization in landfill liner application by conducting consolidation test. The study indicated that the coefficient of consolidation was inversely proportional to the square of the bentonite/silt ratio. The hydraulic conductivity decreased as the compaction pressure was increased. Hydraulic conductivity could be expressed as a function of void ratio. A strong relationship exists between the void ratio and log σ for each bentonite ratio.

2.3 Unsaturated state of soil and measurement of soil suction

The study of classical soil mechanics is based on the assumption that soil is fully saturated consisting of water and solid phase only. But in most of the cases, the soil remains in unsaturated state and consist of three phases: gaseous phase, liquid phase and solid phase. In many geoenvironmental problems, a fourth phase which is the contaminant phase occurs in the soil matrix. This contaminant phase comes from the dissolved contaminant present in the pore water. So the study of unsaturated state of the soil for geoenvironmental problems requires knowledge of the interaction mechanism of these phases.

The characterization of unsaturated soil depends on the accurate measurement of negative pore water pressure or soil suction, which is defined as the amount of energy required to liberate unit volume of water from an unsaturated soil. Total suction present in

the unsaturated soil is composed of matric suction and osmotic suction (Fredlund and Rahardjo1993). Matric suction is attributed to the adsorbed and capillary forces between water and the soil matrix where as osmotic suction results from solutes/dissolved salts present in the pore-solution. Soil suction can be measured either directly or indirectly. Direct method involves the measurement of soil suction directly on the soil, whereas indirect method yield parameters like electrical resistivity, thermal conductivity or relative humidity that can be correlated to soil suction with the help of appropriate calibration equations. The details of the various instruments available for direct and indirect methods of suction measurement with type of suction, their range and equilibration time are given in Malaya (2012).

The measured soil suction values when plotted against the water content yield a characteristic curve, which is termed as soil-water characteristic curve (SWCC) or water retention curve (WRC) or water retention characteristic curve (WRCC). The term WRCC is used in this study. The WRCC is unique for a particular type of soil and has been used by researchers to estimate various unsaturated soil properties such as hydraulic conductivity, shear strength and compressibility. Studies related to the suction measurement for soil are discussed below.

Tripathy et al. (2014) studied the WRCC of three types of clays having different plasticity characteristics using axis-translation, vapour equilibrium, and osmotic technique. The shrinkage paths of the clays was established with the help of clod test and obtained the suction-degree of saturation WRCC by combining the suction-water content WRCC with the clod test result. They found that air entry value of bentonite can be precisely obtained from the suction-degree of saturation WRCC. They also observed that water content at the air entry is greater than shrinkage limit of the soil.

Lin and Cerato (2012) studied the behavior of WRCC of four expansive soils in both untreated and stabilized form. Suction was measured using pressure plate apparatus. It was reported that for highly clayey soils, diffuse double layer formation has significant impact on the WRCCs behavior. The two physical parameter pH and surface conductance were used to account the diffuse double layer effect on the WRCC. Result showed a good correlation between pH and surface conductance with Fredlund and Xing (FX) parameter ‘‘a’’ because the AEV is determined by the diffuse double layer of the samples at their saturated state. However, no clear mechanism was revealed with respect to how pH and surface conductance affect parameter ‘‘a’’. Poor correlation was shown between pH and

surface conductance and parameter ‘‘m’’; while no correlation was found with ‘‘n’’, which may be in part a result of using a small data set.

Pedarla et al. (2012) studied the influence of montmorillonite mineral content on sand-montmorrilonite mix WRCC and gave some important information about the effect of mineral content on the WRCC model parameters of various models. Suction was measured using pressure plate apparatus and WP4 device. It was reported in the study that model parameters of Brooks and Corey (BC), Fredlund and Xing (FX) and van Genuchten (vG) were not similar. The air entry pressure was found to increase with the increase in mineral content in the mix.

Yang et al. (2011) studied the improvement effect of expansive soil by determining the WRCC of lime-expansive soil mix and fly ash-expansive soil mix. Pressure plate apparatus was used to measure the suction in the range of 5 to 1000 kPa. The study found that four indexes, saturated gravity water content, air entry value, residual water content and curve slope, can be used to evaluate the chemical improvement effects on expansive soil.

Zielinski et al. (2011) compared four different methods of determining WRCC for compacted boulder clay. The measurement of soil suction was carried out using i) Indirect method, ii) Deterministic method and iii) Direct method. Indirect method includes the direct contact filter paper method and chilled mirror dew point potentiameter technique. The deterministic method includes the Mercury Intrusion Porosimetery (MIP). The direct measurement was carried out on a macro scale embankment model desiccated under fully controlled environment in the laboratory. Suction was measured using tensiometer and the water content by a time domain reflectometry (TDR) moisture content probe. It was observed that the WRCC obtained using all the four methods matched well.

Agus et al. (2010) studied the suction characteristics of bentonite-sand mixtures containing different proportions of bentonite. Pure bentonite and three different mixtures namely 30:70, 50:50 and 70:30 bentonite-sand were used in the study. It was found that the total suction of bentonite-sand mixtures is primarily a function of water content and bentonite content. The higher percentage of bentonite in the mixture, higher the total suction for the same water content. Again, the effect of compaction conditions were investigated by conducting suction measurement on loose, standard Proctor and enhanced Proctor compaction state. It was found that there were no effects of compaction conditions on the suction of all the mixes.

Gallage and Uchimara (2010) studied the effect of dry density and grain size distribution of the WRCC of sandy soils. A Tempe pressure cell apparatus was used to measure the suction of the soils. The Fredlund and Xing 1994 WRCC model parameters a, n and m were correlated with the basic soil properties. It was found that the a parameter increases with the increase in air entry value, m parameter decreases with the increase in residual suction and n parameter related to the slope of the WRCC curve. Again, the air entry value and residual suction increased with the increase in dry density of the soil. A coarse grained soil had a lower air entry value and residual suction than a fine grained soil. Again, it was found that steeper the slope of the grain size distribution curve, steeper was the slope of the WRCC.

Lee et al. (2010) studied the suction characteristics of unsaturated compacted bentonite. The suction measurement was carried out using an indirect technique by using a humidity sensor which measures the relative humidity and temperature of the compacted bentonite. The total suction was then determined using the Kelvin's equation. From the study, it was found that the suction of the compacted bentonite decreased with increasing water content at a given dry density, and the suction became more for a particular water content when the dry density was more. The effect of temperature on the suction was found to be negligible for water content up to 17%.

Pan et al. (2010) presented a review of different direct and indirect suction measurement techniques and their basic principles of measurement and application. Direct measurement includes axis translation technique, tensiometer and suction probe. Indirect methods were presented in three different sections under matric suction, osmotic suction and total suction measurement methods. It was reported that the matric suction gives correct result if appropriate calibration curve is available. They found squeezing technique as the best for measuring osmotic suction. Total suction below 100 kPa was difficult to obtain from the current techniques as reported in the study.

Young and Qing (2009) studied the WRCC of bentonite sand mixture by measuring suction using a pressure plate apparatus. The study compared the WRCC for different dry density, different time of wetting drying cycle and different proportion of mixes. It was found that bentonite-sand mixtures having different initial dry density, the logarithm of air-entry value increases linearly as dry density increases. In case of bentonite-sand mixtures having different proportions, the air-entry value was influenced by relative filling ratio of pores. Greater bentonite content leads to greater relative filling ratio of pores, which needs a greater air entry value.

Nam et al. (2009) obtained WRCC of a river bank soil using six different methodologies. These were filter paper, dew point potentiameter, vapour equilibrium, pressure plate, tempe cell and osmotic methods. The WRCC's was obtained for different range of suction values using the above techniques and also by combining the above results. From this study, it was recommended that separate technique should be employed for determining the total and matric suction. The dew point potentiameter was recommended for determining the total suction. Again, axis translation technique or osmotic technique was recommended for the matric suction measurement. The fitting parameters for various WRCC models were obtained in this study and compared.

Birle et al. (2008) studied the effect of compaction condition i.e. initial water content and dry density on the WRCC and shrinkage characteristics curve of clay soil. Suction was measured using the chilled mirror dew point technique while the volume change during shrinkage was measured using a vernier caliper. It was found that WRCC and shrinkage curve are independent of the initial compaction condition of the sample. It was also reported that at higher compaction water content the WRCC curves are not same.

Delage et al. (2008) presented a review of different techniques for controlling and measurement of suction. The study discussed axis translation method, osmotic method, high suction tensiometer and high capacity psychrometer. The review presented a detailed discussion on the advantages and disadvantages of these instruments for characterizing unsaturated soil.

Sreedeep and Singh (2008) investigated the influence of suction measurement techniques on the WRCC of three fine grained soils, which include a locally available silty soil, a clayey soil and commercially available white clay. Three types of measuring techniques namely insertion tensiometer (IT), a pressure membrane extractor (PME) and a dew point potentiameter (WP4) were used to measure the suction. The influence of salt was also investigated in this study. The study revealed that the WRCC obtained by using different methodologies did not match each other. It was found that the suction values measured by using WP4 get significantly influenced by the presence of salt in the soil.

Patric et al. (2007) compared the suction measurement data of chilled mirror WP4 technique and filter paper technique and presented a detailed investigation on the various errors which affect the measured suction results. The study came with an observation that errors due to the incomplete equilibration of the sample in the sealed block chamber of

the WP4 device and errors due to the measurement of the water content in the filter paper method affects WRCC.

Zhan et al. (2007) studied the soil-water interaction of natural and compacted expansive soil by obtaining the soil-water characteristics curve using pressure plate apparatus. From the WRCC obtained from natural and compacted specimen, it was found that there was a distinct difference between the WRCC's for suction less than 200 kPa, but both the drying WRCC's tend to merge at suction above 200 kPa. The air entry value of the natural expansive soil was found to be quite low due to cracks and fissures present as compared to the compacted specimen (i.e. 25 kPa).

Puppala et al. (2006) studied the WRCC of two expansive soils under natural and stabilized condition using pressure plate extractor. The stabilizers used were coal ashes which include fly ash and bottom ash, and combined ash and fibers. The fly ash and bottom ash content were varied from 0, 10, 15 and 20%. From this study, it was found that volumetric water content of class F fly ash treated soils get decreased with the increase in percentage of fly ash. This was mainly due to modification of the particle size and cementing effects of the fly ash. The fine particles of fly ash occupied the voids in the expansive soil, and also bond the finer clay particles at contact points. However, there were only very small changes in the WRCC of bottom ash treated soil. The AEV of the stabilized soil with higher percentage of fines was larger than those with no fines. However, the AEV of the bottom ash treated soil get decreased due to the small increase in coarse particle sizes.

Shah et al. (2006) presented the use of two different technique for measuring suction and obtain WRCC of four different types of soils. The study used pressure membrane extractor (PME) and WP4 dew point potentiameter technique for measuring suction. It was reported that WRCC models fitted to the PME data differs each other quite appreciably while the WRCC models fitted to the combined data of PME and WP4 merges well above 10^5 kPa.

Sreedeep and Singh (2006) investigated the determination of osmotic suction by utilizing the results of two devices namely pressure membrane extractor (PME) and WP4 dew point potentiameter. The PME was used for measuring matric suction and WP4 was used to obtain the total suction. The study indicated that the osmotic suction depends strongly on the water content of the soil. Therefore, the osmotic suction of the soil at lower water content might be quite different from that obtained using the pore solution

extraction method. The study also indicated the influence of osmotic suction on the unsaturated soil property.

Thakur et al. (2006) used WP4 dew point potentiameter for measuring high suction range of two fine grained soils and clay. The efficiency of WRCC fitting functions FX and BC for the fine grained soil had been evaluated. From this study, it was found that the above fitting functions are suitable for extremely high suction range of fine grained soil, whereas van Genuchten model is valid only for suction < 20 MPa. It was found that the dry unit weight did not have any effect on suction of the fine grained soil.

Agus et al. (2005) studied the water retention behavior of polymer enhanced bentonite-sand mixture using two techniques: namely axis translation technique (in pressure plate apparatus) and vapour equilibrium technique (in desiccators with salt solution). The results obtained using both the methods were combined to obtain a single WRCC for each specimen. It was found that there was no significant effect of compaction conditions on the WRCC. The air entry value of the material was found to be about 10 kPa, whereas the residual suction was around 40,000 kPa.

Agus and Schanz (2005) compared four different method of suction measurement on bentonite-sand mixtures using non-contact filter paper technique, psychrometer technique, relative humidity sensor (RH) and chilled mirror hygrometer techniques. It was found that chilled mirror hygrometer technique is the best technique for measuring total suction and can be used for assessing the accuracy of the other three techniques.

Sreedeep and Singh (2005) studied the influence of initial water content and dry unit weight on suction of two types of soils: sand and clay. Insertion tensiometer (IT) was used for the suction measurement. It was found that suction decreases with the increase in water content of the sample while the suction remains constant with the change in dry density.

Yang et al. (2004) studied the drying and wetting WRCC of four different types of sandy soil with finer to coarser fractions. They determined the WRCC by using tempe pressure cell and capillary rise tube and compared the behavior with that of the estimated WRCC from the grain size distribution curve. It was found that the shape of the WRCC determined from the soil parameters have consistent relationships with the grain size distribution plot. It was found that coarse grained soil possesses a lower air entry value, lower water entry value and lower residual suction than a fine grained soil. Again, soil with larger porosity had a higher air entry value than soil with low porosity.

Leong et al. (2003) used chilled mirror dew point technique to measure the total suction of two types of soils of Singapore. Soil samples for the suction measurement were prepared for different compaction water content. Three types of compaction effort namely standard, enhanced and modified were used for measuring the suction. The total suction obtained from the dew point technique was compared with the sum of the matric and osmotic suction obtained using null type axis translation and pore fluid squeezer technique. The study indicated that the total suction measured using the dew point technique gives consistently higher value than sum of the matric and osmotic suction measured individually. The discrepancy was found to increase with increase in total suction. The error in the total suction was found to be less than 150 kPa for the range of suction tested in this study.

Likos and Lu (2003) described an automated humidity system for measuring total suction of soils. They used this technique for measuring total suction of four different types of clay soils starting from highly expansive clay to non expansive kaolinite mineral soils. They compared the results with non-contact filter paper technique and found to be comparable. Slight discrepancies found were due to the powdered and aggregate sample in the two techniques.

Ridley et al. (2003) presented three instruments for matric suction measurement with its principle of measurement, procedure for use and interpretation of results. The methods included filter paper method, Imperial college suction probe, and field tensiometer with capacity up to 90 kPa. The paper highlighted the soil suction in natural ground, soil suction in fill and compacted ground, and soil suction in samples recovered from the ground.

Miao et al. (2002) studied the wetting-drying cycle tests of WRCC of an expansive soil using pressure plate apparatus. It was found that the hysteresis potential was reduced as the number of wetting-drying cycle's increases. The influence of stress state on the WRCC was investigated. The hysteresis loops between the drying and wetting curve for preloaded expansive soil specimen were more stable, and the influence of number of wetting and drying cycles were smaller. From the study, it was clear that the WRCC of the preloaded specimen could reflect the soil property function of expansive soil.

Miller et al. (2002) studied the effect of compaction conditions on the WRCC of four types of soils using a pressure membrane apparatus. It was found that with the increase in compactive energy, the WRCC curve shifts upwards. However there was no

significant difference between the WRCC behavior of field compacted and laboratory compacted specimens.

Tinjum et al. (1997) determined WRCC of four clay soils at different compaction water contents (dry, wet and optimum) and compactive effort (standard and modified). They used pressure plate apparatus to measure the suction. It was found from their study that SWCC's are affected by the compaction condition. Higher the compaction water content and compactive effort higher was the air entry value. Also with the increase in plasticity index of the soil, the air entry value increases. They also reported that changes in the WRCC for different compaction condition and plasticity index also affects the vG and BC model fitting parameters.

2.4 Contaminant retention characteristics of fly ash and bentonite

The usefulness of fly ash and bentonite as a low cost adsorbent has been studied by researchers all over the world. Fly ash has been extensively used for the removal of heavy metals from wastewater due to its physical and chemical properties. Moreover, the alkaline nature of fly ash makes it a good neutralizing agent. Few of the major studies found in the literature are discussed below.

Visa et al. (2010) studied the removal of heavy metals from aqueous solution using fly ash collected from Romania and modified with NaOH-2N. The heavy metals used for this study were Cd^{2+}, Cu^{2+} and Ni^{2+}. Batch adsorption study was conducted to see the adsorption property of the fly ash. The effect of contact time was found to be around 30 min or less to complete the adsorption process for the single metal ion solution. The second order kinetic study was done and the experimental results were fitted with the Langmuir isotherm model. The adsorption efficiency of Cu^{2+} was found to be more than the other metals used in this study.

Hsu et al. (2008) used raw fly ash and modified fly ash for the adsorption of Cu^{2+} from waste water. The effect of pH, adsorbent dose and effect of temperature was carried out in this study. The fly ash was found to remove Cu^{2+} from the waste water effectively. The raw fly ash was found to be more effective in removing Cu^{2+} from the waste water than the modified fly ash.

Alinnor et al. (2007) studied the adsorption of Pb^{2+} and Cu^{2+} from aqueous solution by fly ash collected from Nigeria Coal Corporation, Enugu. Batch adsorption study was carried out to see the adsorption of the metals. The effect of contact time, pH

and temperature on the removal of these metals had been investigated in this study. Lead and copper were adsorbed onto the fly ash very rapidly within 20 min, and the equilibrium was achieved within 2 hrs. The retention of the metals was increased with an increase in pH. There was a decrease in uptake of the metals with the increase in temperature.

Papandreou et al. (2007) studied the adsorption of Cu^{2+} and Cd^{2+} from aqueous solution on pellets made from class C fly ash, collected from the Megalopolis power plant in southern Greece. Here, the fly ash was shaped into pellets, having diameter 3-8 mm, high relative porosity and very good mechanical strength. The effect of agitation rate, equilibrium time, pH of solution and initial metal concentration were investigated in this study. The adsorption of both the metals was found to increase with an increase in pH with 100% sorption at pH above 9. The adsorption capacity of pellets was found to increase with an increase in initial metal concentration. Again, the adsorption of Cu^{2+} by the pellets was found to be higher than the Cd^{2+}. This study indicated that the pellets could be used for adsorption of Cu (20.92 mg/g) and Cd (18.98 mg/g), and could be used for their removal from aqueous solution at ambient temperature.

Pehlivan et al. (2006) studied the effectiveness of fly ash on the removal of Cu^{2+} and Zn^{2+} from aqueous solution using the batch sorption studies. The fly ash was obtained from a sugar industry, produced from burning of young brown coal. Batch kinetics and isotherm studies were conducted to determine the adsorption capacity of the sorbents in this study. The affect of contact time, pH, sorbent dose, and initial concentration of adsorbate on the adsorption were studied. The adsorption of the metals was found to increase with the increase in contact time and it had reached equilibrium within 60 min. The adsorption of metals by the fly ash was found to decrease with the decrease in pH of the initial solution. Maximum sorption of both the metals was found to be between pH 5 and 4 for the fly ash. The adsorption of both the metals was found to increase with the increase in adsorbent dosage and the increase in initial concentration of the metal ions. The adsorption data were found to fit very well with the Langmuir and Freundlich models.

Cho et al. (2005) studied the adsorption of heavy metals (zinc, lead, cadmium and copper) from aqueous solution using fly ash as a low cost adsorbent. The fly ash used in this study was collected from a bituminous coal-burning power plant of Korea Electric Power Corporation, Boryung, Korea and was categorized as class F fly ash. The adsorption characteristic of the fly ash was studied under different pH, heavy metal

concentrations and fly ash dosages using both isotherm and kinetic studies. In the study, the heavy metals were found to adsorb very rapidly (within the first 20 min). The equilibrium time for the zinc was found as 2 hr, while for other metals apart from zinc, it was 3 hr. The precipitation of the metals on the fly ash was found to be higher for high pH. The adsorption data fitted well to the Freundlich isotherm

Weng and Huang (2004) studied the adsorption of Zn^{2+} ions from aqueous solution by using fly ash. The fly ash used in this study was collected from the Delmarva Power plant in Wilmington, DE. Batch adsorption experiment was conducted to study the sorption of Zn^{2+} by the fly ash. The study indicated that the amount of Zn^{2+} ions adsorbed gets increased with the increase in fly ash content and pH of solution. The adsorption of Zn^{2+} was found to increase with the decrease in ionic strength for a particular value of pH of the solution. The Langmuir adsorption isotherm model was used to study the adsorption of the Zn^{2+} ion on the fly ash.

Rio and Delebarre (2003) studied the removal of mercury from aqueous solution using two different types of fly ash produced by two circulating fluidized bed plants located in the Northeast and Southeast of France. The kinetic studies of the two types of fly ash indicated that equilibrium adsorption had reached within 72 hrs for both the fly ashes. The rate of adsorption was faster and the steady state removal was higher for the sulfo-calcic fly ashes than for silico-aluminous fly ashes for any value of pH of the aqueous solution. The adsorption capacity for the sulfo-calcic fly ash was found to be 5.0 mg/g, whereas for sillico-aluminous fly ash, the adsorption capacity was found to be 3.2 mg/g.

Rao et al. (2002) investigated the removal of Cr^{6+} and Ni^{2+} from aqueous solution using raw bagase fly ash from sugar mill and coal fly ash from thermal power plant. The affect of hydrogen ion concentration, contact time, sorbent dose, initial concentrations of adsorbate and adsorbent and particle size on the uptake of Cr^{6+} and Ni^{2+} was investigated in this study using batch experiment. The optimum pH for removal of Cr^{6+} and Ni^{2+} by the fly ash was found to be 6 and 8 respectively. The effect of contact time on the rate of uptake of Cr^{6+} and Ni^{2+} was found to be rapid, having maximum adsorption within the first one hour of contact time. This is due to the large number of surface site available for adsorption in the initial time. After that the adsorption was very slow and the saturation was attained within 1.5 to 2 hr for both the metals. Again, the rate of uptake of Cr^{6+} and Ni^{2+} was found to increase with the increase in adsorbent dose. The adsorption efficiency of both the bagase fly ash and thermal power plant fly ash was found to decrease with the

increase in initial concentration of the metals. The uptake of the metals was found to increase with the decrease in particle size due to greater surface area.

Lin and Chang (2001) studied the effect of fly ash on the removal of Cu^{2+} from aqueous solution. The fly ash used in this study was obtained from the China Steel Corporation (Kaohsiung, Taiwan). The study investigated the effect of carbon fraction of fly ash on the removal of Cu^{2+}. The fly ash containing different carbon fractions were prepared by thermal decarbonation in the laboratory. The equilibrium concentration of Cu^{2+} was found to decrease with increasing adsorbent dosage and carbon fraction.

Piekos and Paslawska (1999) studied the characteristics of fly ash in retention of fluoride. Experiments were conducted on various concentrations of fluoride ions to see the uptake of fluoride ions by the fly ash. It was found that the retention of fluoride ions by the fly ash is initially low up to about 24 hrs but it gradually increased leading to almost complete retention at 120-144 hrs. The study showed a double mechanism in the retention of fluoride ions by fly ash, one was chemical binding by calcium hydroxide and the other was physical sorption by residual carbon particles.

Ayala et al. (1998) investigated the adsorption of Cd and Cu by fly ash. The effect of initial metal concentrations, pH, contact time, grain size and ionic strength were investigated in this study. The retention of the metals by the fly ash gets decreased as the pH of the initial solution decreased. The presence of high ionic strength or appreciable quantities of calcium and chloride did not have a significant effect on the removal of cadmium and copper by fly ash. The removal of metals increased as the grain size decreases.

Gupta and Torres (1998) studied the removal of heavy metals like Cu, Pb and Zn from waste water effluent using fly ash collected from Indian River Power Plant, Millsoboro, DE. The treatment of the effluent with the fly ash had significantly reduced the amounts of the heavy metals.

Nhan et al. (1996) studied the hydraulic and contaminants barrier properties of coal fly ash by using synthetic MSW leachate. The ability of the barrier material to attenuate metal ion contaminants was investigated in this study. The study indicated that the hydraulic conductivity of the barrier remains constant at the beginning and then showed a long term linear increase with the leachate volume. The metals carried by the leachate were reduced due to precipitation in the barrier material. The contaminant metals were precipitated in the barrier as either hydroxide or carbonate depending upon the solubility constants of the two solid species.

Pandian et al. (1996) conducted laboratory experiments to study the effectiveness of fly ash for retention of heavy metals. The effects of fly ash types and pH on the retention of heavy metals were investigated in this study. The study indicated that fly ash contains lead ions through the formation of lead hydroxide which gets precipitated in the pore volumes and at the surface of fly ash. It also retained lead ions by adsorption on to the surface sites of silica, alumina and iron oxide. Again, the retention of lead ions by fly ash increased with the increase in initial pH of the solution. It was found from this study that fly ash containing high amount of calcium retains more lead ions than low calcium fly ash. The fly ash was found to retain lead ions permanently when the leachate pH was between 3.5 and 10. Fly ash however released lead ions at very low and very high pH.

2.5 Summary and critical appraisal of literature review

The reviewed literature indicates that there are not many studies exploring the utility of fly ash in waste management projects. It was noted that hydraulic properties such as hydraulic conductivity, water retention characteristics and contaminant interaction characteristics are invariably necessary for establishing the utility of a geomaterial for hydraulic barriers used in waste management. These characterization studies were quite sparse for wide range of geomaterials especially for fly ash, bentonite and its mixes. This was specifically true for Indian fly ashes. There are no discussions on the measurable range of suction for fly ashes. The effect of spatial variability and content of fly ash on WRCC of fly ash-bentonite mix is missing in the literature. Such efforts are needed to understand the possibility of generalizing the WRCC of fly ashes.

Not many studies have investigated the usefulness of shrinkage characteristics for defining the WRCC of high plastic, high volume change soil. WRCC model parameters are an important input for modeling the behavior of unsaturated geomaterials. The influence of WRCC parameter variability on unsaturated behavior modeling needs further investigation. Another important geoenvironmental characteristic is the contaminant retention property of fly ash, which plays a major role in the retention of heavy metals when used in waste containment liners. Reviewed literature showed that heavy metals like Pb^{2+}, Cu^{2+}, Cd^{2+}, Hg^{+}, Ni^{2+}, Zn^{2+} etc. can be successfully removed from the waste water using fly ash. This makes fly ash an excellent material in combination with low permeable soil (bentonite) for waste containment liner construction. However, there were not many studies that reports contaminant retention characteristics of fly ash-bentonite

mixes. The influence of different sources of fly ashes on contaminant retention property also needs to be understood in detail.

2.6 Scope of the present research work

The critical appraisal of the reviewed literature shows that water and contaminant retention characteristics were not investigated in detail for fly ashes and its mixes with expansive soil like bentonite. Such characterizations are required for its utility in projects related to waste containment and agriculture. With this in view, the main objective of this research work was to study the water retention and contaminant retention behavior of different fly ashes and its combination with expansive soil such as bentonite. Following are the different scope of this study to achieve the objective:

1. Measurement of water retention characteristic curve (WRCC) of fly ashes using instruments of various suction ranges to identify the measurable range of suction in fly ashes.
2. To study the influence of fly ash type and fly ash content on the WRCC of fly ash-bentonite mixes.
3. To investigate the WRCC of different qualities of bentonite obtained from various sources and also to study the effect of volume change characteristics on WRCC parameterization.
4. To study the sensitivity of variations in WRCC parameters of fly ash, bentonites and fly ash-bentonite mixes on unsaturated seepage modeling.
5. To study the contaminant retention characteristics of fly ashes, bentonite and selected fly ash-bentonite mixes by considering lead ion (Pb^{2+}) as the model contaminant.

Chapter 3

Experimental Investigation

3.1 General

The experimental investigations carried out for fulfilling the objective of this research work has been discussed in detail in this chapter. It includes the evaluation of various properties of fly ashes and bentonites used in this study and the discussion on methodology adopted.

3.2 Materials used

Non-plastic cohesionless material and high plastic cohesive material were used in this study with an objective of exploring its utility as hydraulic and contaminant barrier. Cohesionless material includes four fly ashes collected from different thermal power plants in India and cohesive materials were four commercially available bentonite. The details of these materials with their source and designation are given in Table 3.1.

Table 3.1 Details of geomaterials used in this study

Sl. No.	Material used	Designation	Source/Remarks
1	Farakka fly ash	FFA	NTPC Farakka, West Bengal
2	Badarpur fly ash	BFA	NTPC Badarpur, New Delhi
3	Neyvelli fly ash	NFA	Neyvelli Lignite Corporation, Tamilnadu
4	Pond ash	PA	NTPC Singrauli, Uttar Pradesh
5	Bentonite 1	B1	Commercially available
6	Bentonite 2	B2	
7	Bentonite 3	B3	
8	Bentonite 4	B4	

NTPC: National Thermal Power Corporation

3.3 Material properties

The geomaterials listed in Table 3.1 were characterized for specific gravity (G_s) using kerosene instead of water (ASTM D854-06), grain size distribution (ASTM D422-63), Atterberg's limit which include liquid limit (LL), plastic limit (PL) and shrinkage limit (SL) (ASTM D4318-05), free swell index (FSI) (IS 2720: Part XL), Proctor compaction characteristics, which include maximum dry unit weight (γ_{dmax}) and optimum moisture content (OMC) (ASTM D698-07), and total specific surface area (SSA) by Ethylene Glycol Monoethyl Ether (EGME) method (Cerato and Lutenegger 2002).

The G_s of materials was determined with the help of small density bottles. Kerosene was used instead of water to nullify the reactivity of the geomaterials with water. The average specific gravity was obtained from minimum of five repeatable test results. The grain size distribution plot of fly ashes and bentonites are shown in Figure 3.1. A steep rise in grain size distribution plot was observed in case of bentonites. This is an inherent problem associated with expansive soil when wet sieve analysis is mixed with hydrometer analysis. This is mainly due to the reactivity of bentonite with water. The determination of Atterberg's limit for fly ashes was not required due to its non-plastic nature. These physical properties were listed in Tables 3.2 and 3.3 for fly ashes and bentonites, respectively. According to USCS classification of soils (ASTM D2487-06), all bentonites belong to CH group.

The chemical oxide composition of fly ashes and bentonites were determined using X-ray Fluorescence (XRF) test (AXIOS, PANalytical, Netherlands) and the results were presented in Tables 3.4 and 3.5. The classification of fly ashes was made based on the oxide composition (SiO_2+ Al_2O_3+ Fe_2O_3) as recommended by ASTM C618-05. The fly ashes FFA, BFA and PA belongs to F type and NFA is C type. The cation exchange capacity was determined by following the guideline presented in IS 2720 (part XXIV 1976). It is defined as the amount of exchangeable cations (Na^+, K^+, Ca^{2+} and Fe^{3+}) that a soil can accommodate. The detail of the methodology for determining CEC as given in IS code of practice is explained below. In the IS method, the sample was first treated with hydrogen peroxide, laboratory reagent grade, (20 volume, 6% w/v H_2O_2) and was boiled thoroughly for 1 hr to remove organic contents. The treated sample was oven-dried and 5 g of it was mixed with 50 ml 1 N Sodium acetate (CH_3COONa) solution with pH= 5. This mixture was digested in a boiling water bath for 30 min., with intermittent stirring, and was later centrifuged at a speed of 5000 to 6000 rpm, for 15 min. The supernatant liquid was discarded and the sample, settled at the bottom of the centrifuge tube was again treated with 50 ml of 1 N CH_3COONa solution (pH=5) and centrifuged. This process was repeated thrice, so as to ensure exchange of all ions in the sample by Na^+. This sample was treated with 1 N Calcium chloride ($CaCl_2$) solution and was again digested and centrifuged as discussed above. This process was repeated thrice, so as to ensure exchange of Na^+ by Ca^{2+}. This sample was treated again with 50 ml 1 N CH_3COONa solution (pH= 7), and was again digested and centrifuged. This operation was performed thrice. The resulting supernatant from the last three steps was collected in a 250 ml volumetric flask, and the concentration of Ca^{2+} present in the solution was

determined using the Flame photometer. The loss on ignition (LOI) of the geomaterials was determined by burning at 500 ^{0}C in muffle furnace. The mineralogical properties of the materials were determined by conducting X-ray diffraction (XRD) test (Model: Brucker AXS D8 model, Canada). The pattern obtained for the fly ashes and bentonites are shown in Figures 3.2(a) and 3.2(b), respectively. The results were used for qualitative identification of the type of minerals present in these materials. It was found that majority of minerals present in fly ash were quartz, calcium oxide (CaO) and magnesium oxide (MgO). The minerals present in bentonite include quartz, aluminium oxide (AlO), montmorillonite, and kaolinite.

The saturated hydraulic conductivity (k_{sat}) of the fly ashes and bentonites was determined by falling head method (IS 2720 part (XVII) 1986) and the results were presented in Table 3.6. A specially designed small sample thickness (10 mm to 15 mm) falling head apparatus (Jibeesh 2013) were used in this study to facilitate quick saturation of bentonite. The advantage of this new setup is that the saturation time of the sample becomes very less due its minimal thickness and the hydraulic conductivity can be measured under no swell condition. The schematic diagram of the new setup is shown below in Figure 3.3. An additional advantage of this new setup is that there is provision of applying vacuum to remove any entrapped air present which facilitates quick saturation. More than 15 days was required for saturation of pure bentonite sample, while for mixes depending on the bentonite content, 7 to 10 days was sufficient for complete saturation.

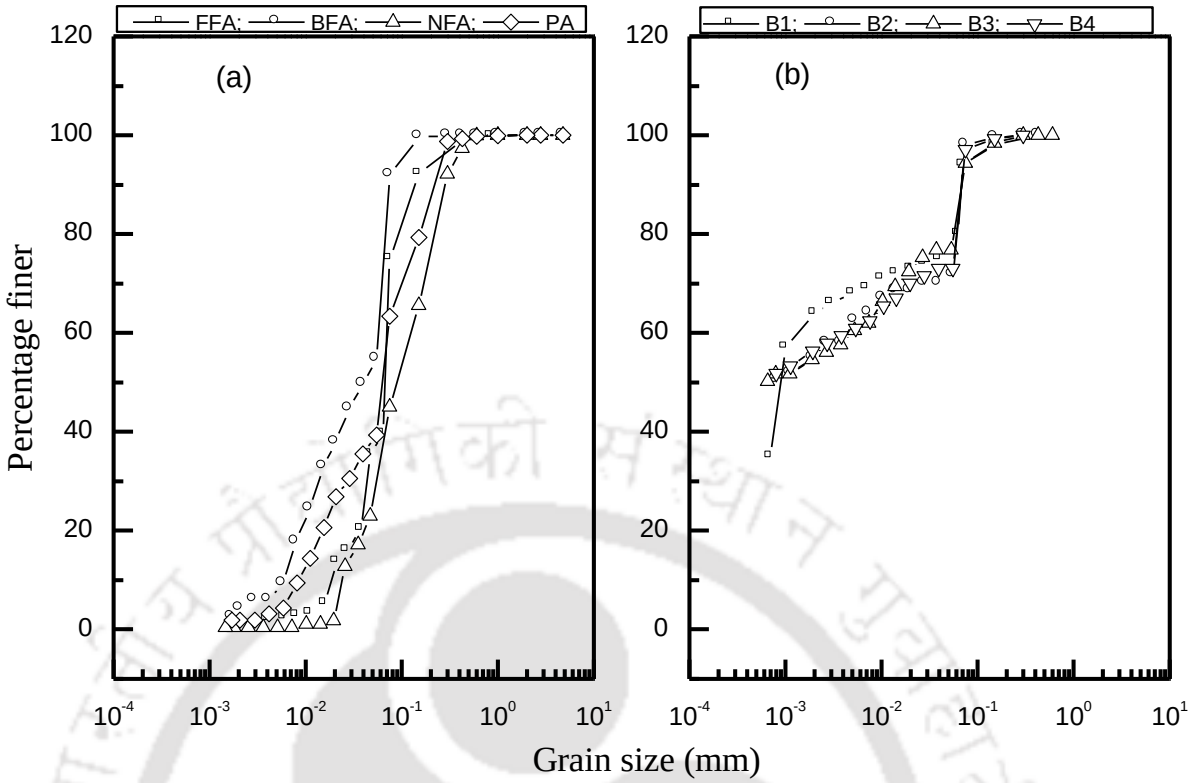

Figure 3.1 Grain size distributions of (a) Fly ashes and (b) Bentonites

Table 3.2 Physical properties of fly ash

Material properties	**Fly ash**			
	FFA	**BFA**	**NFA**	**PA**
Specific gravity, G_s	2.02	1.97	2.46	1.84
Grain size distribution (%)				
Coarse sand (4.75-2mm)	0	0	0	0
Medium sand (2-0.425mm)	0	0	3	0
Fine sand (0.425-0.075mm)	24	8	55	36
Silt size (0.075-0.002mm)	74	88	42	61
Clay size (<0.002mm)	2	4	0	3
Total SSA (m^2/g)- EGME method	12.59	11.54	13.24	10.45
Cation exchange capacity, CEC (meq./100 g)	1.85	1.44	9.04	0.99
Maximum dry unit weight, $\gamma_{d\,max}$ (kN/m^3)	13.8	12.0	15.3	12.1
Optimum moisture content, OMC (%)	20.29	32.0	21.0	19.0

Table 3.3 Physical properties of bentonite

Material properties	Bentonite			
	B1	**B2**	**B3**	**B4**
Specific gravity, G_s	2.71	2.8	2.71	2.76
Grain size distribution (%)				
Coarse sand (4.75-2mm)	0	0	0	0
Medium sand (2-0.425mm)	0	0	0	0
Fine sand (0.425-0.075mm)	5	2	1	3
Silt size (0.075-0.002mm)	31	43	48	41
Clay size (<0.002mm)	64	55	51	56
Atterberg's limits (%)				
Liquid limit, LL (%)	300	310	433	244
Plastic limit, PL (%)	53	48	55	62
Shrinkage limit, SL (%)	14	16	18	16
Plasticity index, PI (%)	247	262	378	182
USCS classification	CH	CH	CH	CH
Free swell index, FSI (%)	980	1433	1700	1600
Total SSA (m^2/g)- EGME method	260	244	428	215
Cation exchange capacity, CEC (meq./100 g)	20.45	15.66	38.18	23.41
Maximum dry unit weight, $\gamma_{d\ max}$ (kN/m^3)	12.4	13.9	13.6	11.5
Optimum moisture content, OMC (%)	37.5	28.89	33.16	49.24

Table 3.4 Chemical composition (% weight) of fly ash

Oxide	Fly ash			
	FFA	**BFA**	**NFA**	**PA**
SiO_2	46.47	67.8	30.1	52.2
Al_2O_3	27.49	12.5	28.8	30.5
Fe_2O_3	1.06	3.8	2.4	2.6
MnO	2.93	1.2	0.04	0.06
MgO	0.06	2.5	2.24	0.08
CaO	2.84	3.9	18.73	1.2
Na_2O	0.56	1.3	0.50	0.12
K_2O	0.84	1.8	0.04	0.13
TiO_2	6.58	0.7	1.75	3.8
P_2O_5	5.20	0.8	0.02	0.12
SiO_2+ Al_2O_3+ Fe_2O_3	75.02	84.1	61.3	85.3
Loss on ignition, LOI (%)	6.17	4.7	5.07	6.60
Classification **(**ASTM C618-05**)**	F	F	C	F

Table 3.5 Chemical composition (% weight) of bentonite

Oxide	Bentonite			
	B1	**B2**	**B3**	**B4**
SiO_2	51.68	57.04	57.51	58.54
Al_2O_3	17.07	13.45	13.07	14.56
Fe_2O_3	2.03	6.90	9.02	9.54
MnO	0.05	0.076	0.098	0.121
MgO	1.95	0.12	0.14	0.12
CaO	0.52	0.51	1.12	0.61
Na_2O	2.36	2.21	2.23	2.20
K_2O	0.60	0.58	0.22	0.69
TiO_2	1.94	1.52	1.67	2.26
P_2O_5	0.05	0.01	0.035	0.034
SiO_2+ Al_2O_3+ Fe_2O_3	70.78	77.39	79.6	82.64
Loss on ignition, LOI (%)	22.69	20.4	18.5	21.6

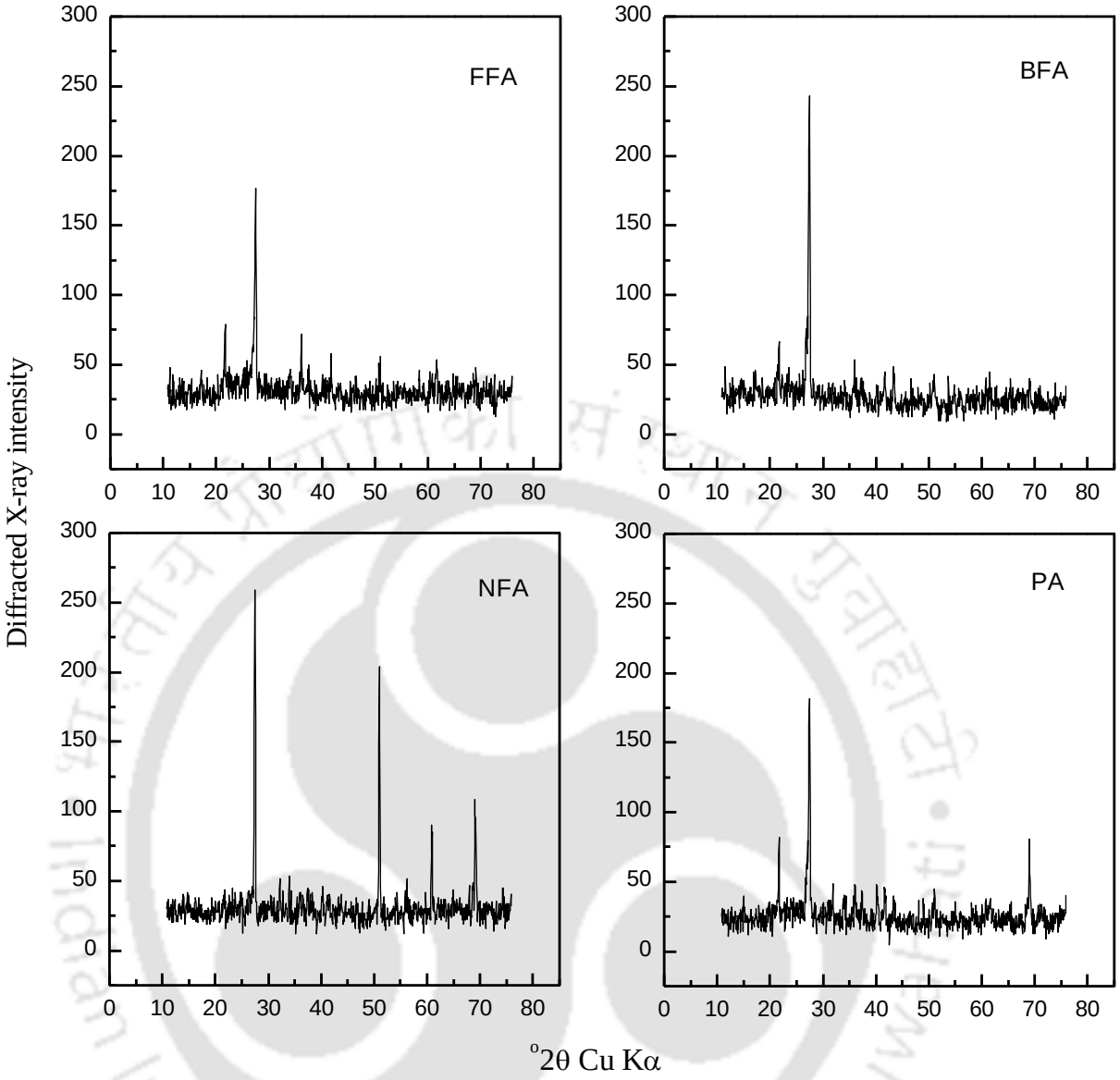

Figure 3.2(a) XRD pattern of fly ashes

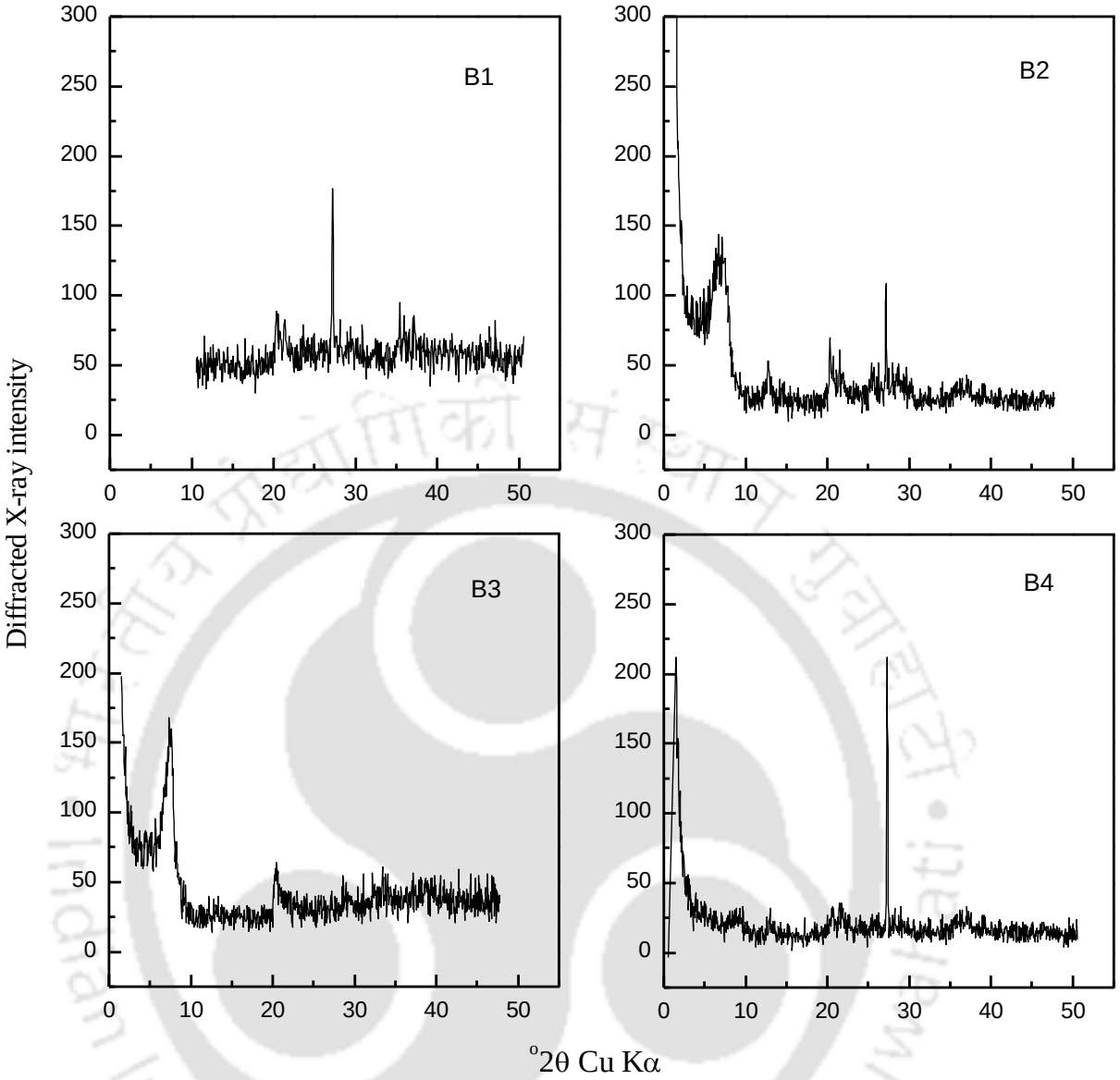

Figure 3.2(b) XRD pattern of bentonites

Table 3.6 Saturated permeability, (k_{sat} m/s) of fly ash and bentonite

Fly ash/ bentonite	***k*sat (m/s)**
FFA	3.22×10^{-7}
BFA	3.72×10^{-7}
NFA	3.19×10^{-7}
PA	3.48×10^{-7}
B1	6.43×10^{-12}
B2	7.0×10^{-12}
B3	3.0×10^{-12}
B4	4.0×10^{-12}

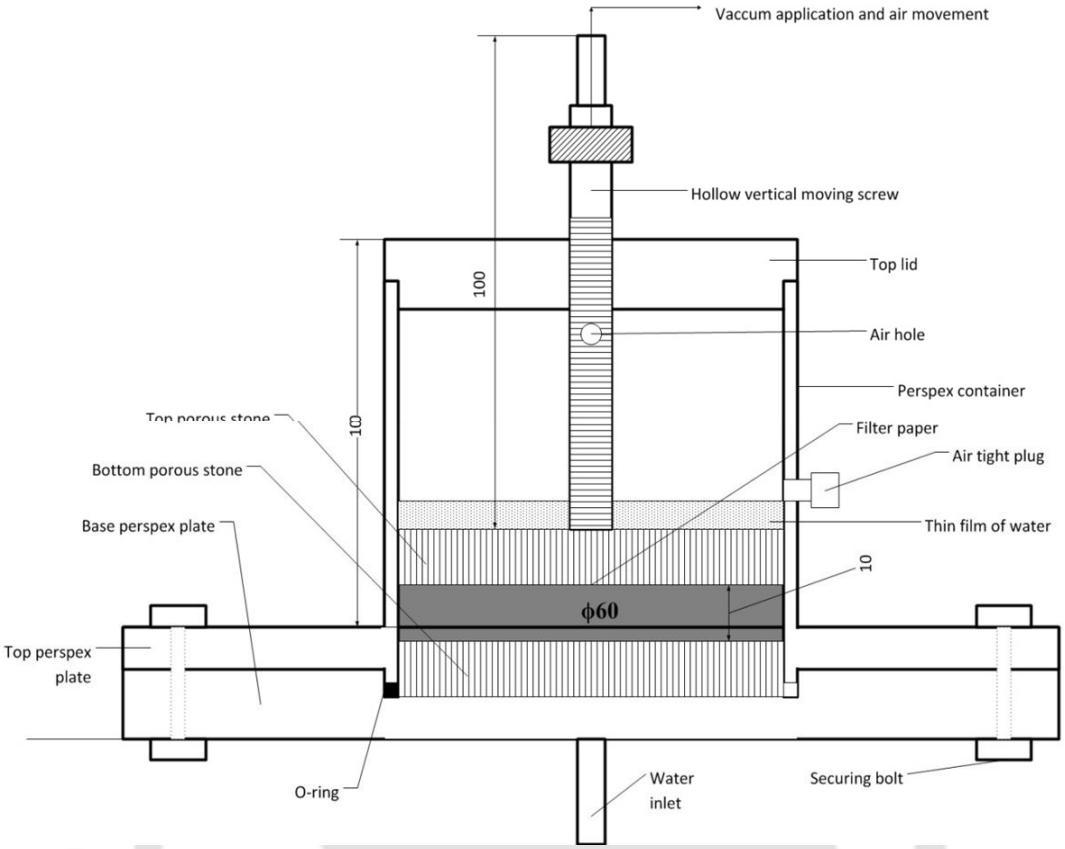

All dimensions are in mm.

Figure not drawn to scale.

Figure 3.3 Schematic diagram of new permeability apparatus (Jibeesh 2013)

The morphological property of the fly ashes and bentonites was studied by conducting Field Emission Scanning Electron Microscope (FESEM) (Maker: Zeiss; model: Sigma) test. The images obtained were shown in Figures 3.4(a) to 3.4(d) for fly ashes and in Figures 3.5(a) to 3.5(d) for bentonites.

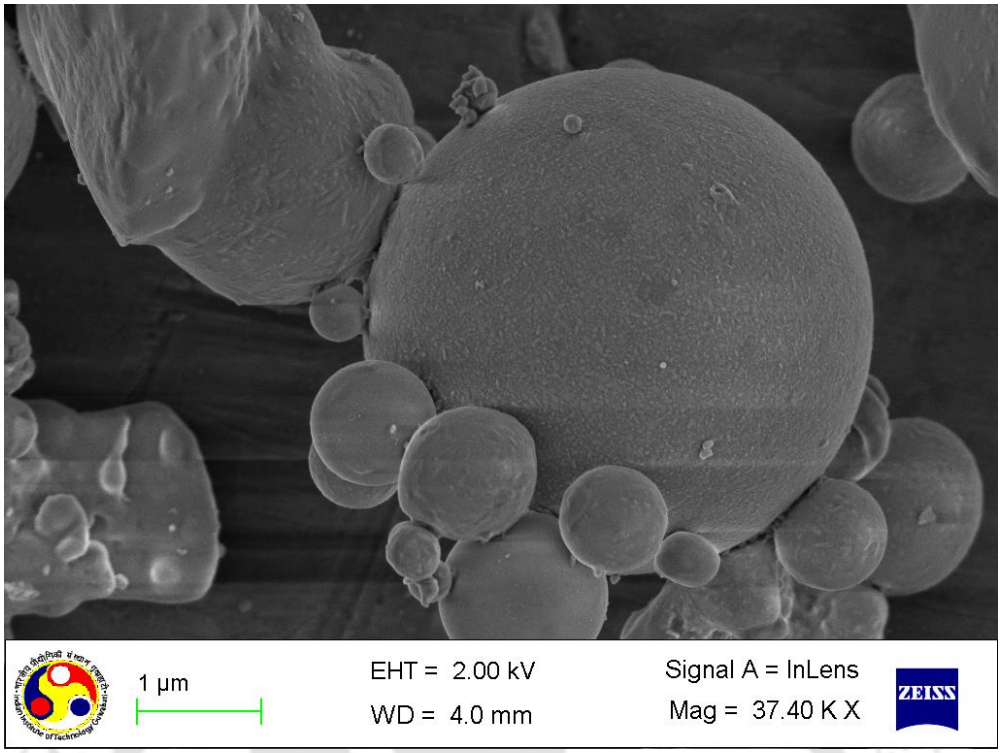

Figure 3.4(a) FESEM image of FFA

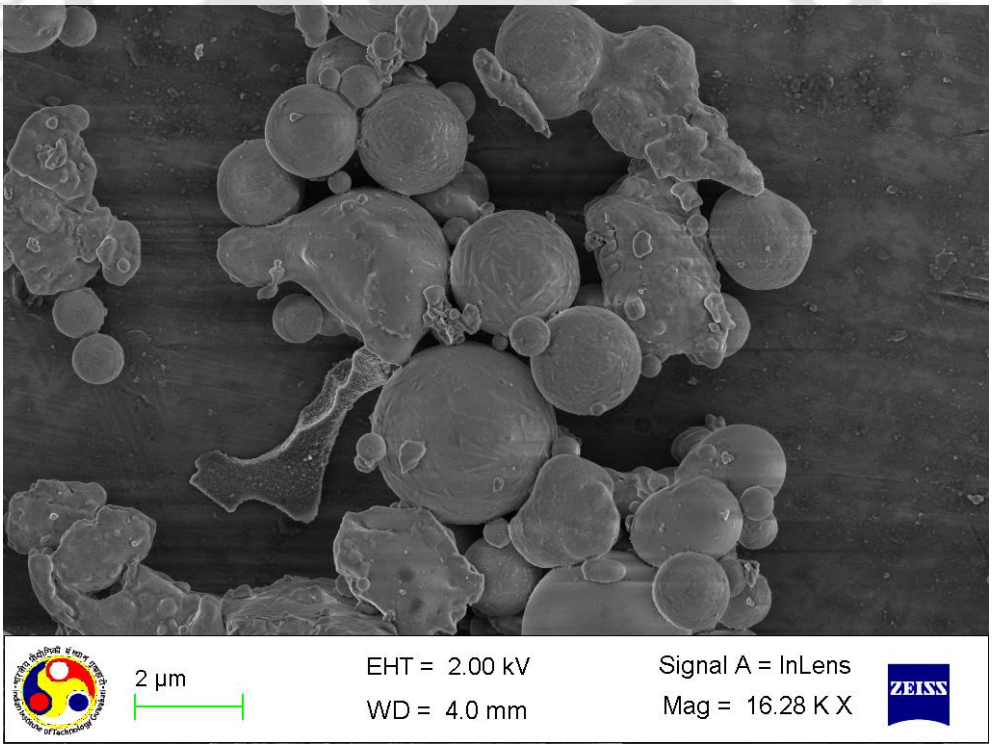

Figure 3.4(b) FESEM image of BFA

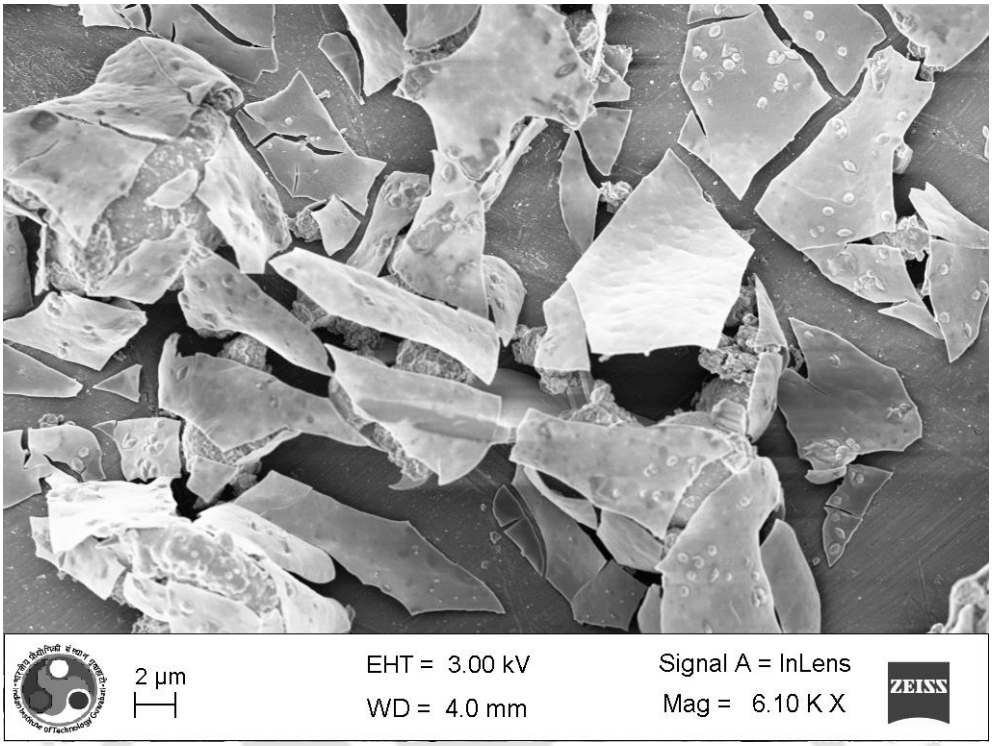

Figure 3.4(c) FESEM image of NFA

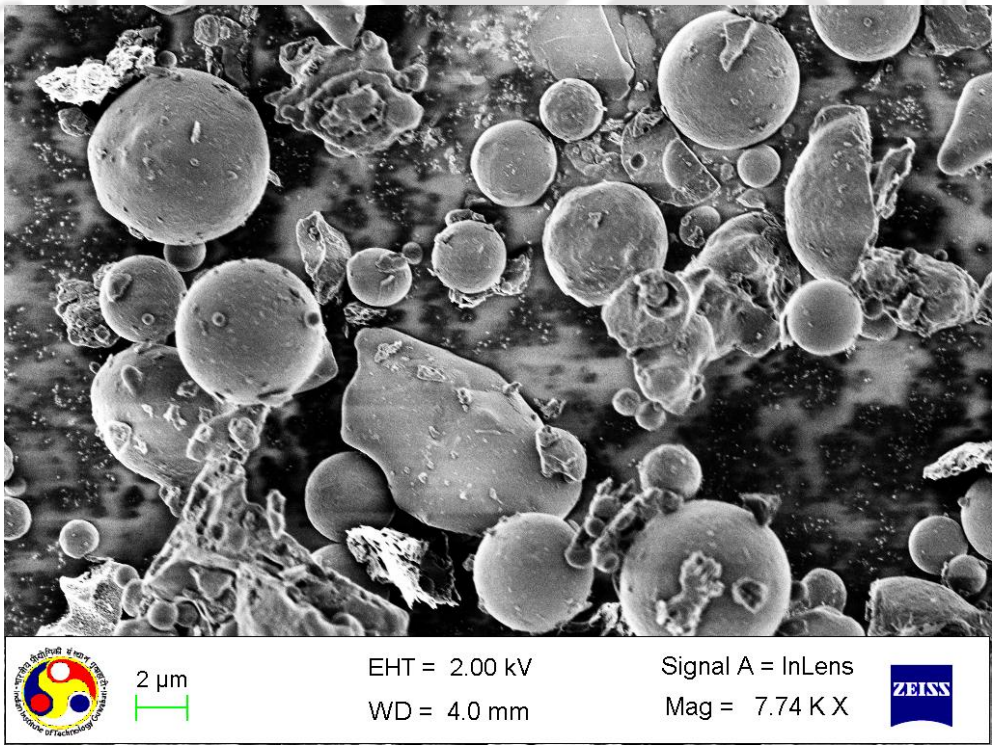

Figure 3.4(d) FESEM image of PA

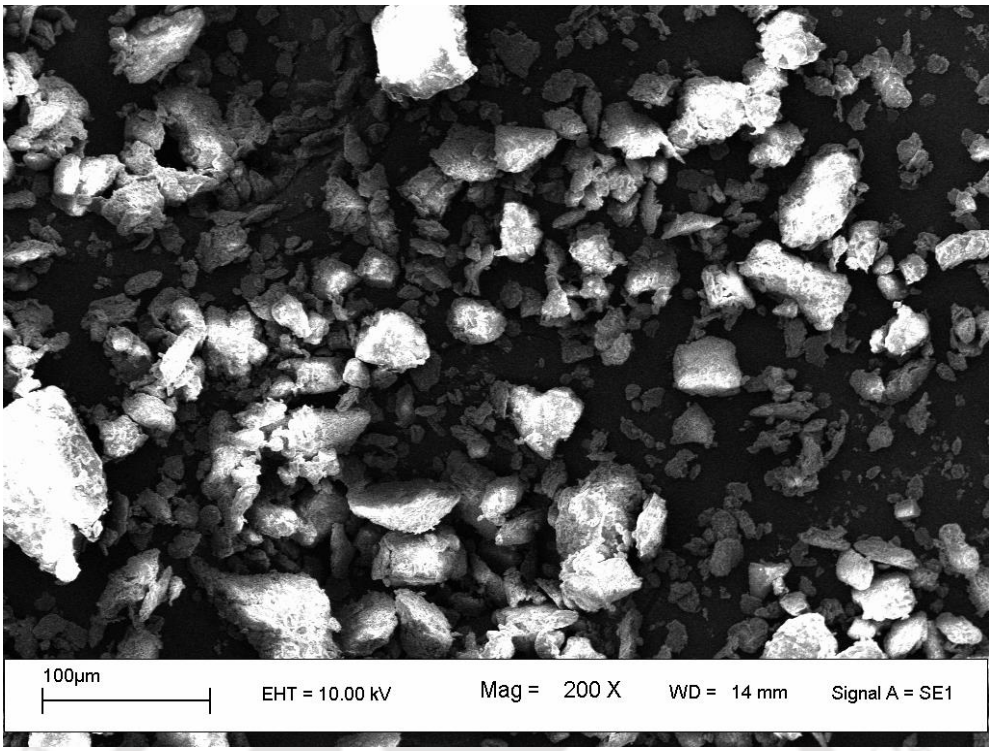

Figure 3.5(a) FESEM image of B1

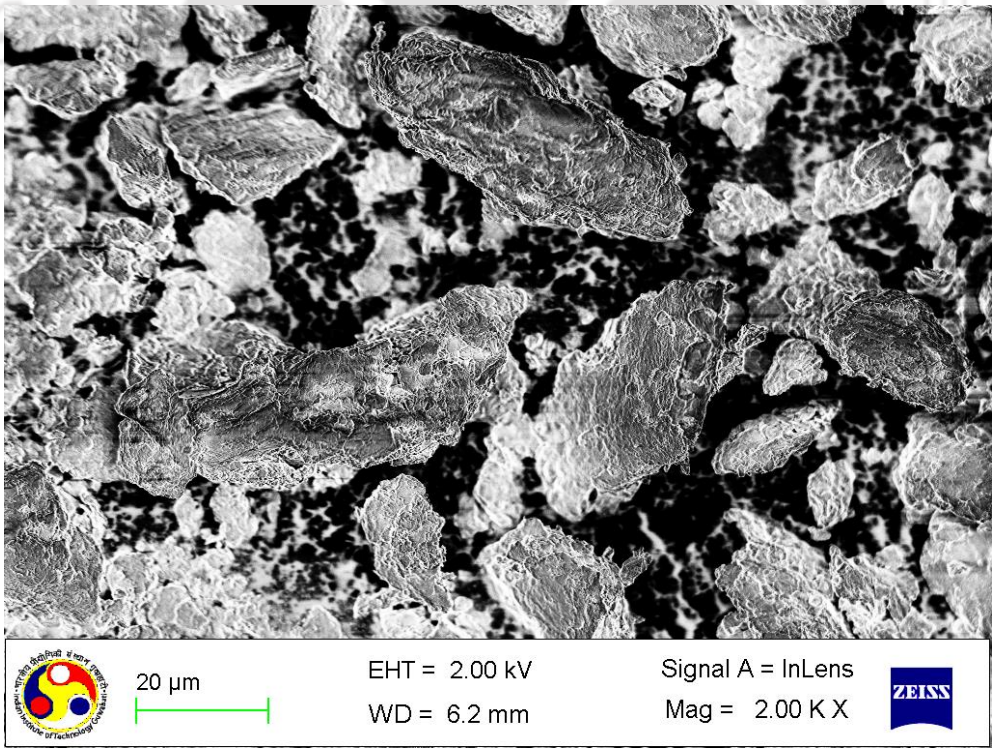

Figure 3.5(b) FESEM image of B2

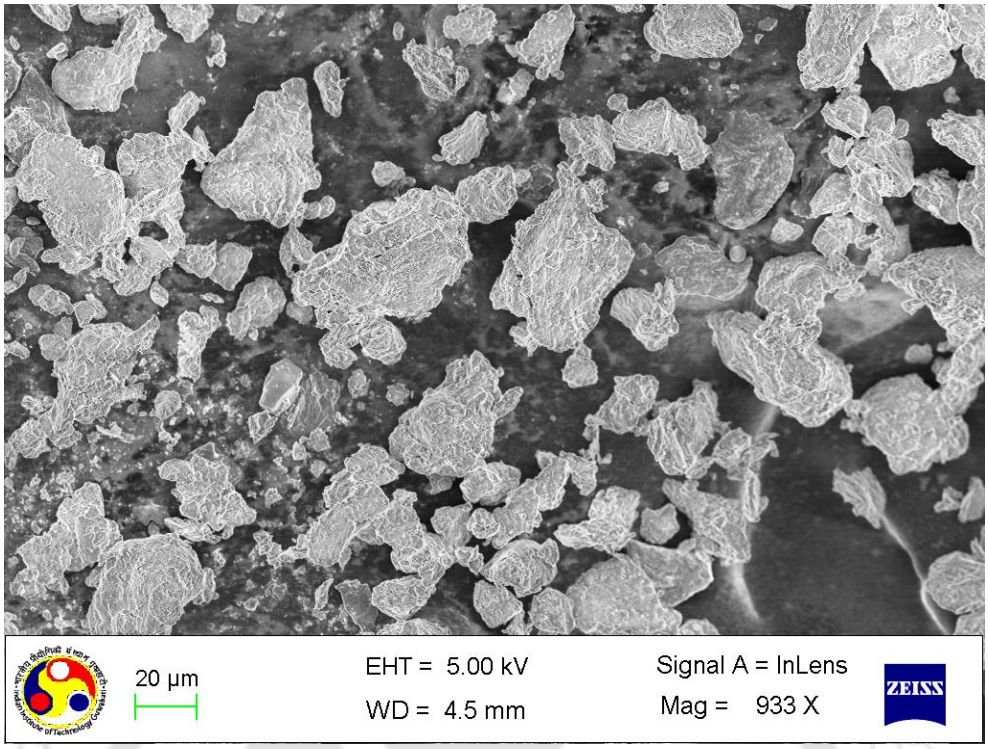

Figure 3.5(c) FESEM image of B3

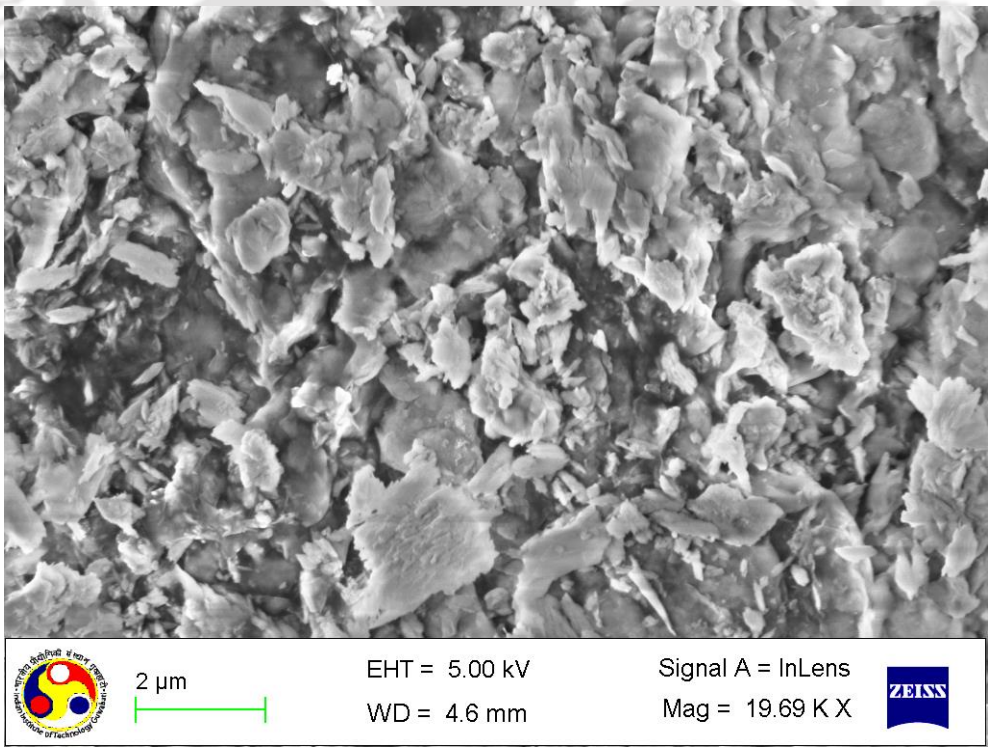

Figure 3.5(d) FESEM image of B4

It was observed that for FFA, BFA and PA, majority of the particles are spherical in shape. This spherical shaped particle indicates the presence of high amount cenosphere in FFA and BFA. The presence of cenosphere in fly ash has already been established by many researchers (Naik et al. 2007; Pandian 1998). The image of NFA showed the presence of sharp platy structure. This might be the presence of glassy particles which are most likely to be found in C class fly ash as reported in the literature (Das and Yudvir 2005; Ilic et al. 2003). The presence of spherical cenosphere in NFA was not seen in the result. The results obtained in bentonite samples indicated a flaky plate like structure.

3.4 Measurement of suction

The measurement of suction in fly ash, bentonite and fly ash-bentonite mixes was performed using different suction measurement instruments namely Tensiometer (TM), Equitensiometer (EQT), Matric potential sensor (MPS) and WP4 dew point potentiameter. The details of each instrument are given below. The T5 tensiometer (TM) as shown in Figure 3.6 is one of the robust instruments for measuring matric suction (ψ_m) directly. It consists of three important parts tensiometer body, shaft and ceramic cup. The tensiometer body is threaded into a transparent acrylic shaft filled with deionized water free from any air bubbles and the other end is connected to ceramic cup of 5 mm diameter and 4 mm long. Such a small dimension facilitates easy insertion, quick equilibration and measurement as compared to the conventional tensiometer. The cup acts as an interface between the soil and shaft and maintains continuity of water through its pores. One of the drawbacks of TM is its low range of suction measurement (< 80 kPa) (accuracy ±0.5 kPa), thereby limiting its application to only cohesionless geomaterials (Malaya and Sreedeep 2010). The working principle and measurement procedure of TM (model T5, UMS, Germany) used in this study were discussed in detail in the literature (Malaya and Sreedeep 2012; Malaya and Sreedeep 2010; T5 User Manual 2001). For measuring suction the tensiometer is inserted into the geomaterial up to the required depth. Due to this the water present in the shaft tries to come into equilibrium with soil pore water. Due to this, the negative pressure of soil water becomes equal to the water tension developed in the tensiometer shaft. The change in the water tension in the shaft water results in deformation of silicon chip present in the tensiometer body. The deformation of the silicon chip results in a change in the specific electric resistance, which is then converted into defined voltage signal via a Wheatstone bridge. The voltage is further converted into the pressure units of hectopascal (hPa). For measuring suction by tensiometer a proper

contact between the tensiometer ceramic cup and the soil is essential. For loose state of soil, it can be easily inserted, while for compacted soil a guide hole of diameter less than the tensiometer shaft is made with a dummy rod and after that the tensiometer is inserted into the soil. This method minimizes the chance of any damage to the tensiomter and ensures a proper contact with the soil below.

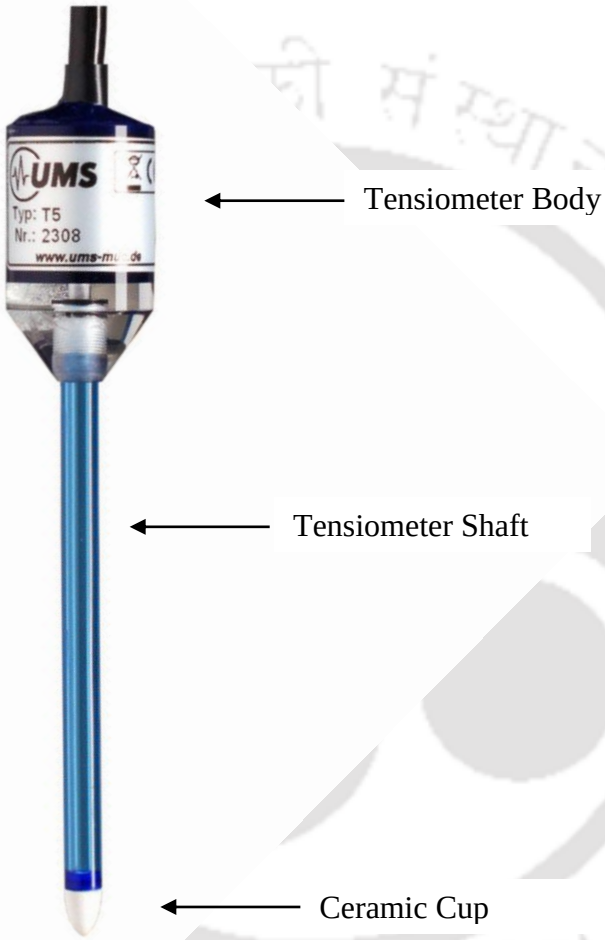

Figure 3.6 Details of T5 tensiometer TM

The measurement range of MPS (model MPS-1, Decagon, USA) is ψ_m< 500 kPa (accuracy ±5 kPa from -10 to -50 kPa and ±20% of reading from -50 to -500 kPa). It consists of two engineered ceramic disks of 32 mm diameter sandwiched between two stainless steel screens and a circuit board as shown in Figure 3.7. The relationship between water content and ψ_m of the ceramic material is well established. When the MPS is inserted into the sample, the water present in the sample tries to equilibrate with the

two ceramic disks. At equilibrium, suction developed in the ceramic disks is equal to the suction in the sample. The MPS circuit board comprises of an oscillator that generates an electromagnetic (EM) field during ψ_m measurement. The EM field charges the ceramic disks around the MPS circuit board. The stored charge is proportional to dielectric permittivity (ε) of the ceramic disks, which is a function of water content and gives the output in millivolt (mV). This mV output is converted into ψ_m based on the general calibration equation given by the manufacturer of the device (MPS-1, Operator's manual 2008).

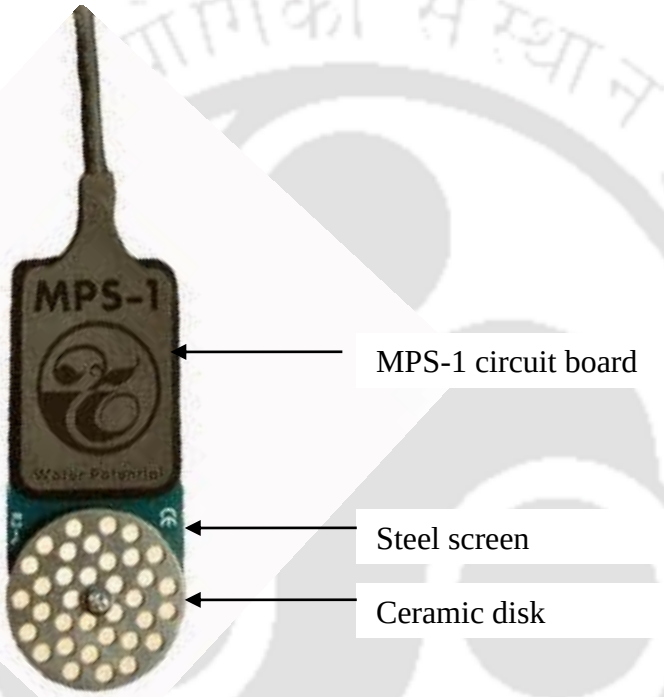

Figure 3.7 Details of MPS sensor

The EQT (model EQ-2, Delta-T Devices, England) measures ψ_m< 1000 kPa (accuracy ±10 kPa from 0 to -100 kPa and ±5% of reading from -100 to -1000 kPa) and consists of two important parts, (i) the ML2x ThetaProbe (ThetaProbe, Type ML2x) (Equitensiometer user's manual, Delta-T Devices 1999), and (ii) a 40 mm diameter and 68 mm long specially formulated porous cylinder known as equilibrium body as shown in Figure 3.8. The measuring rods of the ThetaProbe were embedded into the equilibrium body for monitoring water content in the porous material. Like MPS, the porous material has an established relationship between water content and ψ_m.

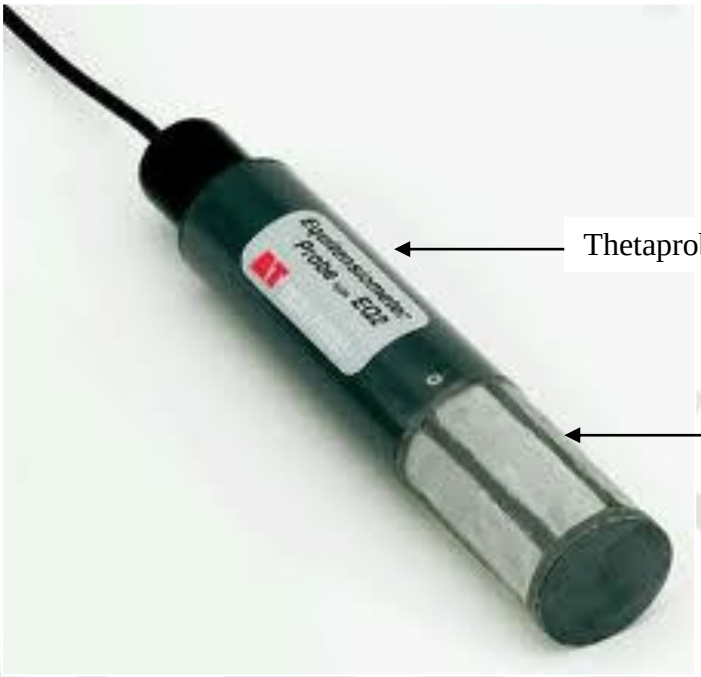

Figure 3.8 Details of EQT sensor

The WP4 dew point potentiameter (model WP4-T, Decagon, USA) as shown in Figure 3.9 can be used to measure total soil suction (ψ) between 1 MPa and 300 MPa (accuracy ±0.1 MPa from 0 to -10 MPa and ±1% from -10 to -300 MPa). The instrument works on the principle of chilled-mirror dew point technique (Leong et al. 2003; WP4 user's manual 2002). The WP4 measurements are considered to be less accurate for suction less than 1 MPa, especially for cohesionless or low plastic soils (Shah et al. 2006). It essentially consists of a sealed block chamber in which the soil sample can be placed in a 15 cm^3 Polyurethane or stainless steel sampling cup. The geomaterial with particular water content induce a specific relative humidity in the head space of the sealed block chamber. Based on the relative humidity of air in the headspace of the block chamber, ψ can be estimated with the help of Kelvin's equation (Malaya 2012; ASTM D6836-02).

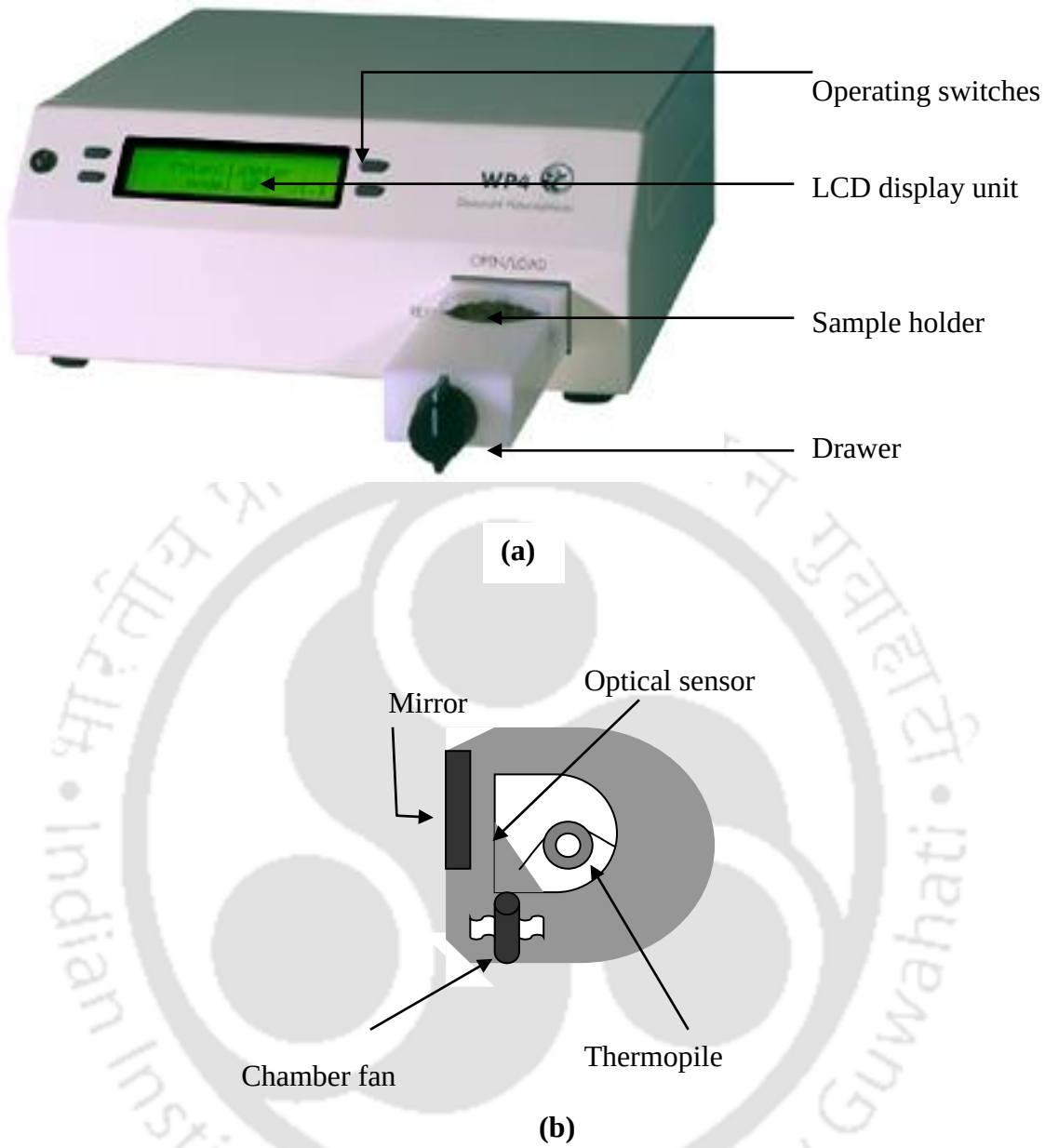

Figure 3.9 Details of (a) WP4 and (b) block chamber

The volumetric water content (θ) (VWC) of the geomaterials was measured using VWC probe EC-5 (model ECH2O-EC5, Decagon, USA) (accuracy ±3% and ±1% with soil specific calibration) (Operator's manual version 5, ECH2O soil moisture sensor 2006). As shown in Figure 3.10, the probe EC-5 has two epoxy-impregnated fibreglass prongs that are inserted into the geomaterial. The dimension of the probe is 8.9x1.8x0.7 cm. The working principle and procedure for measuring θ using EC-5 are discussed in the literature (Malaya and Sreedeep 2010; Bogena et al. 2007). The dielectric permittivity of soil changes with the water content of the soil. The sensor measures the capacitance

property of the soil mass in milliVolt. The mV output is further converted into θ based on the calibration equation. The value of dielectric permittivity of water is 80, while for dry soil and air it is around 4 and 1 respectively. This broad range of permittivity helps in measuring the θ of the soil from saturated to dry state condition.

The probe is equipped with an oscillator working at a frequency of 70 MHz, which generates an electromagnetic field. The electromagnetic field charge the soil around the probe. This stored charge is proportional to permittivity and θ, and is measured by the copper traces of the prongs. The electromagnetic field is maximum near the probes while it gets decreased away from the probe surface. A zone of influence of 50 mm from the edge of the probe surface is reported in the manual for this stored charge. It may be noted that such probes cannot be used with WP4 due to small sample size of the geomaterial. For WP4 measurements, gravimetric water content (w) was measured and converted to $\theta = w(\gamma_d/\gamma_w)$,where γ_d is the dry unit weight of fly ash and γ_w is the unit weight of water. In this study, it was assumed that the shrinkage due to drying is negligible for fly ash because it is a cohesionless geomaterial.

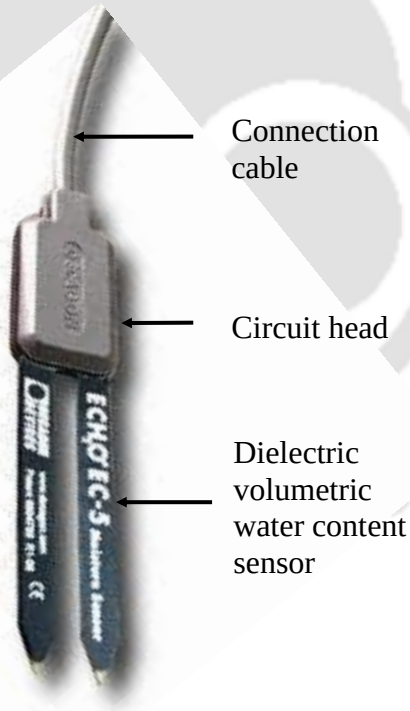

Figure 3.10 Details of ECH2O-EC-5 sensor

3.5 Details of contaminant retention procedure

Contaminant retention characteristics of the geomaterials are very important for landfill liner application together with the water retention characteristics. So, it is necessary to conduct the retention study of the geomaterials and to determine the isotherm parameters of some popular established models. In this study, retention of the geomaterials fly ash, bentonite and fly ash-bentonite mixes was carried out by following the 24 hr batch test as per ASTM D4646-03. The aim of this method was to determine the retention characteristics of the geomaterials in aqueous leachate suspension, which is expressed in terms of sorption coefficient. Lead was used as the model heavy metal contaminant in this study due to its abundance in industrial and municipal wastes. Also, lead causes serious health problem as compared to other heavy metals found in the landfill leachate. Due to this fact, only lead was selected as the heavy metal in this study. The Pb^{2+} metal ion stock solution of 1000 mg/L concentration were prepared by dissolving known amount of analytical grade lead nitrate $Pb(NO_3)_2$ (99% pure) in de–mineralized water prepared through R.O. process (Model: Milli–Q Water, M/S Millipore S.A.S., Molsheim, France). The metal solutions for Pb^{2+} ions were prepared by diluting the stock solution in de–mineralized water. The step by step procedures of the 24 hr batch test are explained in chapter 7 of this thesis.

3.6 Properties of FA-B1 mix

The effect of FA addition on the LL, FSI and k_{sat} of FA-B1 mixes has been determined in this study for all the FAs as given in Table 3.7. It was found that LL and FSI decreases with the increase in FA content in the FA-B1 mix. As expected, k_{sat} value increases with the increase in FA content in the FA-B1 mix. The k_{sat} values of the mixes were used as an input parameter in the unsaturated seepage modeling study in chapter 6.

Table 3.7 LL, FSI and k_{sat} of FA-B1 mixes

Properties	FA	FA content, %		
		30	50	70
LL (%)	FFA	212	153	108
	BFA	189	162	109
	NFA	139	91	69
	PA	221	141	112
FSI	FFA	7.72	6.27	2.09
	BFA	2.2	1.09	0.25
	NFA	3.0	1.5	1.0
	PA	5.0	3.36	1.91
k_{sat}(m/s)	FFA	1.27e-11	1.91e-11	8.01e-9
	BFA	1.76e-11	3.20e-11	1.33e-9
	NFA	2.83e-11	6.41e-11	2.14e-9
	PA	2.83e-11	6.38e-11	2.11e-9

3.7 Summary

The details of materials, its designation and experimental investigations of the basic material fly ash and bentonite and mixes were discussed in this chapter. Further, different instruments and methodology adopted for matric, total suction measurement and volumetric water content measurement was presented in this chapter. Finally, the contaminant retention procedure for batch test is explained.

Chapter 4

Water Retention Characteristic Curve of Fly Ash

4.1 General

Fly ash (FA) has potential applications in geotechnical and geoenvironmental projects, where its water retention characteristic curve (WRCC) is important. The main objective of this chapter was to establish the inherent range of measured suction of FAs using four different instruments: tensiometer (TM), matric potential sensor (MPS), equitensiometer (EQT), and WP4 dew point potentiameter with a varying measurement range as mentioned in section 3.4 (chapter 3). The four suction measurement methodologies used in this study have different ranges of measurement and working principle. Based on the measured results, the variability of WRCC equation parameters of four FAs collected from different thermal power plants were studied. The sensitivity of different range of measured suction on WRCC equation parameters of FA was investigated.

4.2 WRCC of FA

The sample preparation procedure for suction measurements using TM, MPS and EQT was the same. The FA samples were mixed with required quantity of deionized water, packed in a polythene cover and placed in the desiccators for about 24 hr for maturation and uniform distribution of water. The matured sample was then compacted in an in-house fabricated column in three layers by providing adequate number of blows per layer using a circular hand held rammer weighing 600 g to achieve the desired compaction state. The bottom of the column was sealed to prevent any loss of moisture during and after compaction. Measurements using TM were performed in a perspex column of 120 mm diameter and 150 mm height. The MPS and EQT measurements were performed together on the same sample compacted in a poly vinyl chloride (PVC) mold of 200 mm diameter and 150 mm height. This small height of the column ensures homogeneity of compacted FA samples. The details of compaction state for TM, MPS/ EQT and WP4 are listed in Table 4.1, where w is the gravimetric water content, γ_d is the unit weight and S_r is the degree of saturation. For TM, MPS and EQT it was essential to set near zero suction as the initial state for drying WRCC. Therefore, the compacted sample was excessively saturated with water and ponding water on top was removed with a syringe. The initial water content of NFA for

TM measurement was intentionally kept low due to poor response at higher water content. The suction measuring instruments and the EC-5 volumetric water content probe were inserted vertically into the saturated sample and allowed to air dry. For ease of insertion, guide holes with diameter less than the instrument was made in the compacted sample. Special care was taken to ensure that the depth of insertion of all these instruments and EC-5 were the same to avoid any inconsistencies in measurements during drying. The miniature T5 tensiometer was inserted such that its ceramic tip was at a depth equal to the mid height of the EC-5 sensor.

Table 4.1 Compaction state of FA for different measurements

Measurement technique	**FA**	**w (%)**	**γ_d (kN/m^3)**	**S_r**
Tensiometer (TM)	FFA	25.30	13.08	0.99
	BFA	43.70	10.34	0.99
	NFA	14.24	10.15	0.25
	PA	35.90	12.2	0.99
Matric potential sensor (MPS) and Equitensiometer (EQT)	FFA	25.30	13.08	0.99
	BFA	40.08	10.31	0.90
	NFA	41.50	10.61	0.80
	PA	27.30	11.98	0.99
WP4 dew point potentiameter	FFA	38.67	6.07	0.34
	BFA	45.56	7.94	0.62
	NFA	54.52	6.76	0.51
	PA	53.01	7.54	0.68

Specific calibration of EC-5 was performed for all the FAs used in this study. The validity of the customized calibration of EC-5 was ascertained using independent measured data sets that were not used for calibration. No user calibration was performed for EQT and MPS since the suction measurement is based on the equilibrium water content of the porous material integrated with the instrument. This porous material acts as an interface between the geomaterial and the instrument sensor. The equilibrium water content of the porous material would depend upon the suction and water content present in the FA. The factory calibration

of EQT and MPS correspond to the porous interface and not the individual geomaterial in which the measurements are made. The variation in matric suction (ψ_m) and volumetric water content (θ) with drying was continuously recorded with time with the respective data loggers. These data were used to obtain continuous WRCC of the FAs. The drying process was fully governed by evaporation from the top of the sample which closely simulates the actual field boundary condition. The measured variation in ψ_m and θ with drying corresponds to the average value for the sample adjacent to the respective sensors. Keeping in view the macroscopic characterization of the sample, it was presumed that the suction and water content in the sample were uniform for the size of the sensor considered in this study. Therefore, any unforeseen microscopic influence of water content variation along the sensor length was not accounted for in this study.

For WP4 measurements, FA sample was mixed with sufficiently high amount of deionized water and packed in the sample cup by pressing with a spatula. From Table 4.1, it can be noted that the initial dry unit weight was comparatively less for WP4 samples. However, it was already reported in the literature that initial dry unit weight has negligible influence on WRCC (Malaya and Sreedeep 2010; Birle 2008). The sample cup with the specimen was placed inside the block chamber of WP4 for ψ measurement. After each ψ measurement, the specimen was taken out of the WP4 chamber and the weight of the sample cup along with specimen was recorded using a high precision balance. The cup with the sample was then left for air-drying till the next measurement was performed. This process was repeated several times till a near dry state of the sample was attained ($\psi \approx 300$ MPa). At the end of the test, the sample cup with the soil specimen was placed in an oven to determine its dry weight. Using the dry and wet weights of the specimen, the gravimetric water content, w, corresponding to each ψ measurement was back calculated for establishing WRCC. Before using the WP4, its calibration was ensured by measuring ψ of the measuring standard (0.5 M KCl solution) supplied by the manufacturer (WP4 users manual 2002).

The reliability and repeatability of the above instruments were assessed by determining drying WRCC of three independent identical samples of FA. The initial compaction state used for these studies conforms to Table 4.1 and the results are depicted in Figure 4.1. The results of three independent trials of suction measurement clearly indicate the repeatability of the instruments used in this study for the range of measurements and for FAs considered in this

study. For comparing ψ measured using WP4 with ψ_m obtained using TM, MPS and EQT, it needs to be ensured that FAs do not contain any salt or contaminants contributing to osmotic suction (ψ_o) (Sreedeep and Singh 2006). For this purpose, all FAs were repeatedly washed with deionized water (Sreedeep and Singh 2006). After every washing, WRCC of FA was determined using WP4. It was found that the WRCC of original and washed FA matches well for all the FAs. For the sake of brevity, only the result of FFA is presented in Figure 4.2. The result depicted in Figure 4.2 indicates that there is no ψ_o for the FA considered in this study. Therefore, ψ measured using WP4 is equal to ψ_m and hence the results can be compared and combined together with those of TM, MPS and EQT.

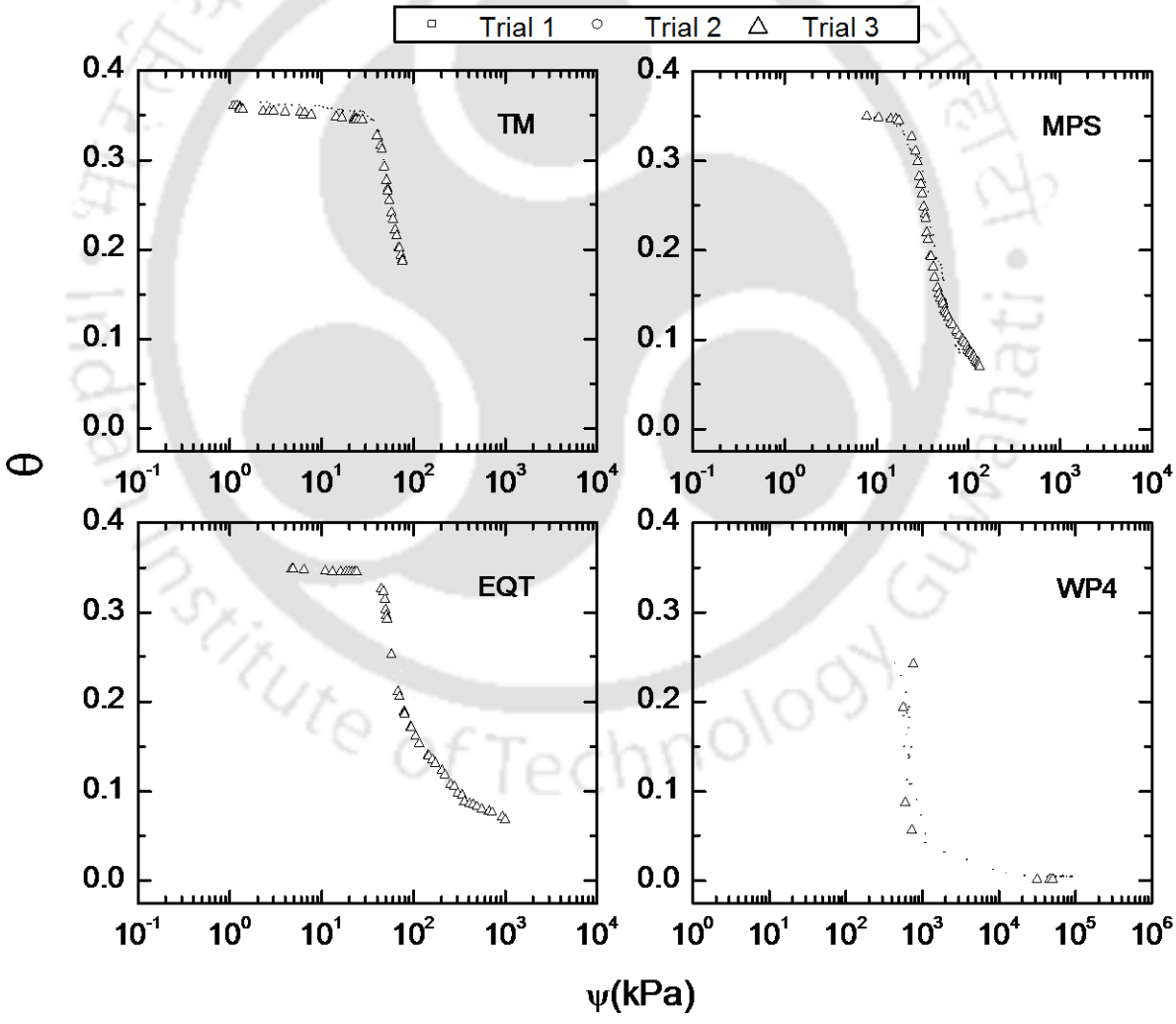

Figure 4.1 Repeatability of measurements using TM, MPS, EQT, WP4 and EC-5 for FFA

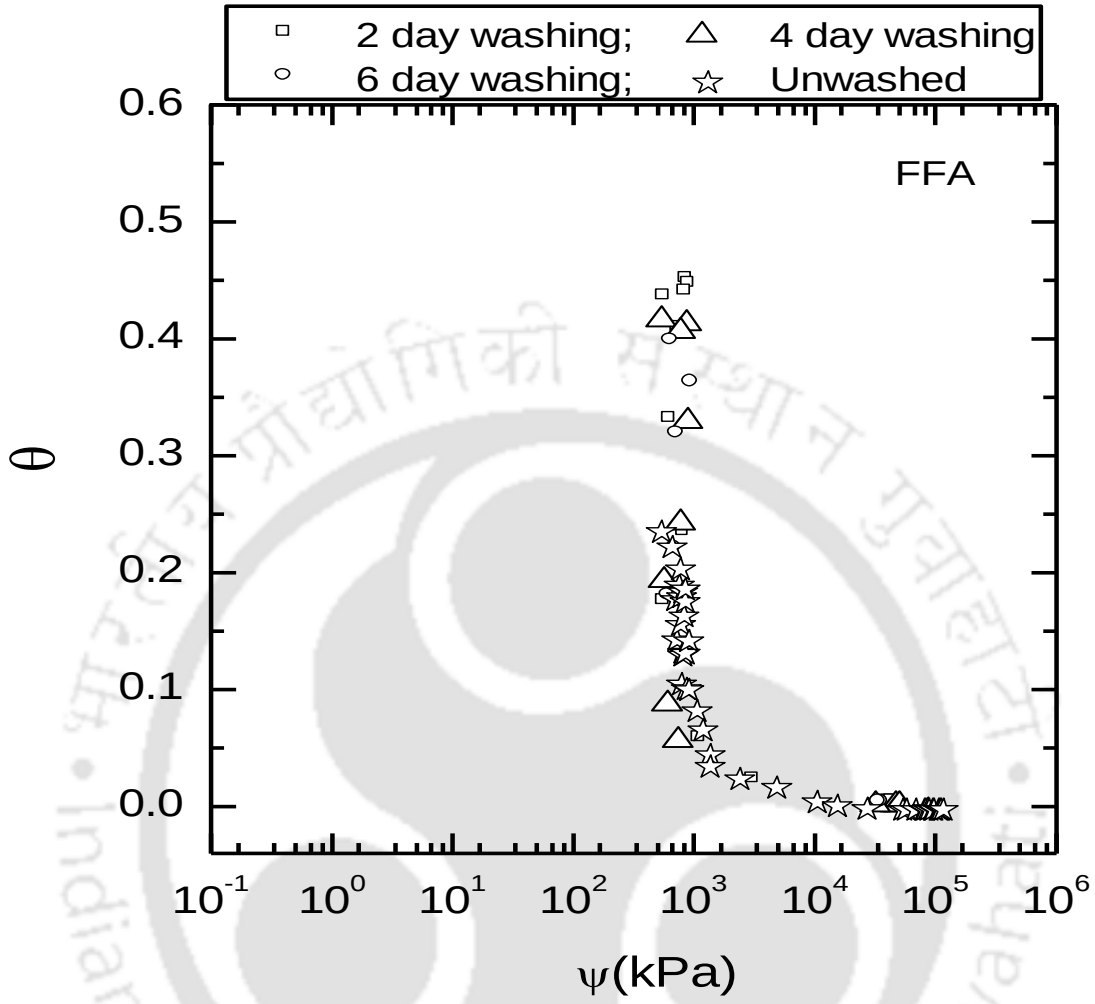

Figure 4.2 Effect of washing on the water retention characteristic of FFA obtained using WP4

Figure 4.3 indicates the variability of WRCCs of FAs obtained using a particular suction-measurement methodology. As expected, ψ_m was found to increase with decreasing θ for all the FAs. The near-saturation portion (initial horizontal portion of the WRCC at low suction) and desaturation portion (decreasing portion) (Malaya and Sreedeep 2012) were quite explicit for Farakka fly ash (FFA), Badarpur fly ash (BFA) and Pond ash (PA). The ψ_m corresponding to desaturation was similar for both FFA and BFA, even though the θ_s (θ of near saturation portion) was not the same. The saturated water content θ_s of PA was similar to that of FFA, but desaturation point was different. This indicates that FAs from different

sources and having different characteristics (Tables 3.1 to 3.2) will exhibit varying WRCCs. It must be noted that the NFA, which was the only class C fly ash considered in this study, did not give a proper continuous WRCC for TM measurements. The variation of ψ_m from 10 kPa to 80 kPa occurred for a θ variation between 0.15 and 0.12. The NFA hardened during drying, and the TM response was erratic. The hardening of NFA might have resulted in the improper functioning of the ceramic interface of the TM. Repeated trials of TM measurement (four times) were not successful for NFA. It is clear that the WRCC obtained from TM measurement for high calcium content geomaterials such as NFA is not reliable. Another important observation is that the θ corresponding to 80 kPa was greater than 0.1 for all FAs considered in this study. This indicates that the residual portion of the WRCC of FA cannot be determined using TM. It is important to understand the implication of this for quantifying WRCC parameters and comparing them with techniques that permit measured suction greater than 80 kPa. Such a study would help to appraise the suitability of TMs for ψ_m measurements of FA.

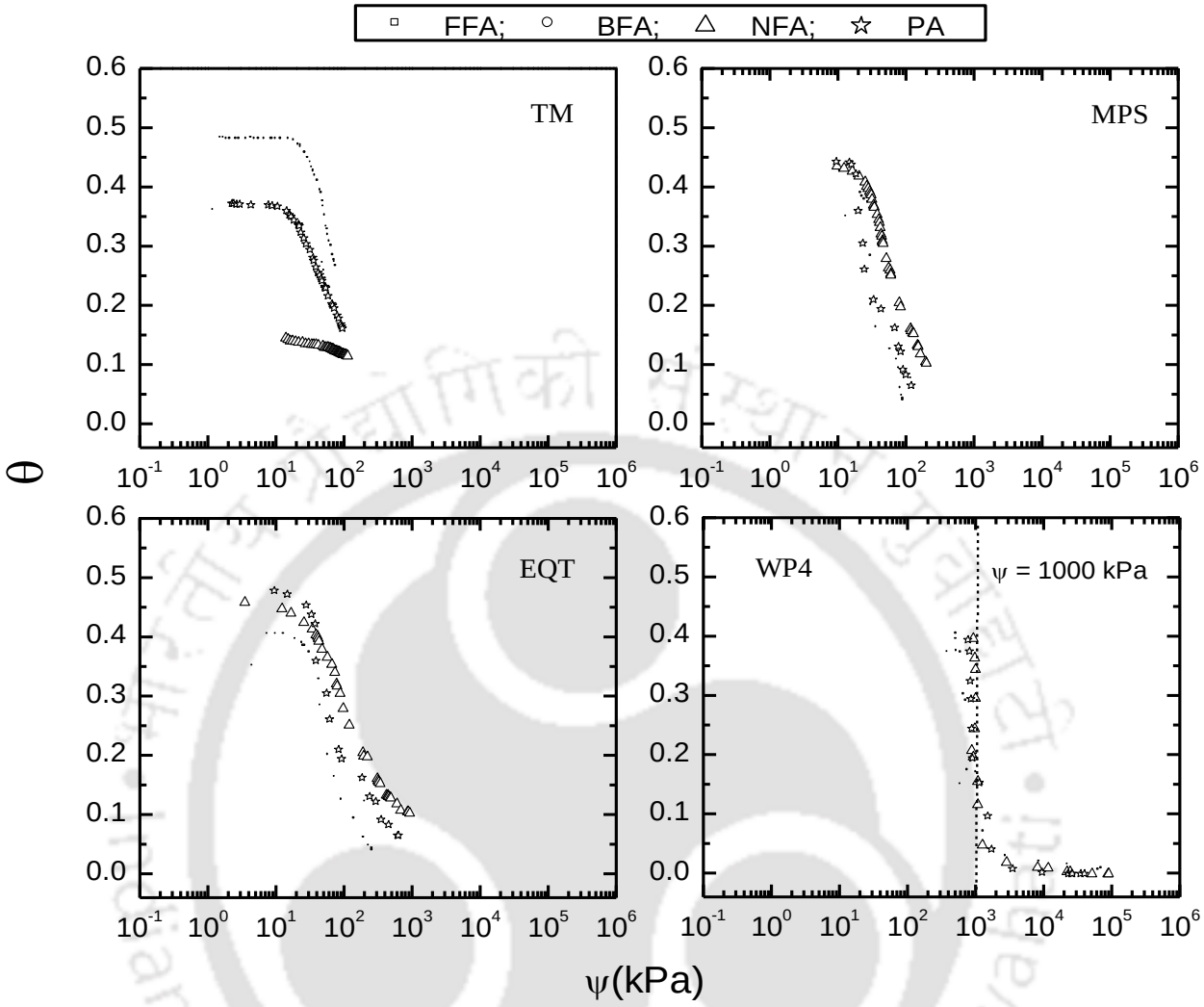

Figure 4.3 WRCC of FAs obtained using TM, MPS, EQT and WP4

The continuous drying WRCC measured using the MPS indicated that the initial near-saturation portion was obtained for all FAs. Desaturation initiated around 20 kPa for FFA, and the maximum ψ_m measured was 150 kPa, corresponding to a θ of 0.05. The figure indicates that the WRCC of FFA approached the residual portion. For BFA and PA, the desaturation stage started from around 25 kPa. For BFA, θ fell vertically at the start of the desaturation stage (at 25 kPa of suction) from around 0.40 to 0.15. A maximum ψ_m of 100 kPa was observed for θ close to 0.01. Such a trend is justified by the poorly graded particle size of BFA listed in Table 3.2 of chapter 3, which allowed the water to escape instantly during the drying process. For PA, the maximum ψ_m correspond to 100 kPa for θ equal to

0.05. Unlike TM, the MPS was able to successfully measure near-saturation and desaturation portion of the WRCC of NFA. The desaturation stage started around 30 kPa and continued up to a maximum ψ_m of 110 kPa corresponding to a θ of 0.1. An interesting observation is that the maximum ψ_m measured was within 110 kPa for all FAs considered in this study, even though the maximum capacity of the MPS was 500 kPa. This might have been due to the discontinuity of FA samples around the sensing portion of the MPS as drying progressed; preventing measurement of ψ_m values greater than 110 kPa. Below 20 kPa, the WRCCs of BFA, NFA, and PA matched reasonably well. In the desaturation portions, it is observed that for a particular θ, ψ_m was marginally higher for NFA, whereas FFA, BFA, and PA yielded similar values. The marginal difference in the WRCC of FAs may be attributed to differences in physical and chemical properties.

The WRCC of FAs measured using the EQT show that the well-defined near-saturation portion continued up to a ψ_m of around 30 kPa for all FAs, even though the θ_s values of the FAs were different. All the FA exhibits a defined desaturation portion as well. The EQT could measure maximum ψ_m values close to 1000 kPa for FFA and NFA, which is the measurement limit of the EQT. However, for BFA and PA, the maximum ψ_m measured was only 300 kPa and 600 kPa, corresponding to a θ of 0.01 and 0.07, respectively. It is interesting to note that all the FAs approached a residual state of suction within 1000 kPa. Therefore, it is apparent that a reliable WRCC for FAs inclusive of saturation, desaturation, and residual portions can be obtained by the measurement range of instrument such as EQT.

When the results obtained from all four methodologies were compared as shown in Figure 4.3, it is clear that data points below 1000 kPa for the WP4 (separated by the dotted line) cannot be considered reliable for materials like FA. Therefore, it is explicit that a WP4 with an accuracy range greater than 1000 kPa will be useful for obtaining residual suction data. The measured ψ values for all FAs merged beyond 1000 kPa with θ less than 0.05. The ψ varied from 10^3 kPa to 10^5 kPa for a minimal change in θ from 0.05 to a near-dry state. The observation highlights that the residual portion of the WRCC is unique for FAs irrespective of their physical and chemical properties. Such an observation is justified by the findings in the literature that water retention characteristics of soil merge at higher suction (Zhou and Yu 2005). The study indicates that a high suction measuring instrument such as WP4 has limited

applications for establishing the WRCC of cohesionless materials like FA. It may be useful only for determining the residual portion of the WRCC of FA.

4.3 Effect of measurement methodologies on WRCC of FA

Figure 4.4 shows a comparison of WRCCs of FAs measured using the different methodologies discussed above. Suction less than 10^3 kPa obtained using the WP4 was presented in the figure to show the difference in WRCC if the desaturation portion is considered irrespective of the accuracy range of the instrument. It can be noted that the desaturation portion based on WP4 results shows steep reduction for all FAs and yields higher suction as compared to other measurement methodologies. For all FAs, TM and EQT results match well with each other, despite some differences in the near-saturation portion, which is due to the variation in measured θ_s. The slope of the desaturation portion obtained using MPS deviates marginally from EQT results towards a higher suction range (> 100 kPa). The influence of such deviations on the quantification of WRCC equation parameters is presented below. For the sake of comparison, WRCC parameters were determined for WP4 results as well.

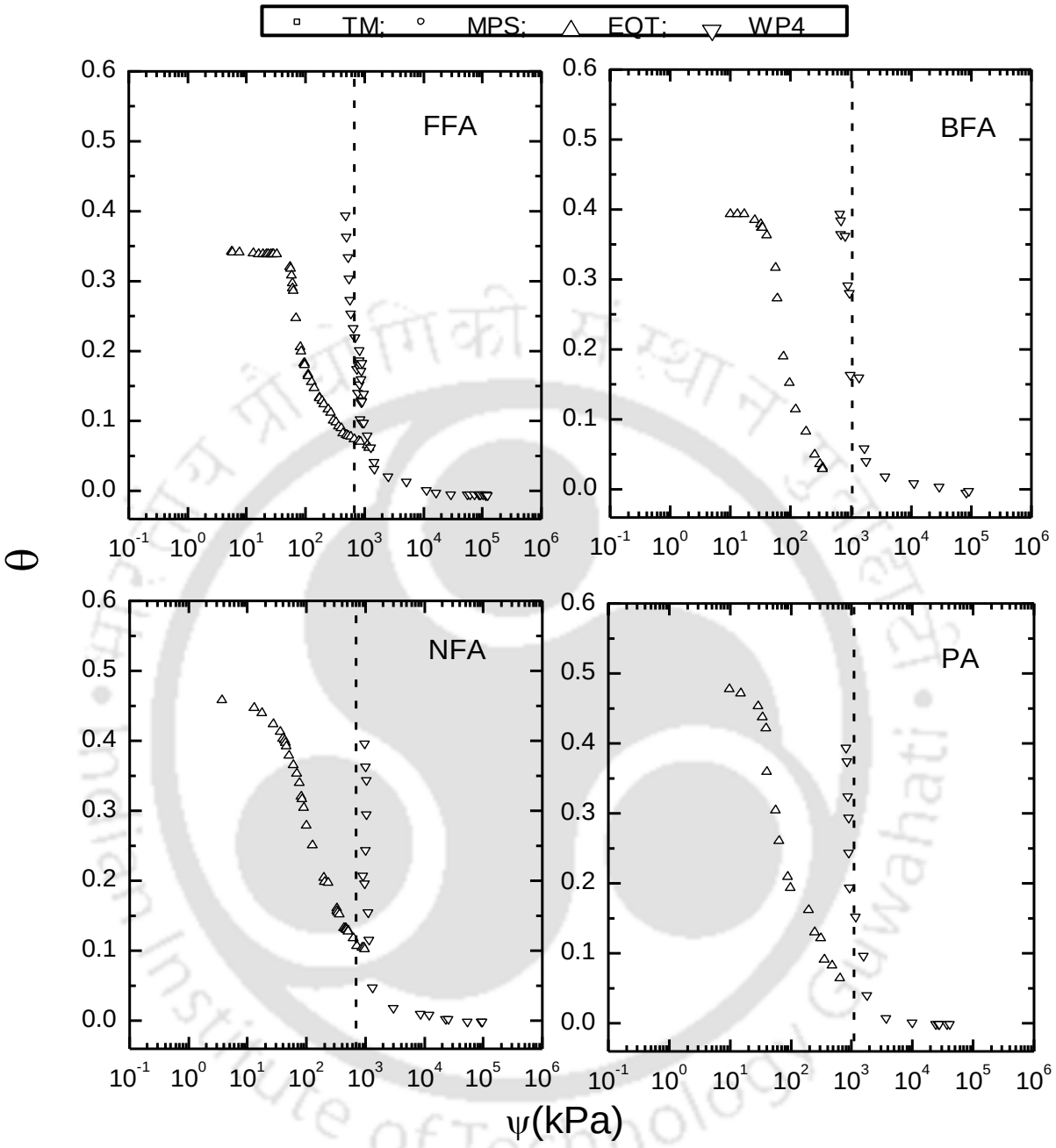

Figure 4.4 Comparison of measured WRCC obtained using different methodologies

4.4 WRCC parameterization of FA

The WRCC of FA was mathematically quantified by fitting Fredlund and Xing (FX) (Fredlund and Xing 1994) and van Genuchten (vG) (van Genuchten 1980) WRCC model to the experimental data. Equations 4.1 and 4.2 represent FX and vG models, respectively.

$$\theta(\psi) = \theta_s \left[1 - \frac{\ln\left(1 + \frac{\psi}{h_r}\right)}{\ln\left(1 + \frac{10^6}{h_r}\right)} \right] \times \frac{1}{\left\{ \ln\left[\exp(1) + \left(\frac{\psi}{a_f}\right)^{n_f} \right] \right\}^{m_f}} \tag{4.1}$$

$$\theta(\psi) = \theta_r + \frac{(\theta_s - \theta_r)}{\left[1 + (a_{vg}\psi)^{n_{vg}}\right]^{m_{vg}}} \tag{4.2}$$

Where, m_{vg}= 1-(1/n_{vg}), θ(ψ) is the volumetric water content at suction ψ; θ_r is the residual volumetric water content; θ_s is the volumetric water content at saturation; a_{vg} and a_f are fitting parameters primarily dependent on the air entry value (AEV); n_{vg} and n_f are fitting parameters that are dependent on the rate of extraction of water from the soil; m_f is the fitting parameter that depends on θ_r; and h_r is the suction (in kPa) corresponding to residual state.

The FX and vG WRCC equation parameters were obtained by using SoilVision 4.21 and RETC code (SoilVision 4.21 2009; van Genuchten et al. 1991). SoilVision is a well-established database software for determining parameters of WRCC equations by following non-linear regression algorithm based on the quasi-Newton method (SoilVision 4.21 2009). To understand the importance of the residual suction data (> 10^3 kPa) measured with the WP4, the results of FFA were combined with the individual TM, MPS, and EQT measurements for WRCC parameter quantification. The WRCC equations fitted to the individual and combined results of FFA are depicted in Figures 4.5 and 4.6. The plots for other FAs were similar and thus not presented here for the sake of brevity. The fitting parameters obtained are listed in Tables 4.2 to 4.5 for individual measurements and combinations. It can be noted from Figure 4.5 that TM data might not be adequate for quantifying the FA as compared to MPS and EQT data, which approaches the residual state. The EQT has the advantage of having a few additional suction data towards the residual portion relative to the MPS. Figure 4.6 shows the utility of using residual suction data from

the WP4 in combination with TM results for better quantification of WRCC equations. However, the influence of combined residual data on MPS and EQT measurements was not significant. The residual portion of the WRCC represented by vG is different from that represented by FX in Figures 4.5 and 4.6. The appended WP4 data with EQT in Figure 4.6 clearly indicate that vG equation defines the residual state better than FX. For better understanding, the WRCC parameters obtained for individual and combination measurements were compared as below.

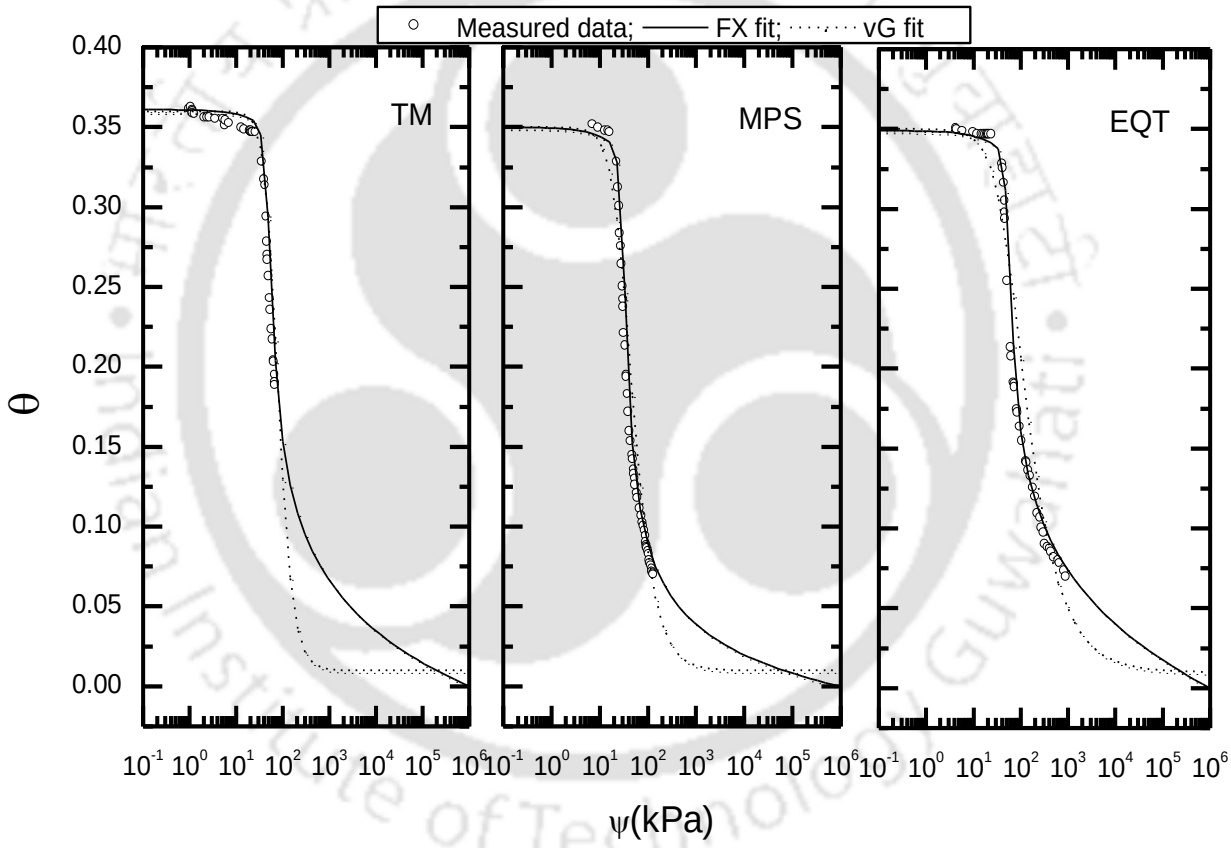

Figure 4.5 WRCC equations fitted to individual measurements of FFA

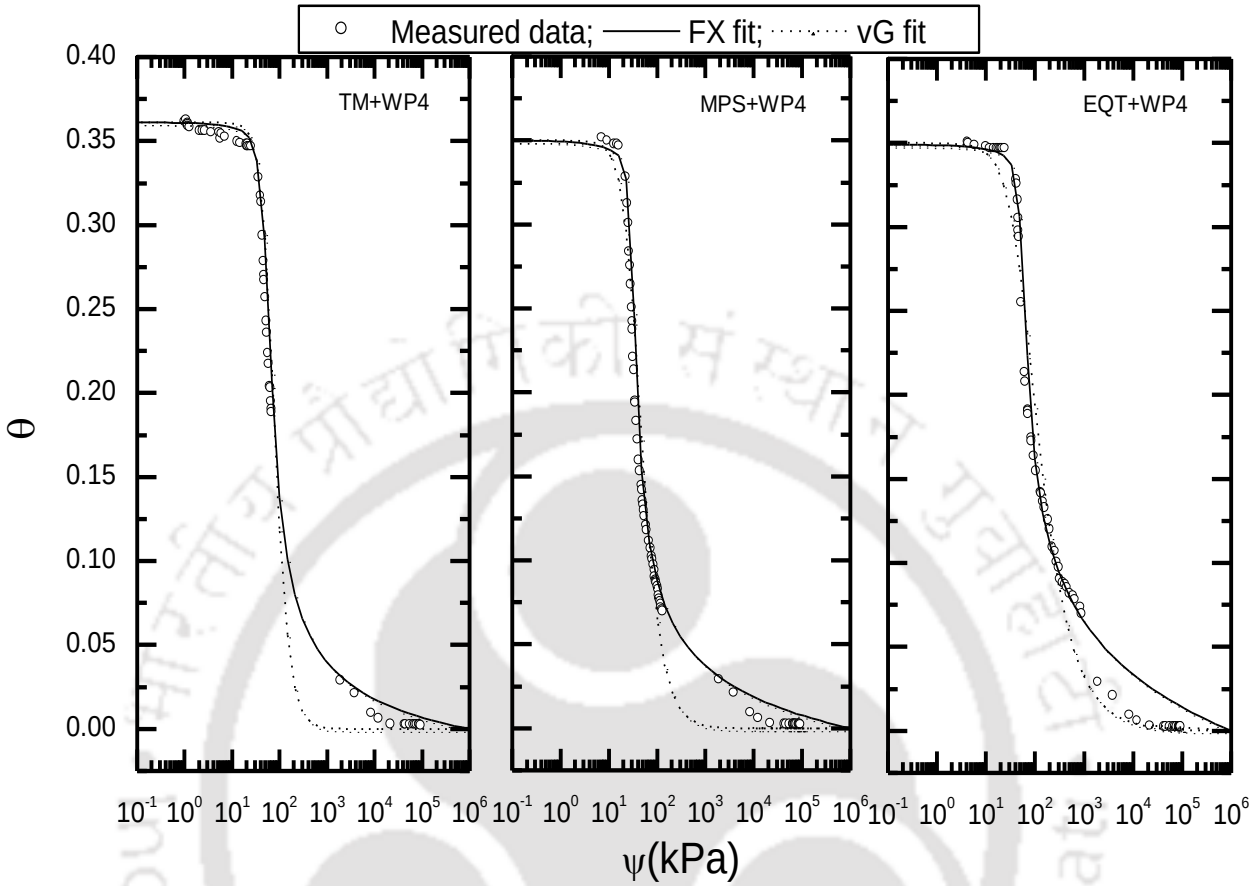

Figure 4.6 WRCC equations fitted to combined measurements of FFA

Tables 4.2 and 4.3 present a comparison of FX and vG WRCC equation parameters, respectively, for all FAs corresponding to individual measurements. For all the cases, parameters obtained based on WP4 results are high. Specifically, the AEV obtained based on WP4 results was one order of magnitude greater than those obtained by other measurement techniques. This is not expected for cohesionless materials such as FA. Similarly, a_f, n_f, and AEV values obtained based on TM measurements were marginally different from MPS and EQT results. Such an observation indicates that the inadequate range of the TM and inaccurate range of measurement by WP4 for suction less than 1000 kPa can lead to improper WRCC equation parameterization. However, it is quite interesting to note that for a particular measurement methodology, all FAs considered in this study exhibited comparable AEV and θ_r. A similar observation was made for vG WRCC, as shown in Table 4.3. All vG parameters based on WP4 measurements exhibited differences in comparison with TM, MPS

and EQT measurements.

Tables 4.4 and 4.5 were presented to study the influence of combined data on WRCC parameterization of FAs. It was noted that a_f, m_f, θ_r, and AEV values of individual and combined results are comparable for all methodologies used in this study. The parameter n_f of TM and TM+WP4 measurements varied marginally, whereas n_f based on MPS and MPS+WP4 was different from EQT results. Again, a_{vg} and n_{vg} parameters based on TM+WP4 measurements varied marginally from TM values and were close to MPS measurements, EQT measurements, and the combination results. The comparison indicates that the values of the parameters were influenced more by the low suction range. This was explicit from the parameters obtained for TM+WP4 measurements, which were close to those obtained for TM results. The WRCC parameters of different FAs varied and cannot be considered unique. However, the implication of marginal parametric variations of FAs corresponding to a particular measurement methodology needs to be further investigated.

Table 4.2 Comparison of FX WRCC parameters of FA for different methodologies

FX Parameter	Materials	Measurement method			
		TM	**MPS**	**EQT**	**WP4**
a_f(kPa)	FFA	44.86	29.02	50.27	696
	BFA	49.17	30.69	49.13	2073
	NFA	-	33.05	49.71	743
	PA	24.67	17.46	33.95	1284
n_f	FFA	6.77	7.81	9.31	6.11
	BFA	3.87	20	4.84	3.49
	NFA	-	3.61	2.01	19.72
	PA	2.69	11.83	4.83	20
m_f	FFA	0.46	0.55	0.37	1.26
	BFA	0.66	0.58	0.93	19.9
	NFA	-	0.66	0.76	0.81
	PA	0.59	0.40	0.56	0.84
θ_r	FFA	0.06	0.04	0.06	0.01
	BFA	0.06	0.04	0.03	0.02
	NFA	-	0.07	0.05	0.001
	PA	0.07	0.08	0.05	0.002
AEV (kPa)	FFA	32.68	22.69	41.23	263
	BFA	32.00	22.69	31.46	421
	NFA	-	20.71	20.71	538
	PA	12.53	14.67	22.69	593
R^2	FFA	0.992	0.901	0.997	0.946
	BFA	0.998	0.970	0.996	0.842
	NFA	-	0.998	0.998	0.900
	PA	0.998	0.976	0.989	0.991

-: Not available

Table 4.3 Comparison of vG WRCC parameters of FA for different methodologies

vG Parameter	Materials	Measurement method			
		TM	**MPS**	**EQT**	**WP4**
a_{vg} (kPa^{-1})	FFA	0.015	0.029	0.017	0.0024
	BFA	0.014	0.024	0.017	0.0015
	NFA	-	0.022	0.018	0.0012
	PA	0.027	0.040	0.024	0.0016
n_{vg}	FFA	3.25	2.40	1.76	3.52
	BFA	2.82	3.57	2.77	3.87
	NFA	-	2.08	1.59	13.36
	PA	1.89	2.25	1.82	3.54
m_{vg}	FFA	0.69	0.58	0.43	0.72
	BFA	0.65	0.72	0.64	0.74
	NFA	-	0.52	0.37	0.93
	PA	0.47	0.56	0.45	0.72
θ_r	FFA	0.01	0.02	0.01	0.02
	BFA	0.01	0.01	0.02	0.02
	NFA	-	0.02	0.05	0.01
	PA	0.01	0.02	0.03	0.02
AEV (kPa)	FFA	30.31	15.46	24.67	251
	BFA	28.88	21.71	29.05	310
	NFA	-	15.46	22.79	586
	PA	12.72	11.28	18.78	335
R^2	FFA	0.989	0.958	0.957	0.979
	BFA	0.997	0.906	0.987	0.953
	NFA	-	0.987	0.994	0.987
	PA	0.995	0.937	0.958	0.979

-: Not available

Table 4.4 Comparison of FX WRCC parameters of FA for combination of methodologies

FX Parameter	Materials	Measurement method		
		TM+WP4	MPS+WP4	EQT+WP4
a_f(kPa)	FFA	53.03	29.02	50.37
	BFA	44.40	30.38	45.92
	NFA	-	31.11	46.45
	PA	29.71	17.47	34.58
n_f	FFA	4.12	7.70	9.8
	BFA	4.64	20	8.21
	NFA	-	4.52	2.23
	PA	2.17	10.31	4.32
m_f	FFA	0.93	0.56	0.41
	BFA	0.47	0.52	0.60
	NFA	-	0.53	0.67
	PA	0.84	0.44	0.61
θ_r	FFA	0.04	0.03	0.05
	BFA	0.07	0.03	0.03
	NFA	-	0.03	0.03
	PA	0.04	0.06	0.05
AEV (kPa)	FFA	32.68	19.71	37.38
	BFA	31.12	18.77	35.58
	NFA	-	19.71	22.69
	PA	14.53	14.67	25.84
R^2	FFA	0.998	0.920	0.995
	BFA	0.991	0.931	0.967
	NFA	-	0.983	0.993
	PA	0.998	0.983	0.990

-:Notavailable

Table 4.5 Comparison of vG WRCC parameters of FA for combination of methodologies

vG Parameter	Materials	Measurement method		
		TM+WP4	MPS+WP4	EQT+WP4
a_{vg} (kPa^{-1})	FFA	0.015	0.028	0.017
	BFA	0.018	0.025	0.017
	NFA	-	0.023	0.018
	PA	0.029	0.041	0.024
n_{vg}	FFA	3.34	2.60	1.84
	BFA	1.70	3.83	3.13
	NFA	-	2.16	1.65
	PA	1.82	2.48	1.87
m_{vg}	FFA	0.70	0.615	0.456
	BFA	0.411	0.738	0.681
	NFA	-	0.537	0.393
	PA	0.451	0.596	0.465
θ_r	FFA	0.01	0.02	0.03
	BFA	0.03	0.02	0.01
	NFA	-	0.01	0.04
	PA	0.02	0.01	0.03
AEV (kPa)	FFA	33.38	19.71	22.79
	BFA	24.99	21.72	34.42
	NFA	-	17.04	20.69
	PA	14.70	10.75	16.23
R^2	FFA	0.994	0.990	0.975
	BFA	0.966	0.938	0.993
	NFA	-	0.983	0.995
	PA	0.989	0.965	0.979

-: Not available

4.5 Summary

This study evaluated suitable suction measurement methodologies and water retention characteristics curves (WRCC) for FAs. Four different suction measurement instruments-tensiometer (TM) (0-80 kPa), matric potential sensor (MPS) (0-300 kPa), equitensiometer (EQT) (0-1000 kPa), and dew point potentiameter (WP4) (1 MPa to 300 MPa) were used to establish WRCCs. It was found that TM is not appropriate for high-calcium materials, which tend to harden during measurement, resulting in poor responses. The limited range of TM does not include all the major portions of the WRCC. All FAs considered in this study approached a residual state of suction within 10^3 kPa. Therefore, a reliable WRCC representing saturation, desaturation, and residual stages can be obtained using instrument

like EQT for FAs. The study indicates that a high-suction measuring instrument like WP4 has limited application for establishing WRCC of cohesionless materials like FA. At the same time, it can be used to determine the residual portion of WRCC of FA precisely. It was noted that the residual data obtained using the WP4 could be appended with a low suction-range instrument such as a TM for better representation of the WRCC. However, the values of the WRCC parameters were found to be influenced more by the low suction range. The vG WRCC equation fitted well for the combination of low and high suction results. The WRCC parameters of FAs obtained based on different measurement methodologies cannot be considered unique. For a particular instrument, there is not much comparison of WRCC parameters of FAs, and thus it cannot be generalized. When high suction measurements of WP4 were appended with TM, MPS, and EQT results, then the WRCC parameters were found to be more comparable than the individual measurements. The overall variation of WRCC fitting parameters for FA for different combinations was listed in this study. The sensitivity of such variations on unsaturated behavior modeling of FA needs to be investigated in detail.

Chapter 5

Water Retention Characteristic of Bentonite and Fly Ash-Bentonite Mixes

5.1 General

The objective of this chapter is to appraise the variability of water retention characteristic curve (WRCC) of different high plastic bentonites (B). Bentonites are known for its high volume change behavior when it interacts with water. The effect of high volume change of bentonite on WRCC and its implication on WRCC parameterization was investigated. The studies reported in the literature to an extent have circumvented the influence of volume change on WRCC by reporting the results in terms of gravimetric water content. However, most of the field applications and mathematical formulations require WRCC in terms of volumetric water content. This study recommends a mandatory approach for determining the WRCC model parameters unambiguously by considering the results of shrinkage characteristics. A robust method was presented for determining volumetric shrinkage curve for bentonite. The influence of fly ash (FA) type and FA content on the WRCC of FA-B mixes was studied in detail. This study was done with an intention of exploring FA-B mixes as hydraulic barriers in waste management projects. The observation from this study would help to understand the possibility of generalizing WRCC of FA-B mixes when FAs from different sources are used.

5.2 WRCC of bentonites

The WRCC of bentonites B1 to B4 plotted in terms of gravimetric water content (w) and total suction (ψ) measured using WP4 corresponding to the initial compaction state given in Table 5.1 were compared as shown in Figure 5.1. The initial water content (w) was kept near to liquid limit (LL) for uniformity and to maintain ψ close to zero. Low initial dry unit weight of the samples was due to high initial w and mild press packing using spatula. The WRCC presented in Figure 5.1 corresponds to continuous drying of the same bentonite sample by following the procedure mentioned in sections 3.6. As expected, it was seen that WRCC of all the bentonites exhibited an increase in ψ with drying due to reduction in w. The initial point of WRCC of bentonites was different due to the difference in initial w, which was attributed to the varying liquid limit (LL) of bentonites. However, as w decreased with drying, the variation in WRCC among different bentonites decreased. There was a drastic reduction in w in the initial stages of measurement which indicated a rapid loss of water from the sample associated with low

water retention at high water content. Except B1, ψ of all bentonites varied from 10^3 kPa to $4x10^5$ kPa, which is within the accurate measurement limits of WP4 instrument used in this study. Above 10^4 kPa, w-ψ variation of all the bentonites coincided and there was minimal change in w with ψ. This indicated that all bentonites have attained residual state completely (Fredlund and Rahardjo 1993).

Table 5.1 Compaction state of bentonites for WRCC measurement

Bentonite	w (%)	γ_d (kN/m^3)
B1	298	2.9
B2	315	2.8
B3	433	2.1
B4	252	3.5

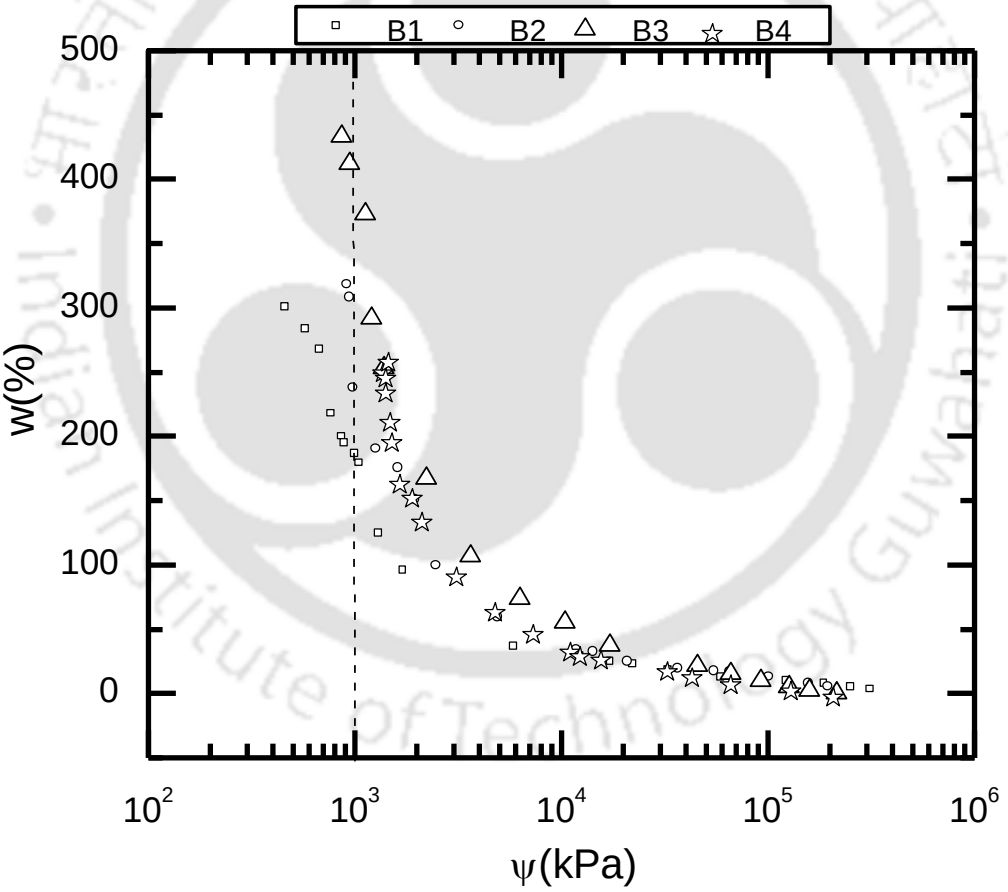

Figure 5.1 WRCC of bentonites presented in terms of gravimetric water content

5.3 Evaluation of osmotic suction (ψ_o) component of bentonite

It was necessary to understand the contribution of osmotic suction (ψ_o) towards the total suction (ψ) of bentonites measured using WP4. It is understood that ψ_o is due to the dissolved salts present in the soil. Therefore, all bentonites were repeatedly washed with deionized water by following the procedure given in section 4.2. After washing with deionized water for 2, 4 and 6 days, WRCC of bentonites was determined using WP4. It was found that the WRCC of original and washed sample matches very well for all the bentonites. For the sake of brevity, only the result of B1 is presented in Figure 5.2. The figure shows that the measured WRCC of unwashed and washed samples matches well. This shows negligible osmotic suction (ψ_o) for all bentonites considered in this study. Therefore, total suction (ψ) measured using WP4 can be considered equal to matric suction (ψ_m). The data presented in Figure 5.2 also ascertains the repeatability of WRCC measurements of bentonites using WP4.

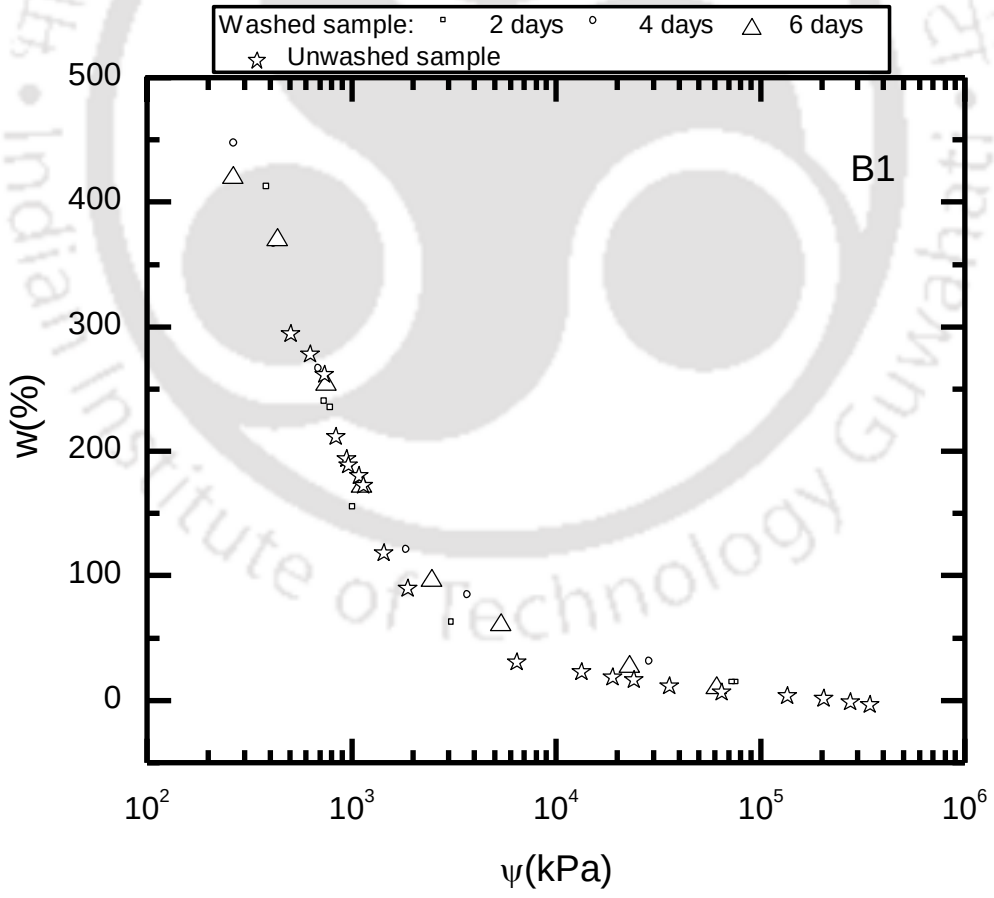

Figure 5.2 WRCC of B1 for washed and unwashed samples

5.4 Shrinkage characteristics of bentonites during air drying

It is an established fact that high plastic soils like bentonites exhibit high shrinkage during drying as compared to soils having less plasticity. The shrinkage characteristics would influence the WRCC of bentonites (Tripathy et al. 2014; Marinho 1994). Therefore, it is important to determine the shrinkage characteristics of different bentonites along with the suction measurement. The usefulness of shrinkage measurements for unambiguous WRCC parameterization was not studied in detail. Bentonite samples with initial compaction state mentioned in Table 5.1 (for maintaining same initial state as in WP4 measurements) were subjected to free shrinkage by air drying for establishing volumetric shrinkage characteristics. Two methods were used for volumetric shrinkage measurement in which the first method adopts the volume determination by conventional mercury displacement technique (IS 2720: part VI (1972)). The limitation of this method is that closely spaced data cannot be obtained. The second method was based on the rubber balloon technique proposed by Tariq and Durnford (1993). Brief descriptions of these two procedures are given below.

Bentonite samples were mixed with required amount of water and kept in the desiccators for almost one week for maturation and uniform distribution of water in the sample. The prepared sample was then divided into two halves for performing volume change measurement by the above two methods. This will ensure same initial water content of the samples for shrinkage measurements and better comparison of the two methods. For the balloon method approximately 100 g of the matured soil sample was taken and carefully placed inside a balloon as shown in Figure 5.3. Due to the elasticity of the balloon the sample remains unconfined throughout the test. The mouth of the balloon was closed with a rubber stopper. The rubber stopper has two openings, one inlet and another outlet for circulation of air inside the balloon. These opening were connected to a valve which can be closed when required. For drying of the sample, air was continuously allowed to pass inside the rubber balloon through the inlet valve by using a low pressure air pump. During this period, the outlet valve was kept open. The low rate of air circulation in and out of the balloon causes slow air drying of the sample. The reduction in volume and weight of the sample was measured at regular interval of time (approximately 12 hr). To measure the volume, the inlet valve was closed and the outlet was connected to a low capacity suction pump. A small suction pressure was applied and the outlet valve was kept closed. This will ensure proper encompassing of the balloon around the shape of the soil sample. The sample with the balloon was then dipped in a small beaker containing water, which was placed on an electronic balance of accuracy

0.01 g. This will give the mass of water displaced by the soil sample based on the Archimedes principle. Also, the weight of the sample was taken in air by directly placing it on the weighing balance. In this manner, the reduction in volume and weight of the sample was recorded with time till there was no further change in volume. The total time required for drying was about 20 days for high plastic soils like bentonites. The sample was taken out of the balloon and was kept in the oven at 105-110 ^{o}C for 24 hrs. The oven dried weight of the sample was noted and w was back calculated for each of the previous reading. Bulk unit weight of the sample was calculated from the measured volume and mass of the sample and thus dry unit weight was obtained. Using the specific gravity (G) and dry unit weight (γ_d), void ratio (e) was calculated corresponding to different stages of drying. The volumetric water content θ was obtained using the relation $\theta = w.(\gamma_d/\ \gamma_w)$, where γ_w is the unit weight of water.

Figure 5.3 Balloon method set up used for volumetric shrinkage measurement

The results were plotted in terms of e versus w and e versus θ for all bentonites as shown in Figure 5.4(a) and 5.4(b), respectively. A 100% saturation line data was calculated for each bentonite and plotted along with the measured data in e-w plot. As seen in Figure 5.4(a), the measured data exactly follows the 100% saturation line till a minimum void ratio (e) was reached and beyond which e approaches a constant value. This indicates that all bentonite samples remains saturated over a wide range of w and

matches well with the observation reported in the literature (Tripathy et al. 2014; Fityus and Buzzi 2009). Three different trials were performed for each bentonite to confirm the repeatability of the measured results. It was found that all the trials gave identical results.

The shrinkage characteristic was also obtained by conventional mercury displacement technique. The matured soil sample was put in the shrinkage disc and was tapped so that any entrapped air inside the sample would escape. The surface of the sample was then leveled with a spatula and was kept for air drying. The change in volume of the sample at different stages of drying was measured with the help of mercury displacement technique as given in IS 2720: part VI (1972) till it reaches near dry state. The corresponding weight of the sample along with the shrinkage dish was also taken with the electronic balance. The change in volume of the sample was calculated at each stage of measurement by subtracting from the initial volume of the sample. The process was repeated till the volume change of the sample became negligible. The sample was then kept in the oven for drying. After 24 hrs, the dry weight was obtained and w was back calculated for previous measurements. Further γ_d and e was calculated by knowing G for different stages of drying as explained earlier.

The disadvantages of mercury method are (a) skilled measurement is required for precise volume displacement, (b) any small error in mercury volume measurement would lead to high error in volume calculation (due to high specific gravity of mercury), (c) initial high w samples cannot be used for shrinkage measurement, (d) closely spaced volumetric shrinkage data could not be obtained, (e) several different samples need to be prepared for measurement at regular intervals, (f) several samples have to be discarded due to excessive cracking resulting from constrained shrinkage due to the boundary effect of shrinkage dish. All the above disadvantages could be effectively alleviated in balloon method discussed above. The important advantage of balloon method is that it is a simple and economical procedure with better control and gives closely spaced shrinkage data for the same soil sample. Therefore, void ratio versus water content variation obtained from balloon method can be termed as volumetric shrinkage characteristics curve (similar to WRCC). The results of balloon method and mercury method were plotted together as shown in Figure 5.4(a). It was found that both the methods of measurements matched very well. This also verifies the accuracy of the balloon method for determining the shrinkage characteristics.

Similar non-linear variation of e versus θ was observed for all bentonites as shown in Figure 5.4(b) exhibiting three well defined stages of drying. For the first stage of drying corresponding to initial high water content portions ($\theta > 0.8$), the decrease in e was

very high as compared to a minimal decrease in θ. This was due to the nearly proportionate total volume reduction of the soil in comparison with the reduction in volume of water during drying. This was followed by second stage where there is significant variation in θ with e till it approaches a constant value of e. In the third stage, θ reduced with constant e, wherein the soil particles would be sufficiently close to each other preventing further change in volume with decrease in w to dry state. The inter granular strength mobilization in third stage would prevent the soil particles from coming close to each other while it approaches oven dried state. Therefore, later portion of the e-θ curve shows a very minimal change in e value even though there was variation in θ.

It can be specifically noted that the desaturation or the air entry point was not obvious from the WRCC results presented in Figure 5.1 for all bentonites. For e-w plot in Figure 5.4(a), S_r was computed and plotted against corresponding e values as shown in Figure 5.5. This plot clearly shows the point of desaturation where S_r becomes less than 1. A horizontal line was drawn at S_r=1. The point where the measured data deviates from the horizontal line was noted and the e value corresponding to this point was considered as the e at desaturation or the air entry point and denoted as e_{ds}. Corresponding to e_{ds} value, θ_{ds} was noted from Figure 5.4(b) which will give the θ at air entry according to the definition of air entry value (AEV) of WRCC (Brooks and Corey 1964). The values of e and θ at the air entry point for different bentonites are listed in Table 5.2. It was found that when the e value increases at air entry point, θ also increases simultaneously. The e_{ds} and θ_{ds} can be considered unique since e-w variation for different trials gave a unique repeatable trend.

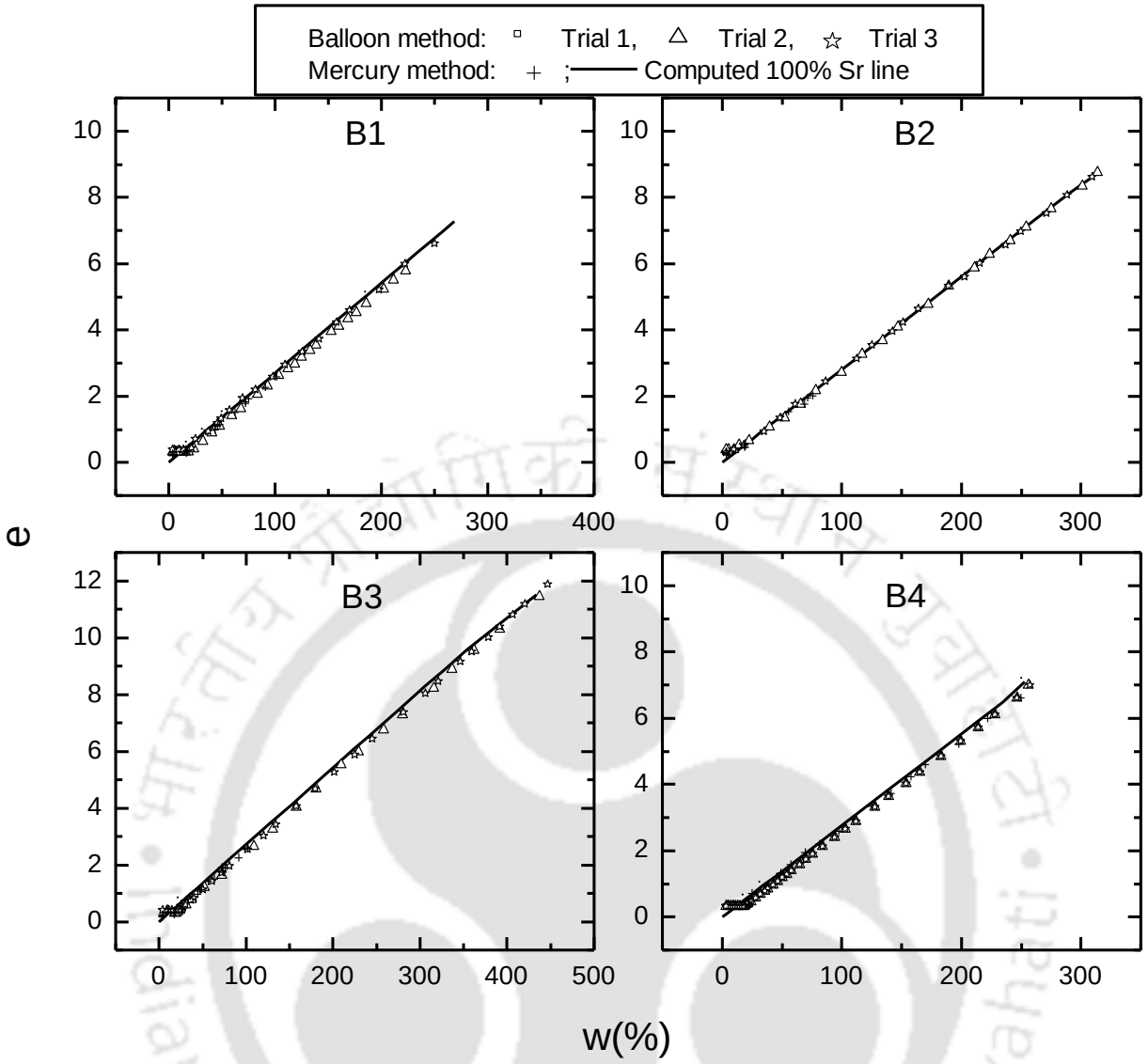

Figure 5.4(a) e-w variation of bentonites during air drying

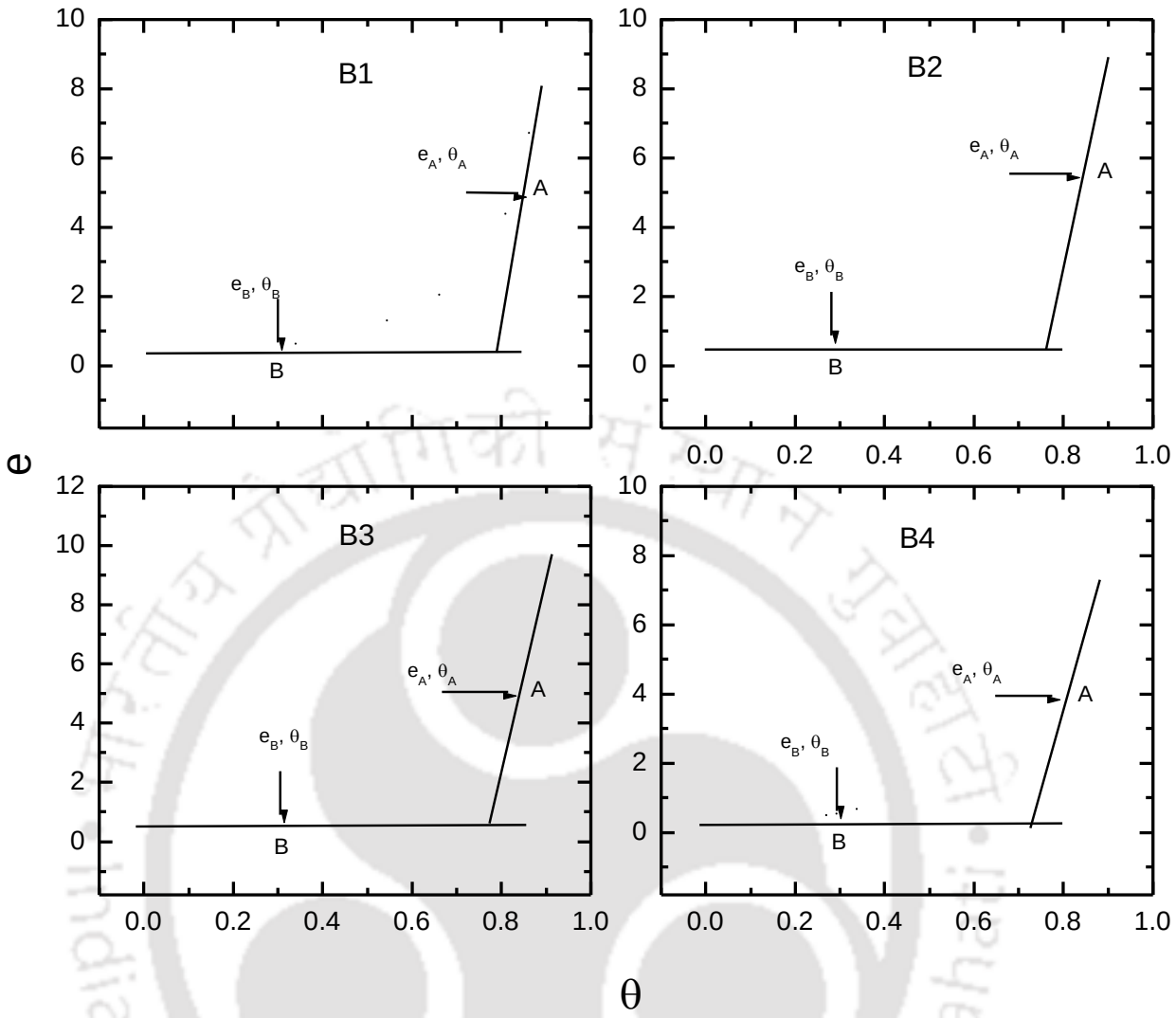

Figure 5.4(b) e-θ variation of bentonites during air drying

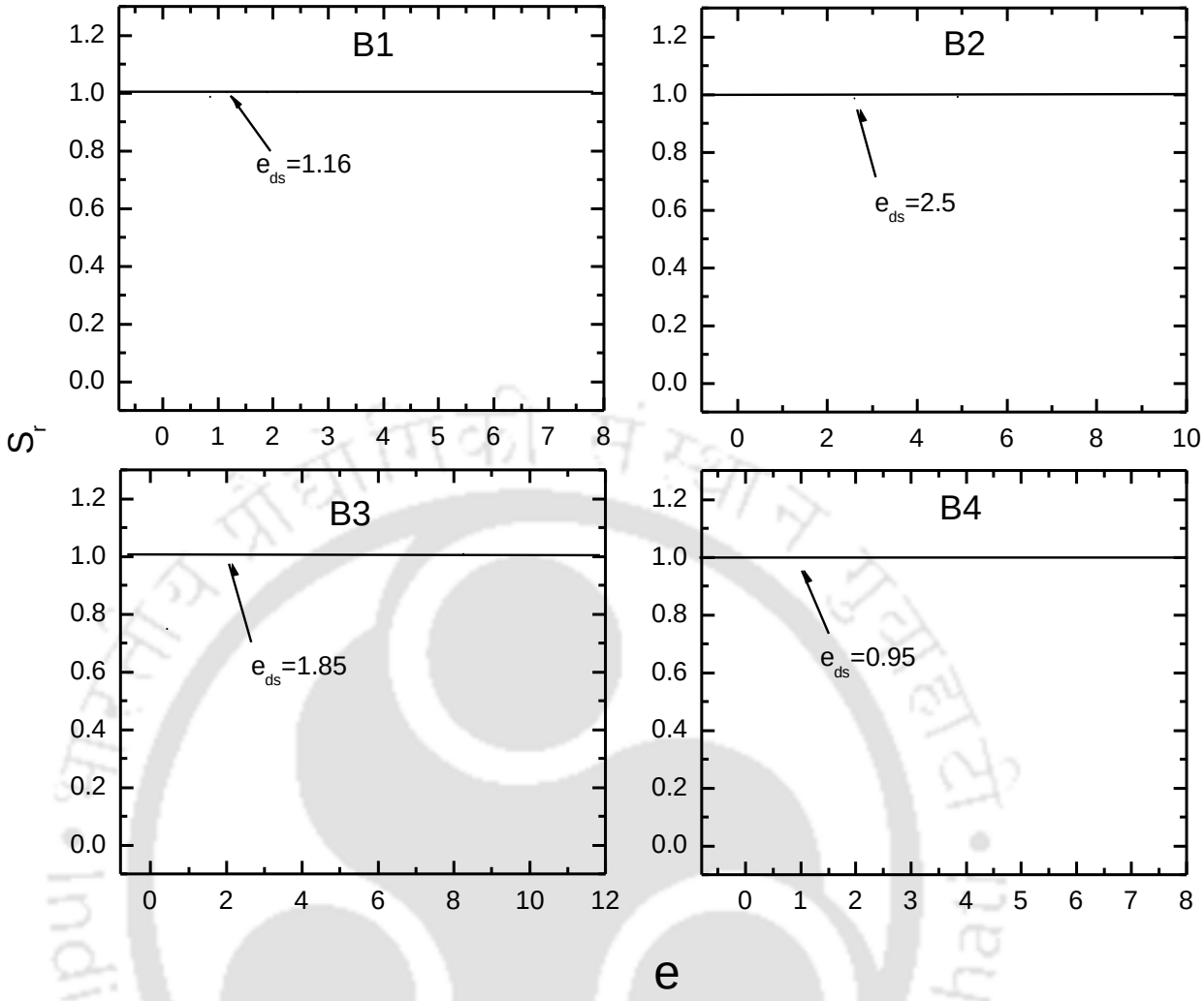

Figure 5.5 Variation of S_r with e for bentonites

Table 5.2 e_{ds} and θ_{ds} at air entry point for bentonites

Bentonite	e_{ds}	θ_{ds}
B1	1.16	0.53
B2	2.5	0.68
B3	1.85	0.62
B4	0.95	0.48

Table 5.2 was compared with e and θ values corresponding to the transition points A and B as shown in Figure 5.4(b). Tangent was drawn on the initial and final portions of e-θ curve. The point where the shrinkage data deviates from the tangent was noted and e, θ values corresponding to this point was tabulated in Table 5.3. It can be noted that e_{ds}, θ_{ds} lies on the transition curve from e_A, θ_A to e_B, θ_B. From this exercise, the physical significance of the transition points A and B could not be clearly understood. Further analysis is required for better understanding of these transition points A and B.

Table 5.3 Summary of transition points A and B on e-θ variation curve

Sample	Deviation point			
	e_A	θ_A	e_B	θ_B
B1	4.98	0.85	0.44	0.30
B2	5.51	0.84	0.49	0.28
B3	5.06	0.84	0.46	0.31
B4	3.93	0.81	0.40	0.29

For different w points in WRCC (Figure 5.1) the corresponding e value was obtained from the e-w relationship of respective bentonites depicted in Figure 5.4(a). It must be noted that the initial points for shrinkage test and WRCC were same. The e value obtained was used to calculate the corresponding dry unit weight (γ_d) and finally the volumetric water content (θ) using the relationship $\theta = w.(\gamma_d/\gamma_w)$, where γ_w is the unit weight of water. Thus WRCC of all the bentonites was expressed in terms of θ as shown in Figure5.6. For the near saturation portion of WRCC, a gradual decrease in θ was found with increase in ψ, unlike the sharp decrease exhibited in w-ψ representation in Figure 5.1. Also, the slope of the residual portion is higher than in w-ψ representation. It was observed that the results of B1 and B2 matches well, which has comparable plasticity characteristics. For a particular θ, B3 is showing a highest ψ while B4 is indicating lowest ψ. This can be attributed to the highest and lowest plasticity characteristics of B3 and B4, respectively as reported in Table 3.3.

A very important apprehension here is whether the data in Figure 5.6 can be used for WRCC parameterization of bentonites like other low plastic soils without any data processing. It may be noted here that low plastic soils may not undergo significant volume change like bentonite. The initial volumetric water content and void ratio designated as θ_i and e_i, respectively, was obtained for all bentonites from Figures 5.6 and 5.4(b). These points were listed in Table 5.4, which shows that θ_i is greater than 0.8. However, data presented in Table 5.2 indicates that θ at air entry (θ_{ds}) is much less than 0.8. This obviously means that the WRCC presented in Figure 5.6 cannot be used directly for parameterization according to the conventional definition of air entry value (AEV), which asserts the actual desaturation point. The following section therefore investigates WRCC parameterization of bentonite in detail.

Comparing e_i and θ_i of WRCC listed in Table 5.4 with e_A and θ_A listed in Table 5.3, it can be noted that the values are close to each other specifically the volumetric water content. It was clear from previous discussion that θ_i will not represent air entry

point for high plastic soils like bentonite. Therefore, it was hypothesized in this study that θ_i or θ_A would represent a state of first appearance of crack in the drying bentonite sample. For convenience, this state was defined as macro air entry value (AEV) because air do enter into the crack. However, bentonite portion around the crack is still under full saturation. The actual AEV at which saturation (S_r) deviates from 100% was designated as micro AEV in this study. The hypothesis in this study was further investigated with crack development experiments as shown in Figure 5.7, wherein θ corresponding to first appearance of crack was noted and tabulated in Table 5.5 as θ_c.

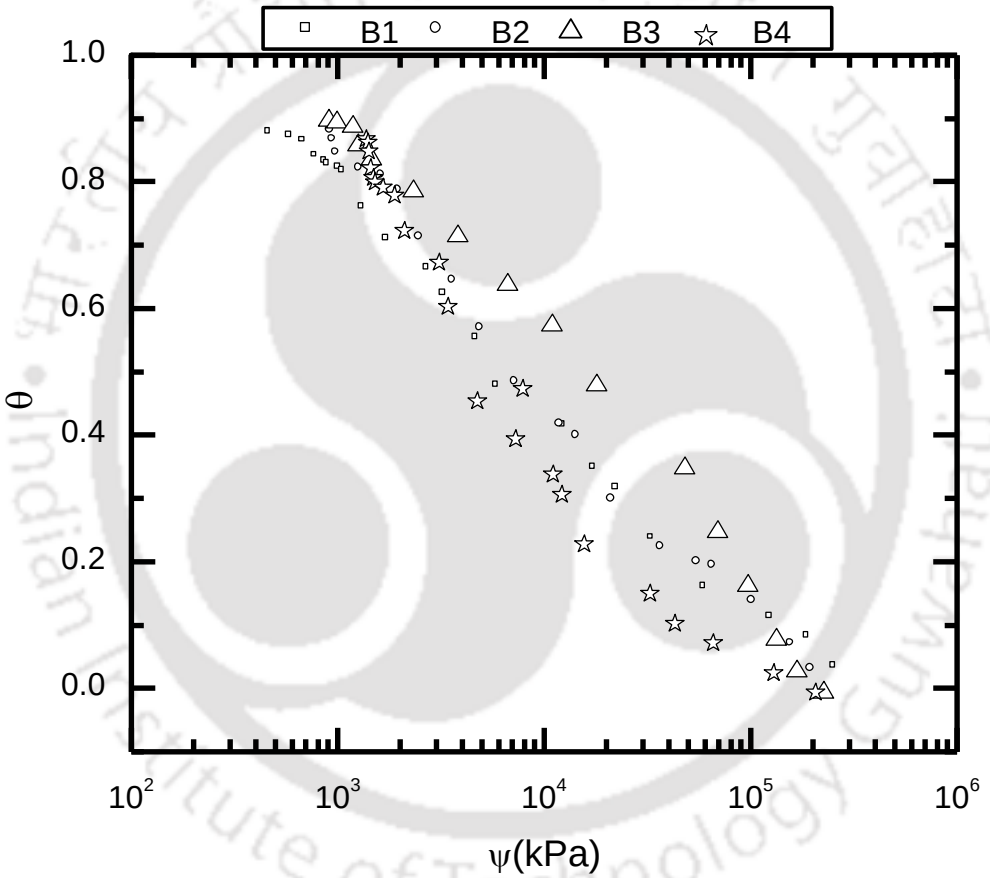

Figure 5.6 WRCC of bentonites in terms of volumetric water content θ

Table 5.4 Details of initial state of bentonites in terms of e_i and θ_i

Bentonite	e_i	θ_i
B1	6.29	0.87
B2	7.41	0.88
B3	8.71	0.90
B4	6.74	0.87

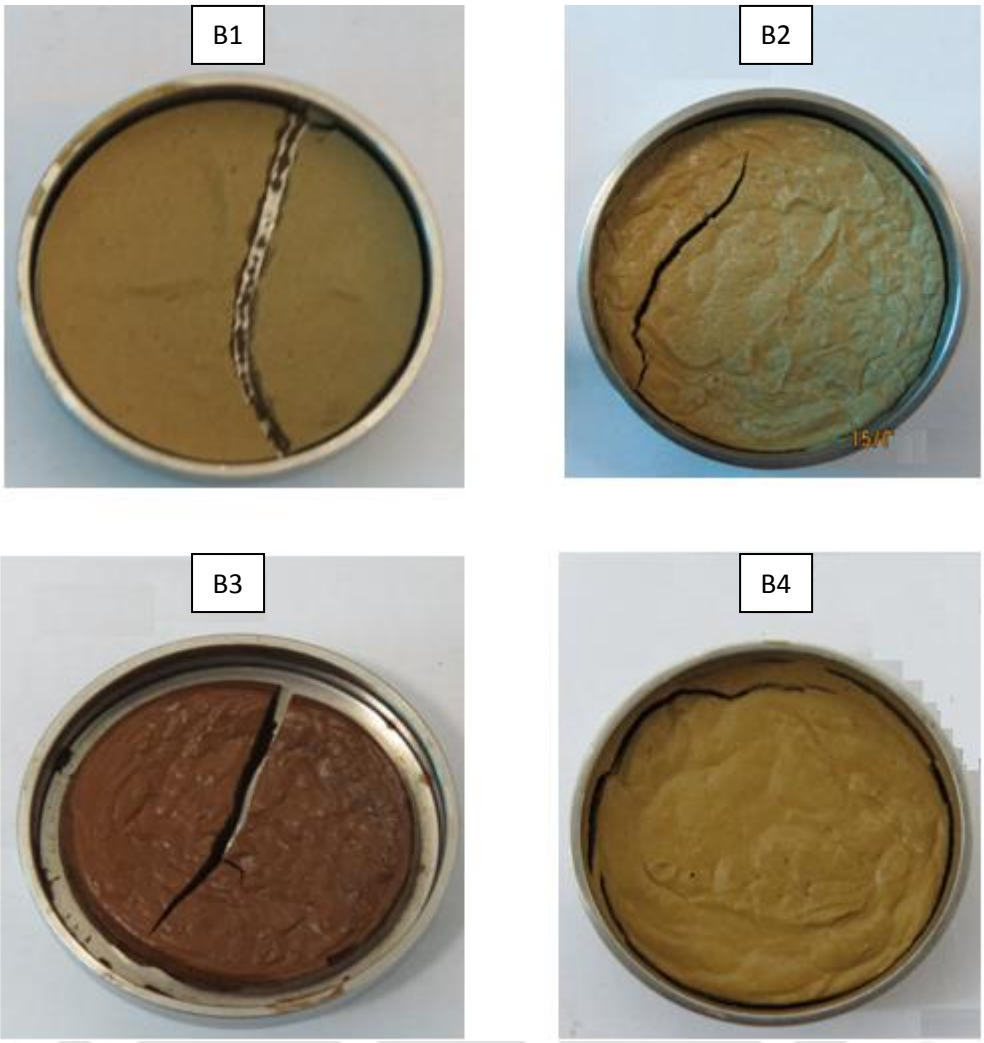

Figure 5.7 Depiction of first development of crack in bentonite samples

Table 5.5 θ_c corresponding to first appearance of crack in bentonite samples

Bentonite	θ_c
B1	0.82
B2	0.87
B3	0.87
B4	0.85

It can be noted from Table 5.5 that volumetric water content at first appearance of crack in the bentonite samples, θ_c, matches relatively well with the corresponding θ_i. This also indicates the physical significance of θ_A related to the first appearance of crack and the concept of macro AEV for high plastic soils like bentonite samples during drying. However, no such physical relevance could be established for the points e_B and θ_B with

respect to WRCC of bentonites other than the fact that θ_{ds} is approximately twice the value of θ_B.

5.5 WRCC parameterization of bentonite

It is clear from previous discussion that WRCC parameterization of bentonite cannot be done directly with the available measured suction data. In this study, two different approaches were used to obtain the WRCC equation parameters of Fredlund and Xing (FX) and van Genuchten (vG) models. The first approach include the full dataset of measured WRCC in terms of θ and ψ (Figure 5.6) by considering macro AEV. The second approach includes selected measured data which strictly adheres to the shrinkage characteristics of bentonites and by considering micro AEV (based on conventional definition of AEV). Bentonite samples remain saturated for a wide range of θ during drying even with the development of cracks, which was confirmed by Figure 5.7 and Table 5.5. Such observation was reported by Fityus and Buzzi (2009) as well. Due to this, there will be ambiguities while defining saturated θ_s and AEV, and would influence the determination of WRCC equation fitting parameters of bentonites. Therefore both the approaches were discussed below to understand the uncertainties associated with the WRCC parameterization of bentonites and proposed an appropriate methodology to alleviate the ambiguities.

5.5.1 Approach 1:

In this approach, bentonite samples were mixed with w close to liquid limit (LL) and then air dried. The whole of the drying data was then used for WRCC parameterization as shown in Figure 5.8 for bentonites B1 to B4. The fitting parameters were obtained by non-linear least square regression method by fitting FX equation to empirical data in graphical software Microcal Origin (Sreedeep and Singh 2006) and vG equation parameters using well established RETC code (van Genuchten et al. 1991). As seen from Figure 5.8, both the FX and vG equation fitted well with the measured data for all the bentonites. The goodness of fit was confirmed by regression coefficient (R^2) which was close to unity. The parameters for both the fits along with R^2 values are listed in Table 5.6. It needs to be specifically noted that for all bentonites there is a well defined near saturation portion of WRCC for θ ranging from 0.8 to 0.9. This approach gave AEV$\leq$ 1400 kPa. However, there is an ambiguity whether θ of 0.8-0.9 would really represent θ_s for high volume change soils like bentonites or such a high value is due to the choice of high w close to LL as the initial point of drying. If the latter is true then this

would cause uncertainties in WRCC parameterization of bentonites, biased by the initial w selected by the user. Such a hypothesis was further investigated and presented in section 5.5.2

Table 5.6 shows the comparison of FX and vG WRCC equation parameters for B1 to B4 using approach 1. It was seen that all the FX parameters except n_f were relatively comparable. The m_f parameter was marginally higher for B1, while it was comparable for B2, B3 and B4. The AEV obtained from the FX model were more or less comparable for all the bentonites. Even though the bentonites were different in terms of its physical properties, the same was not reflected much in WRCC parameter variations. Similar to FX model, there was only a marginal variation in vG parameters for all bentonites. However, it is important to investigate the impact of marginal variation in WRCC parameterization on the unsaturated behavior modeling. This is due to the fact that the reliability of such modeling is entirely dependent upon the input WRCC parameters of soils.

In approach 1, the near saturation portion of WRCC for θ in the range 0.8 to 0.90 was presumed to be due to macro air entry where the cracks started appearing in the sample during drying. This can also be treated as the transition point between structural shrinkage and normal shrinkage (Tang et al. 2011). However, this was not explicit in the experimental trend for drying (Figure 5.4(a)). The macro air entry is different from actual definition of AEV, which indicate the desaturation point. Table 5.2 shows that 0.8-0.9 was much higher than θ_{ds}. For eg: for the range of $0.87 < \theta_s < 0.53$, B1 sample remains saturated due to proportionate shrinkage and reduction in pore volume along with water loss. The user can choose any value of θ_s ranging from 0.87 to 0.53 for parameterization if shrinkage curve was not referred to. Approach 2 was used to circumvent this uncertainty arising due to the ambiguous choice of θ_s by the user.

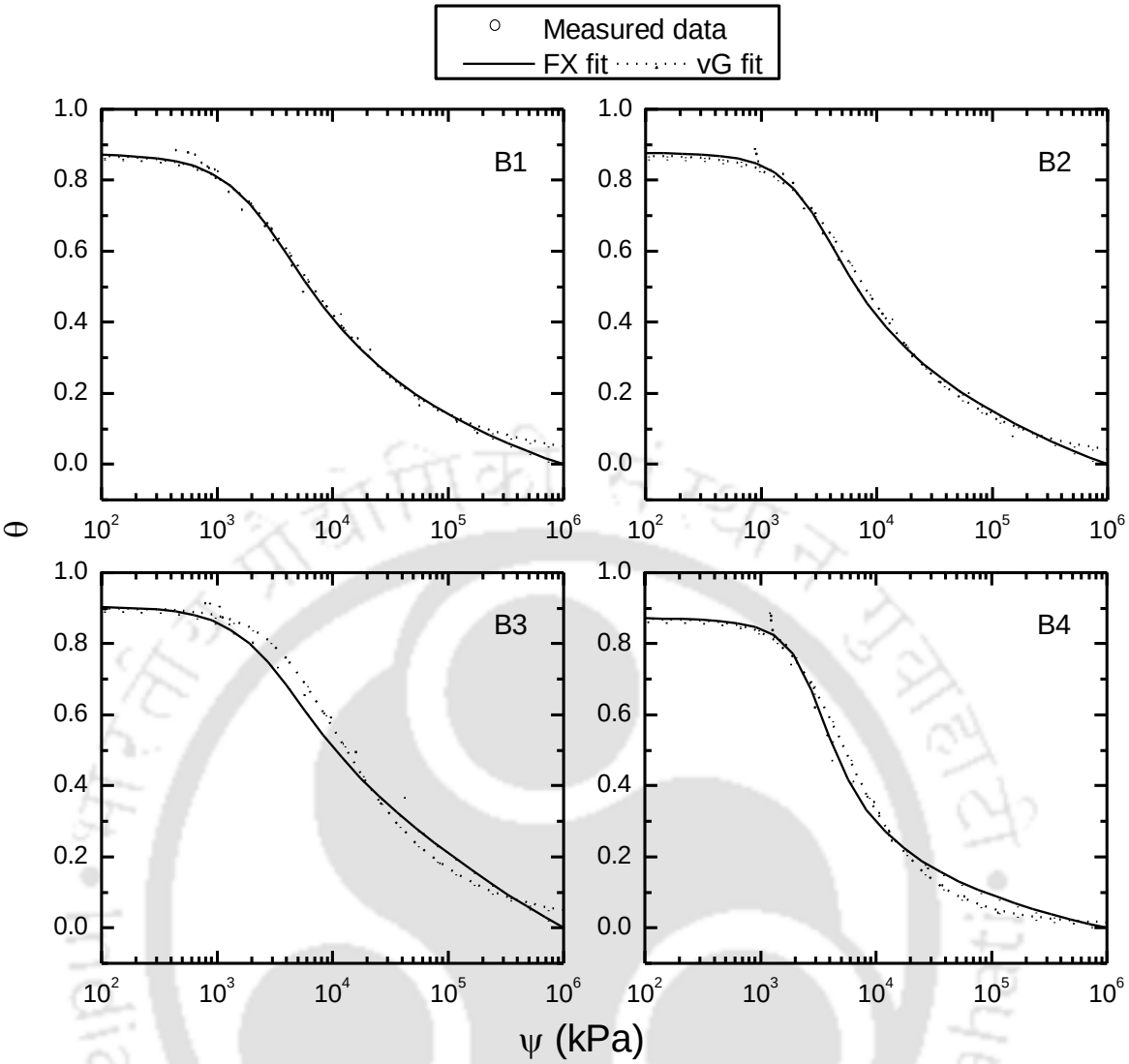

Figure 5.8 WRCC parameterization for bentonites using approach 1

Table 5.6 FX and vG WRCC parameters of bentonites using approach 1

WRCC Model	Fitting parameters	Bentonites			
		B1	**B2**	**B3**	**B4**
FX	a_f (kPa)	2244	2415	2499	2380
	n_f	1.65	2.08	1.59	3.18
	m_f	0.68	0.58	0.56	0.59
	θ_r	0.09	0.12	0.14	0.11
	AEV(kPa)	876	1218	1115	1329
	R^2	0.99	0.99	0.96	0.95
vG ($m_{vg} = 1 - \frac{1}{n_{vg}}$)	a_{vg} x10^{-5}(kPa^{-1})	39	29	18	29
	n_{vg}	1.51	1.58	1.60	1.88
	m_{vg}	0.34	0.37	0.37	0.47
	θ_r	0.08	0.06	0.10	0.07
	AEV(kPa)	876	1218	1930	1329
	R^2	0.99	0.99	0.97	0.98

5.5.2 Approach 2:

In this approach, the shrinkage characteristics of bentonite (e-w) were obtained to determine the variation of S_r with θ. The S_r-θ plot was used to identify the point of desaturation precisely. This point will be unique for a given bentonite, provided initial w is sufficiently high to give 100 % saturation (ψ≈ 0) as explained earlier. The methodology for choosing θ_{ds} corresponding to desaturation point was explained in Figure 5.9 for bentonite B1 as an example. This θ_{ds} was then used as the modified initial θ. The data falling above θ_{ds} were not considered and the remaining data was used for WRCC parameterization. The same procedure was followed for other bentonites. It is explicit that desaturation (S_r< 1) occurs at θ=0.53. This means that when drying initiates from θ= 0.87, B1 remains saturated till θ=0.53. Therefore, air entry and desaturation corresponds to θ=0.53 for B1. This AEV is presumed to be micro AEV which confirm to the conventional definition of AEV (Brooks and Corey 1964). The methodology discussed in approach 2 alleviates the possibilities of multiple initial volumetric water content depending on users and results in unique WRCC parameters for high volume change soils like bentonite. The FX and vG models were fitted to measured data by following the methodology explained in Figure 5.9 and depicted in Figure 5.10 for all bentonites. The AEV obtained using approach 2 will be more physically relevant in line with its definition. The fitted parameters obtained using approach 2 are listed in Table 5.7

Table 5.7 FX and vG WRCC parameters of bentonites using approach 2

WRCC model	Fitting Parameters	Bentonites			
		B1	B2	B3	B4
FX	a_f (kPa)	14000	9520	52000	12528
	n_f	2.5	1.8	2.6	2.41
	m_f	0.55	1.12	1.10	1.05
	θ_r	0.03	0.04	0.016	0.038
	AEV(kPa)	6449	3490	12451	5779
	R^2	0.993	0.977	0.991	0.974
vG ($m_{vg} = 1 - \frac{1}{n_{vg}}$)	a_{vg} x10^{-5}(kPa^{-1})	7	12	4	10
	n_{vg}	1.98	1.92	2.05	2.30
	m_{vg}	0.495	0.479	0.512	0.565
	θ_r	0.03	0.097	0.016	0.025
	AEV(kPa)	6038	3810	10221	4744
	R^2	0.986	0.959	0.989	0.972

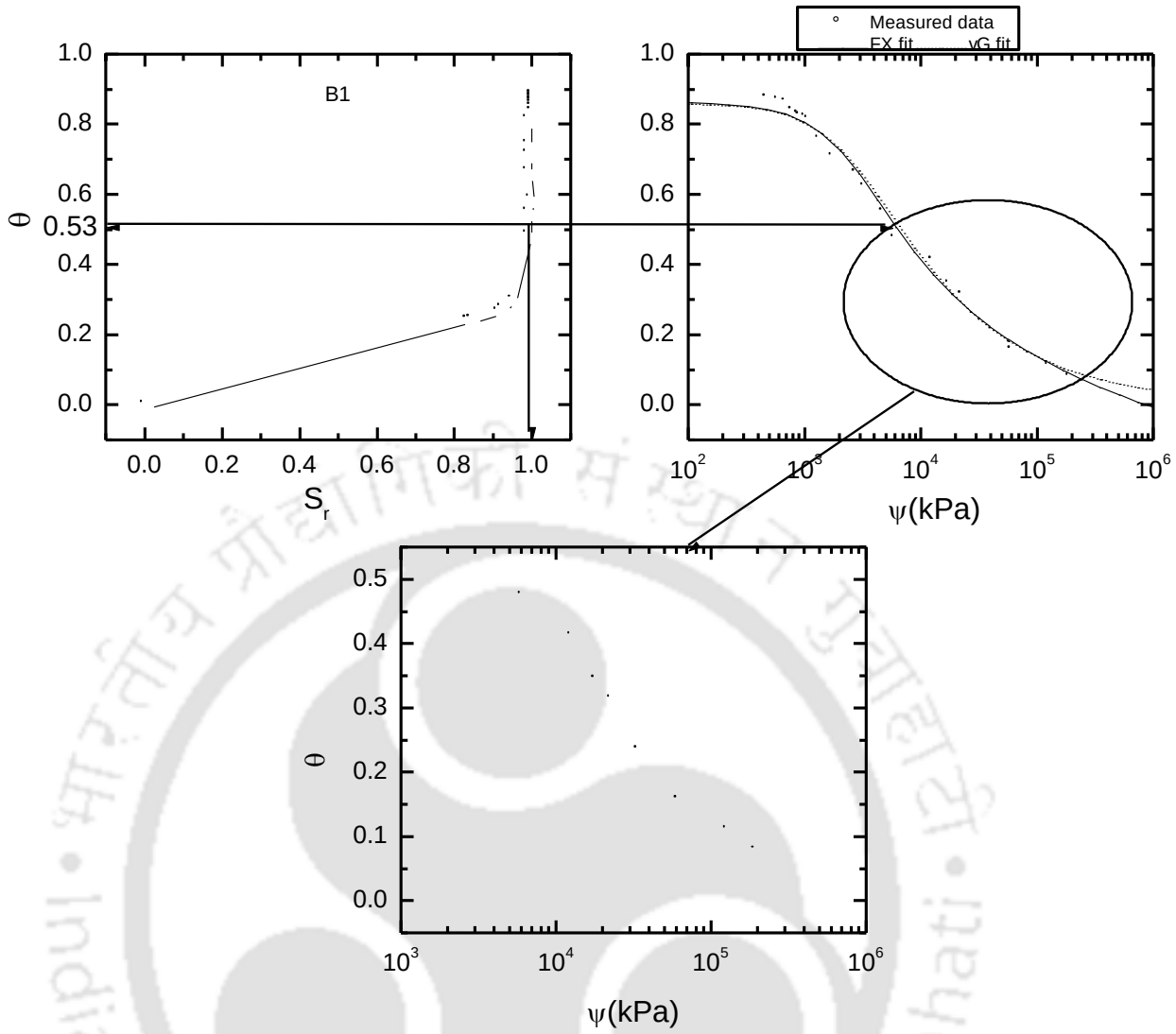

Figure 5.9 Methodology for choosing appropriate range of WRCC for parameterization of B1

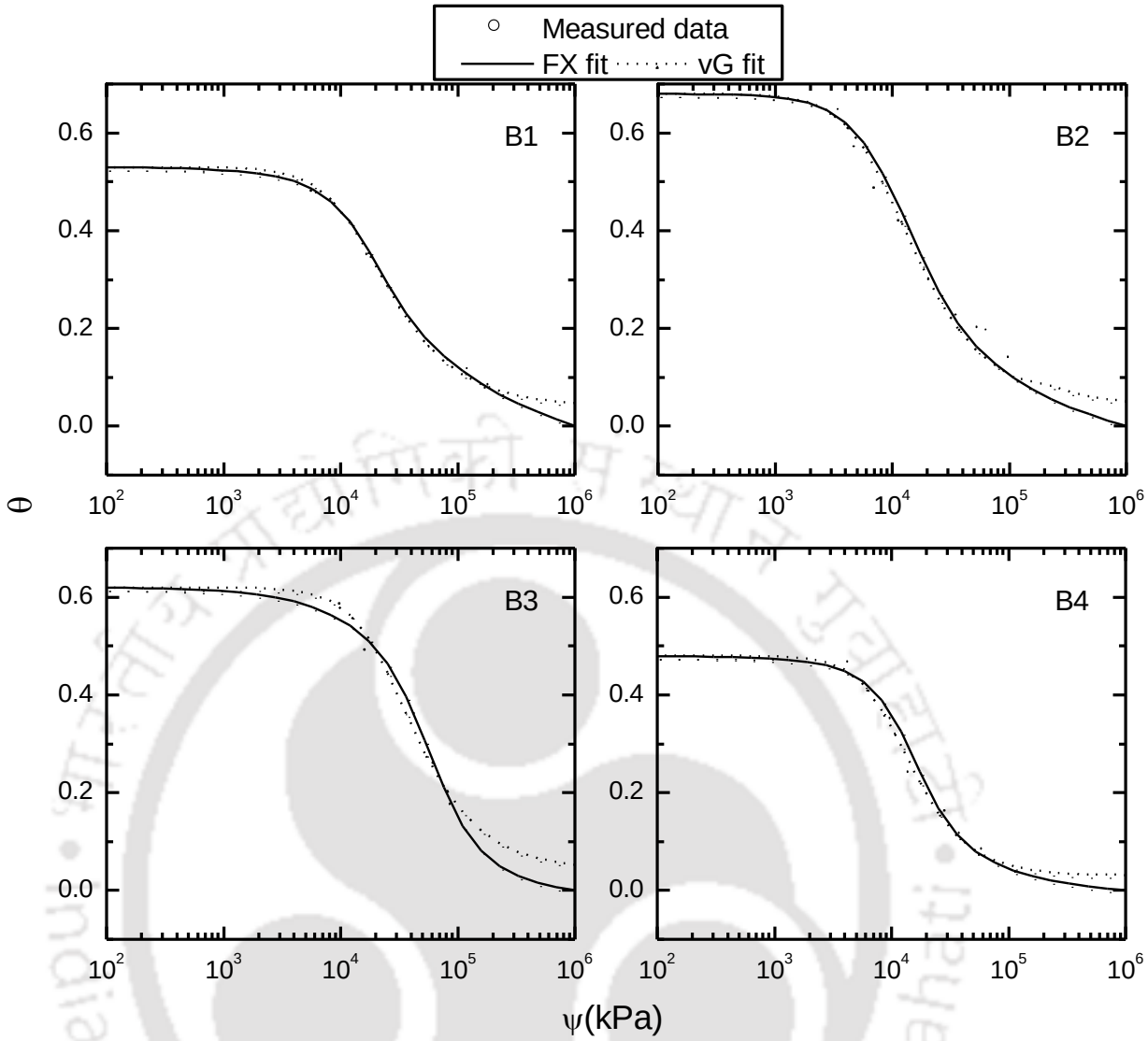

Figure 5.10 WRCC parameterization for bentonites using approach 2

Similar to approach 1, it was observed that both FX and vG fitting gave regression coefficient (R^2) close to unity. Comparing Table 5.6 and 5.7, a lower m_f, n_{vg} and m_{vg} values were observed in approach 1 than in approach 2. The n_f parameter was lower in approach 1 in case of B1 and B3 while it was higher for B2 and B4 in approach 1. The a_f and AEV for FX model obtained from approach 2 were much higher than approach 1. Similarly, the AEV obtained from vG gave higher values in approach 2 than approach 1. These observations indicate that if θ-ψ data was not defined based on shrinkage characteristics, it would lead to erroneous WRCC parameterization for high plastic soils like bentonite. The study recommends approach 2 for unambiguous parameterization of WRCC of high volume change bentonites. The impact of difference in WRCC parameters obtained from approach 1 and 2 was studied further in chapter 6. For completeness, approach 2 was further summarized as follows.

5.6 Recommended procedure for WRCC parameterization for high volume change soils like bentonite

1. The soil specimen was prepared at water content (w) close to liquid limit for determining the shrinkage curve by using precise continuous volume measurement techniques like balloon method used in this study.
2. From the shrinkage test result, e versus w was plotted. For a particular soil, shrinkage curve corresponding to 100% saturation will be unique.
3. Dry unit weight γ_d was determined by knowing specific gravity G and void ratio e. From these result, volumetric water content θ and S_r was computed. Further, S_r versus θ was plotted for determining the point of desaturation at which S_r becomes less than 1. The θ_{ds} corresponding to this point of desaturation will be the initial point used in WRCC data.
4. The continuous suction measurement of the same soil was performed with the same initial condition similar to shrinkage test. The WRCC was obtained in terms of θ versus ψ (considering shrinkage characteristics curve).
5. Only those data with $\theta < \theta_{ds}$ (modified data set) was used for WRCC parameterization.
6. The WRCC model was fitted to the modified data set for WRCC parameterization.

5.7 Influence of compaction condition on WRCC of bentonite

5.7.1 Effect of initial water content on WRCC of bentonite

The effect of initial w on continuous drying WRCC of bentonite was investigated. Literature shows that the initial portions of the WRCC in a cohesionless soil like sand was influenced by the initial water content particularly in the lower suction range (Malaya and Sreedeep 2010). However, the effect of initial water content on WRCC of high volume change cohesive soil like bentonite was not well established. To investigate this, one particular bentonite B1 was selected and samples with six different initial water content (w=35%, 65%, 76%, 112%, 116%, 298%) and γ_d reported in Table 5.8 were prepared and subjected to air drying. The increase in ψ during drying was continuously measured using WP4. The results obtained were plotted as shown in Figure 5.11. It can be noted that irrespective of different initial w, continuous drying WRCCs of B1 matches well. The lowest initial water content, w= 35%, falls in the residual portion of WRCC. All the WRCCs with different initial w approaches residual portion up to 10^5 kPa. This observation of negligible effect of initial w matches with those reported by Marinho and Chandler (1993) and Miller et al. (2002). However, there are studies which have reported the effect of compaction water content on the WRCC (Tinjum et al. 1997). In these studies, axis translation technique was used for ψ measurement where water was expelled under pressure higher than the atmospheric pressure. However, WP4 method adopts slow air drying under atmospheric pressure. The results presented in Figure 5.11 also reiterates the fact that γ_d has negligible influence on the WRCC. The whole of the data point results in a unique WRCC for B1 irrespective of the difference in initial w and γ_d reported in Table 5.8.

Table 5.8 Compaction state for different water content samples for bentonite B1

w (%)	γ_d (kN/m^3)
35	10.1
65	8.9
76	7.7
112	6.1
116	3.6
298	2.9

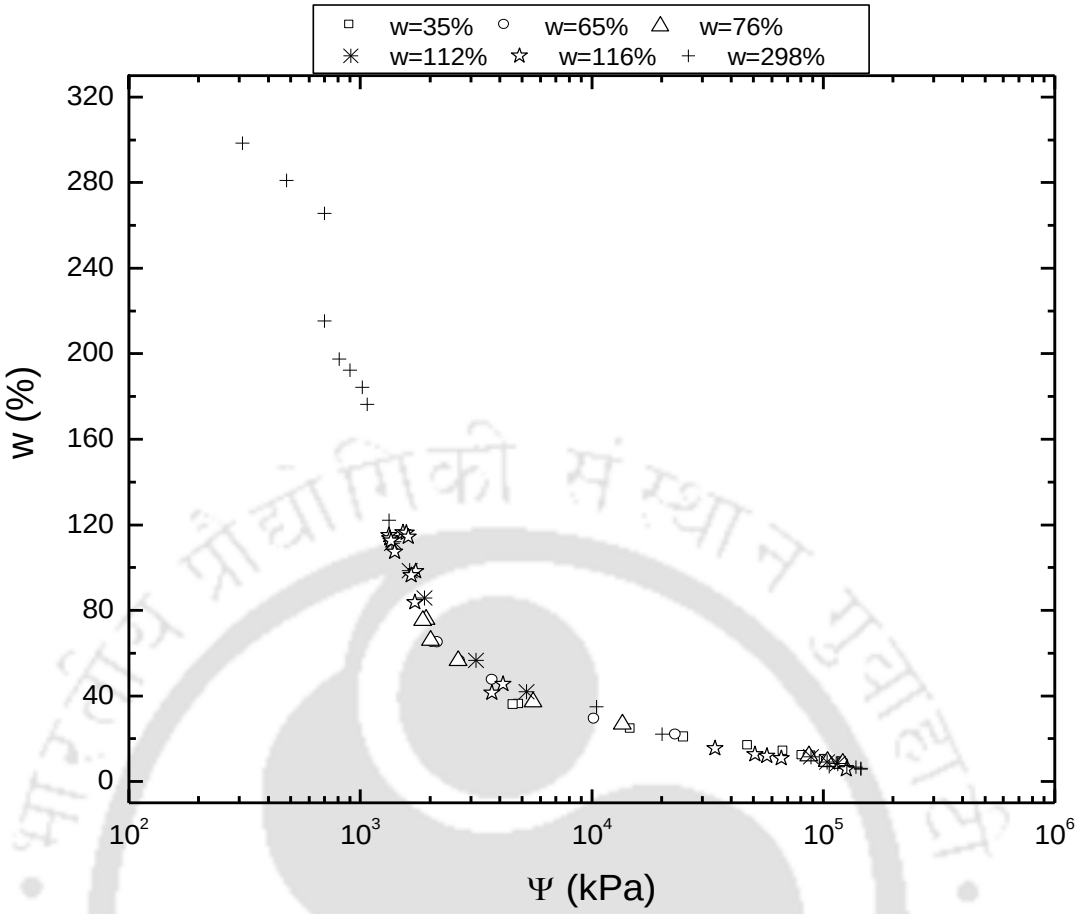

Figure 5.11 Effect of initial water content on w-ψ variation of B1

In addition to WRCC, it was also necessary to verify the effect of initial w on the uniqueness of shrinkage characteristic curve of bentonite. Therefore, the shrinkage characteristics of B1 was investigated for different initial w and e-w variation was plotted as shown in Figure 5.12. The objective was to see whether the shrinkage behavior was unique or not for different initial w. The initial degree of saturation of the sample was ensured to be 100%. It was found that all the samples follows the same shrinkage curve and matches perfectly. The ψ corresponding to w were obtained from Figure 5.11 and plotted as a function of computed θ as shown in Figure 5.13. It was found that θ-ψ plot also shows a unique trend for the three initial w considered in Figure 5.12. Thus it can be summarized that the shrinkage characteristic curve and WRCC of bentonite is unique and matches well irrespective of different initial w and γ_d. However, this observation corresponds to the initial $S_r \approx$ 100% and relative humidity based measurement of ψ at atmospheric pressure (zero stress condition).

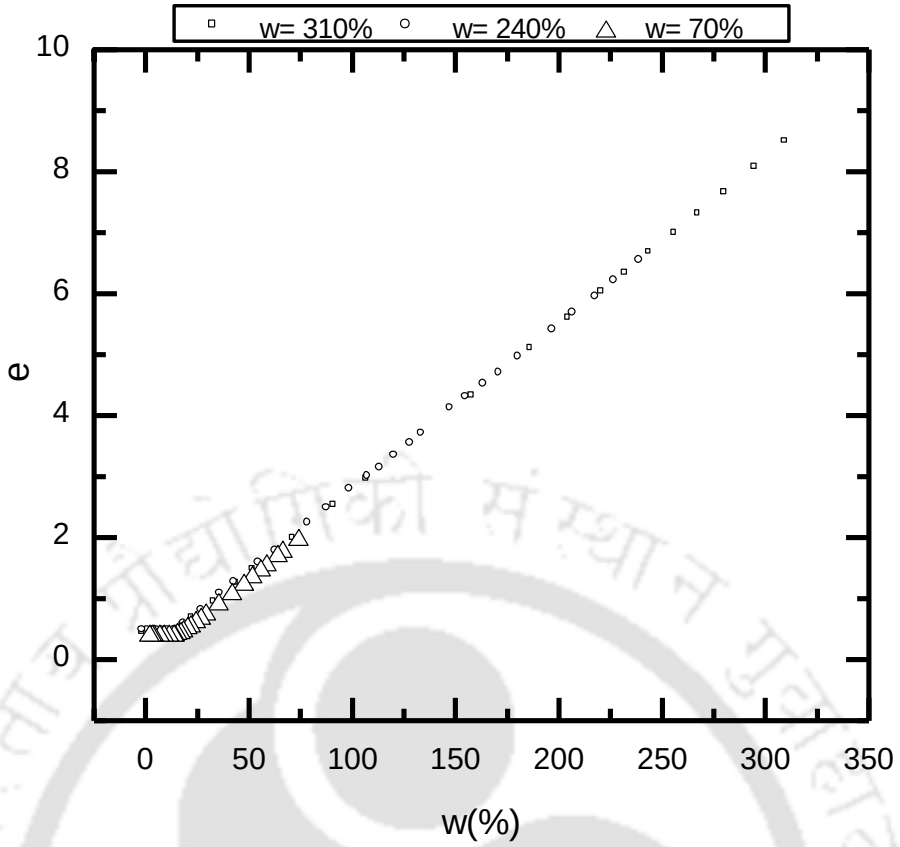

Figure 5.12 Effect of initial water content on e-w variation of B1

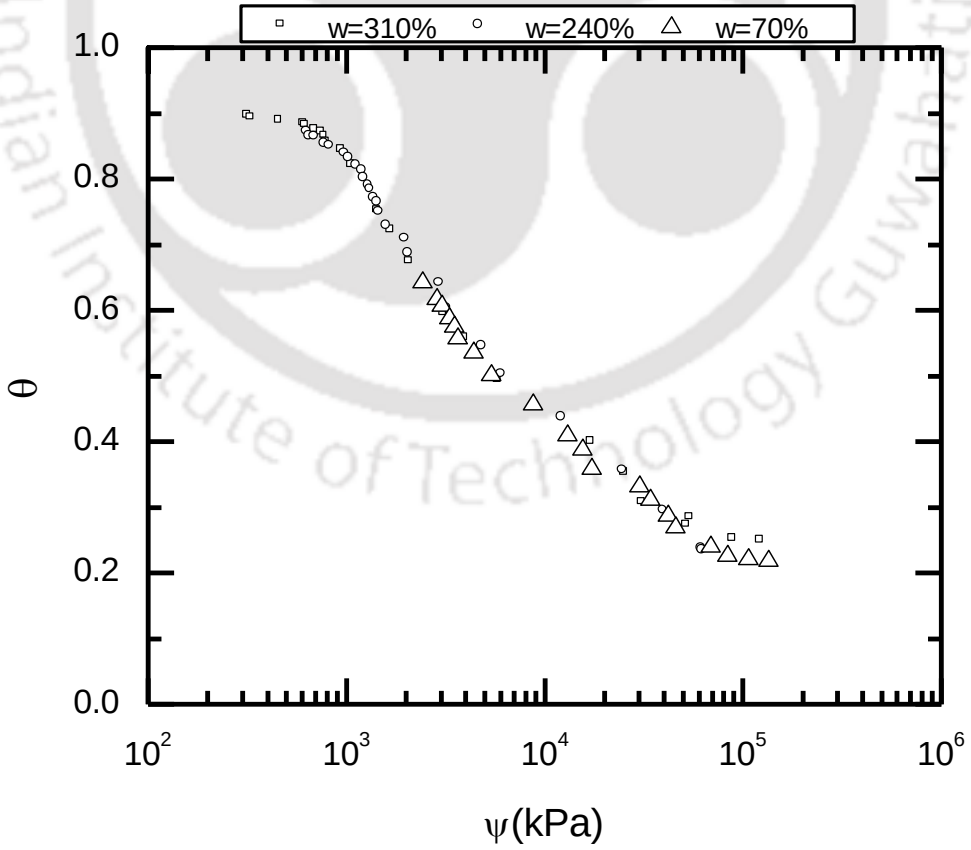

Figure 5.13 Effect of initial water content on θ-ψ variation of B1

5.7.2 Influence of compaction on WRCC of bentonite

The above section mostly focused on initial w with mild press packing of the bentonite with spatula. Therefore γ_d was less for the samples as shown in Table 5.8. In this section, the influence of higher compaction on WRCC of B1 was investigated. The compaction state (γ_d and w) of the samples considered in this study are shown in Figure 5.14 and listed in Table 5.9. For achieving sufficient compaction, initial w was kept low. The curve shown in Figure 5.14 corresponds to Standard Proctor Compaction curve of B1. For obtaining the compacted sample at the desired dry unit weight and water content, hollow sharp steel rings were made with external diameter 35 mm and height 5 mm so that it fits inside the WP4 sample cup. A steel container with known volume was used for compacting the soil sample. The required bulk volume of soil to be compacted was calculated for the given volume of the container to achieve the compaction conditions listed in Table 5.9. The steel ring was pushed into the compacted sample using the sharp edge. After that, the steel ring with soil sample was scooped out from the steel container. The soil sample with the rings was placed in the WP4 sample cups and suction was measured continuously. Figures 5.15 and 5.16 exhibit the WRCC plot for different compacted points in terms of w and θ. It was observed that measured WRCC of all the nine points falls exactly on a single curve. The results show negligible effect of initial compaction w and γ_d on ψ measurement. This observation matches with the observation of negligible contribution of γ_d on ψ measurement reported by Agus et al. (2010) for bentonite-sand mixture. It must be noted that samples were dried under atmospheric pressure, which was different from forced expulsion of water in pressure plate apparatus. The starting point of the WRCC depends on the initial w selected for different samples. To understand the uniqueness of WRCC of bentonite, all the available data for bentonite B1 obtained from section 5.2 to 5.7 were plotted together as shown in Figure 5.17 in terms of w and θ. It can be noted that irrespective of various initial conditions, WRCC of B1 is unique.

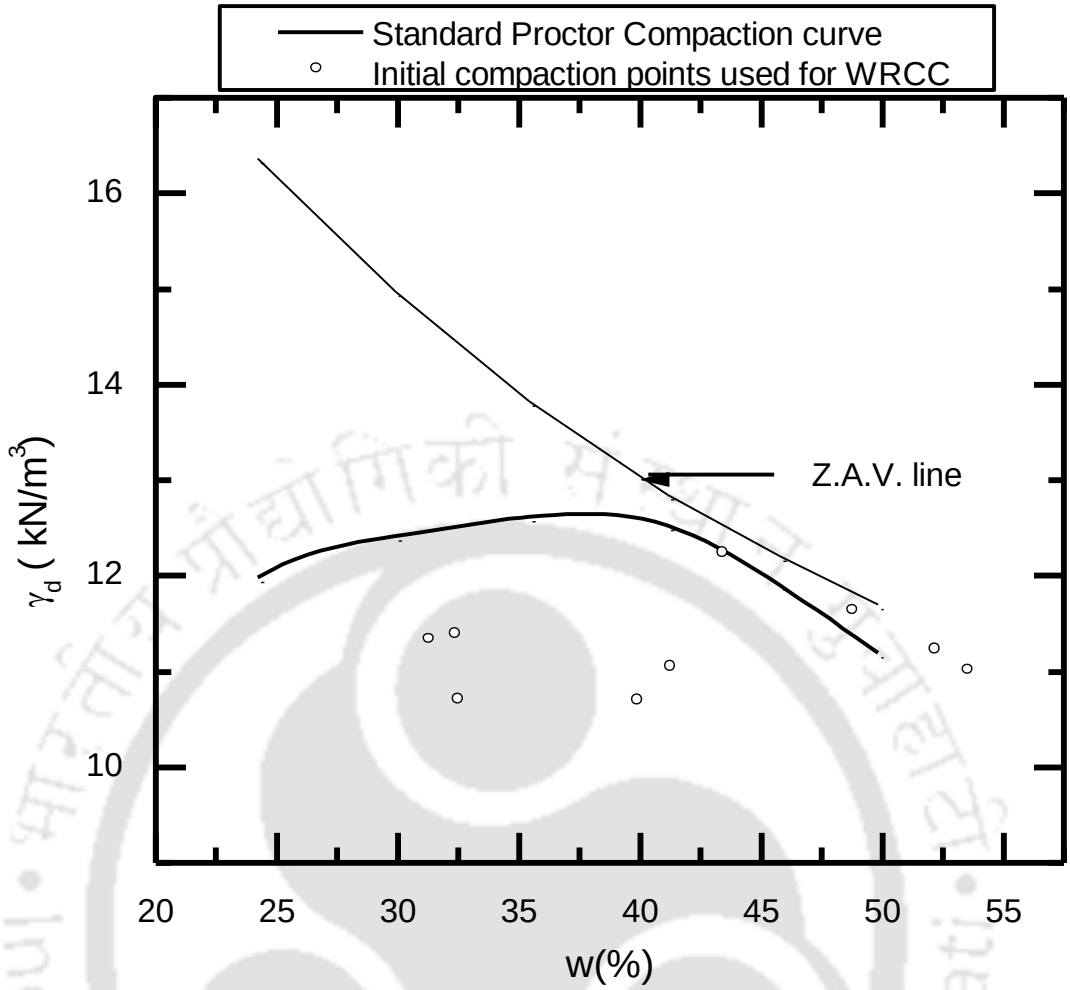

Figure 5.14 Details of initial compaction points used for WRCC of B1

Table 5.9 Initial compaction points used for WRCC measurement of B1

Points	Parameter			
	w (%)	γ_d (kN/m^3)	S_r (%)	θ (%)
1	32.53	11.36	63.68	36.97
2	43.56	12.20	96.71	53.16
3	48.93	11.60	99.25	56.77
4	31.45	11.30	61.27	35.65
5	41.41	11.02	77.04	45.68
6	53.68	10.97	99.06	57.43
7	32.66	10.67	57.49	34.85
8	40.07	10.66	70.43	42.72
9	52.32	11.20	99.89	57.55

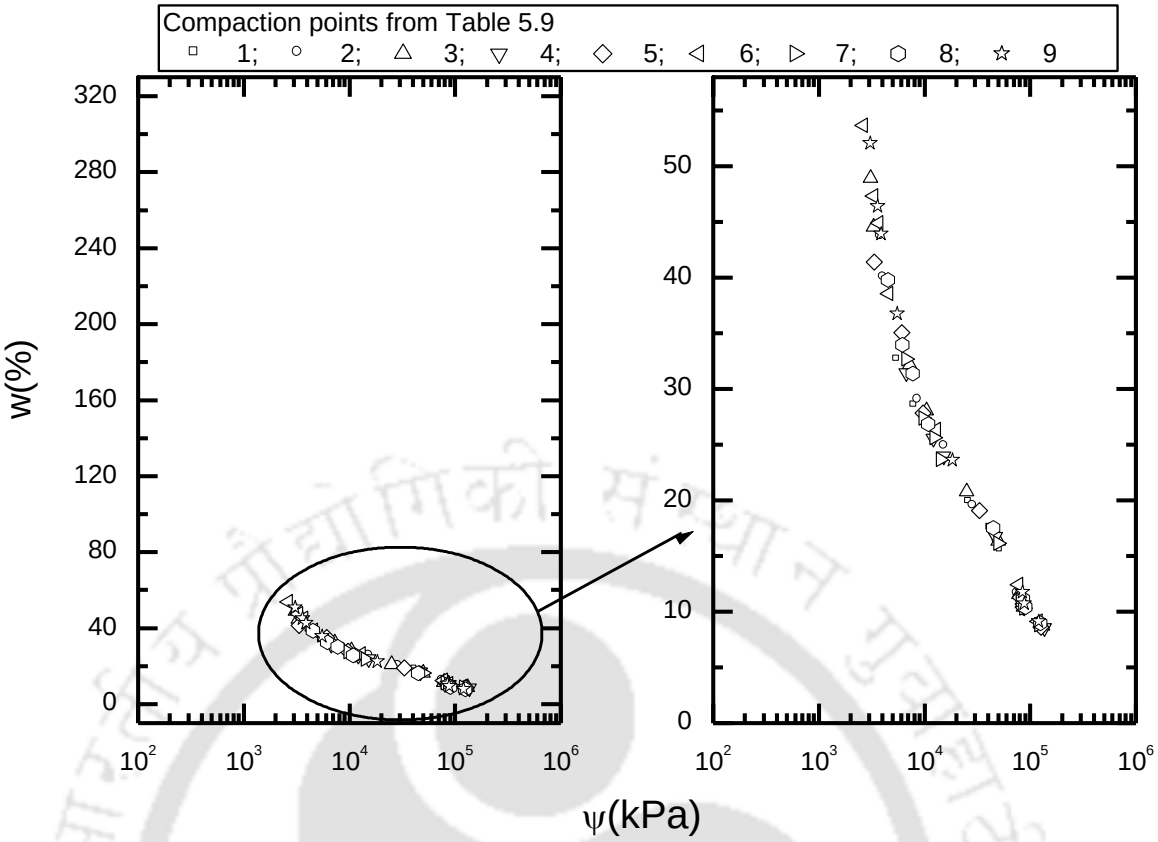

Figure 5.15 Influence of initial compaction condition on WRCC of B1 plotted in terms of w

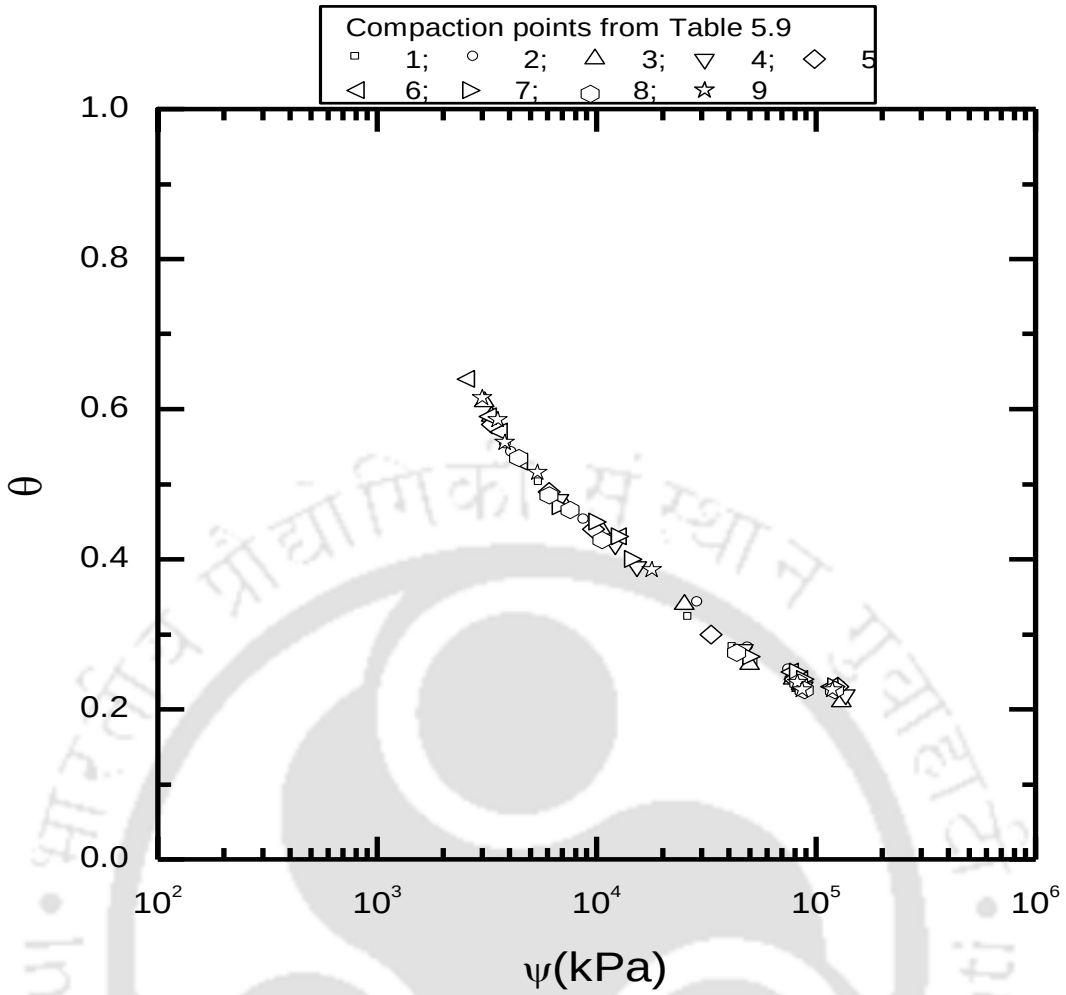

Figure 5.16 Influence of initial compaction condition on WRCC of B1 plotted in terms of θ

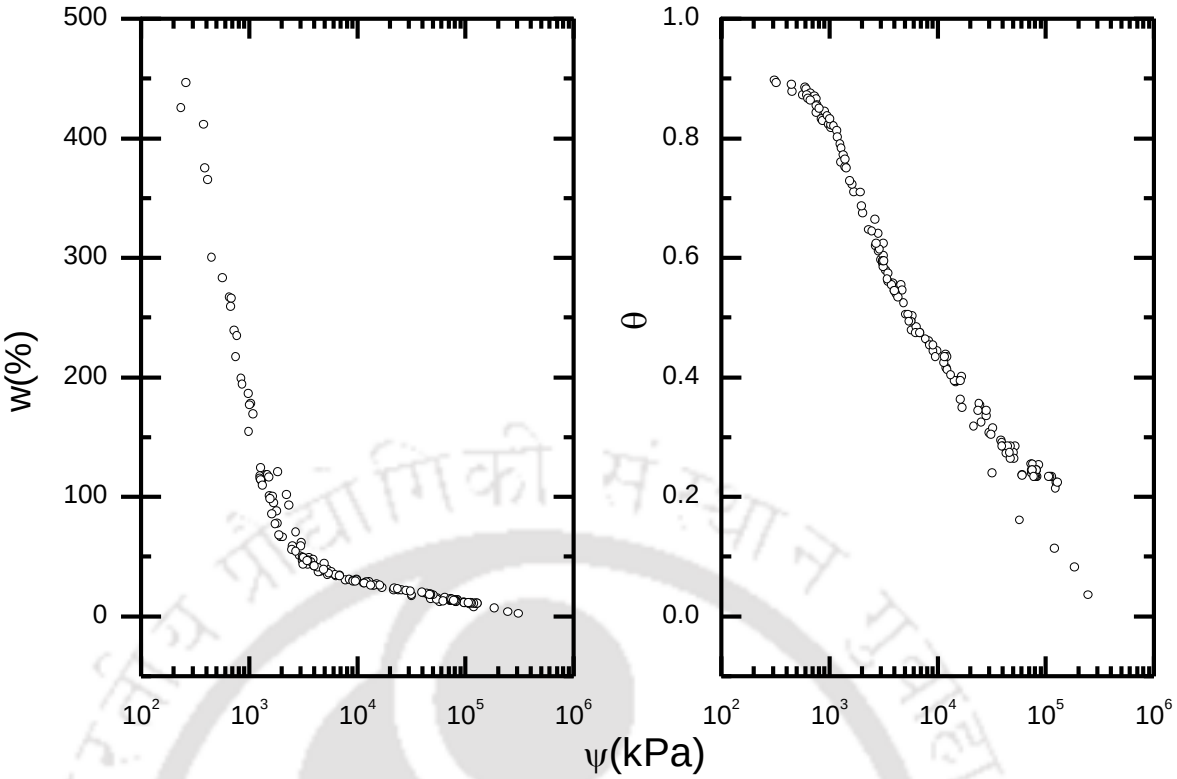

Figure 5.17 Evaluation of uniqueness of WRCC of B1 in terms of w and θ

5.8 Water retention characteristics of fly ash-bentonite (FA-B) mixes

WRCC of fly ash-bentonite (FA-B) mixes is mandatory for proposing it as hydraulic barrier. The effect of FA content and FA type on the measured WRCC of FA-B mixes needs to be studied in detail. The aim was to understand how WRCC of mixes gets affected for the given variation in FA characteristics. For this purpose, bentonite B1 was kept same (selected randomly) and different FAs were mixed with it one at a time. No attempt was made to study the influence of bentonites on FA-B mix. The measured WRCC was compared in terms of bentonite water content (w_b) (Agus et al. 2010) and suction for different FA content. The influence of FA content on the volume change behavior of FA-B mixes was established for the four different FAs used in this study. A critical analysis of the WRCC fitting parameters obtained using the FX and vG model for different FA-B mixes was discussed.

5.9 Preparation of FA-B1 mixes

Each FA used in this study was mixed with B1 in three proportions, 30%, 50% and 70% of dry weight. Both FA and B1 was oven dried at around 105 ^{0}C to remove any hygroscopic moisture present in it. The samples were then dry mixed thoroughly in the

required proportions. Water was added to the mixture using a water sprayer to obtain the target water content. Mixing was done properly and care was taken to achieve a uniform mixture of fly ash-bentonite (FA-B). From now on, FA-B corresponds to bentonite B1 mixed with respective fly ash in different proportion. All the samples were prepared at high water content close to LL similar to bentonites for achieving a minimum measured suction at the start of the measurement. The prepared samples were kept in the desiccators for 24 to 48 hrs to have a uniform distribution of moisture before suction measurement.

5.10 Effect of FA content on WRCC of FA-B1 mixes

Figure 5.18 shows the measured WRCC in terms of w for FA-B1 mixes (30%, 50% and 70%) for the FAs considered in this study. For completeness, WRCC of FA (100%) and B1 (0%) was plotted in the figure as reference. As expected, the WRCC for 30% FA measures the maximum suction and 70% FA measures the minimum for a particular w for all FAs. The WRCC of 50% FA content falls close to the 70 % FA content except in BFA, where there is distinct difference among all the mixes. For all the mixes, w decreases from around 90% to 10% and below this w the drying becomes slow as suction increases to its maximum value. This can be attributed to the presence of very less amount of water in the samples towards the residual state. The low w close to residual state of the sample contributes to considerable increase in suction up to 10^5 kPa attributed to high adsorptive force. Bentonite have high SSA and surface negative (-ve) charge, which can hold the polar water tightly thereby increasing the suction. Similar observation was reported by Agus et al. (2010) for bentonite-sand mixtures. The difference in WRCC due to varying percentage of FA becomes negligible for high suction close to 10^5 kPa, which is in the residual state. Another important observation is that WRCC of FA-B1 mixes falls close to that of B1. There is distinct variation of WRCC of FA-B1 mixes from that of FA even for 70% FA content. This indicates that water retention of B1 dominate the WRCC of all FA-B1 mixes investigated in this study.

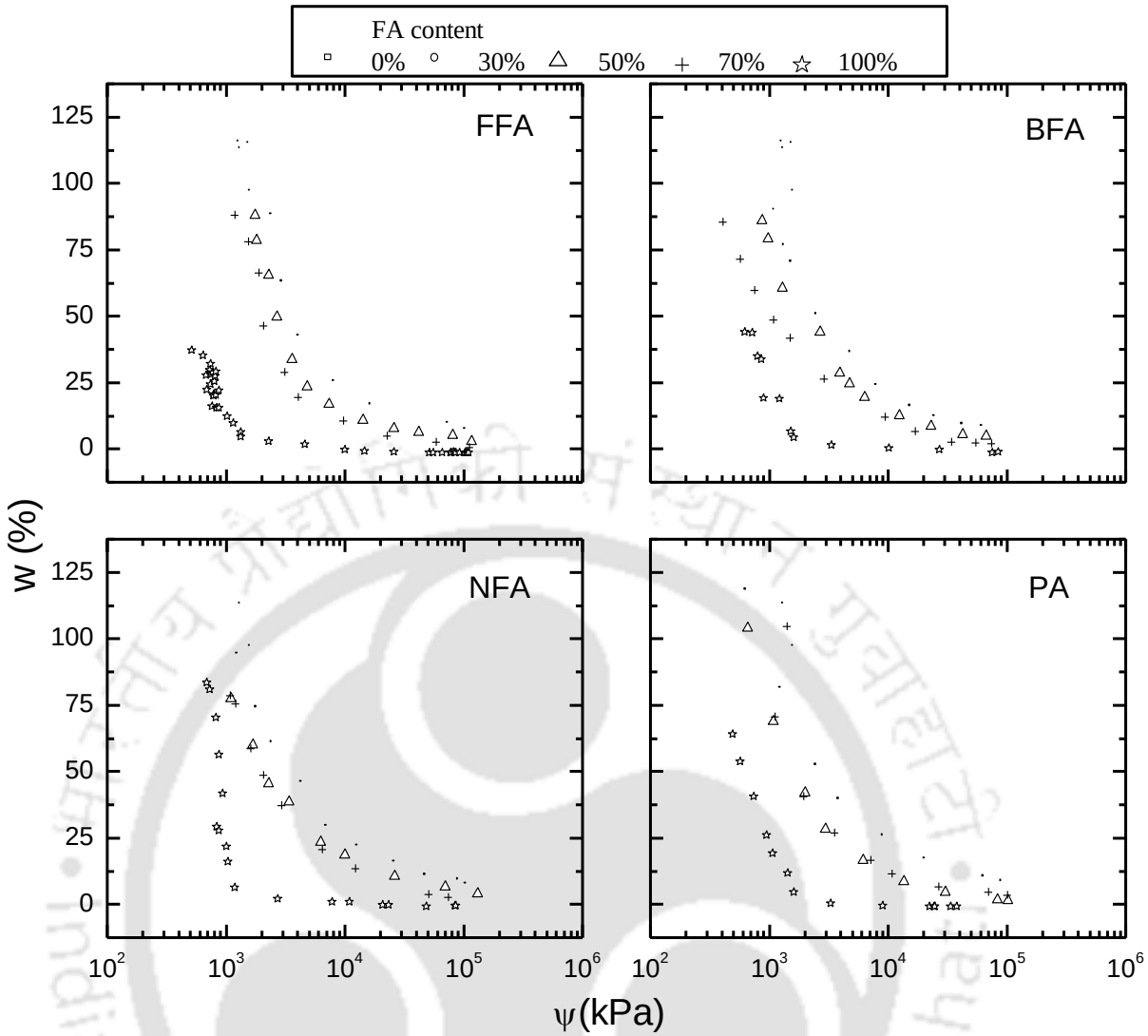

Figure 5.18 Comparison of WRCC of FA-B1 mixes in terms of w

5.11 Effect of FA type on WRCC of FA-B1 mixes

Figure 5.19 shows the effect of FA variability on the measured WRCC of FA-B1 mixes. The measured result shows a distinct influence of FA variability on the measured WRCC particularly at high FA content (70%). The difference in WRCC was not much for low FA content of 30%. For all percentage of FA content, it can be noted that the difference in WRCC was negligible for Ψ> 6000 kPa. This indicates that the effect of variability of FA on WRCC of FA-B1 mixes becomes negligible at higher range of Ψ. The w corresponding to Ψ≈ 6000 kPa was approximately 25% for all FA, which is close to optimum moisture content (OMC) at which hydraulic barrier is compacted. At this w, FAs from different sources gave similar WRCC for FA-B1 mixes. This observation is significant because there need not be a stringent requirement of uniform FA type when it is used as hydraulic barrier compacted at OMC condition. The study highlights that FA

from different sources can be used with confidence in the same project for the construction of hydraulic barriers. This is unlike the natural soil where strict quality check need to be performed for minimizing any uncertainty arising from the spatial variability of material.

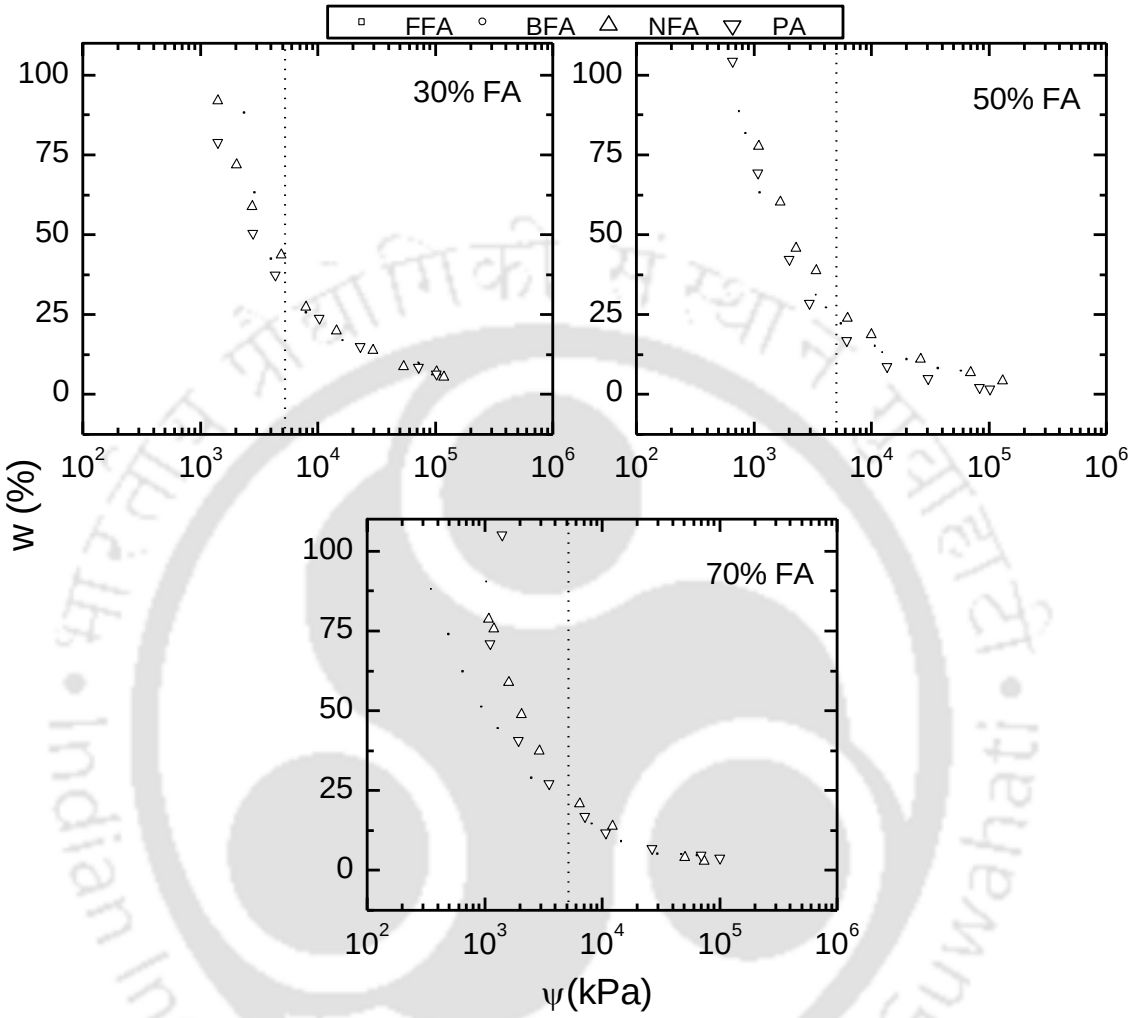

Figure 5.19 Influence of FA variability on WRCC of FA-B1 mixes

5.12 Influence of bentonite water content (w_b) on WRCC of mixes

Agus et al. (2010) reported that total suction of bentonite-sand mixture was strongly controlled by the bentonite water content (w_b) in addition to the percentage of bentonite. The study assumed that the water was absorbed predominantly by the bentonite and the void ratio of the mixture can be regarded as the bentonite void ratio. Based on the above assumption, Agus et al. (2010) have proposed a relationship for calculating w_b (%) as given by equation 5.1. This study also verified the influence of w_b on the WRCC of FA-B1 mixes.

$$w_b = \frac{100 w_m}{\beta} \tag{5.1}$$

where

w_m= water content of the mixture (%)

β= bentonite content in the mixture (%)

Using equation 5.1, w_b was determined for FA-B1 mixes and plotted against total suction as shown in Figure 5.20. The plot indicates that WRCC of FA-B1 mixes in terms of w_b merges and becomes unique irrespective of FA content for FFA and BFA. This observation was similar with those of Agus et al. (2010) for bentonite-sand mixes. For NFA and PA, higher FA content (70%) exhibited some deviation from other mixes. These results were further checked for its repeatability and were found to be consistent. The high calcium content in NFA may have contributed to higher water retention of NFA, which is otherwise not prominent in FFA and BFA. Similarly aging of pond ash resulting from hydro-thermal effect would have altered or increased its porous nature and water retention. Therefore, FA water content would have some contribution to the WRCC of mixes in addition to w_b in the case of NFA and PA and was relevant only for higher FA content (70%). It may be noted that the age of PA could not be established in this study and further investigations are required to prove the hypothesis that aging of FA may alter (or increase) its water retention capacity.

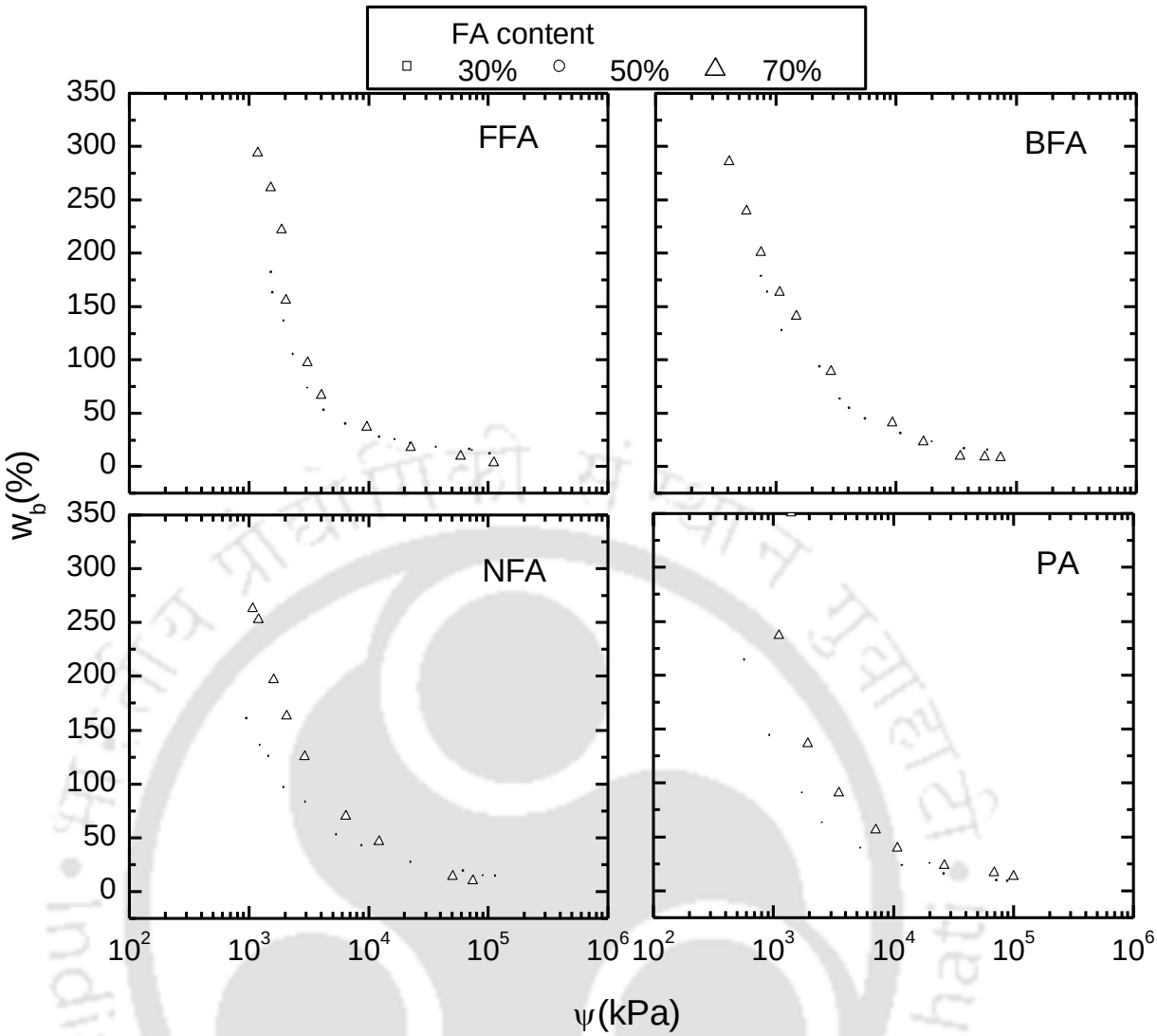

Figure 5.20 Effect of bentonite water content (w_b) on WRCC of FA-B1 mix

5.13 Shrinkage characteristics of FA-B1 mixes

The influence of FA content on the shrinkage characteristics of FA-B1 mixes was established in this study for four different FAs. The volume change measurement at different stages of drying was done with the help of rubber balloon method as explained in section 5.4. The results obtained were plotted in terms of e-w and e-θ as shown in Figures 5.21 and 5.22, respectively. The shrinkage characteristics of 30% and 50% FA content results matched very well while for 70% FA content, the volume change was marginally less as observed from the lower e values at the initial portion of the e-w plot. The 100% S_r line drawn for all the mixes follows the respective measured data well till a minimum e was achieved. For minimum e portion, higher FA content was found to have higher e. This was mainly due to the low shrinkage of high FA content mix. Based on e and w results, S_r and θ was calculated as mentioned before in section 5.4. Figures 5.22

and 5.23 shows e versus θ and S_r versus e, respectively for all FA mixes. The desaturation points were obtained and listed in Table 5.10.

Table 5.10 e and θ at desaturation point for FA-B1 mix

FA	FA content (% of dry weight)					
	30		50		70	
	e_{ds}	θ_{ds}	e_{ds}	θ_{ds}	e_{ds}	θ_{ds}
FFA	1.57	0.55	0.89	0.44	0.96	0.38
BFA	2.10	0.63	1.28	0.51	0.73	0.37
NFA	2.11	0.64	1.56	0.56	0.94	0.43
PA	2.66	0.67	1.90	0.62	1.77	0.58

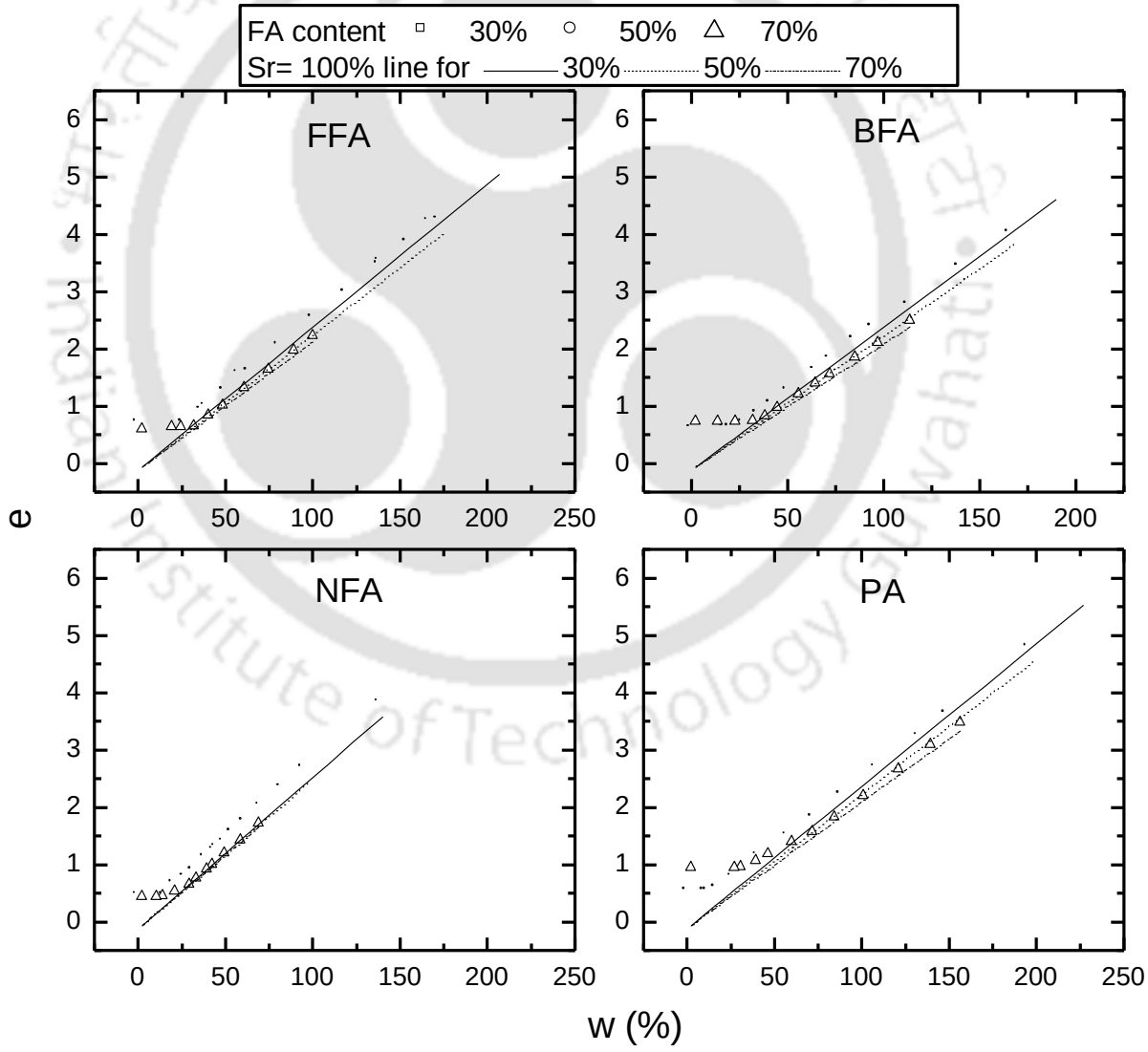

Figure 5.21 Shrinkage characteristics of FA-B1 mix in terms of e-w

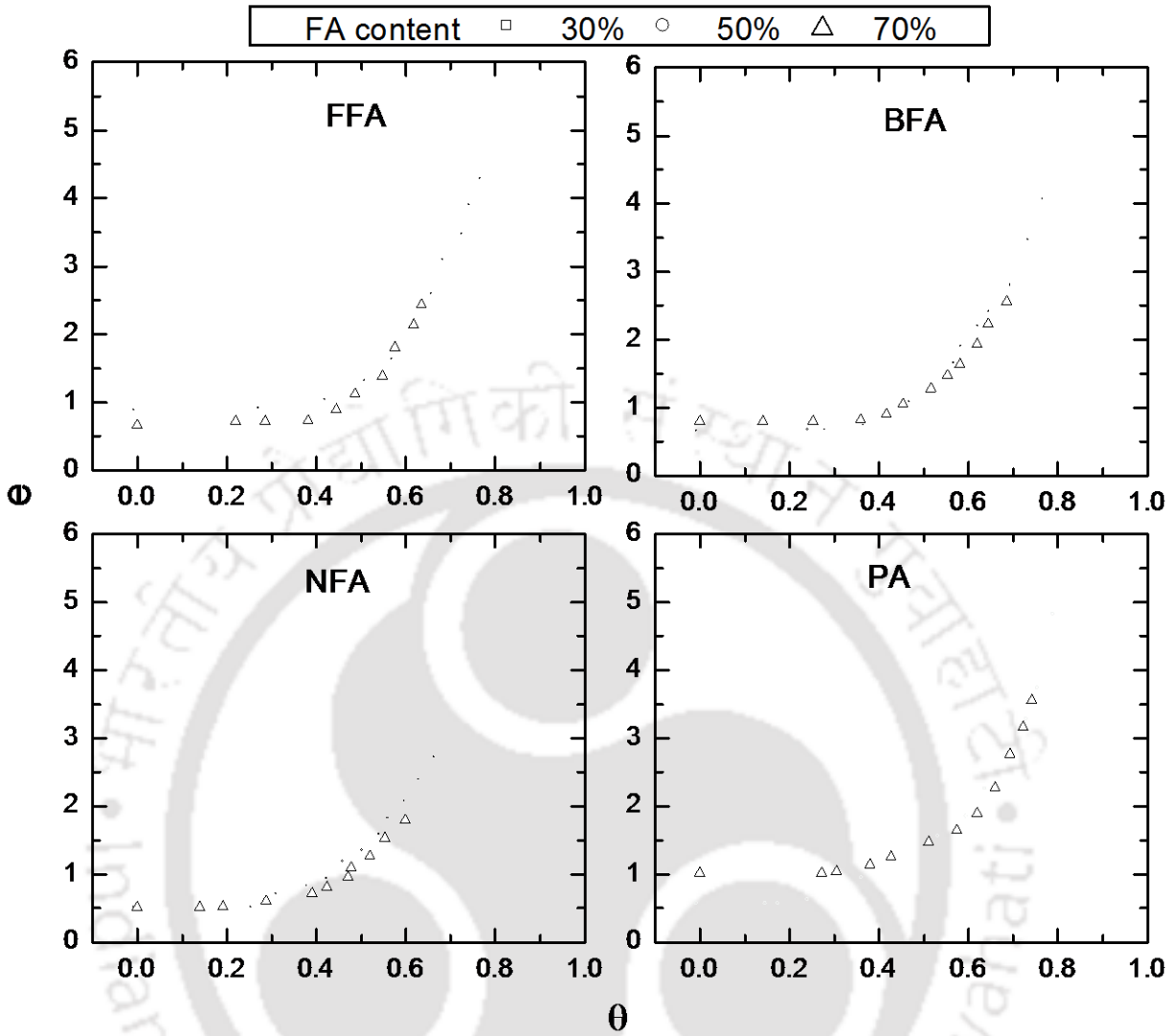

Figure 5.22 Shrinkage characteristics of FA-B1 mix plotted in terms of e-θ

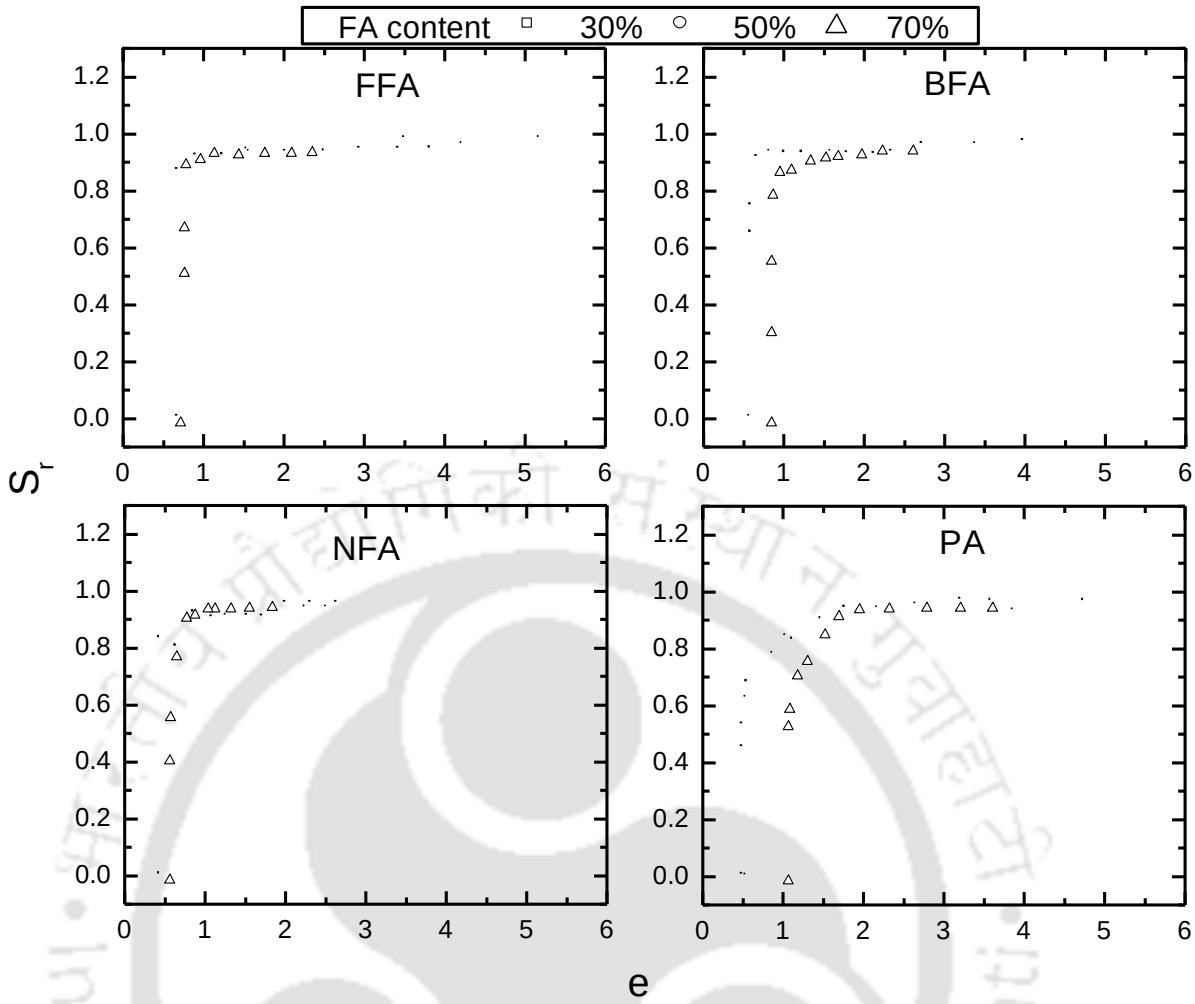

Figure 5.23 Shrinkage characteristics of FA-B1 mix plotted in terms of S_r-e

It was clear from these results that shrinkage characteristics of FA-B1 mixes were influenced by the FA content in the mix. In general, increasing FA content in the mix the e value increases while θ decreases at the desaturation or air entry point. Similar to bentonites, e and θ value at initial (point A) and final (point B) portion (A and B shown in Figure 5.4 (b) of the e- θ plot were obtained and given in Table 5.11. It was found that e and θ value at desaturation falls in the transition portion of the e-θ plot between points A and B.

Table 5.11 Details of e and θ at deviation points A and B for FA-B1 mix

e, θ	FA	FA content, %		
		30	50	70
e_A-e_B	FFA	3.01-1.35	3.12-0.86	1.42-0.75
	BFA	2.58-0.62	1.95-0.67	1.48-0.73
	NFA	2.18-0.84	1.72-0.50	0.98-0.54
	PA	3.32-0.57	2.0-0.57	1.86-1.05
θ_A- θ_B	FFA	0.74-0.46	0.70-0.38	0.55-0.38
	BFA	0.68-0.31	0.61-0.37	0.55-0.37
	NFA	0.64-0.39	0.57-0.27	0.45-0.29
	PA	0.71-0.23	0.70-0.25	0.62-0.35

5.14 WRCC parameterization of FA-B1 mixes

For WRCC parameterization of FA-B1 mixes, the measured WRCC in Figure 5.18 were presented in terms of θ-ψ relationship as shown in Figure 5.24. The θ value corresponding to each measured w points of WRCC were computed by noting the e value from the shrinkage characteristics as explained in section 5.4. It can be noted that different percentage of FA exhibit distinct WRCC when plotted in terms of θ-ψ

Following the methodology explained in approach 2 (section 5.5.2), the WRCC data having $\theta \leq \theta_{ds}$ as given in Table 5.10 were considered for the WRCC parameterization using FX and vG model. The fitted curves for all the mixes are shown in Figure 5.25. The obtained parameters were presented in Table 5.12 and 5.13 for FX and vG model, respectively.

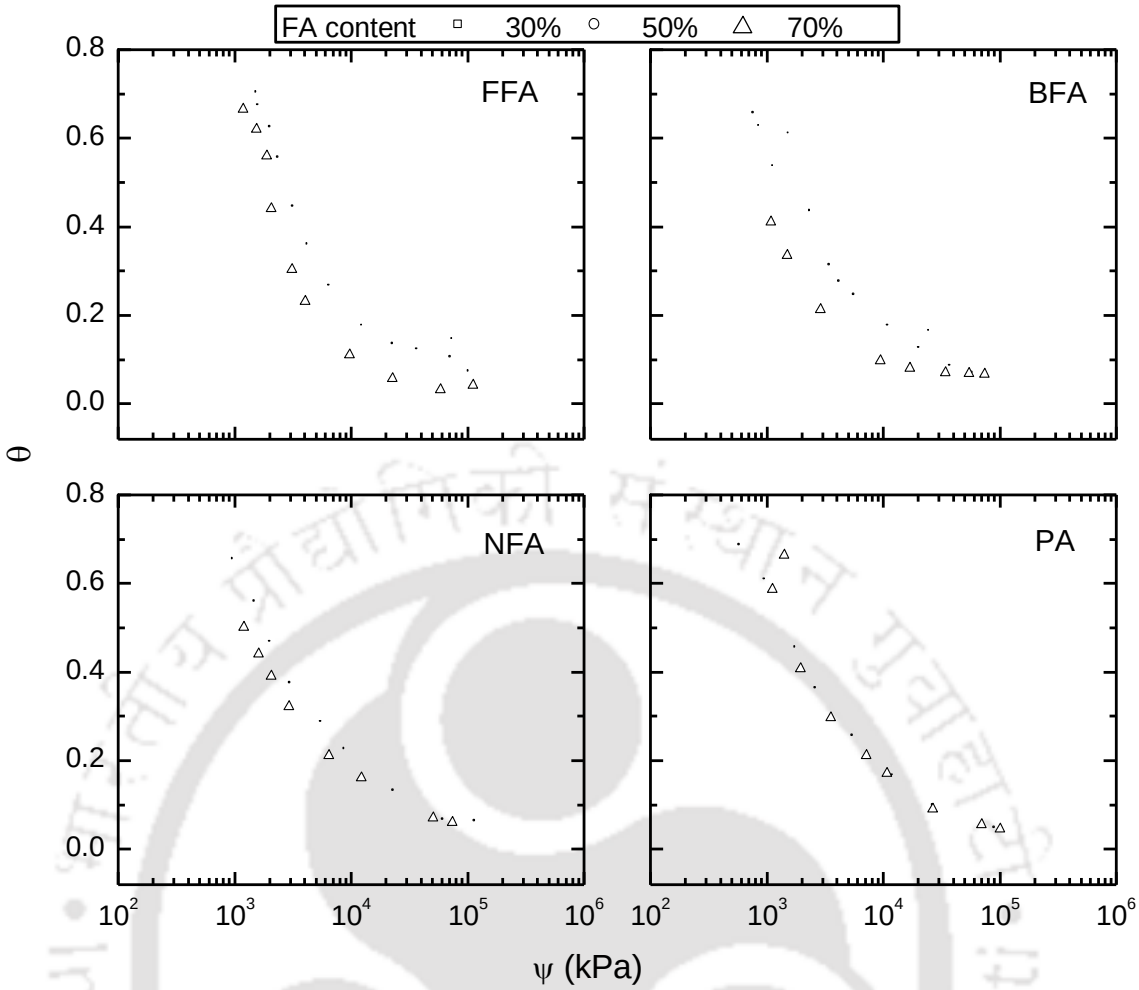

Figure 5.24 Comparison of WRCC of FA-B1 mix plotted in terms of θ-ψ

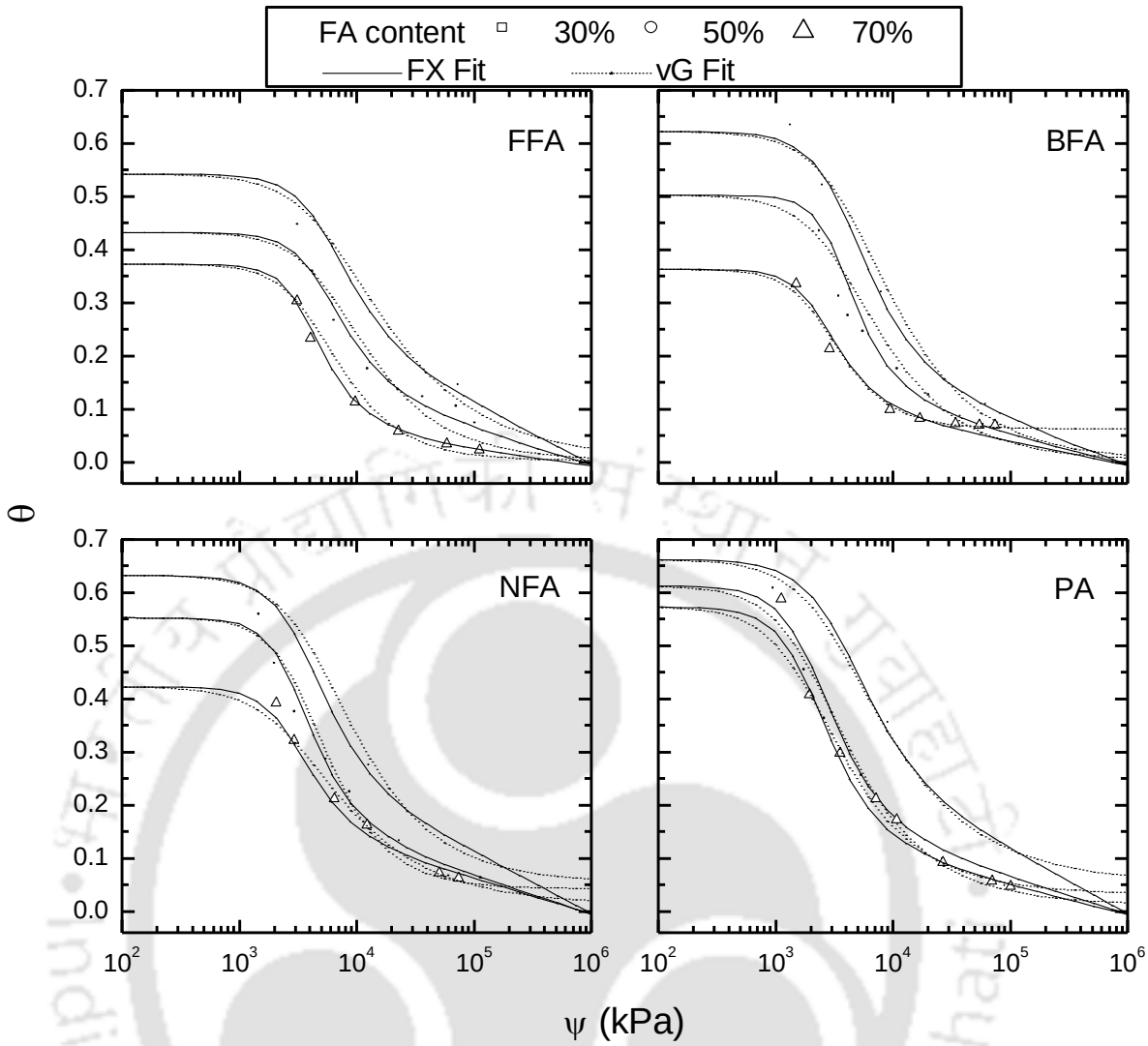

Figure 5.25 WRCC parameterization of FA-B1 mixes

The a_f and AEV parameter shows an expected trend where it decreases with an increase in FA content in the FA-B1 mix. The n_f and m_f parameters for FX model shows comparable values for different types of FAs in all the mixes. The regression coefficient (R^2) gives a high value (> 0.97) for all the mixes. Similar trends were also observed for vG parameters α, n_{vg} and m_{vg}. The value increases with the increase in FA content for all the FAs. The n_{vg} and m_{vg} parameters yield a comparable value for different combination of FA contents and types of FAs. A higher R^2 value (> 0.94) was obtained for vG fitting as well for all FAs. Thus it was found that both the FX and vG model gives a good representation of the measured WRCC of FA-B1 mixes and yields reliable estimates of the fitting parameters.

Table 5.12 FX fitting parameters for FA-B1 mix

FX Parameter	FA	FA content, %		
		30	50	70
a_f (kPa)	FFA	4452	4200	3200
	BFA	3200	2900	1920
	NFA	2800	2400	2200
	PA	2900	1700	1600
n_f	FFA	2.3	2.5	2.98
	BFA	2.2	3.2	2.9
	NFA	2.3	2.8	2.6
	PA	1.9	2.3	2.4
m_f	FFA	0.65	0.75	0.95
	BFA	0.84	0.78	0.75
	NFA	0.68	0.75	0.69
	PA	0.75	0.85	0.90
θ_r	FFA	0.085	0.052	0.045
	BFA	0.041	0.048	0.035
	NFA	0.074	0.051	0.042
	PA	0.092	0.047	0.038
AEV (kPa)	FFA	2152	2100	1723
	BFA	1840	1704	1020
	NFA	1638	1480	1030
	PA	1227	890	840
R^2	FFA	0.99	0.98	0.99
	BFA	0.98	0.99	0.97
	NFA	0.97	0.98	0.97
	PA	0.99	0.98	0.99

Table 5.13 vG fitting parameters for FA-B1 mix

vG Parameter	FA	FA content, %		
		30	50	70
a_{vg} x10^{-5}(kPa^{-1})	FFA	18	18	25
	BFA	25	31	45
	NFA	24	30	38
	PA	35	55	62
n_{vg}	FFA	1.62	1.86	2.12
	BFA	1.75	1.80	2.40
	NFA	1.80	2.20	1.68
	PA	1.65	1.80	1.82
m_{vg} ($m_{vg} = 1 - \frac{1}{n_{vg}}$)	FFA	0.38	0.46	0.53
	BFA	0.43	0.44	0.58
	NFA	0.44	0.54	0.41
	PA	0.40	0.44	0.45
θ_r	FFA	0.082	0.054	0.048
	BFA	0.075	0.044	0.036
	NFA	0.082	0.052	0.043
	PA	0.11	0.052	0.048
AEV (kPa)	FFA	2158	2100	1700
	BFA	1940	1600	1020
	NFA	1638	1480	1030
	PA	1227	670	665
R^2	FFA	0.98	0.96	0.97
	BFA	0.97	0.95	0.95
	NFA	0.97	0.96	0.97
	PA	0.99	0.98	0.99

5.15 Influence of compaction condition on WRCC of FA-B1 mixes

The influence of compaction condition on WRCC of FA-B1 mixes was investigated by considering FFA-B1 mix only. The FA content chosen for the mix was 0%, 50% and 70%. Initial compaction points with similar w and different dry unit weight γ_d selected for the suction measurement were given in Table 5.14. The WRCC was plotted in terms of w-ψ form as shown in Figure 5.26. It can be noted from Figure 5.26 that measured WRCC of all the three cases exactly merge for all the compaction points considered. The results show negligible effect of dry unit weight on the total suction measurement of FA-B1 mix samples. This results matches with the observation of negligible contribution of dry unit weight on suction measurement reported by Agus et al. (2010) on bentonite-sand mixture. Similar observations were obtained by Malya and Sreedeep (2010), Birle et al. (2008), Agus et al. (2005) and Sreedeep and Singh (2005).

Table 5.14 Initial compaction points of FFA-B1 mix used for WRCC measurement

Points	B1 (0% FA)		50% FA		70% FA	
	w (%)	γ_d (kN/m^3)	w (%)	γ_d (kN/m^3)	w (%)	γ_d (kN/m^3)
1	32.53	11.4	17.74	13.4	14.37	12.6
2	43.56	11.4	21.93	13.4	16.98	13.4
3	48.94	11.3	27.0	13.4	20.59	13.7
4	31.45	10.8	16.26	12.8	11.52	12.8
5	41.42	10.8	24.64	12.9	16.29	12.7
6	53.68	10.8	29.73	12.8	22.21	12.7
7	32.67	10.3	22.57	12.3	14.36	10.8
8	40.07	10.2	25.98	12.6	22.21	11.6
9	52.32	10.2	31.43	12.2	21.80	12.1

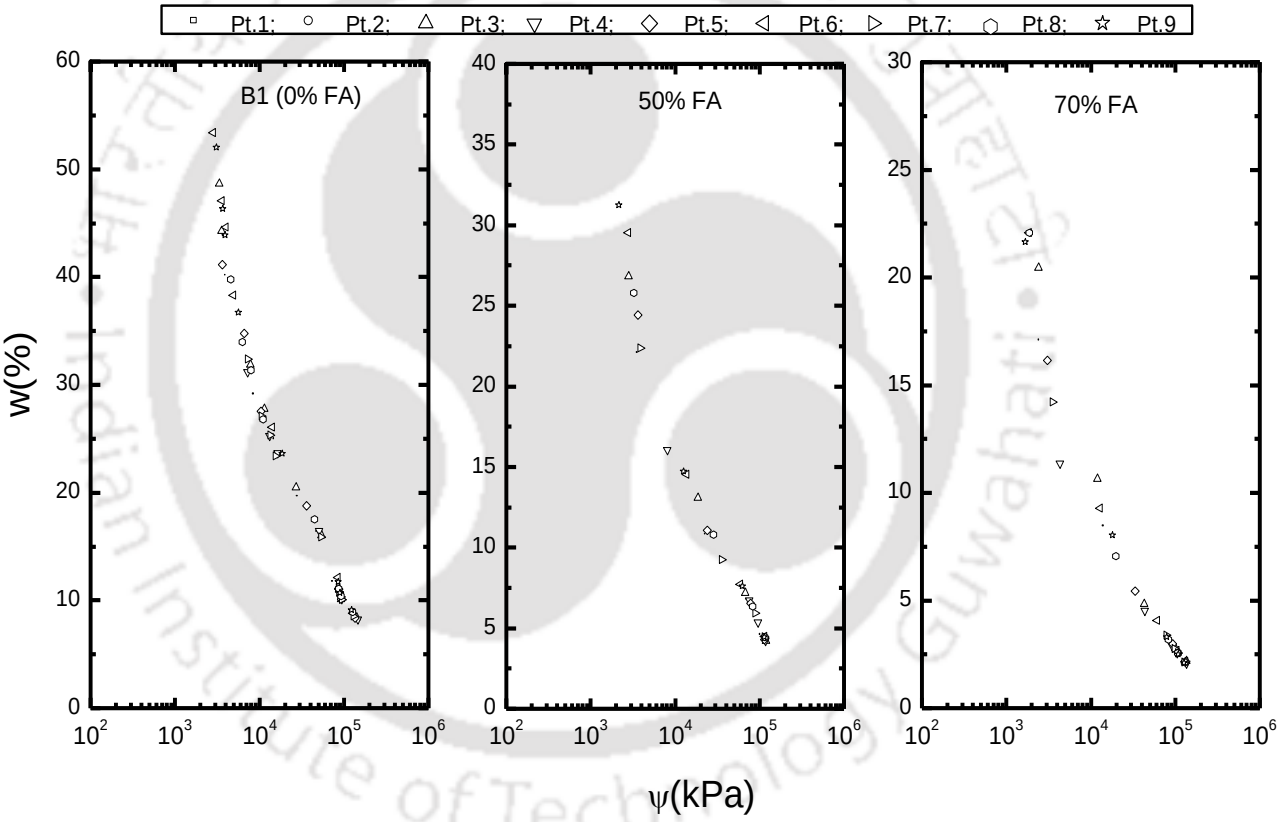

Fig 5.26 Influence of initial compaction condition on WRCC of FA-B1 mix

5.16 Study on the variability of WRCC

It was necessary to understand the extent of variability of WRCC for different bentonites and FA-B1 mixes. For this purpose, the measured WRCC of the four bentonites B1 to B4 was plotted together and the mean FX and vG fitting curve was obtained for the measured results as shown in Figures 5.27 and 5.28 respectively. Considering this fitted curve as the mean curve for the four bentonites, WRCC with ±5%,

±10% and ±20% variation from the mean curve was determined and plotted. It was observed that majority of the measured points of WRCC of all bentonites falls within the 20% variation. The variability of measured data for all bentonites is well within 20% error bar for moderate to low suction range (< 6000 kPa) for the given variation in bentonite characteristics. Marginal difference exists in the range $6000<\Psi<10^5$ kPa for bentonites B3 and B4. At high suction close to residual state, the WRCC data of all bentonites tends to merge. It may be concluded that for bentonites with its liquid limit varying from 244 to 433%, the WRCC variation would be within 20%.

Similarly, percentage variation was plotted for the WRCC of three mixes as shown in Figures 5.29 to 5.31. For this purpose a mean FX and vG curve was plotted by considering the data for all FA type for a particular mix. It was observed that for 70% FA content, most of the measured data falls outside the 5% and 10% variation, while all the data falls within the 20% variation. In case of 50% and 30% FA content, it was observed that majority of the data falls within the 5% and 10% variation except a few points for FFA and PA at higher water content. The variability study indicates that for all the FA-B1 mixes considered in this study, the WRCC variation was within 20% irrespective of the wide difference in the source and type of FAs. The implication of 20% variation of WRCC on the unsaturated behavior modeling of these mixes was investigated in chapter 6.

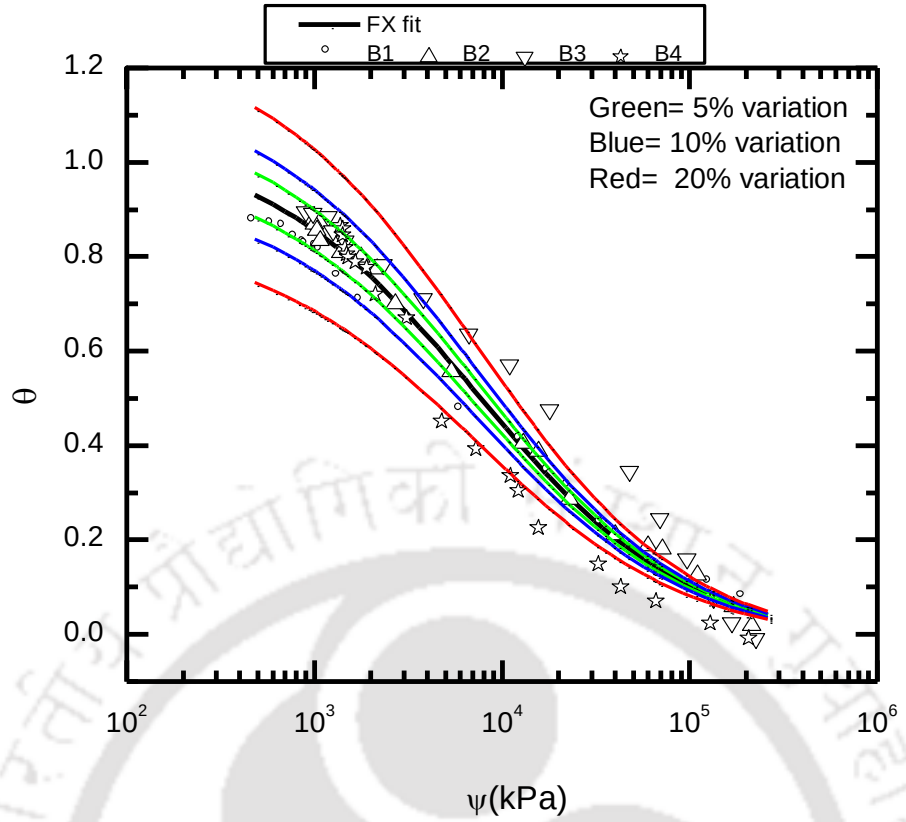

Figure 5.27 Variability of measured WRCC for bentonites with FX model

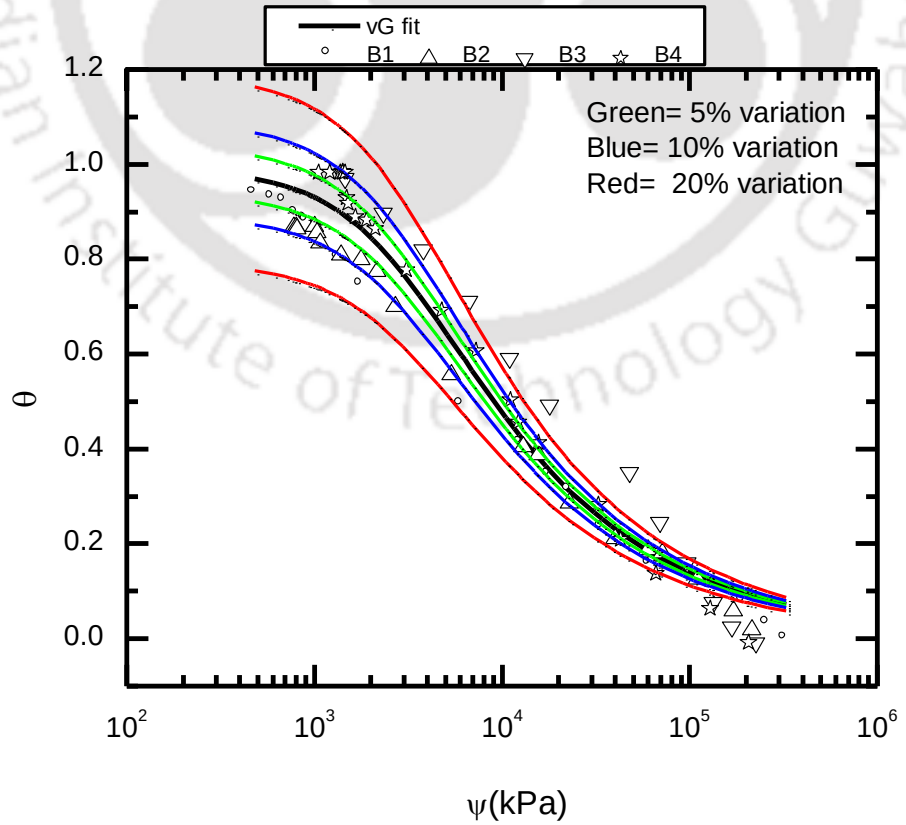

Figure 5.28 Variability of measured WRCC for bentonites with vG model

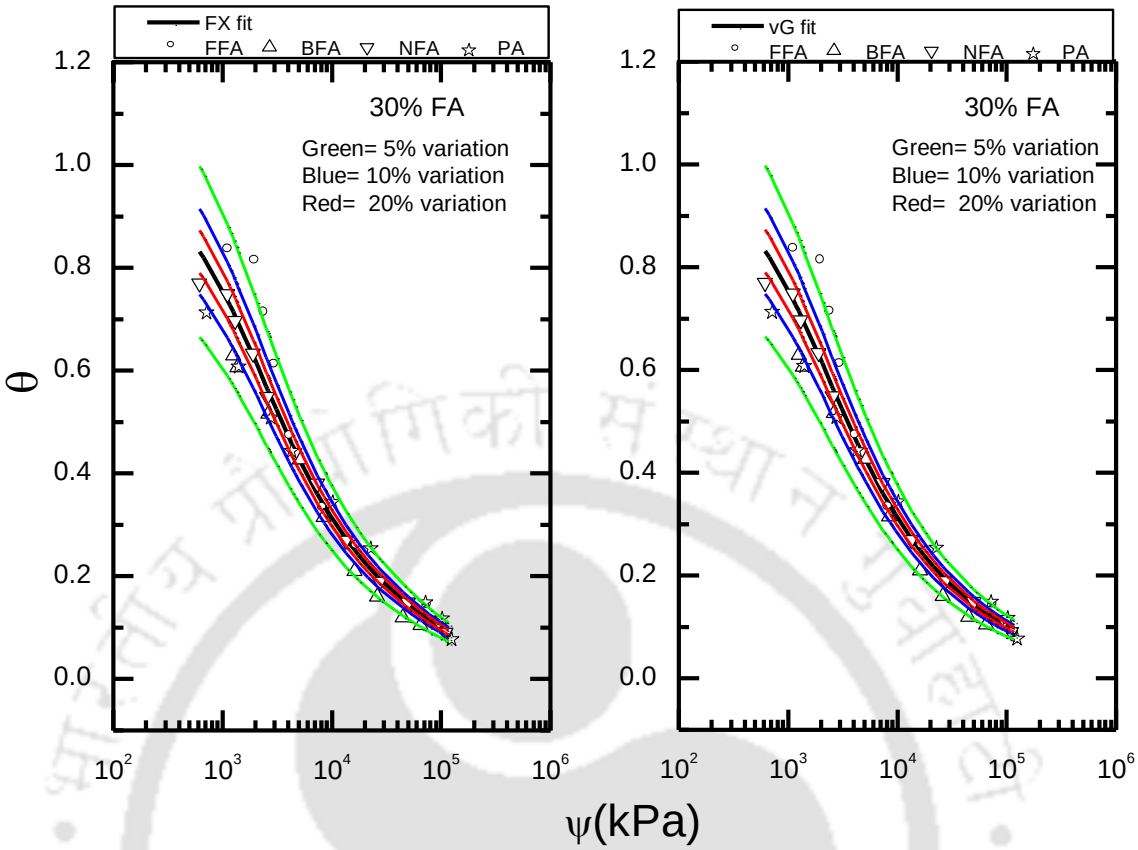

Figure 5.29 Variability of measured WRCC for 30% FA content

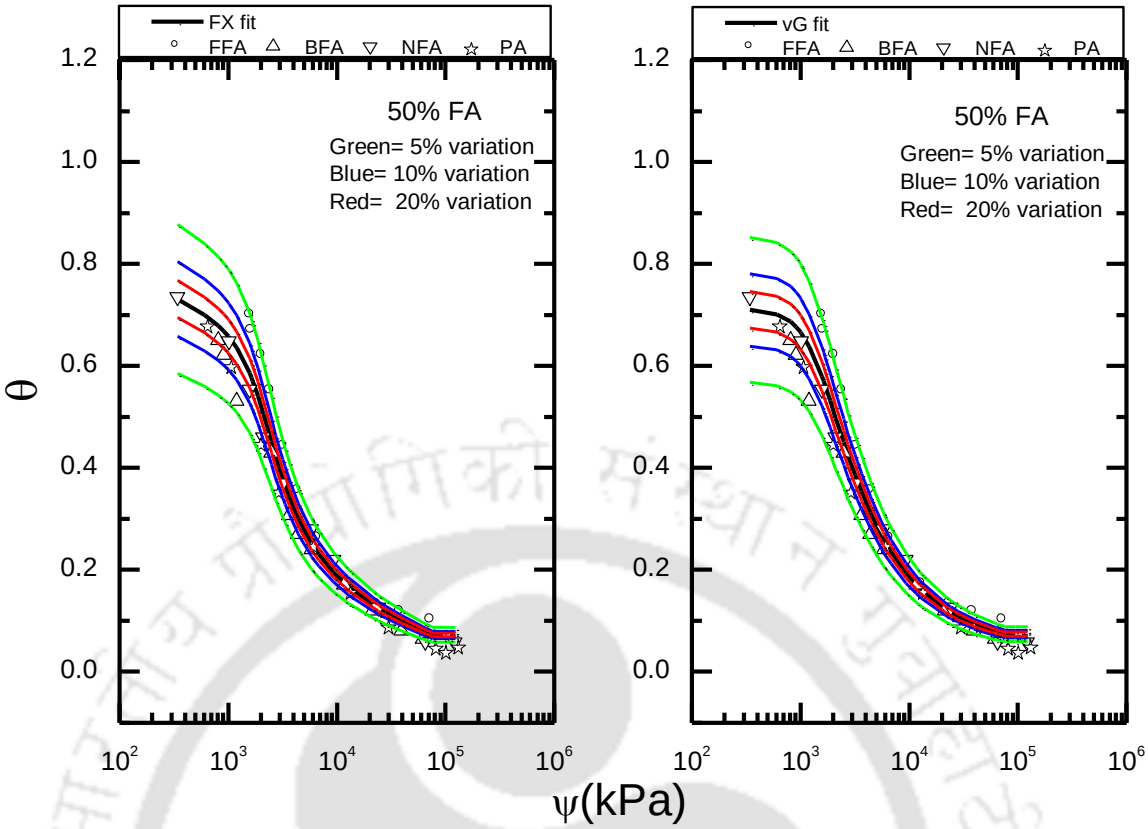

Figure 5.30 Variability of measured WRCC for 50% FA content

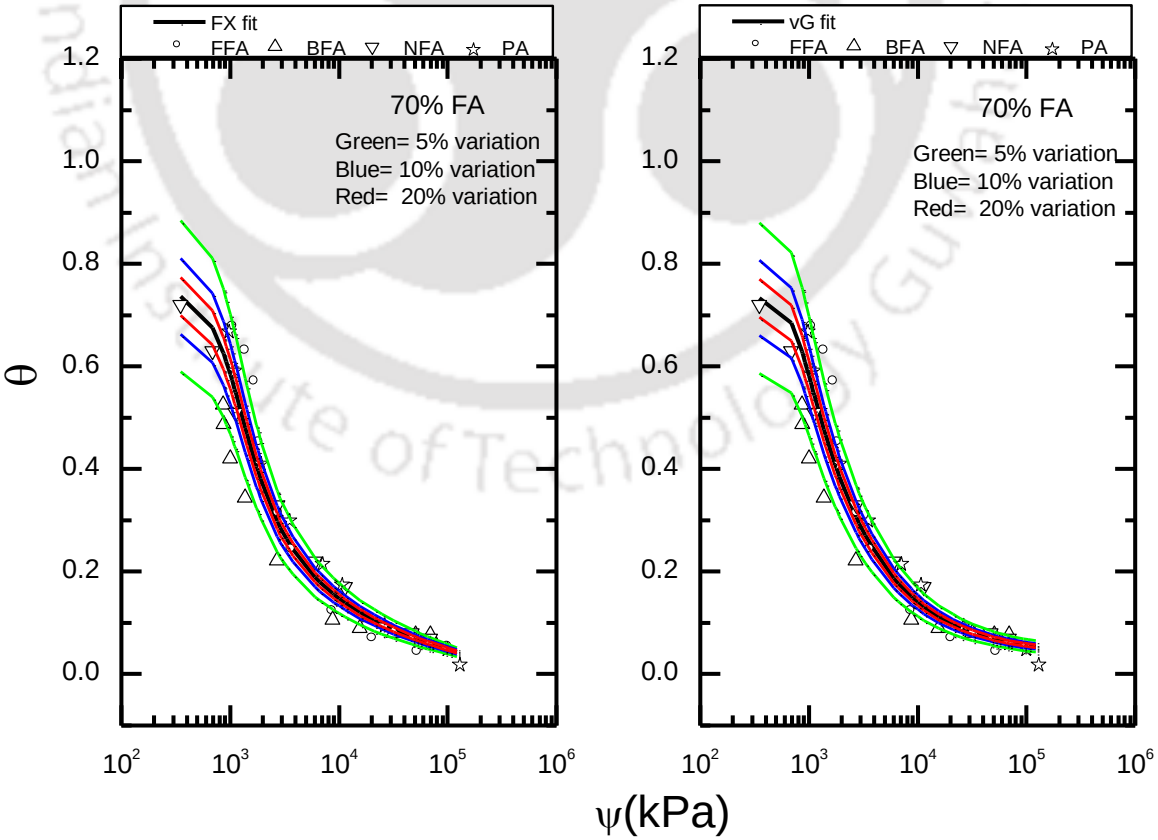

Figure5.31 Variability of measured WRCC for 70% FA content

5.17 Summary

The result of water retention characteristics curve (WRCC) of four different types of bentonites and fly ash-bentonite (FA-B1) mixes was discussed in this chapter. The study established WRCC in terms of gravimetric water content w and volumetric water content θ. For this purpose, extensive studies were conducted to determine shrinkage characteristics. The result of shrinkage test of the bentonites proved that it remains saturated over a wide range of w. The study advocates that for obtaining WRCC fitting parameters accurately, it is essential to establish the shrinkage characteristics of the bentonites. The results of WRCC parameterization clearly highlighted the difference in model parameter with and without the use of shrinkage test result. Based on the present work, a new framework for WRCC parameterization of high volume change soils like bentonite was suggested to overcome ambiguities in obtaining WRCC parameters.

The study indicated the influence of FA type and FA content on the WRCC of FA-B mixes. The result indicates that WRCC of different FA-B mixes cannot be considered unique. As expected, this can be attributed to the effect of different physico-chemical characteristics of the individual FA. A statistical assessment of the variability of WRCCs of bentonites and FA-B mixes was conducted. The study showed that the WRCC of different bentonites with varying plasticity can be represented by a generalized plot with 20% variation. This observation was true for FA-B1 mix as well.

Chapter 6

Influence of WRCC Variation on Unsaturated Seepage Modeling

6.1 General

The previous chapters have discussed the variations in WRCC attributed to different reasons. However, the impact of such variations on unsaturated behavior modeling is not known. Therefore, this chapter investigates the effect of variation in WRCC parameters on unsaturated seepage modeling for specific cases of fly ashes (FAs), bentonites and fly ash-bentonite (FA-B) mixes obtained in the previous chapters. It is essential to understand whether such variations in WRCC parameters results in considerable variation in seepage modeling results or not. Transient seepage analysis was carried out in a two dimensional cylindrical column using a finite element method (FEM) based software SEEP/W, under a specified total head (H) boundary condition. The variation in pore water pressure (PWP) and volumetric water content (VWC) with time was studied for different cases.

6.2 Unsaturated seepage modeling using SEEP/W

Seepage analysis in unsaturated soil is essential to study the movement of water in geotechnical and geoenvironmental problems like design of dams, slope stability analysis, design of waste containment liners/ covers and ground water contamination. Seepage process can be mathematically represented by non-linear partial differential equation (PDE). Transient seepage analysis involves the solution of the PDE under a given set of boundary conditions, initial soil condition and soil properties. In this study, SEEP/W (Geo-Slope International) software was used to study the influence of WRCC variation on unsaturated seepage modeling. Unsaturated seepage modeling using SEEP/W is based on Darcy's law given by Eq. 6.1 below.

$$q = ki \tag{6.1}$$

where,

q= specific discharge

k= hydraulic conductivity

i= hydraulic gradient

Darcy's law was mainly derived for flow in saturated soil. However, Richards (1931) applied continuity principle to the Darcy's equation and derived a general PDE for the water movement in unsaturated soil. The transient form of this equation is known as Richards equation (Richards 1931). SEEP/W uses Richards equation represented by Eq. 6.2 to study unsaturated seepage.

$$\frac{\partial}{\partial x}\left(k_x \frac{\partial H}{\partial x}\right)+\frac{\partial}{\partial y}\left(k_y \frac{\partial H}{\partial y}\right)+Q=\frac{\partial \theta}{\partial t} \tag{6.2}$$

where

H= total head,

k_x= hydraulic conductivity in the x-direction,

k_y= hydraulic conductivity in the y-direction,

Q= applied boundary flux,

θ= volumetric water content (VWC)

t= time

For simplification k_x is kept same as k_y which gives Eq. 6.3

$$k_x\left(\frac{\partial^2 H}{\partial x^2}+\frac{\partial^2 H}{\partial y^2}\right)+Q=\frac{\partial \theta}{\partial t} \tag{6.3}$$

6.3 Types of analysis in seepage modeling

Seepage analysis includes steady state and transient state analysis as discussed below:

6.3.1 Steady state seepage analysis: In steady state analysis, there is no change in volume of water with time. The steady state equation is independent of time variable and do not consider volumetric water content function. It requires only saturated coefficient of permeability as an input function. In steady state analysis, initial pore water pressure (PWP) condition is not required. The output result will give the PWP variations in the problem domain under specified boundary conditions.

6.3.2 Transient state seepage analysis: In transient state analysis, there is a change in volume of water with time. It requires both the coefficient of permeability and coefficient of water volume storage function as an input function for performing seepage analysis. In

order to run the transient analysis for a desired time interval, an initial PWP need to be specified. To study the sensitivity of WRCC (which represent water volume storage function) on unsaturated seepage results, transient analysis was performed in this study.

There are different types of initial conditions available in SEEP/W. In this study, the initial condition was specified as "activation water pressure" with a negative pore water pressure (suction) value corresponding to the residual water content (known from the measured WRCC) of the geomaterial considered. This will define a near dry state of the material as the initial condition for transient analysis, which corresponds to a highly unsaturated state.

6.4 Steps followed in the unsaturated seepage modeling

The different steps followed in performing the unsaturated seepage modeling and the problem domain are discussed below:

i) Generation of the model: A two dimensional cylindrical column with 0.5 m diameter and 1.0 m height was defined in the SEEP/W as shown in Figure 6.1. The region was discretized into small elements by using the automotive mesh command. A uniform meshing of 0.03 m was determined for the whole domain as shown in Figure 6.2. It was found that further reduction in mesh size do not influence the results much. Four noded quadrilateral elements were selected for the meshing.

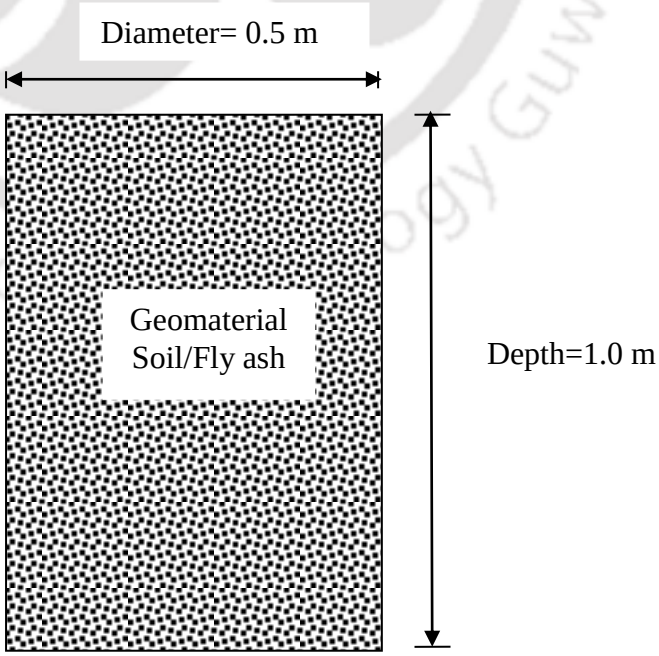

Figure 6.1 Cylindrical column domain for unsaturated seepage modeling

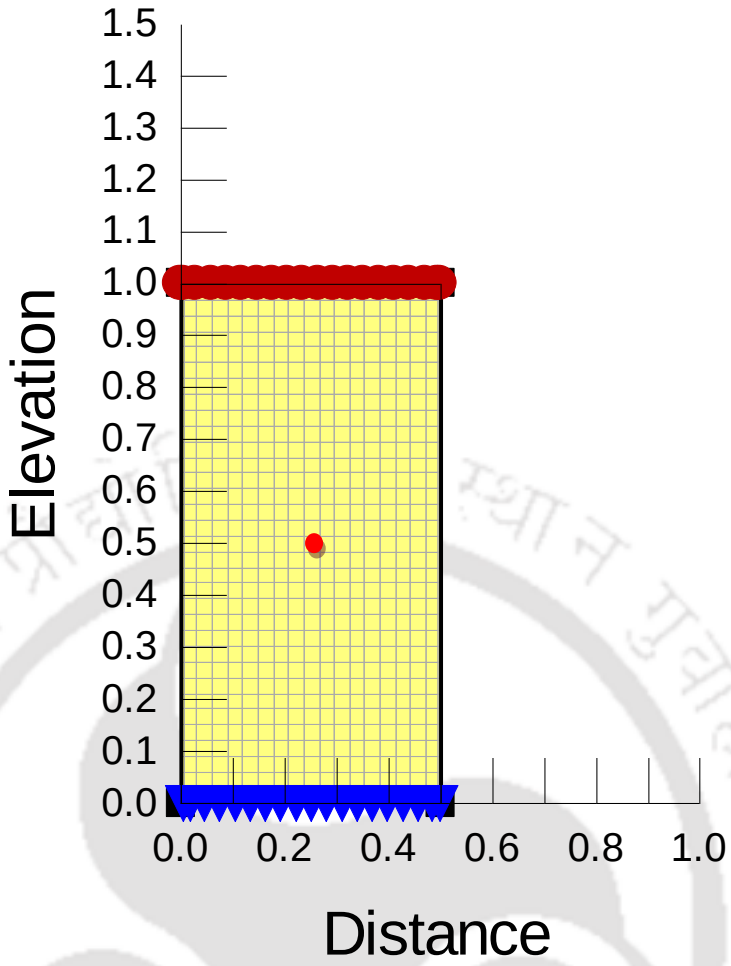

Figure 6.2 Meshing of the soil column in SEEP/W

ii) Assigning material property: For transient analysis, FX WRCC parameters (a_f, n_f, m_f and θ_s) obtained in the previous chapters 4 and 5 and saturated hydraulic conductivity (k_{sat}) as given in Table 3.6 were used as input material properties.

iii) Assigning boundary conditions: The boundary conditions assigned for the problem domain are stated as follows:

i) At the top of the column, a total head (H) of 2.5 m was considered by considering bottom of the column as reference datum. This will give a ponding water condition of 1.5 m at the top of the column.

ii) A unit gradient boundary condition was defined at the bottom of the column to nullify the effect of capillary zone attributed to the presence of water table (SEEP/W 2007, Geo-Slope International).

iii) The sides of the column were defined as no flow boundary.

iv) The initial condition of soil column was maintained as near dry state by fixing the activation water pressure value corresponding to residual state based on the measured WRCC.

iv) Solution of the model: After providing all the necessary input as explained above, the transient analysis was performed for the desired time steps. The results can be viewed at any particular node in the whole domain or at any section within it. In this study, the center node was selected as the reference point for all comparison as shown in Figure 6.2 and PWP and VWC variation with time were plotted. The total time duration was selected in such way that the PWP at the reference point approaches a positive value from an initial negative value corresponding to the residual condition. The variation in PWP from high negative residual suction to positive PWP is attributed to the migration of wetting water front from top to bottom direction of the column.

The difference in PWP and VWC variation with time was compared for specific cases by inputting the appropriate WRCC parameters obtained from previous chapters. The time required for wetting front to saturate 50% of the column depth (represented by t_{50}) as stated above was used as the reference parameter for comparisons. In this manner, the sensitivity of WRCC parameter variations on unsaturated seepage modeling was studied. It may be noted that drying WRCC was measured in this study whereas the unsaturated seepage is a wetting process. However, measurement of wetting WRCC is quite complex especially for fine-grained soil (Lin and Cerato 2013). In the absence of measured wetting WRCC, drying WRCC can be used for unsaturated behavior modeling. Therefore, the seepage results obtained in this study may not be truly representative of the actual field condition. The aim of this study was only to appraise the sensitivity of WRCC parametric variation on unsaturated seepage modeling. Hence, the use of drying WRCC instead of wetting WRCC would not influence the scope of the present study.

6.5 Unsaturated seepage modeling for fly ash (FA)

There are two types of WRCC variations of FA targeted in this section. There were differences in WRCC of different FAs used in this study. It is of interest to know how much of this WRCC variations would translate to unsaturated seepage modeling results. Second aspect is that for the same FA, different methodologies were used for establishing WRCC. The non uniqueness of WRCC attributed to measuring methodologies and its impact on unsaturated seepage modeling needs to be studied. The time t_{50} as discussed above was used as the reference parameter for comparisons.

6.5.1 Influence of FA variability on unsaturated seepage modeling

The WRCC of FAs measured using tensiometer (TM) and equitensiometer (EQT) were used to study the influence of FA variability on unsaturated seepage modeling. For a particular suction measuring methodology (TM or EQT), the variation in unsaturated seepage modeling attributed to different source of FAs were studied in terms of PWP and VWC variation with time. Figures 6.3 and 6.4 indicate the variation of PWP and VWC with time at 0.5m depth (center) of the column for TM and EQT, respectively. It needs to be mentioned here that both the PWP and VWC will change with time due to the downward seepage of water in the column. The values of t_{50} obtained from above for different FAs were given in Table 6.1.

As seen in Figure 6.3 for TM measurements, the variation in PWP with time was found to be similar for FFA, BFA and PA. It needs to be mentioned here that TM measurements could not be obtained for NFA. The time t_{50} for FFA and BFA were comparable while it was marginally high in case of PA. It was also observed that though the saturated θ_s was lower for PA than FFA and BFA still the time required for the water front to reach the 0.5 m depth becomes higher. Comparing the k_{sat} of these FAs listed in Table 6.1, it can be noted that all the FAs have comparable values in the order of 10^{-7} m/s. Thus the results highlight the influence of WRCC fitting parameters of FAs on the seepage modeling results. However, the individual contribution of WRCC parameter on unsaturated seepage modeling was not clear from this comparison.

The results obtained for unsaturated seepage modeling by the EQT measurements for FAs were presented in Figure 6.4. A comparable trend was obtained between the FFA and NFA, while variation was seen for BFA and PA. The t_{50} for all the FAs was in the order FFA<NFA<PA<BFA in case of EQT. Based on the above observations, it can be noted that seepage modeling result i.e. PWP and VWC were affected by the given variation in WRCC parameters for FAs.

It was clear from chapter 4 that the ideal measurable range of WRCC for FA is up to 1000 kPa. The implications of using a low range instrument like TM (0 to 90 kPa) for measuring WRCC of FA need to be understood. Therefore, PWP variation with time obtained based on the WRCC measured using TM and EQT methods were compared for three FAs as shown in Figure 6.5. There is a marginal difference of seepage modeling results obtained based on TM and EQT measurements. For FFA, TM method exhibited higher t_{50} value than EQT, while it is reverse in the case of BFA and PA. The results indicate the need to adopt appropriate range of suction measurement suitable for a given

geomaterial. For brevity, the variations in VWC with time were not presented. The trends were in line with the results of PWP with time.

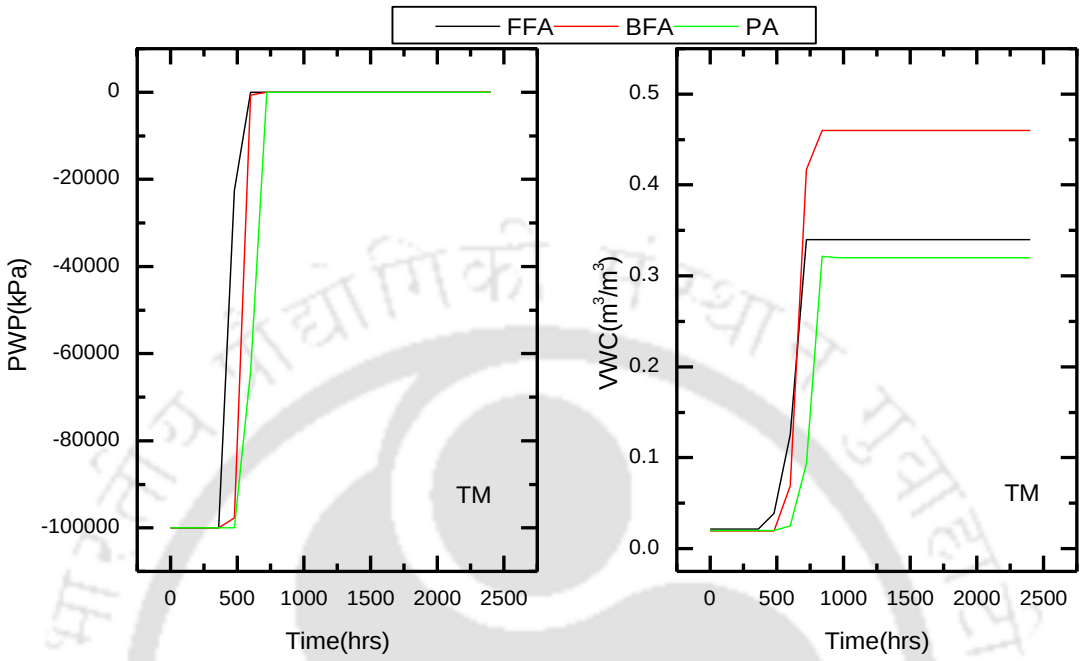

Figure 6.3 PWP and VWC at 0.5m depth for fly ashes based on TM measurements

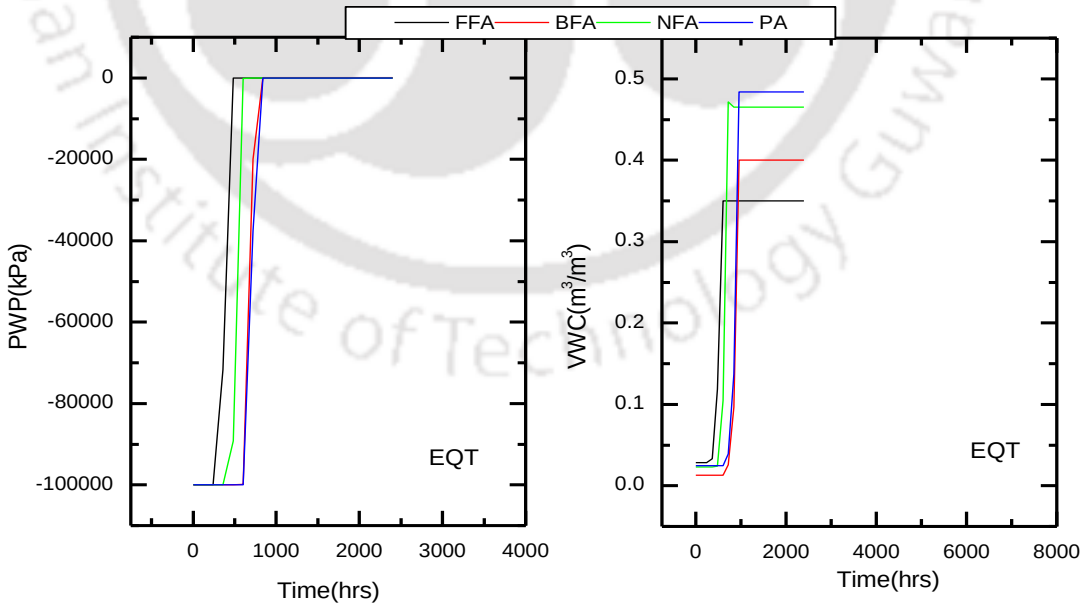

Figure 6.4 PWP and VWC at 0.5m depth for fly ashes based on EQT measurements

Table 6.1 Summary of t_{50} (hrs) determined for FAs based on TM and EQT measurements

Methodology used	**t_{50}(hrs)**			
	FFA	**BFA**	**NFA**	**PA**
TM(0-90 kPa)	550	620	-	750
EQT(0-1000 kPa)	400	890	625	820
k_{sat}x10^{-7}(m/s)	3.22	3.72	3.19	3.48

-: could not be determined

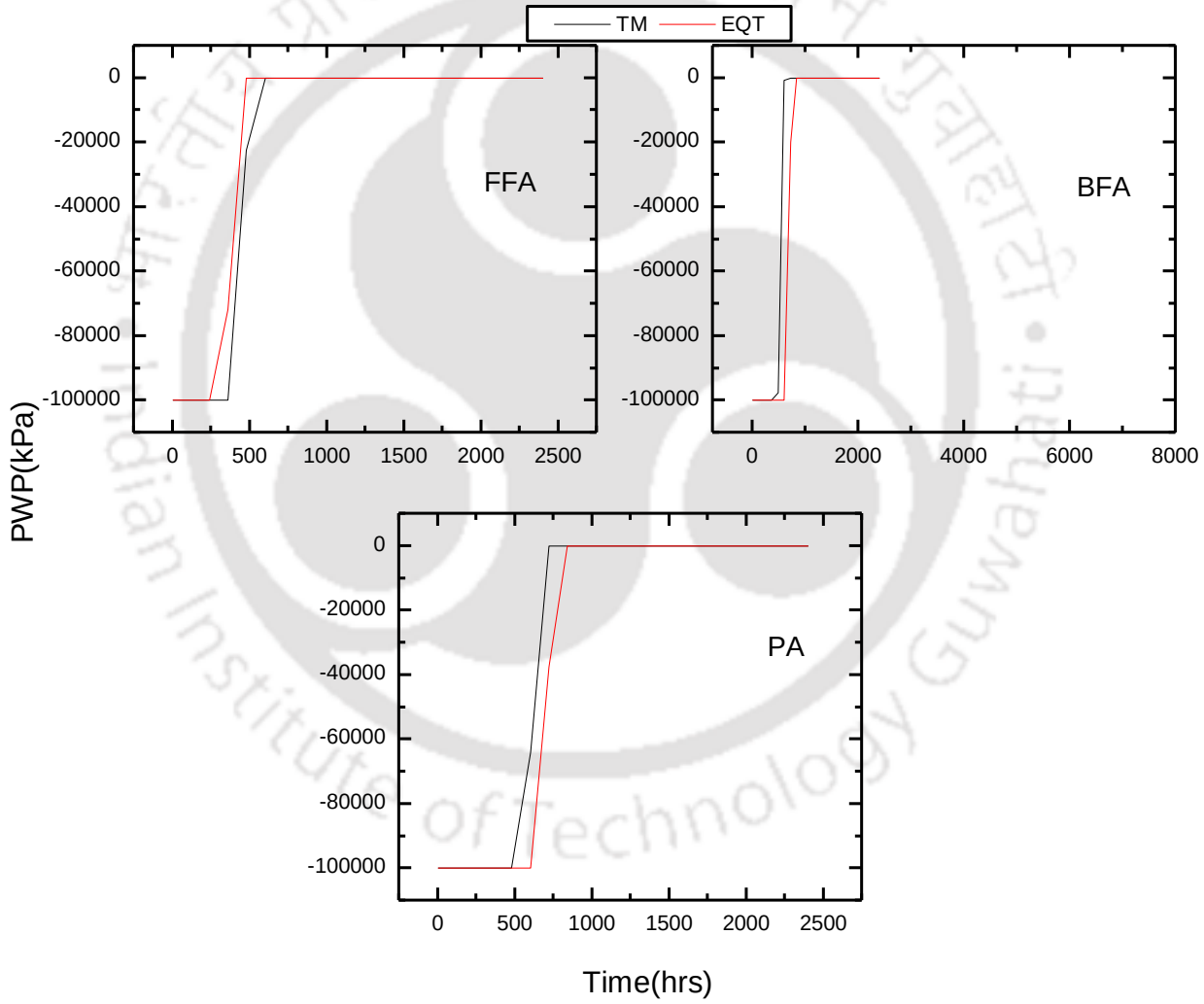

Figure 6.5 Comparison of PWP for TM and EQT

6.5.2 Variation in PWP with time for FAs at same saturated hydraulic conductivity

The above observation and comparison of PWP and VWC with time is influenced by WRCC parameters, saturated hydraulic conductivity (k_{sat}) and unsaturated hydraulic conductivity function of the FAs. The unsaturated hydraulic conductivity function is estimated based on measured WRCC and k_{sat}. This means that both WRCC parameters and k_{sat} would influence unsaturated seepage modeling results presented in section 6.5.1. To understand the influence of only WRCC parameters, k_{sat} was kept same for all the FAs. Figure 6.6 gives the variation of PWP and VWC with time by considering same value of k_{sat} equal to 3.22×10^{-7} m/s and WRCC obtained from EQT measurements for all FAs. The result shows a comparable trend of PWP and VWC for FFA and NFA while BFA and PA showed delayed saturation. Comparing the result of Figure 6.6 (constant k_{sat}) and Figure 6.4 (actual k_{sat}) it was clear that the results were not comparable. This indicates that the variation in the PWP with time for different FAs presented in Figure 6.4 can be attributed to the variation in the WRCC parameters.

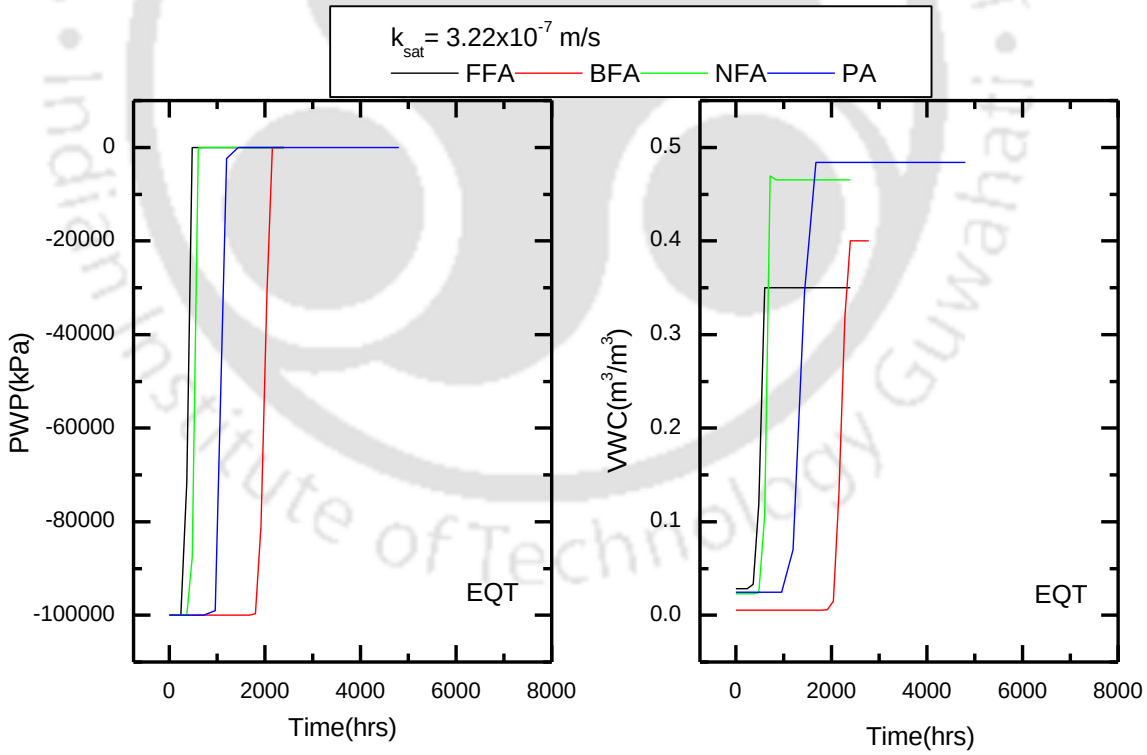

Figure 6.6 PWP and VWC variation of FAs for k_{sat}= 3.22×10^{-7} m/s and EQT measurements

6.5.3 Sensitivity analysis to study the influence of WRCC parameters on unsaturated seepage modeling results of FA

In the previous sections the effect of FA variability and suction measuring range on unsaturated seepage modeling results were investigated. However, it was difficult to understand the influence of individual WRCC parameter on unsaturated seepage modeling results. Therefore the influence of each FX fitting parameters a_f, n_f and m_f on PWP variation with time was investigated by considering the WRCC measured using EQT. For this purpose, the mean and standard deviation of FX WRCC parameters a_f, n_f and m_f of the four FAs (values from Table 4.2) were calculated. Based on the standard deviation, the maximum percentage variation from the mean value was calculated and listed in Table 6.2. Seepage modeling was then performed by varying one parameter at a time up to a maximum percentage variation defined by standard deviation. Mean value of each parameter was considered as the reference value. The results of sensitivity analysis are shown in Figures 6.7 to 6.9 for the three parameters.

Table 6.2 Range of FX WRCC parameters for sensitivity study

FX parameter	Mean	Std. deviation	% variation Mean± Std. deviation
a_f	45.76	7.89	±17
n_f	5.25	3.02	±58
m_f	0.65	0.24	±37

Figure 6.7 shows the sensitivity of a_f parameter on the PWP variation with time for constant reference values of n_f and m_f. Since the maximum variation of a_f was ±17%, its sensitivity on seepage modeling results were obtained up to a maximum percentage variation of ±20% from the mean value. Similarly, the sensitivity of n_f and m_f were obtained for a maximum variation of ±60% and ±40%, respectively as shown in Figures 6.8 and 6.9. It can be noted that even 10% variation in parameters from its reference value has significant effect on seepage modeling results. The extent of influence on seepage modeling results was not similar for positive and negative variation of parameters. For an increase in a_f and decrease in n_f, m_f parameters from its respective mean value results in increased seepage and quick saturation. For all the three parameters investigated, the

sensitivity on seepage modeling results drastically reduces beyond 20% variation from the reference mean value.

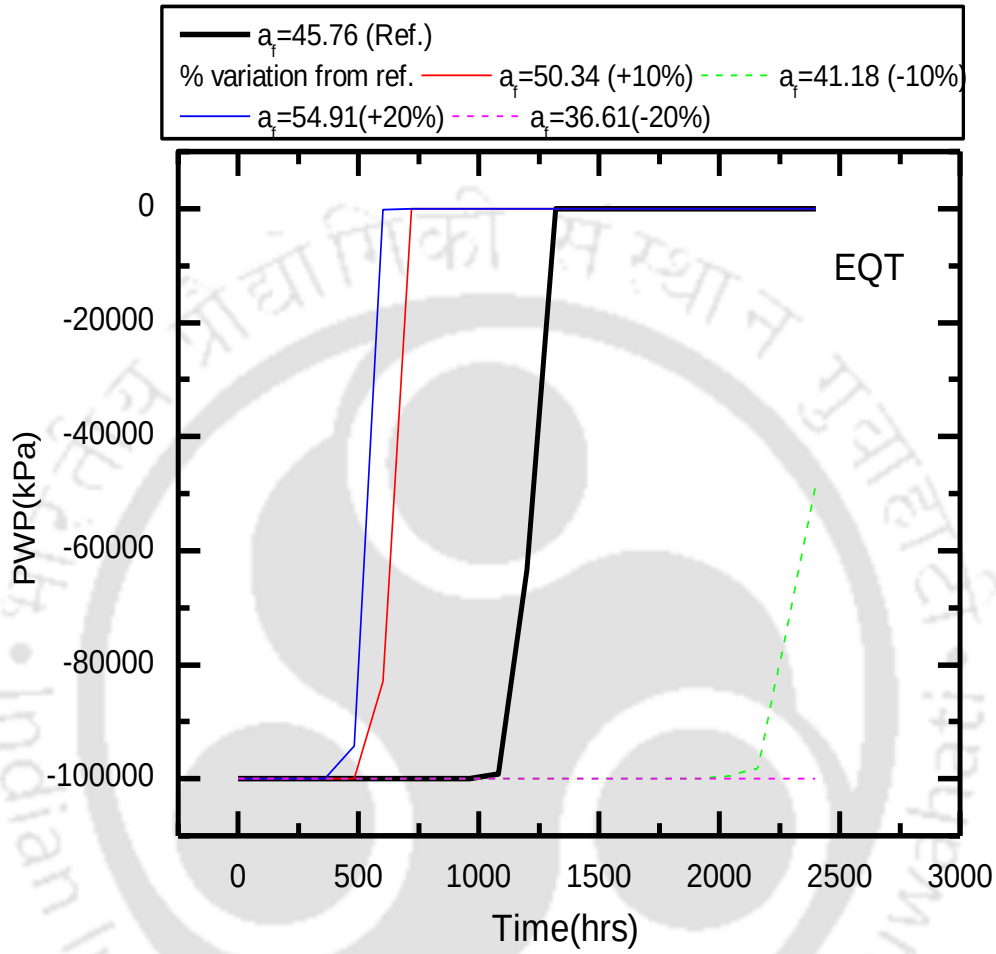

Figure 6.7 Sensitivity of a_f parameter on seepage modeling of fly ash

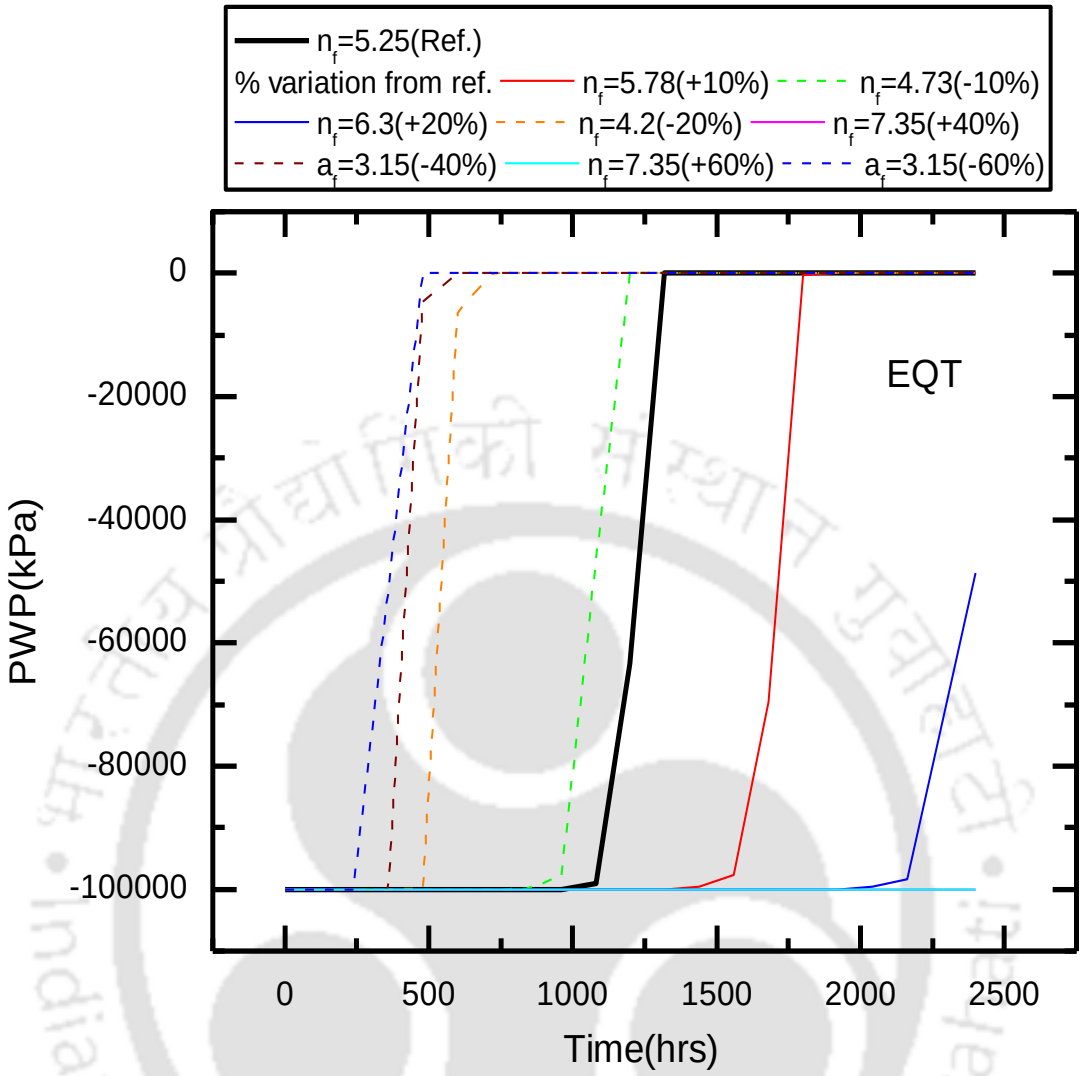

Figure 6.8 Sensitivity of n_f parameter on seepage modeling of fly ash

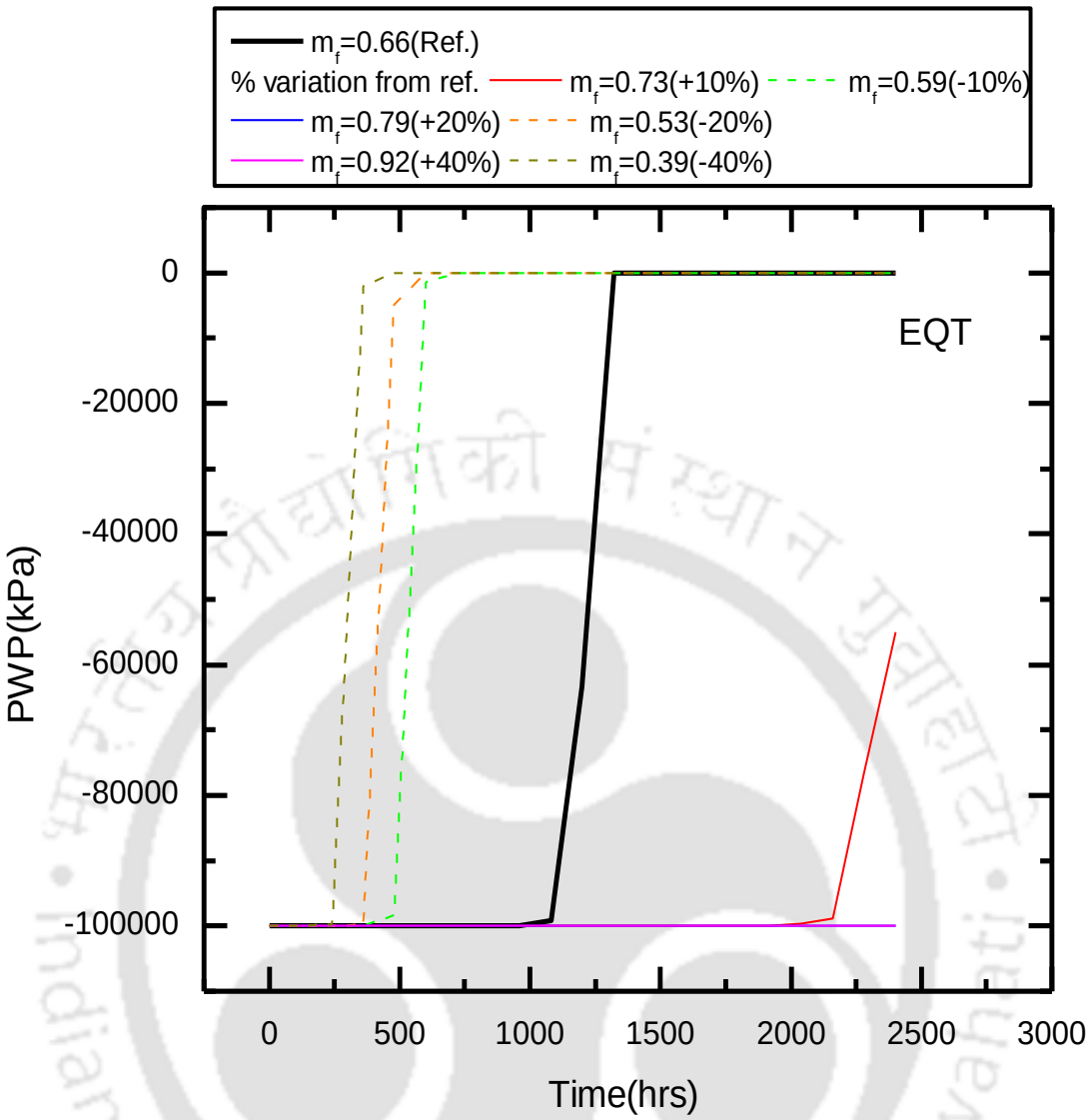

Figure 6.9 Sensitivity of m_f parameter on seepage modeling of fly ash

6.6 Influence of bentonite WRCC on unsaturated seepage modeling

The unsaturated seepage modeling results in terms of PWP and VWC variation with time for the four bentonites were determined for the same model and boundary conditions as discussed in section 6.5. Firstly, the difference in seepage modeling results attributed to bentonite variability was determined for approaches 1 and 2 (discussed in section 5.5.1 and 5.5.2). Further, the sensitivity of approaches 1 and 2 on seepage modeling results was investigated for a particular bentonite. It was clear from section 5.5.2 that approach 2 is appropriate for WRCC parameterization of bentonites. Therefore, the present analysis would help to understand the deviations in unsaturated seepage modeling when approach 2 is not considered.

Figure 6.10 shows the variation of PWP and VWC with time for all bentonites by considering approach 1 for WRCC parameterization. It can be noted that all the bentonites follows a similar trend of decreasing negative PWP and increasing VWC with time. For comparison, the t_{50} for all the bentonites were listed in Table 6.3. As given in Table 6.3, the t_{50} values for B1 to B4 varied in the range of 312450-833333 hrs. Bentonite B2 gave minimum value of t_{50} while B3 gave the maximum t_{50} among all the bentonites. This difference in result can be attributed to the difference in the water retention characteristics and k_{sat} values. As k_{sat} for B3 was the lowest of all, the time taken (t_{50}) was the maximum. This was also clear from the VWC variation with time plot. Though θ_s was comparable for B1, B2 and B4, the final time (t_{50}) for each bentonite was different. It may be noted that the liquid limit of bentonites B1 and B2 were comparable (Table 3.3) based on which a similar soil-water interaction was expected. However, seepage modeling results were not similar for these bentonites. Based on seepage modeling results by considering approach 1, it is apparent that a similar liquid limit may not necessarily mean similar soil-water interaction characteristics for expansive soils.

Figure 6.11 shows the PWP and VWC variation with time by considering approach 2 for WRCC parameterization. It can be noted that PWP variation with time of B1, B2 and B4 were comparable. This observation is different from the observation obtained based on approach 1. For bentonites B1 and B2 with similar liquid limits resulted in similar seepage characteristics. It can also be added here that for bentonites with liquid limit variation from 244% to 310%, the seepage results were comparable However, PWP variation of B3 with liquid limit 433% deviated from the other bentonites. As expected, the time required for saturation is high for B3 as indicated by t_{50} listed in Table 6.3.

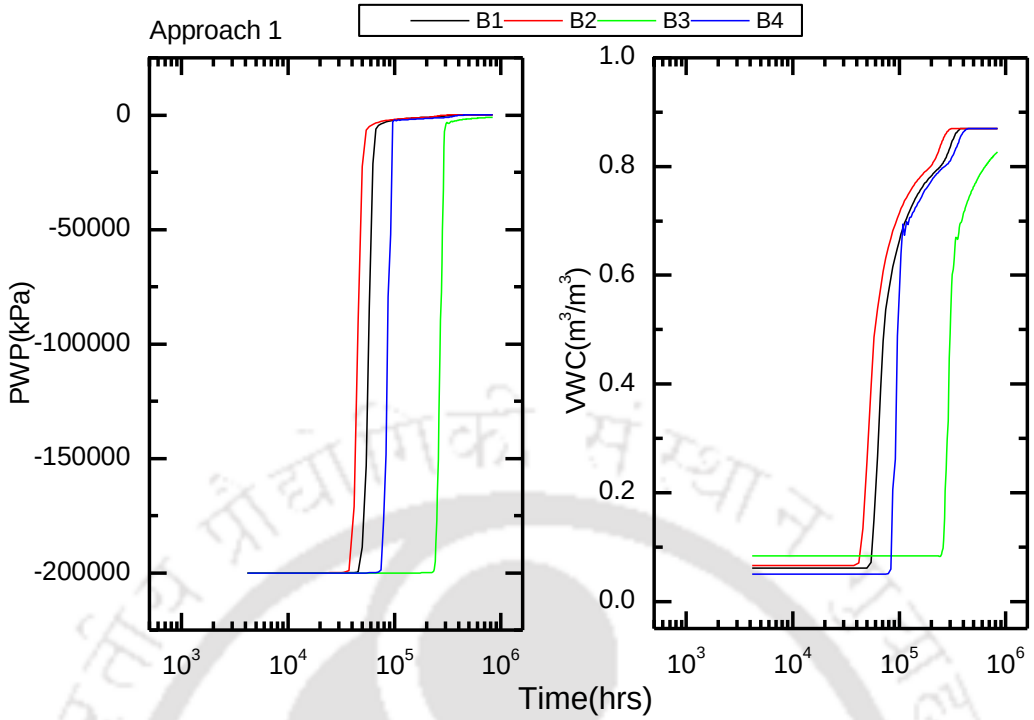

Figure 6.10 Seepage modeling results for bentonites by considering approach 1

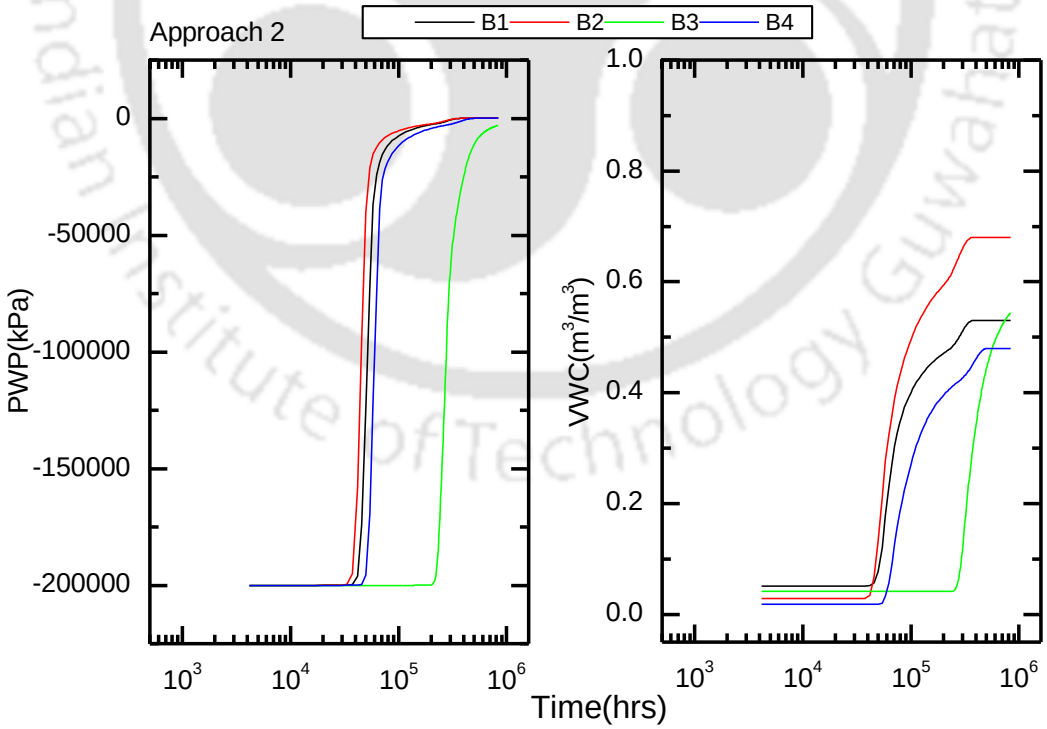

Figure 6.11 Seepage modeling results for bentonites by considering approach 2

Table 6.3 Summary of t_{50} (hrs) for different bentonites obtained by approach 1 and 2

Fitting approach	t_{50} (hrs)			
	B1	**B2**	**B3**	**B4**
Approach 1	383300	312450	833333	450000
Approach 2	433000	362000	1202620	494000

Seepage analysis based on approach 2 indicates that although the WRCC fitting parameters was not same for bentonites B1 to B4, the seepage modeling results were not significantly different. The variation in seepage results of B3 can also be attributed to marginally lower k_{sat} value than B1, B2 and B4. The study highlights that if appropriate approach was selected for WRCC parameterization, then the given variation in WRCC parameters do not have significant influence on seepage modeling results of bentonites with comparable k_{sat} values.

The variation of PWP and VWC with time was specifically compared for approach 1 and 2 for each bentonite as shown in Figures 6.12 and 6.13. It can be noted that there is difference in seepage results of all bentonites obtained based on both the approaches. WRCC based on approach 1 result in early saturation as compared to approach 2 as indicated by t_{50} listed in Table 6.3. Even though there was significant difference in WRCC obtained from both approaches, the same was not observed for seepage results. Referring to the WRCCs it can be noted that θ_s of both approaches was significantly different. However, the time taken for attaining corresponding θ_s in both the approaches was nearly same as shown in Figure 6.13. This could be a possible reason why the seepage modeling results was not significantly different for both approaches.

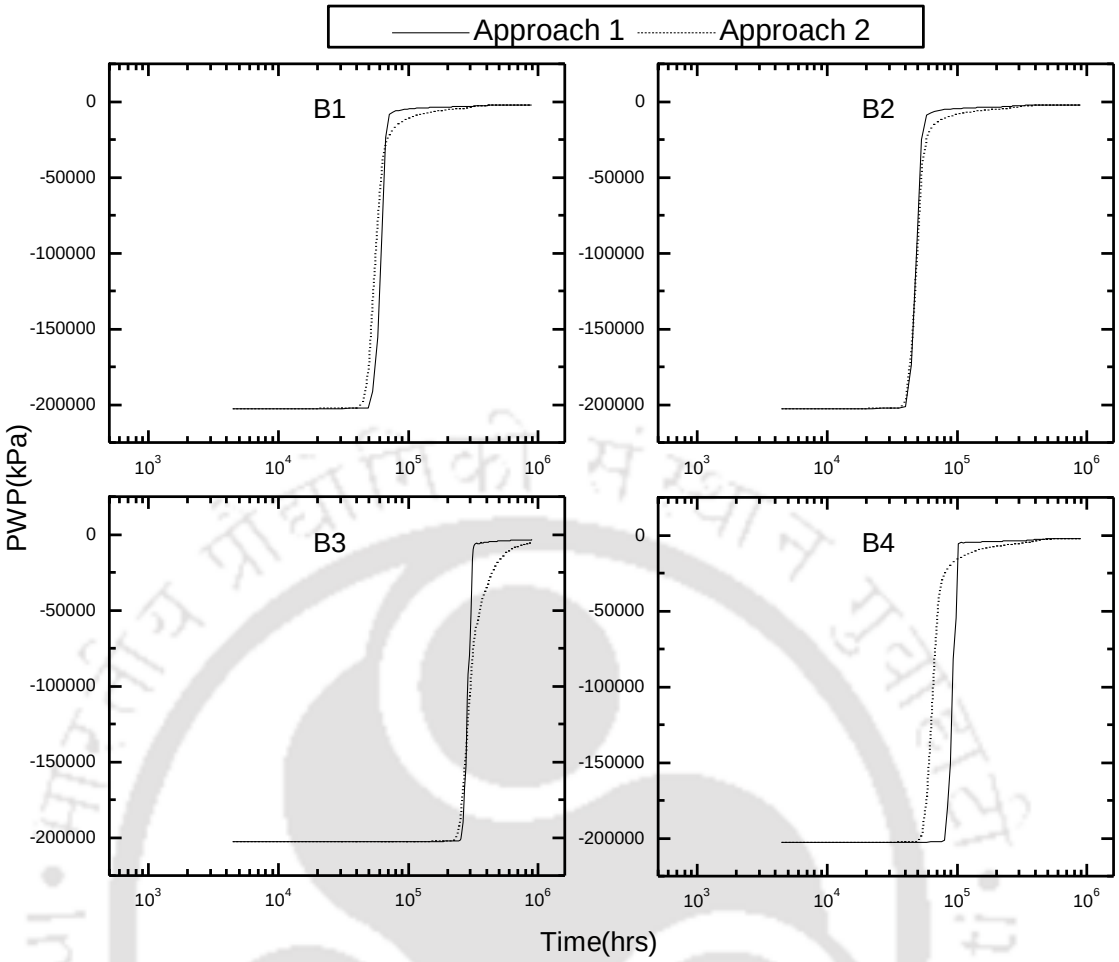

Figure 6.12 Comparison of PWP variation with time based on WRCC obtained from approach 1 and 2

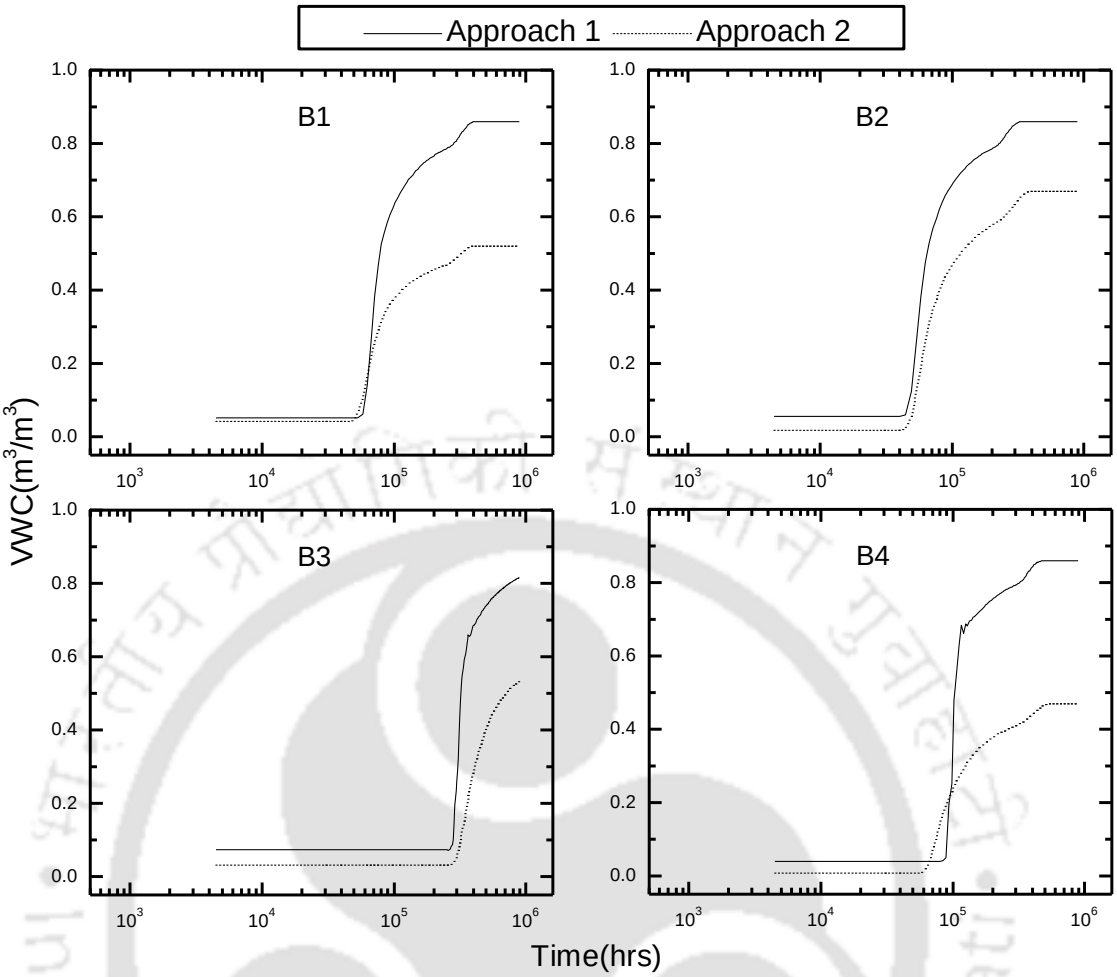

Figure 6.13 Comparison of VWC variation with time based on WRCC obtained from approach 1 and 2

6.7 Influence of FA-B1 mixes on unsaturated seepage modeling results

The influence of FA variability on unsaturated seepage modeling results of FA-B1 mixes was investigated by using the FX WRCC parameter given in section 5.14 for different mixes. The main objective was to investigate the role of FA content and FA variability on unsaturated seepage modeling of FA-B1 mixes.

6.7.1 Effect of FA content on unsaturated seepage modeling of FA-B1 mixes

Figure 6.14(a) to 6.14(d) shows the variation of PWP and VWC with time for the four FAs with FA content varying from 0 to 100%. As expected the variations in PWP and VWC with time were significantly different for varying FA content. The time t_{50} was calculated for these cases and compared in Table 6.4. For 0% FA content (i.e. B1), WRCC based on approach 2 was considered and for 100% FA content the results of EQT

method were used. As FA content increases from 0 to 100%, t_{50} decreased from a high value of 433000 hrs to 400 hrs for 100% FFA.

Table 6.4 Comparison of t_{50} (hrs) for different FA-B1 mixes

FA	% of FA				
	0% (B1)	30%	50%	70%	100%
FFA	433000	179100	70800	550	400
BFA		80800	41666	900	890
NFA		53300	37500	910	625
PA		58972	32939	1150	820

6.7.2 Effect of FA type on the unsaturated seepage modeling of FA-B1 mixes

The influence of FA type on the variation of PWP and VWC with time is shown in Figures 6.15(a) to 6.15(c). It was found that for 30% FA content, the variation of PWP with time for BFA, NFA and PA were comparable while FFA differs from the other FAs. The time t_{50} for NFA and PA was less than the FFA and BFA for 30% FA content. For 50% and 70% FA content, all the FAs showed distinct difference in the PWP variation. As shown in Table 6.4, t_{50} was found to be sensitive to FA type. It is also clear that variation in t_{50} among different FAs was found to be less as FA content in the mix increases.

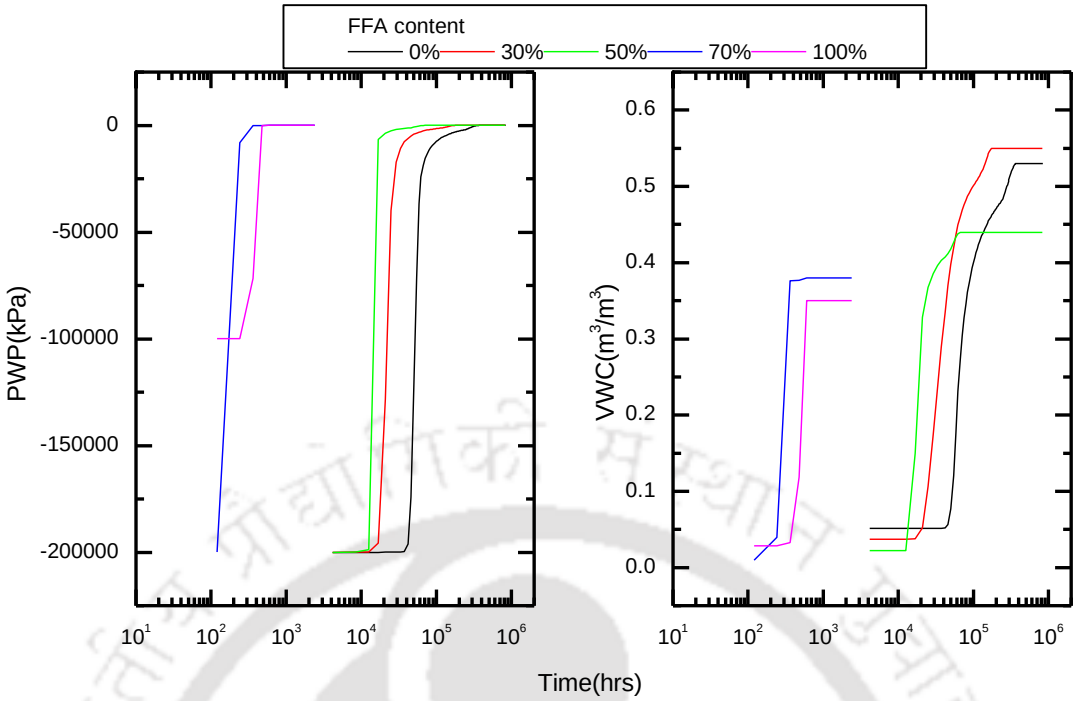

Figure 6.14(a) PWP and VWC variation with time for FFA-B1 mix

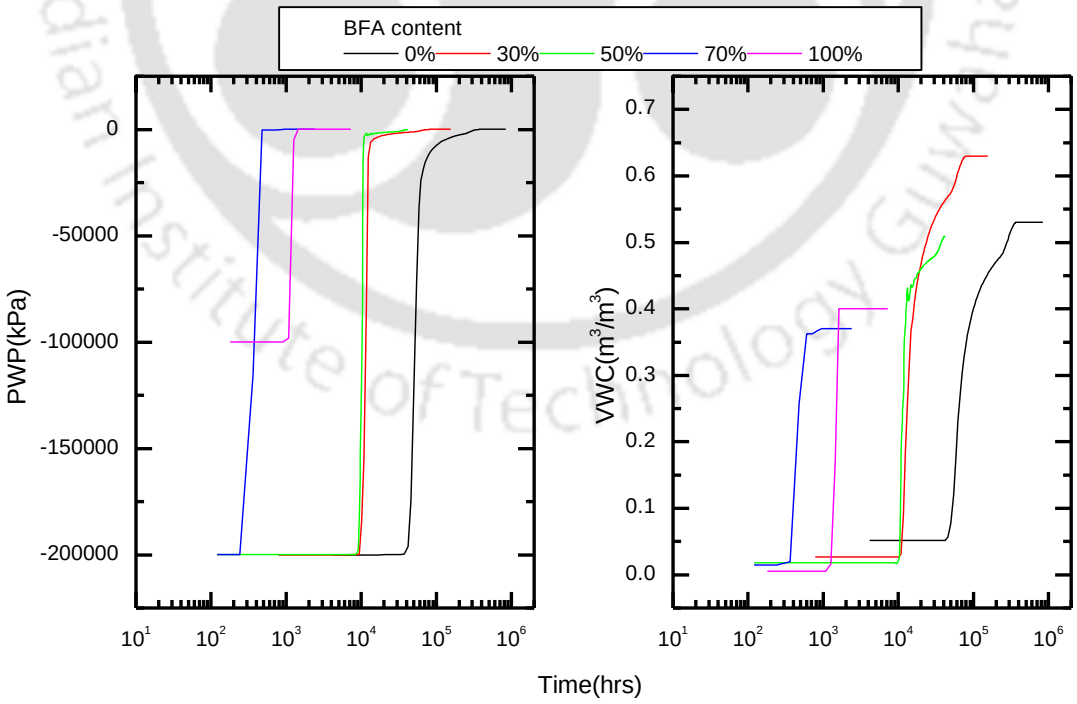

Figure 6.14(b) PWP and VWC variation with time for BFA-B1 mix

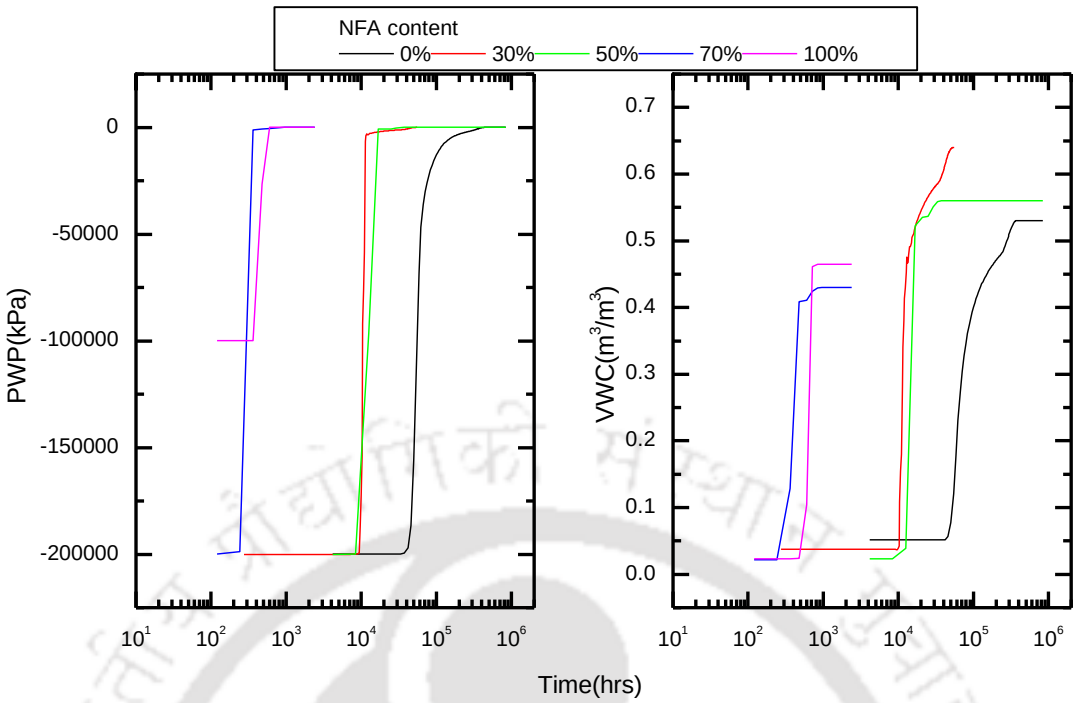

Figure 6.14(c) PWP and VWC variation with time for NFA-B1 mix

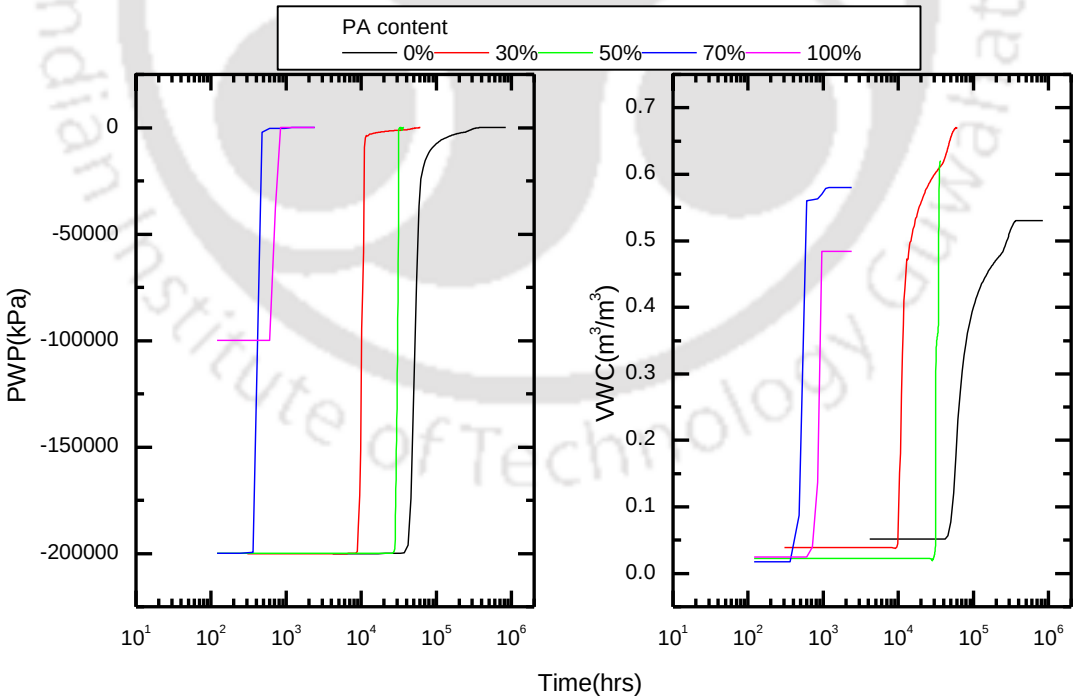

Figure 6.14(d) PWP and VWC variation with time for PA-B1 mix

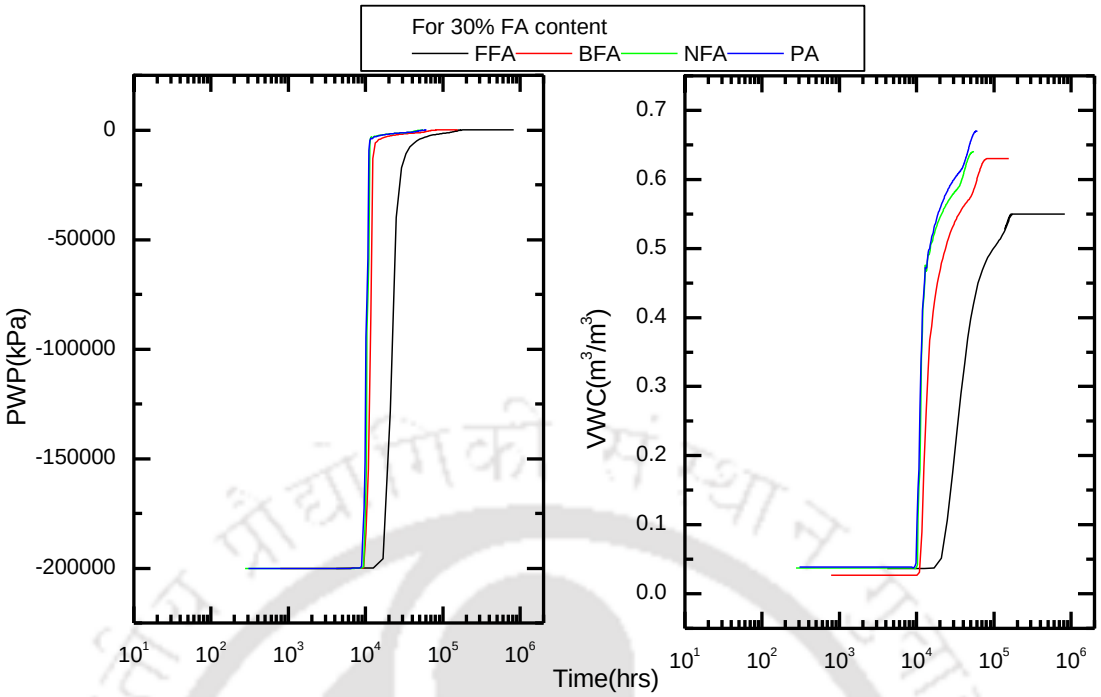

Figure 6.15(a) PWP and VWC variation with time for 30% FA content

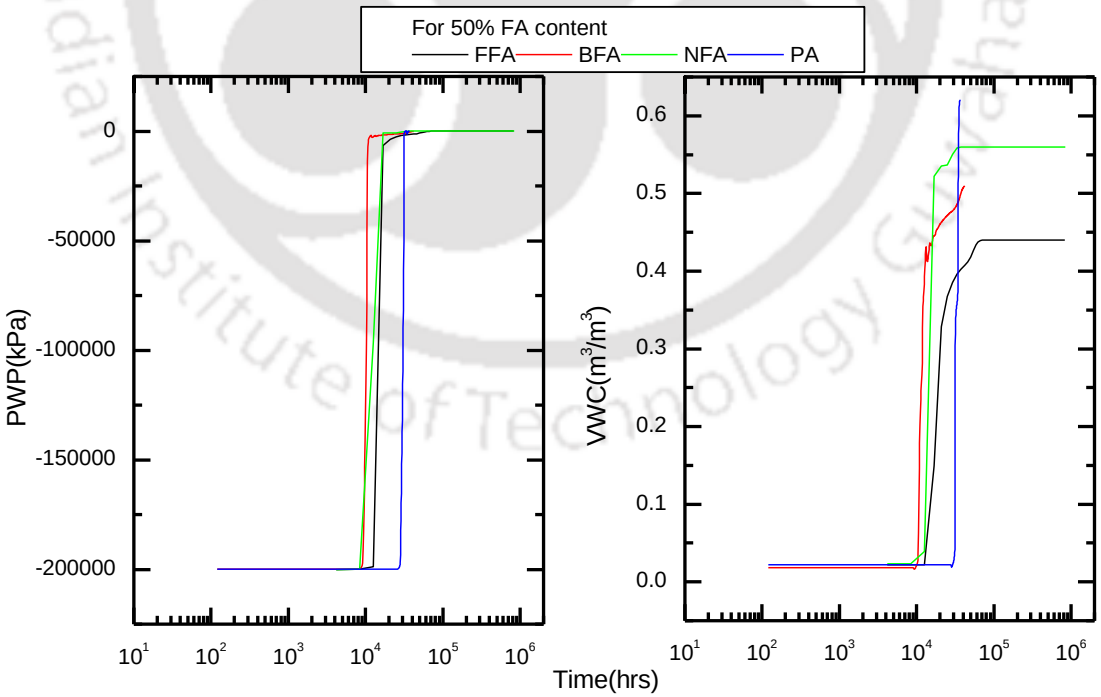

Figure 6.15(b) PWP and VWC variation with time for 50% FA content

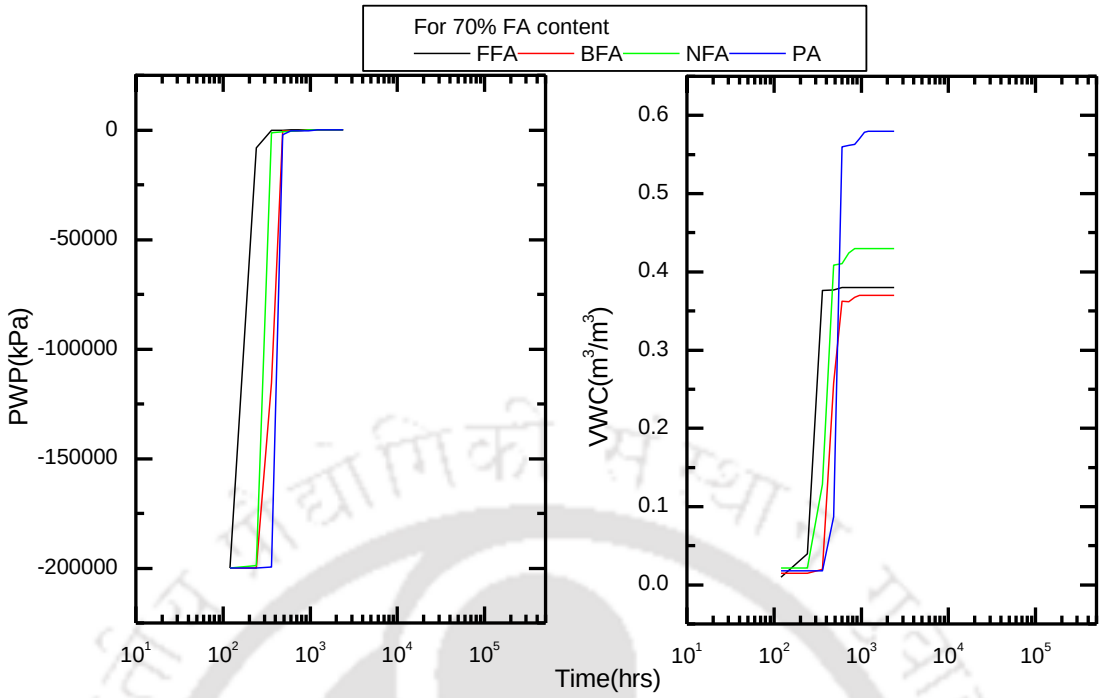

Figure 6.15(c) PWP and VWC variation with time for 70% FA content

6.8 Summary

The sensitivity of WRCC parameter variation on unsaturated behavior modeling was investigated by considering the example of transient seepage analysis for vertical water flow through an unsaturated geomaterial column. The variation in pore water pressure (PWP) and volumetric water content (VWC) with time was studied at the centre of the column. It was found that both PWP and VWC variation with time got affected when WRCC of different fly ashes were used. The influence of suction measurement range on unsaturated seepage modeling result was also found to be considerable. It was established from this study that variation in PWP with time for different fly ashes was mainly due to the variation in the WRCC parameters since the k_{sat} value of all the fly ashes were comparable.

The seepage modeling results of bentonites was investigated for the WRCC parameter obtained using two approaches i.e. with and without the use of shrinkage test results. The PWP and VWC variation with time for the first approach (without shrinkage test) showed considerable difference among all the bentonites. However, the PWP variation for B1, B2 and B4 in the second approach (with shrinkage test) showed comparable result, which was expected due to similarity in bentonite characteristics. This

observation demonstrates the appropriateness of approach 2 for WRCC parameterization of bentonites.

The seepage modeling result obtained for FA-B1 mixes showed considerable influence of FA content and FA type. For any FA type, the difference in t_{50} (i.e. time required for saturating half of the column depth) were found to be decreased with the increase in FA content in the mix. The study also shows that the variation in t_{50} among different FAs was found to be less as FA content in the mix increases.

Chapter 7

Lead Retention Characteristics of Fly Ashes and Fly Ash-Bentonite Mixes

7.1 General

The retention characteristics of different fly ashes (FAs) and fly ash-bentonite (FA-B1) mixes were studied with lead metal, Pb^{2+} as the model heavy metal contaminant. The study investigated the removal efficiency of different FAs and mixes by conducting 24 hr batch equilibrium test. Retention equilibrium studies with varying initial metal ion concentration were investigated under uncontrolled pH conditions. The main objective of this study was to analyze the potential of fly ash (FA) and its mixes with bentonite in retaining heavy metal like lead, when it will be used in liners. The influence of spatial variability of FA on retention characteristics of FA-B1 mixes will be investigated.

7.2 Retention process and isotherm

The term retention refers to all the processes by which contaminants are removed by solid surface from liquid like wastewater and landfill leachate through different mechanisms such as sorption, complexation and precipitation (Ruthven 1984). Since the study was performed under uncontrolled pH and temperature, no distinction was made among the above mentioned retention mechanisms. Any process leading to the removal of contaminants by soil solids was considered as retention.

When a solution of contaminant pass through a known amount of soil solids, retention occurs till equilibrium is reached. The equilibrium state is characterized by the solute concentration retained on the solid adsorbent (q_e) and corresponding equilibrium solute concentration (C_e) left back in the liquid phase. For a particular solid, q_e versus C_e values can be obtained for different range of initial solute concentrations. The variation of q_e with C_e for a particular contaminant-soil solid interaction can be quantified by curve fitting empirical isotherm equations to the measured data. In this study, two popular isotherm models reported in the literature (Poly and Sreedeep 2011), Langmuir isotherm and Freundlich isotherm, were used. Brief descriptions of this model with their assumptions are given below.

i) Langmuir isotherm model: The Langmuir isotherm is the equilibrium non-linear relationship between q_e and C_e which represents retention on a set of distinct localized monolayer sites. The isotherm was developed based on the concept that a solid surface

posses finite number of retention sites. According to this model, retention occurs uniformly on the active sites of the solid and the retained molecule does not have any effect on the other incident molecule. The Langmuir isotherm equation is given below:

$$q_e = \frac{bq_m C_e}{1 + bC_e} \tag{7.1}$$

where q_m is the maximum amount of contaminant retained per unit mass of the soil solid to form a complete monolayer on the surface and b is a constant related to the affinity of the binding sites (bond energy).

ii) Freundlich isotherm model: Freundlich isotherm states that the retention process may be multilayered due to the heterogeneity of the surface charges. The Freundlich equation is expressed as

$$q_e = K_f C_e^{1/n} \tag{7.2}$$

where K_f and n are constants representing the relative retention capacity of adsorbent and intensity of adsorption respectively.

7.3 Materials and methods

The four FAs FFA, BFA, NFA.PA were mixed with one bentonite B1 (randomly chosen) in the ratio 50:50. These FA-B1 mixes were subjected to lead retention study. The details of various physico-chemical properties are already mentioned in Table 3.2 to 3.5. The designation used to represent the 50:50 FA-B1 mixed was FFA50, BFA50, NFA50 and PA50. Lead (Pb^{2+}) was selected as the model contaminant due to its prominence in hazardous landfill leachate and hence a better representative model contaminant.

High purity lead nitrate ($Pb(NO_3)_2$) salt of analytical reagent grade (Merck, Germany) was used to prepare 1000 ppm stock solution. Concentrated HNO_3 acid of approximately 3 ml was added to the calculated quantity of $Pb(NO_3)_2$ salt for proper digestion. The ultrapure deionized water was then added to the salt in required quantity to make it 1000 ppm. Magnetic stirrer was used to have a uniform mixing of the salt with water. Solutions of different concentrations were prepared by appropriate dilution of the

stock solution with deionized water and the measured initial concentration ranged from 1.39 ppm to 987 ppm.

The method used for contaminant retention study was the batch test mentioned in ASTM D4646-2008. The details of the procedure is given in section 3.5. The FAs and B1 was oven dried at 60 ^{0}C to remove any moisture present in it. Soil mass of 2.5 gm was used for all FAs, bentonite and 50:50 mix. The oven dried sample was placed in a conical flask and 50 ml solution of desired concentration was added to maintain liquid to solid ratio of 20 (L/S=20). The initial pH of the solution was adjusted to 5 before the start of the experiment by adding 0.1 N NaOH or 0.1 N HCl buffer. This was done to avoid any initial precipitation of lead ions in the solution. The conical flask containing the samples and the solution were then placed on a horizontal shaker at a constant speed of 200 rpm for 24 hr. After this, the solutions were centrifuged at 2000 rpm for 10 minutes in order to separate the solids and liquid. The supernatant was then collected using a pipette and was filtered through a 0.45 μm filter paper. The filtrate was then analyzed using Atomic Absorption Spectrophotometer (AAS) (Varian, model: Spectra AA- 55B) for the equilibrium Pb^{2+} ion concentration left in the solution after the batch test. The concentration retained (q_e) on the solid surface was determined using the following formula:

$$q_e = (C_i - C_e) \times \left(\frac{V_l}{M_s} \right) \tag{7.3}$$

where

V_l= Volume of solution used in Batch test (50 ml)

M_s= Mass of solid used in Batch test.

C_i= Initial concentration of solution in ppm

C_e= Equilibrium concentration in ppm after 24hr batch test.

7.4 Results of batch equilibrium retention studies

The results of the retention equilibrium studies for different FAs and FA-B1 mixes are shown in Figures 7.1 and 7.2, respectively. From Figure 7.1, it was observed that q_e for all the FAs remain same up to 2.5 mg/g for equilibrium concentration of Pb^{2+} up to 100 ppm. With further increase in initial concentration, the free surface site of the FA gets

progressively saturated and becomes exhausted. This is shown by the inclined portion of the isotherm as shown in Figure 7.1 for FFA, BFA and PA. Similar trend was reported in the literature by Poly and Sreedeep (2011) and Younus (2010). The FFA and BFA isotherms were nearly comparable indicating similar retention capacity for Pb^{2+} ions. The PA exhibited marginally low retention among all the FAs at high concentration range. The retention characteristics of NFA was different from other FAs The presence of high amount of calcium oxide (CaO) (Table 3.4) increased the pH of the resulting solution above 8 for lower concentration as given in Table 7.1. The high pH in case of NFA was due to the hydration of CaO and release of OH^- ions. This eventually increased the pH of the resulting solution causing the precipitation of Pb^{2+} ions as $Pb(OH)_2$ at higher pH (Pandian et al. 1996). This means that retention mechanism of NFA was predominantly governed by the precipitation process than sorption for lower initial concentration. The exact quantification of the amount of sorption and precipitation for NFA for different initial concentration of Pb^{2+} was not attempted in this study. It is interesting to see that FA retains Pb^{+2} ions even though it has limited specific surface area (SSA). It was found in the literature that FA particles have spherical shaped hollow pockets called cenospheres which acts as a storage house for most of the contaminants. The presence of this hollow cenospehere was also observed in the FESEM image of the FAs used in this study (Figure 3.4(a) to 3.4(d)).

Figure 7.2 shows the Pb^{2+} retention characteristics of B1 and 50:50 FA-B1 mixes. As expected, there is a drastic increase in the retention of mixes as compared to FA alone. This can be attributed to the high SSA of B1. For the concentration range investigated in this study, the results of FA-B1 mixes were close to the results of B1. This indicates that there is not much influence of FA in the 50:50 FA-B1 mix and most of the retention was predominantly governed by high specific surface area of B1.

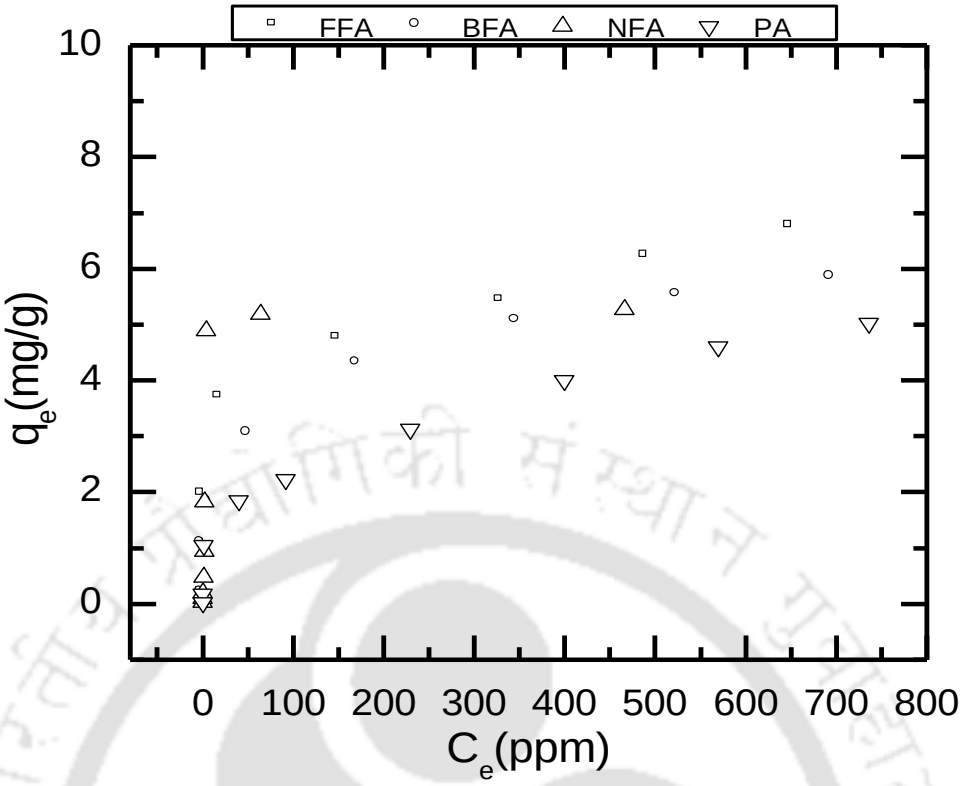

Figure 7.1 Lead retention studies for different FAs

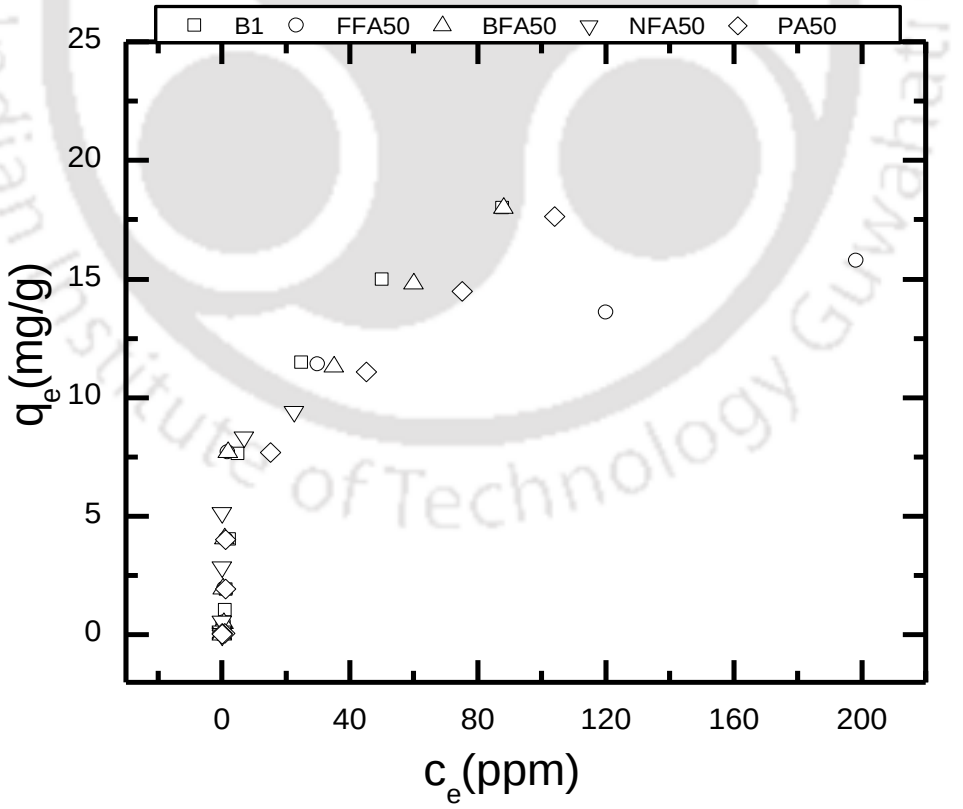

Figure 7.2 Lead retention studies for bentonite B1 and FA-B1 mixes

Table 7.1 Initial and final pH value for different solution concentration and mixes

pH		Concentration range, ppm								
		1.39	9.3	53.9	97.77	203.5	386.3	600	800	987
Initial pH		5.3	5.5	5.4	5.7	5.5	5.4	5.5	5.1	5.2
Final pH	FFA	7.3	7.16	7.1	7.2	6.0	5.5	5.6	5.1	5.2
	BFA	6.7	6.81	6.7	5.9	5.5	5.3	5.5	5.2	5.0
	NFA	9.15	9.3	9.6	8.8	8.2	7.8	7.5	6.9	6.8
	PA	7.15	7.18	7.3	6.8	5.3	7.1	6.5	5.1	4.9
	B1	7.8	7.62	7.5	7.7	7.5	5.3	6.1	5.4	6.5
	FFA50	6.78	7.22	7.42	7.9	7.6	7.5	7.2	6.5	5.8
	BFA50	6.22	7.01	6.44	7.3	7.4	7.2	6.5	6.1	5.8
	NFA50	7.63	6.78	7.87	8.2	8.6	8.3	8.2	7.1	7.5
	PA50	6.8	7.6	8.22	7.04	7.7	7.3	6.5	5.4	5.6

7.5 Comparison of Freundlich and Langmuir isotherm model parameters

The non-linear Freundlich and Langmuir isotherm model were fitted to the measured retention data as shown in Figure 7.3 and the fitting parameters were listed in Table 7.2 for all the FAs and mixes. It was observed that both the models fitted well with the experimental data with R^2> 0.9. The values shown in Table 7.2 are important inputs for assessing contaminant migration studies of FA based liners

Based on the K_f and q_m values of Freundlich and Langmuir isotherm model respectively, the retention capacity of different FAs follows the order FFA>BFA>NFA>PA and for B1 and FA-B1 mixes it follows the order B1>PA50>BFA50> NFA50>FFA50.

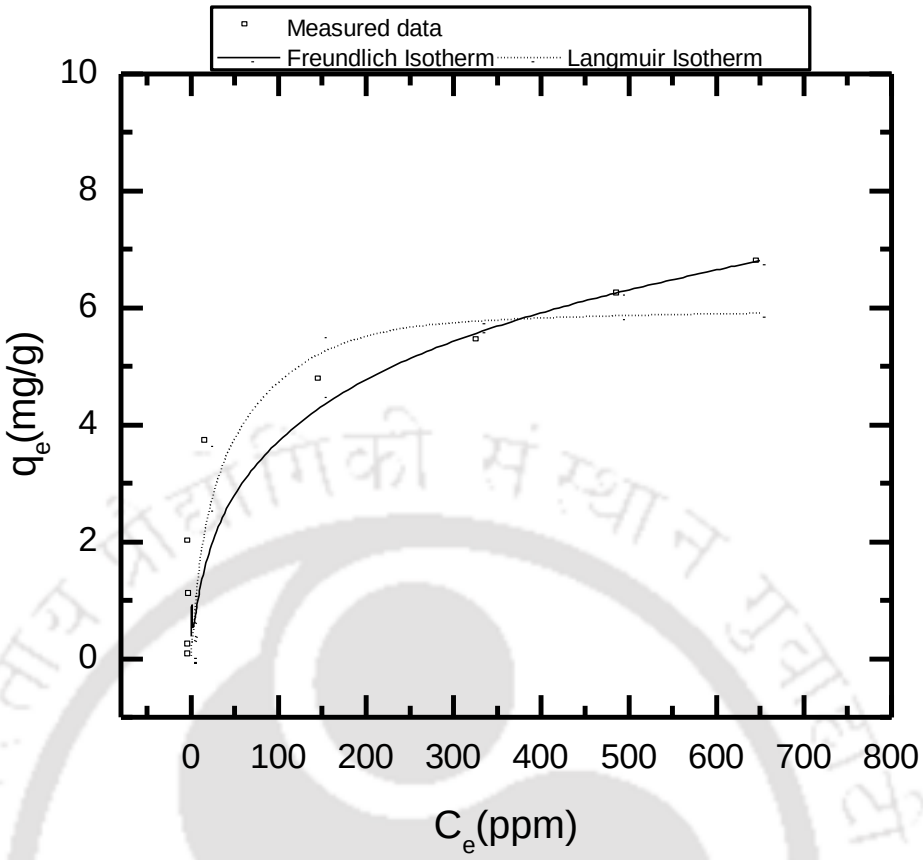

Figure 7.3 Freundlich and Langmuir isotherm model fitted to FFA

Table 7.2 Freundlich and Langmuir isotherm model parameters for fly ash and its mixes

Materials	Freundlich Isotherm			Langmuir Isotherm		
	K_f	n	R^2	q_m(mg/g)	b	R^2
FFA	1.12	3.63	0.91	6.02	0.08	0.91
BFA	0.97	3.58	0.99	5.65	0.03	0.95
NFA	0.95	3.61	0.98	5.41	0.04	0.96
PA	0.52	2.93	0.98	5.52	0.01	0.94
B1	4.45	4.45	0.96	18.54	0.10	0.98
FFA50	2.91	3.11	0.90	14.32	0.35	0.91
BFA50	3.28	2.65	0.94	15.38	0.47	0.90
NFA50	3.21	2.8	0.98	18.02	0.03	0.93
PA50	3.5	3.0	0.97	20.68	0.04	0.90

7.6 Percentage removal of Pb^{2+} by FA and FA-B1 mixes

The removal of Pb^{2+} ions was compared for various initial metal ion concentration as shown in Figures 7.4 and 7.5 for fly ash and its mixes. It was found that the metal removal efficiency decreased with the increasing initial metal ion concentrations. A drastic fall in the percentage removal efficiency was observed for the range of initial concentrations 100 ppm to 500 ppm. Above 500 ppm, there is not much change in removal efficiency. The removal efficiency of FFA, BFA and NFA were comparable while PA exhibited the lowest removal. A minimum of 30% to 35% removal was observed in FAs for the maximum initial concentration of around 1000 ppm. This low value of percentage removal would be still significant while using FA for waste containment liners in place of sand. This is mainly because sand is an inert material and do not remove any heavy metals. Thus FA offers an added advantage of contaminant removal from landfill leachate. It is worth noting that a good removal efficiency (> 90%) was observed for all the FA-B1 mixes.

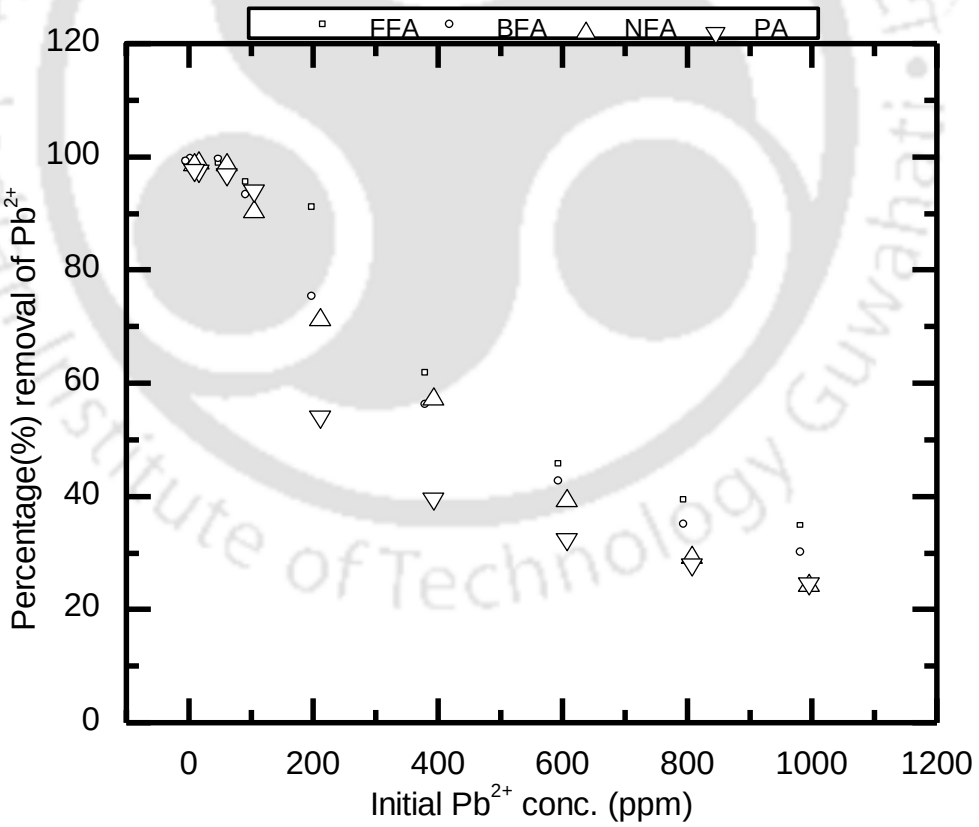

Figure 7.4 Percentage (%) removal of Pb^{2+} by FAs

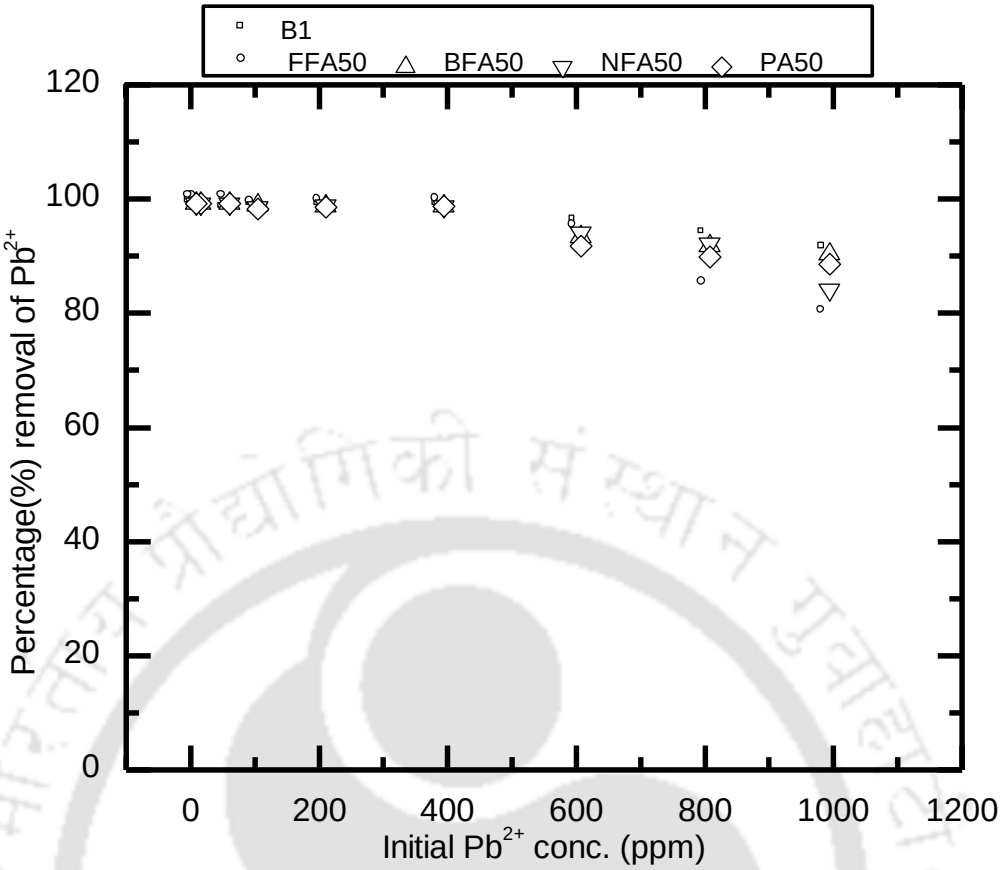

Figure 7.5 Percentage (%) removal of Pb^{2+} by FA-B1 mixes

7.7 Summary

The retention characteristics of the fly ashes (FAs), bentonite B1 and FA-B1 mixes were studied by conducting batch equilibrium study using a single metal model contaminant Pb^{2+}. Based on the adsorption results, it was found that retention of FFA, BFA and NFA were found to be comparable while PA indicates a slightly lower retention. The use of FA from different sources with bentonite B1 (in 50:50 mix) does not change the retention characteristics much and was comparable with that of the latter. The study demonstrates the added advantage of a fly ash based contaminant retention liner compared to inert sand based liner due to the contaminant retention characteristics of the former.

Chapter 8

Conclusions

The conclusions presented below were drawn based on the measured water retention characteristic curve (WRCC) of fly ash, bentonite and fly ash-bentonite mixes, sensitivity of WRCC model parameters on unsaturated seepage modeling and lead (Pb^{2+}) interaction on fly ash, bentonite and fly ash-bentonite mixes.

- The present study identifies the measurable range of suction as 0-1000 kPa for fly ash. This range of measured suction encompasses near saturation, desaturation and residual saturation portions of water retention characteristic curve.
- The WRCC fitting parameters obtained using different methodologies are not unique for fly ashes considered in this study and hence cannot be generalized.
- A new framework for WRCC parameterization of high volume change soils like bentonite was suggested to overcome ambiguities in obtaining WRCC parameters. This was done based on experimentally measured volumetric shrinkage characteristics of bentonites.
- The extent of influence of fly ash type and content on the WRCC of fly ash-bentonite mixes was brought forth.
- Statistical assessment of the variability of WRCCs of bentonite and fly ash-bentonite mixes showed that the variability of WRCC for materials from different sources was within 20%.
- The WRCC results of all the materials merged towards the residual portion. This observation has its significance because most of the landfill liners are compacted at optimum moisture content (OMC). For a high volume change soils like bentonite, OMC will be close to residual state. This means that bentonites from different sources can be used with a minimal quality check for the construction of liners.

- The variation in pore water pressure (PWP) with time obtained from unsaturated seepage modeling for different fly ashes was mainly due to the variation in the WRCC parameters since the k_{sst} value of all the fly ashes were comparable.
- The seepage modeling results of bentonites indicated significant variation in PWP and volumetric water content (VWC) with time for WRCC parameters obtained using two approaches (i.e. with and without the use of shrinkage test results).
- The seepage modeling result obtained for fly ash-bentonite mixes showed considerable influence of fly ash types and fly ash content.
- Fly ash acts as good sorbent for Pb^{2+} which is an added advantage of using fly ash instead of sand for constructing landfill liners.
- The Pb^{2+} sorption result of 50:50 fly ash-bentonite mix showed that results were close to bentonite sorption results, which was mainly attributed to high specific surface area of the latter.

Major contributions from this study

1. Establishing the range of measurable suction for Indian fly ashes and determination of WRCC parameters.
2. Proposing a systematic methodology based on shrinkage characteristic curve for determining WRCC of high plastic bentonites.
3. Measurement of WRCC of fly ash-bentonite mixes and studying the sensitivity of fly ash types and fly ash content on the WRCC of fly ash-bentonite mix.
4. Investigating the sensitivity of variation in WRCC parameters on unsaturated seepage modeling for different cases considerd in this study.
5. Understanding the potential of different fly ashes, bentonite and fly ash-bentonite mixes for the retention of heavy metal such as lead and comparing their removal efficiency.

Chapter 8

Conclusions

The conclusions presented below were drawn based on the measured water retention characteristic curve (WRCC) of fly ash, bentonite and fly ash-bentonite mixes, sensitivity of WRCC model parameters on unsaturated seepage modeling and lead (Pb^{2+}) interaction on fly ash, bentonite and fly ash-bentonite mixes.

- The present study identifies the measurable range of suction as 0-1000 kPa for fly ash. This range of measured suction encompasses near saturation, desaturation and residual saturation portions of water retention characteristic curve.
- The WRCC fitting parameters obtained using different methodologies are not unique for fly ashes considered in this study and hence cannot be generalized.
- A new framework for WRCC parameterization of high volume change soils like bentonite was suggested to overcome ambiguities in obtaining WRCC parameters. This was done based on experimentally measured volumetric shrinkage characteristics of bentonites.
- The extent of influence of fly ash type and content on the WRCC of fly ash-bentonite mixes was brought forth.
- Statistical assessment of the variability of WRCCs of bentonite and fly ash-bentonite mixes showed that the variability of WRCC for materials from different sources was within 20%.
- The WRCC results of all the materials merged towards the residual portion. This observation has its significance because most of the landfill liners are compacted at optimum moisture content (OMC). For a high volume change soils like bentonite, OMC will be close to residual state. This means that bentonites from different sources can be used with a minimal quality check for the construction of liners.

- The variation in pore water pressure (PWP) with time obtained from unsaturated seepage modeling for different fly ashes was mainly due to the variation in the WRCC parameters since the k_{sst} value of all the fly ashes were comparable.
- The seepage modeling results of bentonites indicated significant variation in PWP and volumetric water content (VWC) with time for WRCC parameters obtained using two approaches (i.e. with and without the use of shrinkage test results).
- The seepage modeling result obtained for fly ash-bentonite mixes showed considerable influence of fly ash types and fly ash content.
- Fly ash acts as good sorbent for Pb^{2+} which is an added advantage of using fly ash instead of sand for constructing landfill liners.
- The Pb^{2+} sorption result of 50:50 fly ash-bentonite mix showed that results were close to bentonite sorption results, which was mainly attributed to high specific surface area of the latter.

Major contributions from this study

1. Establishing the range of measurable suction for Indian fly ashes and determination of WRCC parameters.
2. Proposing a systematic methodology based on shrinkage characteristic curve for determining WRCC of high plastic bentonites.
3. Measurement of WRCC of fly ash-bentonite mixes and studying the sensitivity of fly ash types and fly ash content on the WRCC of fly ash-bentonite mix.
4. Investigating the sensitivity of variation in WRCC parameters on unsaturated seepage modeling for different cases considerd in this study.
5. Understanding the potential of different fly ashes, bentonite and fly ash-bentonite mixes for the retention of heavy metal such as lead and comparing their removal efficiency.

Chapter 9

Limitations of the Study and Future Scope of Research

1. This study do not account for the interaction of bentonite and fly ash with time. It is essential to understand the compatibility of geomaterials when fly ash is mixed with bentonite and its effect on water and contaminant retention characteristics (time effect or aging effect) before it can be applied in practice.
2. The significance of transition volumetric water content such as θ_A and θ_B stated in chapter 6 could not be fully understood from this study. The relevance of these points and its correlation with saturation, desaturation and residual characteristics of WRCC need to be further investigated.
3. A detailed investigation to establish the hypothesis of macro and micro air entry value proposed in this study need to be performed.
4. To carry out contaminant retention characteristics for fly ashes, bentonite and fly ash-bentonite mixes for other heavy metals to gain more confidence.

Chapter 9

Limitations of the Study and Future Scope of Research

1. This study do not account for the interaction of bentonite and fly ash with time. It is essential to understand the compatibility of geomaterials when fly ash is mixed with bentonite and its effect on water and contaminant retention characteristics (time effect or aging effect) before it can be applied in practice.
2. The significance of transition volumetric water content such as θ_A and θ_B stated in chapter 6 could not be fully understood from this study. The relevance of these points and its correlation with saturation, desaturation and residual characteristics of WRCC need to be further investigated.
3. A detailed investigation to establish the hypothesis of macro and micro air entry value proposed in this study need to be performed.
4. To carry out contaminant retention characteristics for fly ashes, bentonite and fly ash-bentonite mixes for other heavy metals to gain more confidence.

List of Publications from this Research work

International Journal:

1. **Abhijit**, D., Malaya, C., and Sreedeep, S. (2013). A study on tensiometer measurements in salt laden soil used for irrigation scheduling. *Journal of Geotechnical and Geological Engineering*, Springer, 31(4), 1349-1357.

2. **Abhijit, D.** and Sreedeep, S. Evaluation of measurement methodologies used for establishing water retention characteristic curve of fly ash." *Journal of Testing and Evaluation*, ASTM, 43(5), 7.

Manuscript under preparation:

1. Water retention characteristic of high plastic bentonites: Importance of volumetric shrinkage curve (part I).
2. Water retention characteristic of high plastic bentonites: parameterization and its effect on unsaturated seepage modeling (part II).
3. Study on the variability of water retention characteristic of fly ash-bentonite mixes.
4. Sensitivity of WRCC parameters on unsaturated seepage modeling of fly ash-bentonite mixes.
5. Contaminant retention characteristic of fly ash-bentonite mixes.

International Conference:

1. **Abhijit, D.** and Sreedeep, S. (2014). Evaluating the utility of tensiometer for establishing water retention characteristics curve of fly ash. *Geo-Congress conference* 2014, ASCE, Atlanta, Georgia.

2. Malaya, C., **Abhijit, D.,** and Sreedeep, S. (2011). A study on the influence of measuring methodologies on soil-water characteristic curve of a locally available soil, *Third International Postgraduate Conference on Infrastructure and Environment* 2011, The Hong Kong Polytechnic University, Hong Kong.

National Conference:

1. **Abhijit, D.,** Malaya, C., Srikanth, V., and Sreedeep, S. (2012). Comparison of suction measurement technique for class F fly ash. *Indian Geotechnical Conference*: IGC 2012, New Delhi, India.
2. **Abhijit, D.,** Babloo, k., and Sreedeep, S. (2012). An appraisal on the variability of water retention characteristics of Indian coal ashes. *Indian Geotechnical Conference*: IGC 2012, New Delhi, India.
3. Malaya, C., **Abhijit, D.,** and Sreedeep, S. (2011). Evaluation of estimated suction-water content relationship of a locally available soil. *Indian Geotechnical Conference*, IGC 2011, Kochi, India.
4. **Abhijit, D**., Malaya, C., and Sreedeep, S. (2010). Fly ash water retention with reference to agricultural application. *Fourth International Conference on Plants and Environmental Pollution* 2010, National Botanical Research Institute, Lucknow, India.

References

1. Abeele, W. V. (1986). The influence of bentonite on the permeability of sandy silts. *Journal of Nuclear and Chemical Waste Management*, 6, 8l-88.
2. Agus, S. S., Schanz, T., and Fredlund, D. G. (2010). Measurement of suction versus water content for bentonite-sand mixtures. *Canadian Geotechnical Journal*, 47, 583-594.
3. Agus, S. S., Arifin, Y. F., and Schanz, T. (2005). Hydro-mechanical characteristics of a polymer-enhanced bentonite-sand mixture for landfill applications. *International Workshop on Hydro-Physico-Mechanics of Landfill*, Lirigm, Grenoble 1 University, France, 21-22 March 2005.
4. Agus, S. S. and Schanz, T. (2005). Comparison of four methods for measuring total suction. *Vadose Zone Journal*, 4, 1087-1095.
5. Ahmaruzzaman, M. (2010). A review on the utilization of fly ash. *Progress in Energy and Combustion Science*, 36, 327–363.
6. Alinnor, I. J. (2007). Adsorption of heavy metal ions from aqueous solution by fly ash. *Fuel*, 86, 853–857.
7. Amadi, A. A. (2011). Hydraulic conductivity tests for evaluating compatibility of lateritic soil-fly ash mixtures with municipal waste leachate. *Geotechnical and Geological Engineering*, Springer, 29, 259-265.
8. ASTM D2487-06 (2008). Standard practice for classification of soils for engineering purposes (Unified Soil Classification System). Annual Book of ASTM Standards, ASTM International, West Conshohocken, PA, USA.
9. ASTM D4646-03 (2008). Standard test methods for 24-h batch type measurement of contaminant sorption by soils and sediments. Vol. 04.08, Annual Book of ASTM Standards, ASTM International, West Conshohocken, PA, USA.
10. ASTM D422-63 (2007). Standard test method for particle-size analysis of soils. Annual Book of ASTM Standards, ASTM International, West Conshohocken, PA, USA.
11. ASTM D698-07 (2007). Standard test method for laboratory compaction characteristic of soil using standard effort (12400 ft-lb/ft^3 (600 kN-m/m^3)). Annual Book of ASTM Standards, ASTM International, West Conshohocken, PA, USA.

12. ASTM D854-06 (2006). Standard test method for specific gravity of soil solids by water pycnometer. Annual Book of ASTM Standards, ASTM International, West Conshohocken, PA, USA.
13. ASTM D4318-05 (2005). Standard test methods for liquid limit, plastic limit, and plasticity index of soils. Vol. 04.08, Annual Book of ASTM Standards, ASTM International, West Conshohocken, PA, USA.
14. ASTM C618-05 (2005). Standard specification for coal ash and raw or calcined natural pozzolan for use in concrete, Annual Book of ASTM Standards, ASTM International, West Conshohocken, PA, 2005.
15. ASTM D6836-02 (2003). Test methods for determination of the soil water characteristics curve for desorption using a hanging column, pressure extractor, chilled mirror hygrometer, and/ or centrifuge. Vol. 04.08, Annual Book of ASTM Standards, ASTM International, West Conshohocken, PA, USA.
16. Ayala, J., Blanco, F., Garcia, P., Rodriguez, P., and Sancho, J. (1998). Austrian fly ash as a heavy metals removal material. *Fuel,* 77, 1147–1154.
17. Birle, E., Heyer, D., and Vogt, N. (2008). Influence of the initial water content and dry density on the soil–water retention curve and the shrinkage behavior of a compacted clay. *Acta Geotechnica*, 3, 191–200.
18. Bogena, H. R., Huisman, J. A., Oberdorster, C., and Vereecken, H. (2007). Evaluation of a low-cost soil water content sensor for wireless network applications. *Journal of Hydrology*, 344, 32-42.
19. Brooks, R. H. and Corey, A. T. (1964). Hydraulic properties of porous medium. *Hydrology*, Paper No. 3. Civil Engineering Department, Colorado State University, Fort Collins, Colorado.
20. Cerato, A. B. and Lutenegger, A. J. (2002). Determination of surface area of fine-grained soils by the ethylene glycol monoethyl ether (EGME) method. *Geotechnical Testing Journal,* ASTM, 25 (3), 1-7.
21. Chalermyanont, T. and Arrykul, S. (2005). Compacted sand-bentonite mixtures for hydraulic containment liners. *Songklanakarin Journal of Science and Technology*, 27 (2), 313-323.
22. Cho, H., Oh, D., and Kim, K. (2005). A study on removal characteristics of heavy metals from aqueous solution by fly ash. *Journal of Hazardous Materials,* B127, 187–195.
23. Çokça, E. and Yilmaz, Z. (2004). Use of rubber bentonite added fly ash as a liner

material. *Waste Management*, 24, 153-164.

24. Cowland, J. W. and Leung, B. N. (1991). A field trial of a bentonite landfill liner. *Waste Management & Research*, 9, 277-291.
25. Das, S. K. and Yudhbir. (2006). Geotechnical properties of low calcium and high calcium fly ash. *Geotechnical and Geological Engineering*, Springer, 24, 249-263.
26. Das, S. K. and Yudhbir. (2005). Geotechnical characterization of some Indian fly ashes. *Journal of Materials in Civil Engineering*, ASCE, 17, 544-552.
27. Delage, P., Romero, E. E., and Tarantino, A. (2008). Recent developments in the techniques of controlling and measuring suctions in unsaturated soils. Unsaturated soils: Advances in geo engineering- Toll et al. (eds), Taylor & Francis group, London, 33-52.
28. ECH2O soil moisture sensor (2006), Operator's manual version 5, Decagon Devices, U. S. A.
29. Edil, T. B., Acosta, H. A., and Benson, C. H. (2006). Stabilizing soft fine-grained soils with fly ash. *Journal of Materials in Civil Engineering*, ASCE, 18 (2), 283-294.
30. Equitensiometer User's Manual (1999). Delta-T Devices,
31. Fityus, S. and Buzzi, O. (2009). The place of expansive clays in the framework of unsaturated soil mechanics. *Applied Clay Science*, 43 (2), 150-155.
32. Fredlund, D. G. (2002). Use of the soil-water characteristics curve in the implementation of unsaturated soil mechanics. Proceedings, *Third International Conference on Unsaturated Soils*, UNSAT 2002, Vol. 3, Balkema, Recife, Brazil, 887-902.
33. Fredlund, M. D. (1998). Unsaturated seepage modeling made easy. *Geospec*, Geotechnical news.
34. Fredlund, D. G. and Xing, A. (1994). Equations for the soil-water characteristics curve. *Canadian Geotechnical Journal*, 31 (3), 521-532.
35. Fredlund, D. G. and Rahardjo, H. (1993). Soil mechanics for unsaturated soils. John Wiley and Sons, Inc., New York.
36. Gallage, C. P. K. and Uchimura, T. (2010). Effects of dry density and grain size distribution on soil-water characteristic curves of sandy soils. *Soils and Foundations*, 50 (1), 161-172.

37. Ghosh, A. and Subbarao, C (1998). Hydraulic conductivity and leachate characteristics of stabilized fly ash. *Journal of Environmental Engineering*, 124 (9), 812-820.
38. Gleason, M. H., David E. D., and Gerald, R. E. (1997). Calcium and sodium bentonite for hydraulic containment applications. *Journal of Geotechnical and Geoenvironmental Engineering*, ASCE, 123 (5), 438-445.
39. Gupta, G. and Torres, N. (1998). Use of fly ash in reducing toxicity and heavy metals in waste water effluent. *Journal of Hazardous Materials*, 57, 243–248.
40. Heineck, K. S., Lemos, R. G., Flores, J. A. A., and Consoli, N. C. (2010). Influence of particle morphology on the hydraulic behavior of coal ash and sand. *Geotechnical and Geological Engineering*, Springer, 28, 325–335.
41. Horiuchi, S., Kawaguchi, M., and Yasuhara, K. (2000). Effective use of fly ash slurry as fill material. *Journal of Hazardous Materials*, 76, 301-337.
42. Hsu, T. C., Yu, C. C., and Yeh, C. M. (2008). Adsorption of Cu^{2+} from water using raw and modified coal fly ashes. *Fuel*, 87, 1355–1359.
43. IS 2720: Part XXIV (1976). Methods of test for soils: Determination of Cation Exchange Capacity. Indian Standards Institute, New Delhi, India, 3-10.
44. IS 2720: Part VI (1972). Methods of test for soils: Determination of shrinkage factors. Indian Standards Institute, New Delhi, India, 3-11
45. IS 2720: Part XL (1977). Methods of test for soils: Determination of free swell index of soils. Indian Standards Institute, New Delhi, India, 3-4.
46. IS 2720: Part XVII (1986). Methods of test for soils: Laboratory determination of permeability. Indian Standards Institute, New Delhi, India, 8-12.
47. Ilic, M., Cheeseman, C., Sollars, C., and Knight, J. (2003). Mineralogy and microstructure of sintered lignite coal fly ash. *Fuel*, 82, 331-336.
48. Iyer, R. S. and Scott, J. A. (2001). Power station fly ash- a review of value-added utilization outside of the construction industry. *Resources, Conservation and Recycling*, 31, 217-228.
49. Jibeesh, C. M. (2013). Compaction and hydraulic performance evaluation of bentonite fly ash mixes. Master of technology thesis submitted to Department of Civil Engineering, IIT Guwahati, India.
50. Kalyanshetti, M. G. and Thalange, S. B. (2013). Effect of fly ash on the properties of expansive soil. *International Journal of Scientific & Engineering Research*, 4 (5), 37-40.

51. Kaniraj, S. R. and Gayathri, V. (2004). Permeability and consolidation characteristics of compacted fly ash. *Journal of Energy Engineering,* 130 (1), 18-43.
52. Kaniraj, S. R. and Gayathri, V. (2003). Geotechnical behavior of fly ash mixed with randomly oriented fiber inclusion. *Geotextiles and Geomembranes,* 21, 123-149.
53. Khan, A. A., Muthukrishnan, M., and Guha, B. K. (2010). Sorption and transport modeling of hexavalent chromium on soil media. *Journal of Hazardous Materials,* 174, 444-454.
54. Kumar, P. B. R. and Sharma, R. S. (2004). Effect of fly ash on engineering properties of expansive soils. *Journal of Geotechnical and Geoenvironmental Engineering,* ASCE 130 (7), 764-767.
55. Lam, L., Fredlund, D. G., and Barbour, S. L. (1987). Transient seepage model for saturated-unsaturated soil systems: a geotechnical engineering approach. *Canadian Geotechnical Journal,* 24, 565-580.
56. Lee, J. O., Cho, W. J., and Kwon, S. (2010). Suction and water uptake in unsaturated compacted bentonite. *Annals of Nuclear Energy,* 38, 520-526.
57. Leong, E. C., Tripathy, S., and Rahardjo, H. (2003). Total suction measurement of unsaturated soils with a device using the chilled-mirror dew-point technique. *Geotechnique,* 53 (2), 173-182.
58. Leong, E. C. and Rahardjo, H. (1997). Review of soil-water characteristic curve equations. *Journal of Geotechnical and Geoenvironmental Engineering*, ASCE, 123 (12), 1106-1117.
59. Likos, W. J. and Lu, N. (2003). Automated humidity system for measuring total suction characteristics of clay. *Geotechnical Testing Journal*, ASTM, 26 (2), 1-12
60. Lin, B. and Cerato, A. B. (2013). Hysteretic soil water characteristics and cyclic swell–shrink paths of compacted expansive soils. *Bulletin of Engineering Geology and the Environment,* 72, 61-70.
61. Lin, B. and Cerato, A. B. (2012). Investigation on soil-water characteristic curves of untreated and stabilized highly claye expansive soils. *Geotechnical and Geological Engineering*, Springer, 30, 803-812.
62. Lin, L. C. and Benson, C. H. (2000). Effect of wet-dry cycling on swelling and hydraulic conductivity of GCLs. *Journal of Geotechnical and Geoenvironmental Engineering,* ASCE, 126 (1), 40-49.

63. Lin, C. J. and Chang, J. E. (2001). Effect of fly ash characteristics on the removal of Cu(II) from aqueous solution. *Chemosphere*, 44, 1185–92.
64. Malaya, C. (2012). A study on measuring methodologies and critical parameters influencing soil suction-water content relationship. Ph. D. thesis submitted to Department of Civil Engineering, IIT Guwahati, India.
65. Malaya, C. and Sreedeep, S. (2012). Critical evaluation of the drying water retention characteristics of a class F Indian fly ash. *Journal of Materials in Civil Engineering*, ASCE, 24 (4), 451-459.
66. Malaya, C. and Sreedeep, S. (2010). A study on the influence of measurement procedures on suction-water content relationship of a sandy soil. *Journal of Testing and Evaluation*, ASTM, 38 (6), 1-9.
67. Marinho, F. A. M. (1994). Shrinkage behaviour of some plastic soils. Ph. D. thesis submitted to the University of London, Imperial College of Science, Technology and Medicine.
68. Marinho, F. A. M. and Chandler, R. J. (1993). Aspects of the behavior of clays on drying. *Unsaturated Soils, Geotechnical Special Publication*, ASCE, New York, 39, 77–90.
69. Mishra, M. K. and Karanam, U. M. R. (2006). Geotechnical characterization of fly ash composites for backfilling mine voids. *Geotechnical and Geological Engineering*, Springer, 24, 1749-1765.
70. Miao, L., Liu, S., and Lai, Y. (2002). Research of soil-water characteristics and shear strength features of Nanyang expansive soil. *Engineering Geology*, 65, 261-267.
71. Miller, C. J., Yesiller, M. N., Yaldo, K., and Merayyan, S. (2002). Impact of soil type and compaction conditions on soil-water characteristic. *Journal of Geotechnical and Geoenvironmental Engineering*, ASCE, 128 (9) 733-742.
72. MPS-1. (2008). Operator's Manual, Version 3.0.
73. Nam, S., Gutierrez, M., Diplas, P., Petrie, J., Wayllace, J. A., Lu, N., and Munoz, J. J. (2009). Comparison of testing techniques and models for establishing the SWCC of riverbank soils. *Engineering Geology*, 110, 1-10.
74. Naik, H. K., Mishra, M. K., and Behera, B. (2007). Laboratory investigation and characterization of some byproducts for their effective utilization. *1st international conference on managing the social and environmental consequences of coal mining in India*, New Delhi, November 19-21, 1-10.

75. Nhan, C. T., Graydon, J. W., and Kirk, D. W. (1996). Utilizing coal fly ash as landfill barrier material. *Waste Management,* 16 (7), 587 595.
76. Ogata, N. and Komine, H. (1993). Permeability changes of bentonite-sand mixture before and after swelling. *Elsevier Science Publishers B. V.*, N 03/3, 357-362
77. Pal, S. K. and Ghosh, A. (2014). Volume change behavior of fly ash-montmorillonite clay mixtures. *International Journal of Geomechanics,* 14 (1), 59 68.
78. Palmer, B. G., Edil, T. B., and Benson, C. H. (2000). Liners for waste containment constructed with class F and C fly ashes. *Journal of Hazardous Materials,* 76, 193-216.
79. Pan, H., Qing, Y., and Young, L. P. (2010). Direct and indirect measurement of soil suction in the laboratory. *Electronic Journal in Geotechnical Engineering,* 15, 1-14.
80. Pandian, N. S. (2004). Fly ash characterization with reference to geotechnical applications. *Journal of Indian Institute of Science,* 84, 189-216.
81. Pandian, N. S., Rajasekhar, C., and Sridharan, A. (1998). Studies of the specific gravity of some Indian coal ashes. *Journal of Testing and Evaluation,* ASTM 26 (3), 177-186.
82. Pandian, N. S., Rajasekhar, C., and Sridharan, A. (1996). Fly ash as a pre-filter material for the retention of lead ions. *Journal of Testing and Evaluation,* ASTM 24 (3), 181-186.
83. Papandreou, A., Stournaras, C. J., and Panias, D. (2007). Copper and cadmium adsorption on pellets made from fired coal fly ash. *Journal of Hazardous Materials,* 148, 538–547.
84. Patric, P. K., Olsen, H. W., and Higgins, J. D. (2007). Comparison of chilled mirror measurements and filter paper estimates of total soil suction. *Geotechnical Testing Journal,* ASTM 30 (5), 1-8.
85. Parsa, J., Munson-McGee, S. H., and Steiner, R. (1996). Stabilization/solidification of hazardous wastes using fly ash. *Journal of Environmental Engineering,* ASCE, 122 (10), 935-940.
86. Pedarla, A., Puppala, A. J., Chittoori, B. S., Hoyos, L. R., Zapata, C., and Houston, S. L. (2012). Influence of mineral montmorillonite on soil suction modeling parameters. *Geo Congress conference,* ASCE, Oakland, CA, March 25-29, 2012, 1126-1135.

87. Pehlivan, E., Cetin, S., and Yanik, B. H. (2006). Equilibrium studies for the sorption of zinc and copper from aqueous solutions using sugar beat pulp and fly ash. *Journal of Hazardous Materials,* 135, 193–199.
88. Piekos, R. and Paslawska, S. (1999). Fluoride uptake characteristics of fly ash. *International Society for Fluoride Research,* Fluoride, 32 (1), 14-19.
89. Poly, B. and Sreedeep, S. (2011). Influence of soil-multiple contaminant retention parameters on contaminant fate prediction. *Journal of Hazardous, Toxic, and Radioactive Waste,* 15 (3), 180-187.
90. Prakash, K. and Sridharan, A. (2009). Beneficial properties of coal ashes and effective solid waste management. *Practice Periodicals of Hazardous, Toxic, and Radioactive Waste Management,* 13 (4), 239-248.
91. Prashanth, J. P., Sivapullaiah, P. V., and Sridharan, A. (2001). Pozzolanic fly ash as a hydraulic barrier in landfills. *Engineering Geology,* 60, 245-252.
92. Puppala, A. J., Punthutaecha, K., and Vanapalli, S. K. (2006). Soil-water characteristics curve of stabilized expansive soils. *Journal of Geotechnical and Geoenvironmental Engineering,* ASCE 123 (6) 736-751.
93. Rao, M., Parwate, A. V., and Bhole, A. G. (2002). Removal of Cr^{6+} and Ni^{2+} from aqueous solution using bagasse and fly ash. *Waste Management,* 22, 821–830.
94. Rio, S. and Delebarre, A. (2003). Removal of mercury in aqueous solution by fluidized bed plant fly ash. *Fuel,* 82, 153–159.
95. Ridley, A. M., Dineen, K., Burland, J. B., and Vaughan, P. R. (2003). Soil matrix suction: some examples of its measurement and application in geotechnical engineering. *Geotechnique,* 53 (2), 241-253.
96. Richards, L. A. (1931). Capillary conduction of liquids through porous medium. *Physics*, 1, 318-333.
97. Ruthven. (1984). Principal of adsorption and absorption processes. John Wiley & Sons, Inc. New work.
98. Seepage Modeling with SEEP/W (2007). An engineering methodology, Geo-Slope International Ltd.
99. Shafique, S. B., Rahman, K., Yaykiran, M., and Azfar, I. (2010). The long-term performance of two fly ash stabilized fine-grained soil sub bases. *Resources, Conservation and Recycling,* 54, 666-672.
100. Shanthakumar, S., Singh, D. N., and Phadke, R. C. (2008). Characterization of fly ash from various locations of electrostatic precipitator. *The 12th international*

conference of International Association for Computer Methods and Advances in Geomechanics (IACMAG), 1-6 October, 2008, Goa, India.

101. Shah, P. H., Sreedeep, S., and Singh, D. N. (2006). Evaluation of methodologies used for establishing soil-water characteristics curve. *Journal of ASTM International*, 3 (6), 1-11.

102. Shang, J. Q., Wang, H. L., Kovac, V., and Fyfe, J. (2006). Site-specific study on stabilization of acid-generating mine tailings using coal fly ash. *Journal of Materials in Civil Engineering*, ASCE, 18 (2), 140-151.

103. Sivapullaiah, P. V. and Baig, M. A. A. (2011). Gypsum treated fly ash as a liner for waste disposal facilities. *Waste Management*, 31, 359-369.

104. SoilVision 4.21.001. (2009). A knowledge-based database system for saturated/ unsaturated soil properties. SoilVision Systems Ltd., Saskatoon, Saskatchewan, Canada.

105. Sreedeep, S. and Singh, D. N. (2008). A critical review of the methodologies employed for suction measurement for developing the SWCC. *The 12th International Conference of International Association for Computer Methods and Advances in Geomechanica (IACMAG)*, 1988-1993.

106. Sreedeep, S. and Singh, D. N. (2005). A study to investigate the influence of soil properties on suction. *Journal of Testing and Evaluation*, ASTM, 33(1), 1-6.

107. Sreedeep, S. and Singh, D. N. (2006). Methodology for determination of osmotic suction of soils. *Geotechnical and Geological Engineering*, Springer, 24, 1469-1479.

108. Tang, C. H., Shi, B., Liu, C., Suo, W. B., and Gao, L. (2011). Experimental characterization of shrinkage and desiccation cracking in thin clay layer. *Applied Clay Science*, 52, 69-77.

109. Tariq, A. and Durnford, D. S. (1993). Soil volumetric shrinkage measurements: a simple method. *Soil Sci*., 155, 325-330.

110. T5 User Manual (2001). Version 1.8, UMS GmbH, Munich.

111. Thakur, V. K. S., Sreedeep, S., and Singh, D. N. (2006). Laboratory investigations on extremely high suction measurements for fine-grained soil. *Geotechnical and Geological Engineering*, Springer, 24, 565-578.

112. Thieu, N. T. M., Fredlund, M. D., and Huang, V. Q. (2001). Seepage modeling in a saturated/unsaturated soil system. *International Conference on the Land and Water Resources, MLWR*, October 20-22, Hanoi, Vietman.

113. Tinjum, J. M., Benson, C. H., and Boltz, L. R. (1997). Soil-water characteristic curves for compacted clays. *Journal of Geotechnical and Geoenvironmental Engineering*, ASCE, 123 (11), 1060-1069.
114. Tripathy, S., Tadza, M. Y. M., and Thomas, H. R. (2014). Soil-water characteristic curves of clays. *Canadian Geotechnical Journal*, 51, 869-883.
115. van Genuchten, M. Th., Leij, F. J., and Yates, S. R. (1991). "The RETC code for quantifying the hydraulic functions of unsaturated soils", Report No. EPA/600/2-91/065, R. S. Kerr Environmental Research Laboratory, U. S. Environmental Protection Agency, Ada, OK.
116. van Genuchten, M. T. (1980). A closed-form equation for predicting the hydraulic conductivity of unsaturated soils. *Soil Science Society of America Journal*, 44 (5), 892-898.
117. Visa, M., Bogatu, C., and Duta, A. (2010). Simultaneous adsorption of dyes and heavy metals from multi component solutions using fly ash. *Applied Surface Science*, 256, 5486–5491.
118. Viotti, P., Papini, M. P., and Gamba, C. (2005). Contaminant transport in an unsaturated soil: laboratory tests and numerical simulation model as procedure for parameters evaluation. *Ecological Modeling*, 182, 131-148.
119. Weng, C. H. and Huang, C. P. (2004). Adsorption characteristics of Zn(II) from dilute aqueous solution by fly ash. *Colloids Surfaces A: Physicochem. Eng. Aspects*, 247, 137–143.
120. WP4 User's Manual (2002). Decagon Devices, Inc., USA.
121. Yang, H., He, C., Xiao, J., and Zhan, W. (2011). Analysis on improvement effect of expansive soil by soil-water characteristics curve. *Geotechnical Special Publication*, ASCE, 222, 272-279.
122. Yang, H., Rahardjo, H., Leong, E. C., and Fredlund, D. G. (2004). Factors affecting drying and wetting soil-water characteristic curves of sandy soils. *Canadian Geotechnical Journal*, 41, 908-920.
123. Yeheyis, M. B., Shang, J. Q., and Yanful, E. K. (2010). Feasibility of using coal fly ash for mine waste containment. *Journal of Environmental Engineering*, ASCE, 136 (7), 682-690.
124. Yeo, S. S., Shackelford, C. D., and Evans, J. C., (2005). Consolidation and hydraulic conductivity of nine model soil-bentonite backfills. *Journal of Geotechnical and Geoenvironmental Engineering*, ASCE, 131(10), 1189-1198.

125. Younus, M. M. and Sreedeep, S. (2012). Evaluation of bentonite-fly ash mix for its application in landfill liners. *Journal of Testing and Evaluation*, ASTM, 40 (3), 1-6.
126. Younus, M. M. (2010). Laboratory investigations to maximize the utility of fly ash for landfill liner. Mtech thesis submitted to Department of Civil Engineering, IIT Guwahati, India.
127. Young, L. P. and Qing, Y. (2009). Test study on soil-water characteristic curve of bentonite-sand mixtures. *Electronic Journal in Geotechnical Engineering*, 14, 1-8.
128. Zha, F., Liu, S. U. Y., and Cui, K. (2008). Behavior of expansive soils stabilized with fly ash. *Journal of Natural Hazards*, 47, 509-523.
129. Zhan, L. T., Chen, P., and Ng, C. W. W. (2007). Effect of suction change on water content and total volume of an expansive clay. *Journal of Zhejiang University Science A*, 8 (5), 699-706.
130. Zhou, J. and Yu, J. L. (2005). Influences affecting the soil-water characteristic curve. *Journal of Zhejiang University Science*, 56A (8), 797-804.
131. Zielinski, M., Sentenac, P., Atique, A., Sachez, M., and Romero, E. (2011). Comparison of four methods for determining the soil water retention curve. Unsaturated Soils- Alonso & Gens (eds), Taylor & Francis Group, London, ISBN 978-0-415-60428-4.